

# Durham E-Theses

---

## *Cultural evolution of material knot diversity*

SCANLON, LAUREN, ABIGAIL

### How to cite:

---

SCANLON, LAUREN, ABIGAIL (2019) *Cultural evolution of material knot diversity*, Durham theses, Durham University. Available at Durham E-Theses Online: <http://etheses.dur.ac.uk/12994/>

### Use policy

---

The full-text may be used and/or reproduced, and given to third parties in any format or medium, without prior permission or charge, for personal research or study, educational, or not-for-profit purposes provided that:

- a full bibliographic reference is made to the original source
- a [link](#) is made to the metadata record in Durham E-Theses
- the full-text is not changed in any way

The full-text must not be sold in any format or medium without the formal permission of the copyright holders.

Please consult the [full Durham E-Theses policy](#) for further details.

# Cultural Evolution of Material Knot Diversity

Lauren Abigail Scanlon

Submitted for the degree of Doctor of Philosophy

September 2018

## Abstract

In this thesis we discuss the cultural evolution of knot tying with an overview of the knots widely used and a multi-disciplinary analysis using mathematical knot theory and models exploring human learning and evolution.

In order to assess the knots commonly tied we analyse the knots appearing in the largest collection of material knots; the Ashley Book of Knots, using knot theory to assess their diversity. This analysis identifies 162 distinct mathematical knots appearing in the guise of over 500 different material knots, suggesting a selection for these particular knots.

To identify and explore the biases affecting the oblique transmission of knot tying we present a study comparing the successful replication of two of the simplest knots, the granny knot and the reef knot. The experimental results suggest a bias towards tying granny knots over reef knots through the identification of a bias towards the repetition of features previously tied, using a mathematical model and Approximate Bayesian Computation to fit the model to the experimental data.

With the aim of exploring the diversity in the Ashley Book of Knots, we use a model of social and asocial learning on knot types and a fitness analysis from an NK fitness landscape. Both models suggest highly accurate social learning and mutation through crossing changes is necessary to facilitate the diversity seen in the Ashley Book of Knots. Analysing the crossings present in the knots seen in the Ashley Book of Knots suggests a selection for knot features that increase the complexity of the knot and increase crossing number but also an introduction of redundant features, suggesting the knots used regularly are not optimal.

# Cultural Evolution of Material Knot Diversity

Lauren Abigail Scanlon

A Thesis presented for the degree of  
Doctor of Philosophy



Department of Anthropology and  
Department of Mathematical Sciences  
University of Durham  
England

September 2018

# Contents

<b>Abstract</b>	<b>i</b>
<b>Declaration</b>	<b>x</b>
<b>Acknowledgements</b>	<b>xi</b>
<b>1 Introduction</b>	<b>1</b>
1.1 Knotting . . . . .	1
1.1.1 History . . . . .	1
1.2 Introduction to cultural evolution . . . . .	3
1.2.1 Cultural evolution . . . . .	3
1.3 Introduction to knot theory . . . . .	7
1.3.1 History . . . . .	7
1.3.2 Definitions and examples . . . . .	8
1.4 Project outline . . . . .	14
1.4.1 Questions . . . . .	14
<b>2 A study of knots in material culture</b>	<b>15</b>
2.1 Introduction . . . . .	15
2.2 Mathematical analysis of ABOK . . . . .	20
2.3 Results . . . . .	23
2.3.1 Overall trends . . . . .	23
2.3.2 Distribution of knots (to be used in Chapters 4 and 5) . . . .	28
2.3.3 Knots omitted . . . . .	30
2.3.4 Uses of knots . . . . .	33



---

2.4	Conclusion . . . . .	41
<b>3</b>	<b>An analysis of the transmission of granny and reef knots</b>	<b>44</b>
3.1	Introduction . . . . .	44
3.2	Experiment . . . . .	51
3.2.1	Participants . . . . .	52
3.2.2	Procedure . . . . .	52
3.2.3	Results . . . . .	54
3.3	Parametric model . . . . .	62
3.3.1	Assumptions . . . . .	62
3.3.2	Equations . . . . .	62
3.3.3	Equilibria . . . . .	65
3.3.4	Stability . . . . .	68
3.4	Applying the model to experimental results . . . . .	72
3.4.1	ABC method . . . . .	72
3.4.2	ABC results . . . . .	73
3.5	Conclusion . . . . .	81
<b>4</b>	<b>A social and asocial learning model of knot transmission</b>	<b>85</b>
4.1	Introduction . . . . .	85
4.2	Model of social and asocial learning . . . . .	87
4.2.1	Braid words on two strands . . . . .	88
4.2.2	Braid words on three strands . . . . .	106
4.3	Conclusion . . . . .	126
<b>5</b>	<b>A fitness landscape analysis of knots and links</b>	<b>130</b>
5.1	Introduction . . . . .	130
5.2	Knot NK model . . . . .	132
5.2.1	Fitness from ABOK . . . . .	141
5.2.2	Identifying fit crossings . . . . .	152
5.3	Conclusion . . . . .	158
<b>6</b>	<b>Conclusions</b>	<b>162</b>

---

<b>A</b>	<b>Appendices</b>	<b>168</b>
A.1	Chapter 3 Appendix . . . . .	168
A.1.1	Questionnaire information . . . . .	168
A.1.2	Posterior simulations . . . . .	171
A.1.3	Equations . . . . .	177
A.1.4	Equilibria equations . . . . .	179
A.1.5	Barycentric coordinates . . . . .	180
A.2	Chapter 4 Appendix . . . . .	181
A.2.1	Social and asocial learning model . . . . .	181
A.3	Chapter 5 Appendix . . . . .	185
A.3.1	Random walks on NK landscapes . . . . .	190
	<b>Bibliography</b>	<b>193</b>

# List of Figures

1.1	A projection of the unknot . . . . .	8
1.2	Two projections of the trefoil knot . . . . .	8
1.3	The Reidemeister moves . . . . .	9
1.4	Composition of trefoil knots . . . . .	11
1.5	DT code of the trefoil knot . . . . .	12
1.6	Crossings in braid words . . . . .	13
1.7	Braid representation of the trefoil knot . . . . .	13
2.1	Bowknot reduced to trefoil knot . . . . .	22
2.2	Image of splice . . . . .	31
2.3	Image of single strand knot . . . . .	32
2.4	Image of loop knot . . . . .	32
2.5	ABOK crossing number mean and standard deviation per use . . . .	34
2.6	Reduced crossing number mean and standard deviation per use . . .	34
2.7	Plot of the difference in redundancy between usage levels . . . . .	36
2.8	Plot of the difference in redundancy between prime and composite knots . . . . .	38
2.9	Plot of the difference in redundancy between appearance levels . . . .	40
3.1	Shoelace knot . . . . .	46
3.2	Trefoil knot . . . . .	47
3.3	Granny knots . . . . .	48
3.4	Reef knots . . . . .	48
3.5	Granny knots . . . . .	50
3.6	Reef knots . . . . .	50

3.7	Video used in experiment . . . . .	53
3.8	Trefoils tied in experiment . . . . .	54
3.9	Posterior simulation of knots tied . . . . .	57
3.10	Posterior simulation of granny and reef knots . . . . .	58
3.11	Decision tree for equation parameters . . . . .	64
3.12	Evolutionary trajectories . . . . .	66
3.13	Line plots . . . . .	67
3.14	Density plot . . . . .	71
3.15	Histogram of simulated parameters . . . . .	73
3.16	Evolutionary trajectory for knot frequencies . . . . .	76
3.17	Equilibrium values from sampled parameter values . . . . .	77
3.18	Decision tree for handedness and repetition . . . . .	78
4.1	Example of crossing changes on Hopf Link . . . . .	89
4.2	Networks for two strand braids . . . . .	94
4.3	Contour plots two strand braids . . . . .	103
4.4	Networks three strand braids . . . . .	109
4.5	Contour plots three strand braids . . . . .	123
5.1	Network for braids on two strands in an $N = 3$ , $K = 1$ landscape . .	140
5.2	Distribution of squared Euclidean distance on $3 \leq N \leq 5$ and $1 \leq$ $K \leq N - 2$ landscape . . . . .	147
A.1	Posterior simulation of trefoils tied given hand written with . . . . .	171
A.2	LL posterior simulation . . . . .	172
A.3	RR posterior simulation . . . . .	173
A.4	LR posterior simulation . . . . .	174
A.5	RL posterior simulation . . . . .	175
A.6	Posterior simulation of first knot tied given stage 1 bias . . . . .	176

# List of Tables

2.1	Layout of the ABOK database . . . . .	21
2.2	Prime knots in ABOK . . . . .	24
2.3	Prime links in ABOK . . . . .	26
2.4	Composite knots and links in ABOK . . . . .	27
2.5	Distribution of knots and links up to eight crossings in ABOK . . . .	29
2.6	Redundancy in high and low usage knots . . . . .	37
2.7	Redundancy in prime and composite knots . . . . .	39
2.8	Redundancy in high and low appearance knots . . . . .	41
3.1	Knots tied in experiment . . . . .	55
3.2	Granny and reef knots tied . . . . .	56
3.3	Knots and trefoils tied . . . . .	59
3.4	Parameter values . . . . .	74
3.5	Knots at equilibria . . . . .	75
3.6	Knots frequencies under random and non-random error . . . . .	77
3.7	Probability of cultural transmission under a parametric approach . .	79
3.8	Probability of cultural transmission under a linear approach . . . .	79
3.9	Comparison of parametric and linear approach . . . . .	81
4.1	Braid words from $\sigma_1\sigma_1$ . . . . .	90
4.2	Fertility levels . . . . .	96
4.3	Amount of parents . . . . .	98
5.1	Possible braids on two strands on an $N = 3$ landscape . . . . .	134
5.2	Proportion of fittest knots and links . . . . .	137

5.3	Frequency of braids in ABOK for $K = 1$ on two strands . . . . .	142
5.4	Fitness in an $N = 3$ and $K = 1$ . . . . .	145
5.5	Distance values for $3 \leq N \leq 8$ and $1 \leq K \leq N - 2$ landscapes . . . .	146
5.6	Probability of metric values for $3 \leq N \leq 5$ and $1 \leq K \leq N - 2$ landscapes . . . . .	148
5.7	Random walk results $3 \leq N \leq 5$ and $1 \leq K \leq N - 2$ landscapes . . .	151
5.8	ABOK frequencies for $N = 3$ and $K = 1$ landscape . . . . .	153
5.9	Crossing fitness in an $N = 3$ , $K = 1$ landscape . . . . .	154
5.10	Fitness of crossing types in $3 \leq N \leq 7$ and $K = 1$ landscapes . . . . .	155
5.11	Fitness of crossing types in $3 \leq N \leq 7$ and $K = 2$ landscapes . . . . .	156
5.12	Fitness of crossing types in $3 \leq N \leq 7$ and $K = 3$ landscapes . . . . .	157
5.13	Fitness of crossing types in $3 \leq N \leq 7$ and $K = 4$ landscapes . . . . .	157
A.1	Effect of hand written with on trefoil tied . . . . .	168
A.2	Effect of gender on performance . . . . .	169
A.3	Effect of experience on performance . . . . .	169
A.4	Effect of knowledge on performance . . . . .	170
A.5	Effect of knowledge on performance . . . . .	170
A.6	Fitness values for $3 \leq N \leq 5$ and $1 \leq K \leq N - 2$ landscapes . . . . .	185
A.7	Fitness values for $N = 6$ and $1 \leq K \leq 4$ landscapes . . . . .	186
A.8	Fitness values for $N = 7$ and $1 \leq K \leq 5$ landscapes . . . . .	187
A.9	Fitness values for $N = 8$ and $1 \leq K \leq 6$ landscapes . . . . .	188
A.10	Fitness values for $N = 8$ and $1 \leq K \leq 6$ landscapes . . . . .	189
A.11	Random walk results $N = 7$ and $1 \leq K \leq 5$ landscapes . . . . .	190
A.12	Random walk results $N = 8$ and $1 \leq K \leq 2$ landscapes . . . . .	191
A.13	Random walk results $N = 8$ and $3 \leq K \leq 6$ landscapes . . . . .	192

# Declaration

The work in this thesis is based on research carried out at the Departments of Anthropology and Mathematical Sciences at the University of Durham, England. No part of this thesis has been submitted elsewhere for any other degree or qualification and it is all my own work unless referenced to the contrary in the text.

**Copyright © 2018 by Lauren A. Scanlon.**

“The copyright of this thesis rests with the author. No quotations from it should be published without the author’s prior written consent and information derived from it should be acknowledged”.

# Acknowledgements

Thank you to my supervisors Jeremy Kendal, Andrew Lobb and Jamie Tehrani for their support and guidance over the past four years. Thank you to all the SPOCK team both at Durham and Bristol for making this project possible and the Leverhulme Trust for their funding. Thank you for all the members of CCBC for useful discussions and advice.

Thank you to the International Guild of Knot Tyers, especially Colin Byfleet, for their welcome and useful conversations on knotting. Thanks to Antonio, Ben, David, Fabian and Kate for providing company on the PhD process and for always being up for a trip to the pub and to Sara for all the espresso martinis.

Thanks to my mum, dad, Bev and Gab for their support even if they had no clue what I was working on and to Nick for keeping me sane.



*Dedicated to*

Grandad

# Chapter 1

## Introduction

### 1.1 Knotting

#### 1.1.1 History

Knots are an important and ancient technology, with archaeological evidence suggesting knots played a crucial role in the development of early humans, along with the use of fire and the wheel. It is difficult to say when the first knot was used, as knots are usually made of perishable material and so are subject to decay, but artefacts which probably require knots have been found dating as far back as 300,000 years ago [1]. Such material knots can be found in sites where bodies and artefacts have been preserved in conditions with sub-zero temperatures, a completely dry environment or other conditions which prevent decomposition [2]. For example, knots were found as part of the “Ice Man’s” equipment when he was discovered in 1991 south of the Italian-Austrian border. His body and equipment had been frozen solid and preserved for over 5,400 years. Other preserved knots such as nooses [2], textiles and fishing lines have also been found in various countries in bogs, dating as far back as 3500 BC with knots also observed from Ancient Egypt in both archaeological remains and texts [3], the earliest dating to 1350 BC and found in Middle Egypt.

Knots have appeared in ancient folktales, such as the story of Alexander the Great and the Gordian Knot in 33 BC [4], a complicated knot that was to be untied

by the future King which Alexander cut with his sword defeating the problem. Knots are not only used for practical purposes but are also used in decorative handicraft in Chinese folk art, with the earliest knots dating back around 18,000 years [5]. Another purpose for knots are those known as quipus which appear in the archaeological record between 1100 to 1532 AD, used by the Inca people both as part of numerical and administrative records [6] [7]. Early work suggested that the system of knots tied to form the quipu were used solely as a numerical record, with each the knot type and position in the system denoting a number [6], but more recent analysis suggests these knot systems were also used for administrative records [7] with knots referring to individuals forming a census record.

There have been attempts to categorise the many knots tied, most notably by Clifford Ashley in *The Ashley Book of Knots* (ABOK) [8]. His work contains over 3,800 knots, with information on how to tie them, who ties them and what they are used for. Although an immense amount of knots are included here, they are predominantly tied by Western cultures so may only give us a small snapshot of the actual amount of knots used.

Interest in knot tying may be for practical use or of a theoretical interest. The International Guild of Knot Tyers (IGKT) [9] represent many people from various backgrounds across many countries, with both a practical and theoretical interest in knot tying. The IGKT have been involved in various research into knot tying, including being involved in a project to type up Henry North Grant Bushby's series of manuscripts; "Notes on Knots" [10] currently located in the Mariner's Museum [11]. Bushby's work comprises eight volumes with over 1,900 handwritten pages including hand drawn and inked knot images. His work details drawings and instructions on how to tie many knots but also includes analysis of knot forms and an attempt at knot classification. Involved in these volumes are properties and classification of torus knots and knot equivalence, work previously uncredited.

There are over 82 uses of knots given in ABOK with over 3,800 knots detailed. These uses range from those used by fishermen to tree surgeons and medical surgeons with the knots included in each domain ranging from just a handful to many. Various websites contain instructional videos and images detailing knot tying across ranges

of use from Ian’s Shoelace Site [12], focusing on the various forms and correct tying of the shoelace knot, to Grog’s Animated Knots [13] giving a wider range of domains. The Human Relations Area Files ethnographic database [14] also contains 1,900 references to knotting across 228 different cultures.

Knot tying is also observed in the animal kingdom with weaver birds using knots to form their nests and attract mates [15], the hagfish tying itself in knots which travel from its head to its tail in order to escape predators [16] and great apes being seen to use knots in their nests [17].

Knots are so easily tied and so widely used it leads to the question as to why knots are used and what causes certain knots to be used more than others, evidenced by the diversity of knots documented in ABOK. Knots are also studied mathematically but look a little different to those tied by humans. The properties of these knots are well studied in the field of knot theory giving us tools with which to characterise the variation in material knots. We can use cultural evolutionary theory to investigate the factors that may lead to certain knots being more culturally successful than others through the study of variation, selection and inheritance in socially learned behaviours.

## 1.2 Introduction to cultural evolution

### 1.2.1 Cultural evolution

Cultural evolution is the study of information transmitted socially. This information may be beliefs, languages, attitudes or skills, such as knot tying, and may be transmitted purposefully such as through teaching or acquired through observation and imitation [18]. Boyd and Richerson define culture as “information capable of affecting individual’s behaviour that they acquire from other members of their species” [19] which does not include information learned individually or inherited genetically. Mesoudi describes cultural evolution as a process of “descent with modification” [18] where socially learned behaviour is passed on within a population with intentional improvements or accidental modifications through learning errors. Claidire et al. [20] discuss cultural evolution in terms of cultural attraction with

attractors increasing the frequency of cultural traits over generations, the effect of these attractors can be affected by multiple factors in the transmission process.

In this way the cultural information will be modified through this process of transmission. This process can be affected by who people look to for social information, what is transmitted and how it is transmitted. Many biases are studied which affect this process.

Learners may be biased to make them more likely to acquire information from prestigious members of society which may aid the acquisition of preferential information [21] or acquire information which appears to be being used widely through conformity bias, increasing the frequency of certain traits [22]. Some biases may cause optimisation of the information or skills inherited but others may be detrimental or of no benefit to the learner in the performance of the skill [23].

Certain variants of the information or skill may be favoured through a content bias to acquire certain variants of traits causing an increased frequency in that variant. Morin discusses the preference for direct-gaze in portraits and suggests this is the result of a “cognitive attraction” process, with direct-gaze in portraits catching the attention of both adults and newborns [24], causing increased likelihood to paint portraits with direct-gaze and the variant to increase in frequency.

These biases or factors may be instrumental in the dominance of certain knot types over others or may dictate the way in which knots are learned and used.

## Models of cultural evolution

Cultural evolution can be analysed with mathematical models of the transmission process. Cavalli-Sforza and Feldman were among the first to model the transmission of cultural traits with a model adopted from evolutionary biology [25]. They used a simple differential equation to model the frequency of a trait in the population and the probability it is inherited, enabling them to study the dynamics of the transmission of that trait over time. A similar modelling approach has also been taken by Boyd and Richerson [26] again using models adopted from evolutionary biology to develop models of cultural evolution. These models allow for the inspection of the inheritance of traits from one generation to another allowing for both vertical and

oblique transmission to be modelled.

Modelling the transmission process of a cultural trait can be useful to determine the manner in which it evolved. Acerbi and Bentley [27] contrast neutral models that contain no assumed bias with models including content and context biases to assess population level frequency data across multiple domains. Their findings determine that in some of the contexts the neutral model explains the data best, suggesting an unbiased-copying process was sufficient in that context whereas other domains required biased-copying to explain the frequency of the most common traits in the data.

These biases at the individual level can cause the emergence of population level patterns seen in the frequency of individual traits. However Kandler et al. observe that although biases and transmission at the individual level dictate the frequency of a trait at population level, when comparing multiple transmission models different initial dynamics can cause the same result at the population level [28]. Using a simulation model they conclude it is possible to distinguish the individual-level processes that could potentially have produced the observed data and to exclude those that most likely did not.

Markov models are used to simplify the evolutionary process as they can be used to represent the frequency of a trait in a given generation of the population solely as a function of the previous generation, in a memoryless system, analysing the change of the frequency of that trait in discrete time steps over generations [29] [30]. This is useful for simplifying and analysing the evolutionary process and focusing on change and evolution between generations.

Transition matrices are often used to represent these Markov chains, representing the probability a given trait is adopted in a stochastic matrix [31] in a way that represents the “attraction” of that trait. In this way the change in the frequency of a trait can be explored over generations, with the “attraction” of a particular trait incorporating underlying biases affecting these frequencies [20].

### Experiments analysing the transmission of knots

The transmission of information is often analysed using transmission chain experiments [32]. These experiments simulate the evolutionary process through the passage of information between participants. The information can be transmitted in multiple ways in order to analyse the difference between methods of cultural transmission or various forms of the information can be compared using synchronised chains.

Knot tying has been studied through the use of transmission chain experiments. Muthukrishna et al. [33] explore the effect of group size on the maintenance of knot complexity by using a transmission chain with the task of replicating knots from instructional videos created by previous participants in the chain. Two chains were compared, one in which each participant could only learn from one instructional video created by a previous participant and the other in which they could use five instructional videos created by previous participants. The knots in each chain declined in accuracy but the knots in the chain with one demonstration declined more rapidly than those in the chain with more demonstrators. The summary was that a larger group size is more likely to maintain cultural complexity. This finding gives an insight into knot tying and suggests that in order to have more complex knots they need to be used by a large group size.

Along with group size, the process of transmission in knot tying has been explored through transmission chain experiments. Caldwell et al. [34] explore the affect of teaching on knot tying. They had three groups each with a different method of transmission and explored the affect of the different transmission processes on a range of knots of varying complexity. The first group named “End State Only” had just a tied version and an image of the tied knot, the second named “Intermediate States” had the tied version, an image of the tied knot and images of stages in the knot tying process and the third named “Teaching” had the tied knot, the image and the intermediate states, along with a demonstration from an “expert” with the “expert” giving instruction and feedback. Participants were asked to tie one knot each using the resources provided given which group they were in. The knots were rated for complexity given the number of steps in their instruction on

www.animatedknots.com [13]. It was found that the “Teaching” condition facilitated the correct replication of all knots over the other two conditions and the more complex knots were tied correctly more often in that condition. This suggests that more complex knots may be more difficult to learn correctly through social learning and require full demonstrations and instructions to ensure complexity is maintained. This suggests if complex knots are used they are optimised for the purpose as when they are taught and learned demonstrators must ensure complexity is maintained. However the classification for complexity used in this study was just based on the number of steps in their instruction on www.animatedknots.com, not determined by any properties of the knot so may not be truly representative.

These studies show the importance of the learning process in knot tying but do not include any definitive measure as to whether knots are tied correctly or their complexity. A mathematical analysis of knots is needed to quantify these measures.

## 1.3 Introduction to knot theory

### 1.3.1 History

Most modern stories about Knot Theory start with the tale of Lord Kelvin’s belief that atoms were knots of vortices in the ether [35] and so by classifying all knots you could classify all chemical elements. However properties and relations of knots were studied earlier than this with the study of linking integrals by Gauss in 1833. Research into knots was continued by his student Listing who depicted the difference between projections of the left and right handed trefoil knot and the equivalence of both handed versions of the figure-eight knot, leading the figure-eight knot to be sometimes called Listing’s knot [36].

Knot tables enumerate all distinct knots up to a certain amount of crossings. The first knot tables were given by Peter Guthrie Tait [37] and listed all knots of up to ten crossings. There are now various knot tables online such as Knot Atlas [38] and KnotInfo [39], giving various projections of knots and links and their properties. In 1998 Hoste et al. tabulated all knots up to 16 crossings resulting in over 1.7 million distinct knots [40] with these appearing in the database Knotscape [41].



### 1.3.2 Definitions and examples

**Definition 1.3.1** A knot is a simple closed curve embedded in three-dimensional space  $\mathbb{R}^3$ .

Intuitively, we can think of a knot as a piece of string, passed over and under itself in some way, then the ends glued together forming a closed loop.

**Definition 1.3.2** The unknot is a knot with no crossings, and is represented by a closed loop.

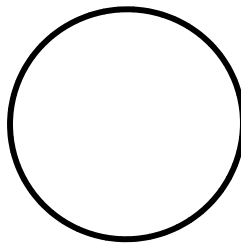


Figure 1.1: A projection of the unknot on  $\mathbb{R}^2$

**Definition 1.3.3** A link is a knot formed of more than one closed loop.

Again, we can think of a link as two or more pieces of string, passed over and under each other in some way, then the ends glued together, creating several linked closed loops.

As knots and links are 3-dimensional objects it is often useful to represent these knots by a 2-dimensional projection. However there are various ways to take a 2-dimensional projection of a 3-dimensional object and so some way to decide whether two projections represent the same knot is required.

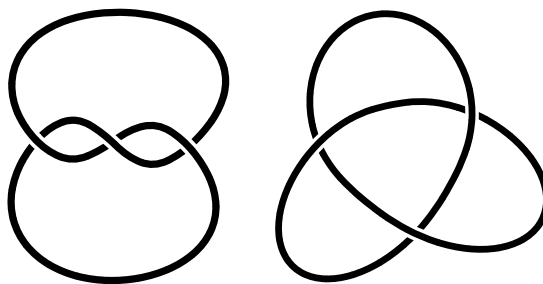


Figure 1.2: Two projections of the trefoil knot on  $\mathbb{R}^2$

The Reidemeister moves [42] are a method used to determine whether two projections represent the same knot or link. There are three Reidemeister moves given as follows:

R1 move - A twisted loop can be undone or added to a strand.

R2 move - A strand can be tucked under or pulled out from under another strand.

R3 move - A strand can be pulled under or over a crossing to lie on the other side of it.

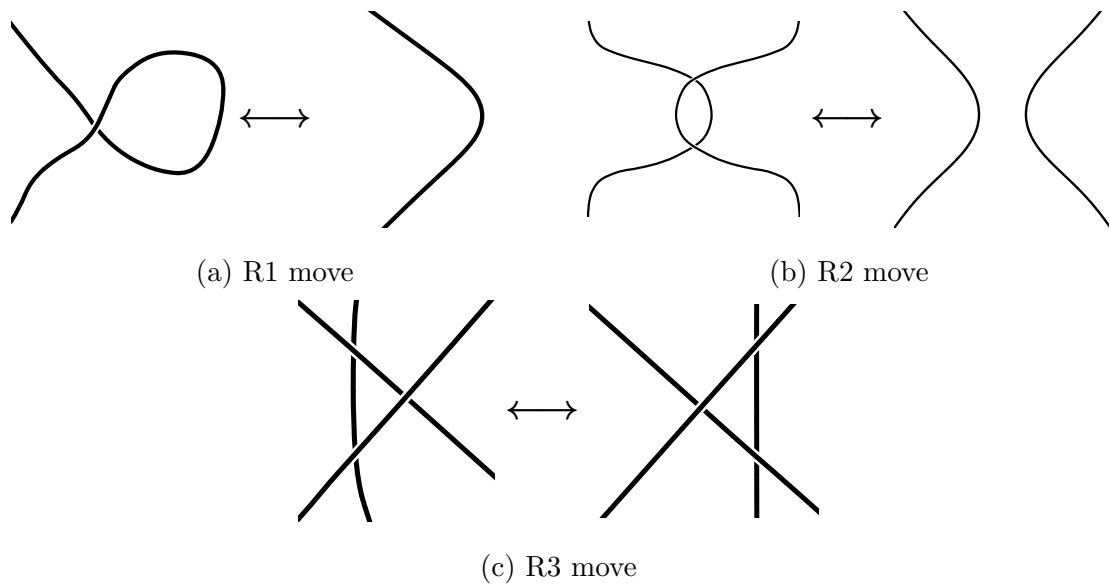


Figure 1.3: The Reidemeister moves; 1.3a shows the R1 move, the equivalence between a twisted loop and a strand, 1.3b shows the R2 move, the equivalence between a two separate strands and one strand tucked under another and 1.3c shows the R3 move, the equivalence of a strand on either side of a crossing.

**Definition 1.3.4** Two projections represent the same knot or link if one can be deformed into the other through a sequence of Reidemeister moves.

If we can find a sequence of Reidemeister moves connecting two projections then they represent the same knot or link.

However this sequence can be very difficult to find. In some cases it might be difficult to determine whether a sequence exists at all or is simply difficult to find. It is simpler to use knot or link invariants. These are properties attributed to a knot or link that can be calculated from a projection that will return the same

result if the projections represent the same knot or link, as they are invariant under Reidemeister moves.

If two projections of a knot or link give a different invariant result then they definitely represent different knots or links. However returning the same result does not necessarily mean the projections represent the same knot or link so sometimes a variety of methods is used for confirmation. One such invariant is the Jones polynomial.

**Definition 1.3.5** The Jones polynomial is denoted  $V_K(t)$  for knots and  $V_L(t)$  for links. Each knot and link is assigned a polynomial in the variable  $t^{1/2}$  by analysing the crossings in the knot or link. [43]

Polynomials of the unknot, and the left and right handed trefoils are given below;

$$V_{\text{unknot}} = 1 \quad (1.3.1)$$

$$V_{\text{right trefoil}} = t + t^3 - t^4 \quad (1.3.2)$$

$$V_{\text{left trefoil}} = t^{-1} + t^{-3} - t^{-4} \quad (1.3.3)$$

We see that the Jones polynomial of the right trefoil is the same as the left handed version, but the powers of  $t$  on each have opposite sign, demonstrating that they are mirror images of one another.

The HOMFLY-PT polynomial is calculated in a similar manner to the Jones polynomial and is often called the generalised Jones polynomial but is a polynomial in two variables,  $m$  and  $l$ . The HOMFLY-PT is denoted  $P(K)$  for knots and  $P(L)$  for links and again we have  $P(\text{unknot}) = 1$  for the unknot. [44]

Knot and link compositions can be formed by taking connected sums of knots or links. This is formed by taking a knot or link and joining them together, by almost fusing the strands from one to the other. In a practical way, a composition of two knots can be formed by tying one in a piece of string, then tying another in the same string afterwards, with no crossings from the second looping back through the first.

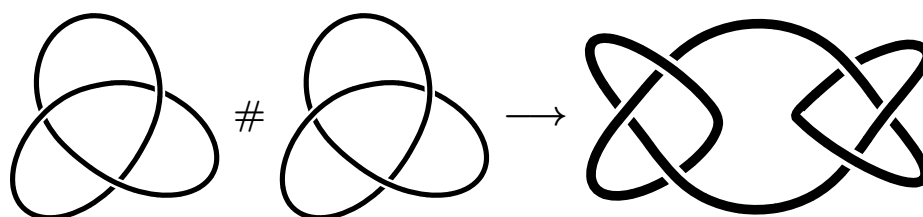


Figure 1.4: The trefoil is a prime knot but two can be joined together to form a composite knot of two trefoils. This can be thought of tying one trefoil after another in the same piece of string.

**Definition 1.3.6** A knot is called prime if in its decomposition as a connected sum, one of the factors is the unknot. A knot is called composite if it is not prime. The unknot is a prime knot.

**Definition 1.3.7** The Dowker-Thistlethwaite (DT) code for a knot is a sequence of even integers that represent the crossings in a knot or link. It is calculated by picking a starting point on the knot and walking along it, numbering each crossing in turn, until each crossing is labelled twice. If an even number is on an under crossing it is given a minus sign, whereas if it is on an over crossing, it is positive. [45]

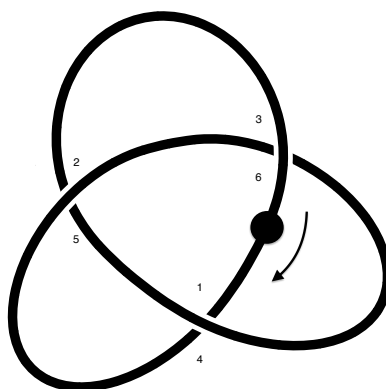


Figure 1.5: The trefoil has DT code 4 6 2. Starting at the black dot and passing through each crossing in turn we get pairs of crossings (1,4), (3,6), (5,2). The DT code is given by just stating the even numbers in the order of the odd numbers paired with them.

All knots and links can be represented as the closure of a braid. A braid is a collection of strands, which can be thought of as strings, arranged vertically with the ends fixed at the top and bottom. Crossings can only occur between neighbouring strands and occur vertically. A braid word is formed using symbols that represent each crossing in the braid.



(a) A left over right crossing between the first and second strand is denoted  $\sigma_1$ . (b) A right over left crossing between the first and second strand is denoted  $\sigma_1^{-1}$ .



(c) A left over right crossing between the  $i$ -th and  $j$ -th strand is denoted  $\sigma_i$ .

Figure 1.6: The crossings in a braid are represented by symbols  $\sigma_i$  and  $\sigma_i^{-1}$  where  $\sigma_i$  denotes a crossing with the  $i$ -th strand crossing over the  $j$ -th strand in the braid and  $\sigma_i^{-1}$  denoting the  $j$ -th strand crossing the  $i$ -th. The symbols representing each crossing are read off top to bottom to result in a word representing that braid.

The closure of a braid is formed by taking a braid and joining each bottom strand to its corresponding strand at the top. These closures give a knot or a link. In this way each knot or link has a minimal braid representation, that is a braid with the fewest crossings on fewest strands giving that knot or link.

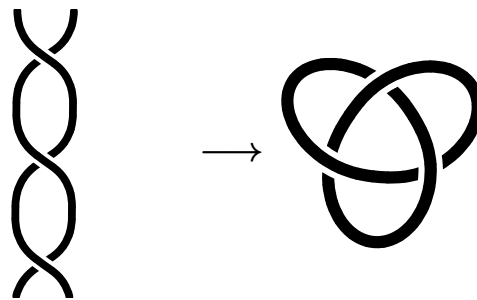


Figure 1.7: A braid representation of the trefoil knot is given by three left over right crossings between strands one and two. This results in a braid word  $\sigma_1\sigma_1\sigma_1$ . When the strands are joined top to bottom the resulting knot is the trefoil knot.

The properties of knots and links discussed above will be used in order to analyse the knots tied in material culture.

## 1.4 Project outline

### 1.4.1 Questions

In this thesis we use a combination of knot theory and cultural evolutionary theory to explore the following questions;

- How many possible knots are utilised in material culture and why not more or fewer?
- Are the knots needlessly complicated or optimised for their purpose?
- What are the common features in knot design and how are they preserved?
- What features affect the fidelity of knot transmission?

In order to explore the possible knots utilised in material culture and their common features, the knots appearing in the Ashley Book of Knots have been classified mathematically to identify how many distinct mathematical knots are used and what features they have in common. This method and analysis is discussed in Chapter 2. The work presented in Chapter 2 includes work presented in the published form from a paper for which I am the sole author [46].

To explore the transmission and complexity of these knots an experiment and model investigating the transmission of some of the simplest knots, granny and reef knots, was used. This method and analysis is discussed in Chapter 3.

To further explore the features in knot design, their preservation and an explanation to the possible knots and complexity of those used in material culture, a model exploring the transmission applicable to all knots and links was created. This model and analysis is explored in Chapter 4.

A further analysis exploring the features in knot design is discussed in Chapter 5, using  $NK$  fitness landscapes to assess the common features in knots and links exploring the optimisation of knots for their purpose.

# Chapter 2

## A study of knots in material culture

This chapter includes work presented in the published form from reference [46].

### 2.1 Introduction

Knots are an important part of our everyday life. From our shoelaces to securing loads, knots are an essential tool for many of us. They are used the world over, in almost every society. The Human Relations Area Files ethnographic database [14] contains 1,900 references to knotting across 228 different cultures. It is not just humans who use knots, knots have been found elsewhere in the animal kingdom. Certain gorillas tie knots in their nests, tying granny knots out of saplings and creepers as well as the slightly more complex reef knot [17]. The Ploceidae or Weaver Bird builds its nest out of knots, weaving an intricate pattern to attract a mate [15]. Knots are part of both human and animal life, woven into important rituals and everyday practices.

Knots are an important part of human's material culture and part of human history and development. But, given knots are something we use daily, have we ever stopped to wonder why we use the particular knot we do for a given purpose? For example, many of us regularly tie our shoelaces, going through the motions and not really thinking about the knot we are tying. Why do we tie our shoelaces in



this way? Is it the optimal knot for the purpose or do we just blindly follow the algorithm we are taught as children?

Many people have a keen interest in knot tying, for example sailors and climbers, but other professionals need to know and use knots regularly too. An attempt has been made by Ashley among others to collect and create an encyclopaedia of knots and their uses [8], focusing on those in modern Western cultures. From the Ashley Book of Knots (ABOK) we can gain insight into the range of knots used and discover some of the history behind how and why these knots are tied. Ashley's book contains over 3,800 knots and while he goes to a great length to provide as much information as he can for each knot, some knots are repeated and some knots do not have a lot of information given. However, from Ashley's work we can put together a picture of the landscape of knots used, for a range of applications, and get an idea of which knots are best suited for these applications.

Pairing Ashley's work with other studies may provide us with more information about knot usage. Studies into knot strength and suitability have been carried out in studies comparing different types of rope and different knots tied, a factor extremely important to those who use knots for purposes such as climbing. It is known that when a knot is tied in a piece of rope it weakens the rope so it is important to choose the knot and rope carefully.

Pieranski et al. [47] studied the strength of knots by finding the breaking point of knots when under strain. In order to pinpoint easily the location of the breaking point cooked spaghetti was knotted and then put under strain by being pulled gently by hand. These tests were recorded by a digital camera with high recording speed so the video could be viewed later and the knot breakage determined. The knots in this experiment were denoted by their notation in the Rolfsen Knot Table [48]. In Pieranski et al.'s study it was found that the weakest knot of all was the overhand knot (knot  $3_1$ ). It was also noted that knot strength increased as the crossing number of the knot increased, which is what we may expect. The exceptions to this rule were the knot  $7_1$ , which was worse than all knots of six crossings, and the figure-eight knot, (knot  $4_1$ ) which was stronger than all knots of five and six crossings, and knot  $7_1$ . It was found that the knot breakage did not occur in the internal region

of the knot, breakage was close to the entry to the knot. These studies give us an idea of the suitability of knots for certain purposes and leads us to question why the overhand knot ( $3_1$ ) is so widely used for a range of purposes when it is shown to be the weakest knot of all.

In addition to the strength of climbing knots, the vast range of possibilities of neck tie knots has been studied. Fink and Mao [49] attempt to predict all aesthetic neck tie knots by modelling their construction through random walks. They define a neck tie knot by a sequence of moves describing the wrapping of the neck tie by the orientation and location of the tucks used to tie it. These moves can be represented as walks on a triangular lattice and so the space of possible neck tie knots can be determined. Fink and Mao demonstrate that there are 85 possible sequences and so 85 possible distinct ways to tie a neck tie. It is interesting to note that whilst there are 85 possibilities, only four of these are commonly used as ways to tie a neck tie. Whilst Fink and Mao only considered neck ties tied with the wide end of the neck tie, Hirsch et al. [50] extended the neck tie knot possibilities by including those tied with the thin end. This takes the number of possible neck ties, with up to 13 moves, up to a staggering 177,146. One thing is clear from these studies, the number of possible neck tie knots is huge, but only a fraction are observed in real life, leading us to question the reasons behind this.

The range of evidence in ABOK and that gathered through studies suggests there is a huge range of diversity in knots, but these studies do not suggest why. An answer to this may lie in the way we learn.

Transmission chain experiments are often used to explore the effect of teaching techniques on a sample of the population. The behaviour which is observed in these experiments may be indicative of the population as a whole. Linear transmission chains operate through a “grapevine” method. Information is passed through a chain of participants in which each participant learns the information, attempts to recall it, and then passes it to the next participant in the chain. The changes that occur in the chain can be measured and give an indicator of the degradation of information in the wider population [32]. Different samples can be manipulated to more accurately model the population or hypothesis which is being tested. Thin

chains, in which information is passed from one person to one other, can be used to simulate one-to-one learning, for example via a teacher or a parent. In these chains the teaching method can be varied to study the effects of different forms of instruction. Fat chains, in which individuals learn in a group and are replaced by others over time, can be used to simulate group learning and are useful to see the effects of behaviours such as conformity. Multiple chains can be run at the same time with different instructions to study the effect of instruction or members of chains can be replaced to model the introduction of new members to a population. These chains are useful for studying how information is passed within a population, but they may also help understand why information is transmitted, by enabling us to analyse the effects of conformity or expert knowledge on the transmission of information.

Knot tying has been used as a tool by Muthukrishna et al. in experiments to test the effect of multiple models on learning [33]. As knot tying only requires a piece of rope it makes an accessible tool with which to experiment. In this study the group of participants were asked to tie a series of knots commonly used by rock climbers. The study ran through two chains, each with ten generations. In both chains participants would learn how to tie the knots from the generation before them. In the first chain participants were only allowed to learn from one model in the generation before them. In the second, participants could learn from five models in the generation before. The first generation in both chains were trained by the experimenter to become “experts” at tying the knots. Other generations created an instructional video for the tying of the system of knots by a camera strapped to their head. The next generation would then be given this video along with a score which measured how well the participant tied the knot series. This score was measured on a scale used when assessing sutures when training surgeons and was judged by human raters [51]. The results showed that knot tying skills declined throughout all generations but declined more slowly in those in the five-model chain than the one-model. One of the issues with the experiment was that the participants in the five-model chain did not have time to view all of the instructional videos presented to them. Another issue was the way the knots were judged. The knots were given

a score based on a set of requirements observed by a rater, but the knots were not studied to determine whether they were mathematically the same. However, the way this study was set up gives us a good idea of a way in which to approach knot transmission chain experiments and that the sample size of demonstrators may affect the fidelity of transmission.

In order to explore the difference between individual and social learning, Derex et al. [52] ran a virtual experiment concerning net building and fishing. Participants were required to construct a net on a square grid using a limited amount of rope of various thicknesses and knots of various sizes. Nets were tested and given a score based on how many fish the simulated net caught. During each of the fifteen trials, participants could view their previous net and score. The participants were placed into different groups under three different treatments, participants were unaware of who was in their group and which treatment they were in. In the individual learning treatment, participants could see the last trial and cumulative score of the rest of their group members. In the product copying treatment, participants could see the different scores of each of their group members and the corresponding nets. In the process copying treatment, participants could see the different scores of each of their group members, the corresponding nets and the step-by-step information for building that net. Participants had 30 seconds in the individual learning treatment to view the information and 90 seconds for the other two treatments. The nets were scanned pixel by pixel for similarity and scored. The process similarity was judged by viewing the net building actions as characters in a string and so the similarity of the string was measured. Scores for net building improved throughout all treatments and younger participants generally performed better than other participants. The difference between performance in the individual and product learning treatments was not significant but the process copying treatment demonstrated a significant advantage. The importance of social learning of the knotting process is indicated by this virtual net building task, however the results could have been skewed by the fact that the task was virtual and the observation that the age of participants made a difference on performance. We may expect social learning mechanisms to be also important for knot learning as nets are made up of a system of knots.

Pairing knot studies with an assessment of the knot learning environment, we attempt to answer our research questions using the methods described in the next section.

## 2.2 Mathematical analysis of ABOK

The Ashley Book of Knots (ABOK) is regarded as the authority on knotting. As it contains over 3,800 knots we may wonder exactly how many different knots appear. This book seems the natural place to start to search for answers to our questions; why are there so many knots in material culture, what are the common features in knot design and how many of the possible knots are utilised?

I have created a database of the knots found in the Ashley Book of Knots [8]. The layout of the ABOK database and explanation of the fields is given below.

Layout of the Ashley Book of Knots (ABOK) database	
ABOK No.	The knot number it first appears as in Ashley
Also appears as	Any other numbers the knot appears as in Ashley
Knot Name	Name as given in Ashley
Crossing number ABOK picture	Crossing number as given by picture in Ashley
Handedness	Whether the knot diagram has positive or negative writhe for chiral knots, otherwise noted as amphichiral
Knot	Common name used by mathematicians (if there is one)
Prime	Whether the knot is prime or composite
Knotplot input	Knotplot input if known (based on Conway notation)
Knot Atlas notation	Knot Atlas notation if known (for larger knots Knotscape notation is used)
Crossing number	Reduced diagram crossing number
Link	Whether or not knot is a link of two or more components
Number of components	If link how many components it is made of
Linking no	Linking number if knot is a link of two or more components
Notes	Any notes relating to considering knot as joined ends
Related knots	Any related knots mentioned by Ashley
Uses	Uses given by Ashley
Use comments	Any comments on usage
ABOK classification	Ashley's classification, Important, Strong, Practical etc.
Alternative names	Any alternative names given by Ashley
ABOK Image	Original image from Ashley
KnotPlot Video	Video showing deformation from Ashley's knot to a known mathematical knot

Table 2.1: Layout of the ABOK database used to analyse material knots

To identify the knots in ABOK, I take Ashley's image of a knot and join the free ends in such a way as to create no new crossings. If there is no such way to join the ends without creating new crossings, I join the ends by creating the minimal amount of new crossings. This may result in choices of whether to create an over or under crossing and so, I consider all cases.

For knots tied in more than one piece of string, or around an object, the knot (and object) is considered as a link, with the free ends joined in the way best suited to the function of the knot. If no way is immediately obvious, all ways to join the ends are considered.

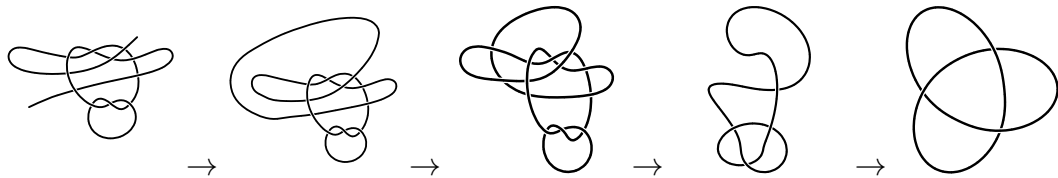


Figure 2.1: This figure shows the Bowknot (ABOK number 1212) with its ends closed, then reduced to the trefoil ( $3_1$ ).

If the knot is prime with 16 crossings or less or a link with 12 or less crossings, I identify it with its knot name as found on KnotAtlas [38] or Knotscape [41] if the knot is larger. The knots are distinguished using their Dowker-Thistlethwaite notation [45] and their HOMFLY-PT polynomials [44] [53], using the identification tools on KnotInfo [39], LinkInfo [54] and Knotscape. I also create a video using the program KnotPlot [55] showing this reduction, as shown in Figure 2.1.

For some knots, joining the ends in any one way is not appropriate or too many cases need to be considered. Knots like these have been excluded from analysis for now.

## 2.3 Results

### 2.3.1 Overall trends

In the ABOK database I have listed the material knots found in ABOK, then given the mathematical name of the knot they relate too. First, let us look at the number of times each mathematical knot appears as a distinct knot in ABOK.



## Prime knots

Prime knots found in ABOK						
Crossing number	Knot	Occurrences		Crossing number	Knot	Occurrences
3	3 <sub>1</sub>	45		10	10 <sub>121</sub>	1
4	4 <sub>1</sub>	14			10 <sub>124</sub>	1
5	5 <sub>1</sub>	12			10 <sub>139</sub>	2
	5 <sub>2</sub>	14			10 <sub>140</sub>	1
6	6 <sub>1</sub>	6			10 <sub>157</sub>	1
	6 <sub>2</sub>	5		11	11a351	2
	6 <sub>3</sub>	6			11a362	1
7	7 <sub>1</sub>	3			11a367	1
	7 <sub>2</sub>	4			11n19	1
	7 <sub>3</sub>	1			11n38	1
	7 <sub>4</sub>	3			11n98	1
	7 <sub>5</sub>	1			11n138	1
	7 <sub>6</sub>	1			11n141	1
	7 <sub>7</sub>	3			11n145	1
8	8 <sub>1</sub>	1		12	12n488	1
	8 <sub>3</sub>	1			12n647	1
	8 <sub>5</sub>	1			12n764	1
	8 <sub>12</sub>	1		13	13a3097	1
	8 <sub>13</sub>	1			13a3861	1
	8 <sub>16</sub>	1			13n4694	1
	8 <sub>18</sub>	2			13n4003	1
	8 <sub>19</sub>	4			13n4639	1
	8 <sub>20</sub>	3		14	14n21324	1
	8 <sub>21</sub>	4			14n27326	1
9	9 <sub>1</sub>	1		15	15a69858	1
	9 <sub>30</sub>	1			15a84903	1
	9 <sub>35</sub>	1			15n103184	1
	9 <sub>40</sub>	2			15n125031	1
	9 <sub>41</sub>	2			15n133979	1
	9 <sub>44</sub>	3			15n135983	1
	9 <sub>47</sub>	1			15n41185	1
	9 <sub>48</sub>	1			15n52069	1
10	10 <sub>1</sub>	2		16	16a357530	1
	10 <sub>109</sub>	1			16n259418	1
	10 <sub>120</sub>	1			Total	189

Table 2.2: Frequencies of all the identifiable prime knots in ABOK

Let us look first to the number of prime knots found in the database. Table 2.2 shows a table showing the amount of times each prime knot appears in ABOK of up to 16 crossings.

Unsurprisingly, we see the trefoil (knot  $3_1$ ) is the most common knot occurring in ABOK. This may be expected, given it is the simplest non-trivial prime knot. Overall we see the trend that as crossings increase, occurrence decreases. If we equate complexity with higher crossing numbers, this gives the conclusion that as complexity increases, popularity of usage decreases.

Perhaps the most interesting thing to note is the crossing numbers that do not fit this decreasing pattern. We see there are relatively high occurrences of knots of five and eight crossings. Comparative to the one knot of four crossings (the figure-eight knot), both knots of five crossings occur frequently. As the figure-eight knot is of relatively low crossing number it does not occur as often as we may expect.

Another thing to note is that all knots of under eight crossings appear at least once, we start to see gaps when we look to knots of eight crossings or more. Is this purely because there are so many knots of eight or more crossings that it would be unnecessary to tie them all, or something more? We also look to common families of knots, for example the -foil series (trefoil ( $3_1$ ), cinquefoil ( $5_1$ ), septafoil ( $7_1$ ), etc) we have all knots in this sequence up to knot  $11a367$ . Why do further knots in this sequence not appear, given they can be formed from the former by adding only one twist?

The unknot has been excluded from this table although it occurs in ABOK often in the guise of a slipknot. These knots do not function as the unknot so an alternative way to analyse these knots may be needed.

### Prime links

In a similar way to prime knots, we give a table of prime links in Table 2.3. Again this table shows the occurrence of each individual link of up to 11 crossings. The unlink is omitted for the same reasons as the unknot previously.

It is unsurprising to see the prevalence of the Hopf Link, being the simplest non-trivial link. We start to see more links with lower crossing numbers missing than

Prime links found in ABOK						
Crossing number	Link	Occurrences		Crossing number	Link	Occurrences
2	<i>L2a1</i>	48		8	<i>L8n2</i>	1
4	<i>L4a1</i>	14			<i>L9a37</i>	1
5	<i>L5a1</i>	8			<i>L9a40</i>	1
	<i>L6a1</i>	3		9	<i>L9n10</i>	2
	<i>L6a2</i>	2			<i>L9n11</i>	4
6	<i>L6a3</i>	6			<i>L9n13</i>	1
	<i>L6a4</i>	1			<i>L9n17</i>	1
	<i>L6n1</i>	1			<i>L9n9</i>	2
	<i>L7a1</i>	5			<i>L10a48</i>	1
	<i>L7a2</i>	1			<i>L10a89</i>	1
7	<i>L7a3</i>	1			<i>L10a98</i>	1
	<i>L7a5</i>	2		10	<i>L10n30</i>	1
	<i>L7a6</i>	1			<i>L10n32</i>	1
	<i>L7a7</i>	1			<i>L10n44</i>	1
	<i>L7n1</i>	1			<i>L10n50</i>	1
	<i>L8a11</i>	1			<i>L10n53</i>	1
	<i>L8a13</i>	2			<i>L10n63</i>	1
8	<i>L8a6</i>	1		11	<i>L11n195</i>	2
	<i>L8a8</i>	4			<i>L11n252</i>	1
	<i>L8a9</i>	2			Total	130

Table 2.3: Frequencies of all the identifiable prime links in ABOK

for the prime knots, with two links of under eight crossings not appearing,  $L6a5$  and  $L7n2$ . We see a high amount of links with seven and nine crossings appearing, relative to those of four and five crossings. Is this solely because there is a much wider range of higher crossing links to choose from?

### Composite knots and links

Composite knots and links found in ABOK						
No. factors	Knot	Occurrences		No. factors	Knot	Occurrences
2	$3_1\#3_1$	12		2	$L5a1\#8_{20}$	1
	$3_1\#4_1$	1			$L5a1\#L7n2$	1
	$3_1\#5_1$	8		3	$3_1\#3_1\#3_1$	6
	$3_1\#5_2$	3			$3_1\#3_1\#5_2$	1
	$3_1\#7_3$	1			$3_1\#3_1\#7_3$	1
	$3_1\#7_7$	1			$3_1\#3_1\#L4a1$	1
	$3_1\#8_{20}$	1			$3_1\#3_1\#L6a3$	2
	$3_1\#9_{14}$	1			$3_1\#3_1\#L4a1$	1
	$3_1\#L2a1$	4			$3_1\#3_1\#L5a1$	2
	$3_1\#L4a1$	1			$3_1\#3_1\#L6a4$	1
	$4_1\#4_1$	1			$3_1\#4_1\#L2a1$	1
	$4_1\#L2a1$	4			$3_1\#5_1\#L2a1$	1
	$5_1\#L2a1$	1			$3_1\#5_2\#L2a1$	1
	$5_2\#L2a1$	2			$3_1\#L2a1\#3_1$	1
	$6_1\#6_1$	2			$3_1\#L9n19\#3_1$	1
	$6_1\#L2a1$	1			$4_1\#4_1\#4_1$	1
	$6_3\#L8n6$	1			$6_3\#L2a1\#6_3$	1
	$6_3\#L9n12$	1		4	$3_1\#3_1\#3_1\#3_1$	1
	$L2a1\#L2a1$	1			$3_1\#3_1\#L2a1\#6_3$	1
	$L2a1\#L4a1$	1			$3_1\#L2a1\#3_1\#L5a1$	1
	$L2a1\#12n437$	1		6	$3_1\#3_1\#3_1\#3_1\#3_1\#3_1$	1
	$L4a1\#L6a1$	1			Total	78

Table 2.4: Frequencies of all the identifiable composite knots and links in ABOK

Table 2.4 shows the number of composite knots formed of individual prime knots and links. Unsurprisingly the most common prime knot appearing in a composition is the trefoil ( $3_1$ ). Composite knots range from those formed of only two prime knots up to those formed of six prime knots. The prime knots and links appearing in most compositions are of relatively low crossing number, giving a composition with higher crossing number.

### 2.3.2 Distribution of knots (to be used in Chapters 4 and 5)

In Chapter 4 the distribution of knots and links from ABOK up to 8 crossings will be used for model analysis, as these form the knots and links appearing most commonly. The frequency of knots that will be used is as follows;

Distribution of knots and links found in ABOK						
Crossing number	Knot/Link	Occurrences		Crossing number	Knot/Link	Occurrences
0	$0_1$	111		7	$L7a6$	1
	$unlink$	20			$L7a7$	1
2	$L2a1$	48			$L7n1$	1
	$L2a1\#unlink$	1			$3_1\#4_1$	1
3	$3_1$	45			$3_1\#L4a1$	1
4	$4_1$	14			$5_1\#L2a1$	1
	$L4a1$	14			$5_2\#L2a1$	2
	$L2a1\#L2a1$	1		8	$8_1$	1
5	$5_1$	12			$8_3$	1
	$5_2$	14			$8_5$	1
	$L5a1$	8			$8_{12}$	1
	$3_1\#L2a1$	4			$8_{13}$	1
6	$6_1$	6			$8_{16}$	1
	$6_2$	5			$8_{18}$	2
	$6_3$	6			$8_{19}$	4
	$L6a1$	3			$8_{20}$	3
	$L6a2$	2			$8_{21}$	4
	$L6a3$	6			$L8a6$	1
	$L6a4$	1			$L8a8$	4
	$L6n1$	1			$L8a9$	2
	$3_1\#3_1$	12			$L8a11$	1
	$4_1\#L2a1$	4			$L8a13$	2
	$L2a1\#L4a1$	1			$L8n2$	1
7	$7_1$	3			$3_1\#5_1$	8
	$7_2$	4			$3_1\#5_2$	3
	$7_3$	1			$4_1\#4_1$	1
	$7_4$	3			$6_1\#L2a1$	1
	$7_5$	1			Total	415
	$7_6$	1				
	$7_7$	3				
	$L7a1$	5				
	$L7a2$	1				
	$L7a3$	1				
	$L7a5$	2				

Table 2.5: Distribution of knots and links up to eight crossings in ABOK

### Handedness and chirality

Chirality of all prime knots seen of eight crossings or fewer has been included in the ABOK database. For knots which are chiral, the handedness of the knot has been included. Of all 137 prime knots of eight crossings or fewer, 24 were amphichiral and 113 chiral knots. Of the 113 chiral knots, the diagram given by Ashley was found to have positive writhe for 47 knots and negative for 66 knots.

This does not necessarily mean that whenever a specific knot is tied, the right or left handed version is always used, it could just mean that when Ashley has drawn that specific knot he happens to have favoured the right or left handed version. Looking specifically at the trefoil ( $3_1$ ), the trefoil appears as the right handed version 22 times and the left handed 23 times, suggesting no real preference for either.

#### 2.3.3 Knots omitted

A few types of knots were omitted from the ABOK analysis and mentioned in Chapter 2. These knots are shown below with a reason for their omission. These knots can represent whole chapters in ABOK.

#### Splices

Splices were not included in the ABOK analysis. Splicing is a method used to join two ropes together by interweaving the strands and is intended to be a permanent join of the two ropes. As the strands are not interwoven together in the manner of a traditional mathematical knot and it is difficult to determine the rope ends and the manner with which to join these to form a closed curve these have been excluded from the analysis.

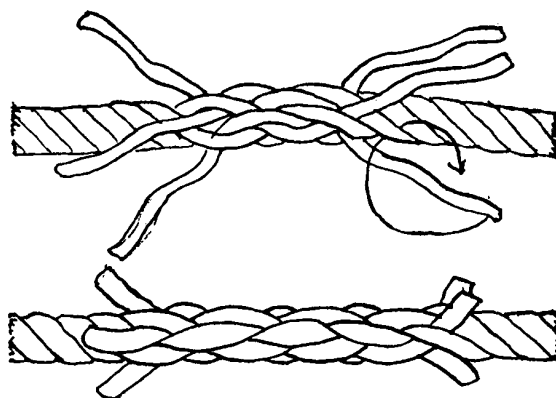


Figure 2.2: The Sailor's Short Splice ABOK #2634 is used to join two ropes by interweaving the strands by sailors and is found in running rigging, cargo and deck gear and in ground tackle [8]. The ends are not easy to identify and the method of tying does not lead it to be easily classified mathematically.

### Single strand knots

Single strand knots have been excluded from the analysis for similar reasons to the splices. The single strand knots are made by fraying a rope and tying the individual sections to form a knot then weaving the frayed ends together to reform the rope. They are used decoratively and to give holds in the rope for climbing or other purposes. Again the ends are not easy to identify and the knot is formed of just one piece of rope split making it difficult to classify mathematically and hence they have been excluded.



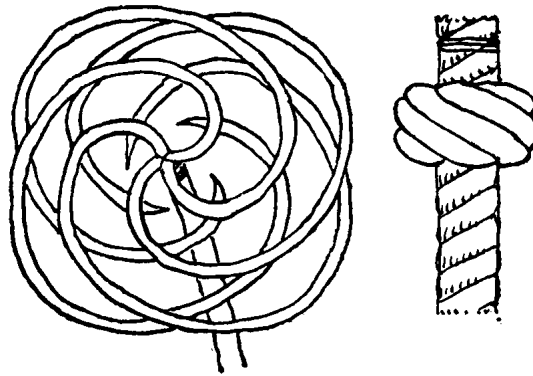


Figure 2.3: The Double Matthew Walker Knot ABOK #691 is a Multi-Strand Stopper Knot used as a terminal knot in a rope usually to prevent unreeving [8]. It is an example of a knot tied in one strand by fraying the ends leading it to be not easily identified mathematically.

### Loop knots

Many knots in ABOK are tied with a loop and as such represent the unknot mathematically however they do not function as such when used. These knots have been included in the ABOK analysis but are classified as the unknot as that is what they represent with the ends joined. The knot below is easily recognised as the trefoil knot,  $3_1$ , if the knot tied just in the looped rope is considered, but overall is the unknot. Other knots of this form are not so easily recognised. This may lead to some misclassification in the ABOK analysis.

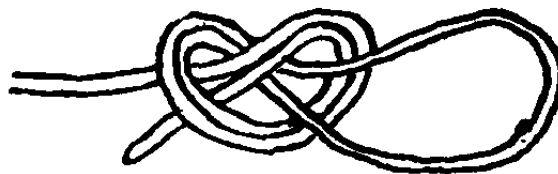


Figure 2.4: The Loop Knot ABOK #290 is a simple, strong and secure Leader Loop used by Fishermen, tied in the leader of a fishing line [8]. It has the form of the unknot but is formed of a trefoil,  $3_1$ , in the looped rope, leading it to be misclassified.

### 2.3.4 Uses of knots

The mathematical knots that appear in ABOK appear in the form of many material knots given by Ashley. In this section we will refer to the crossing number of the knots as they appear in ABOK as the crossing number in the ABOK picture and to the crossing number of the mathematical knot they represent as the reduced crossing number. The difference between the crossing number in the ABOK picture and the reduced crossing number is used to measure the redundancy in the knot, as these crossings will be able to be removed using Reidemeister moves [42].

There are 83 different uses given in ABOK with knots associated with them, with some uses having only one or two knots associated with them and others many more. For example, there are only one or two knots associated with bell ringing or candle making but there are 58 distinct material knots associated with usage by the fisherman. These relate to 30 distinct mathematical knots, making it the usage with the highest amount of distinct material knots associated with it.

We explore relationships in the ABOK data for each range of uses to assess the factors affecting the knots appearing related to each use.

We see there is a linear relationship between the mean crossing number in the ABOK picture for each use with the standard deviation of the crossing number in the ABOK picture. This means that looking at the knots associated to each use, if there is a high mean crossing number then the range of different crossing numbers is likely to be high. This relationship is the same for the final reduced crossing number meaning this link between mean and standard deviation is not affected by redundant features.

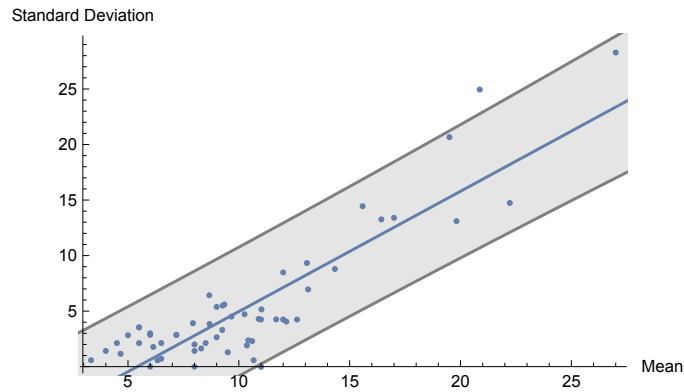


Figure 2.5: ABOK crossing number mean and standard deviation per use. Each point represents the mean and standard deviation of the amount of crossings per knot per use in the Ashley Book of Knots given by the picture representing that knot. There is a linear relationship between these two values as shown by the blue line with the grey line representing the 95% confidence interval. The data shown here is calculated for uses that have more than one knot associated to them.

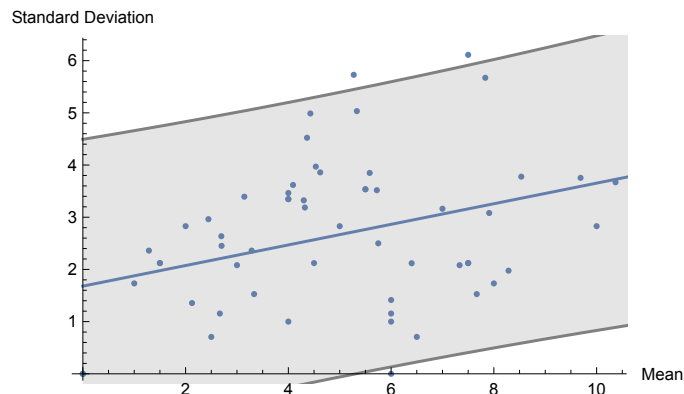


Figure 2.6: Reduced mathematical crossing number mean and standard deviation per use. Each point represents the mean and standard deviation of the reduced amount of crossings per knot per use in the Ashley Book of Knots given by the crossing number of the mathematical knot they relate to. There is a linear relationship between these two values as shown by the blue line with the grey line representing the 95% confidence interval. The data shown here is calculated for uses that have more than one knot associated to them.

However it is not the case that uses that have more knots associated with them than others, have higher mean crossing number or standard deviation as there is

little relationship between these factors. It is also not the case that uses that utilise more distinct knots use knots with higher overall crossing number.

This relationship between the mean crossing number and standard deviation means that uses that utilise knots with higher crossing number are likely to use a wider range of knots than uses utilising lower crossing number knots. This relationship is the same whether we take the crossing number from the ABOK picture or the reduced crossing number of the mathematical knot they represent so this relationship is not affected by redundant features.

This would suggest that utilising a wide range of knots is necessary to use more complex knots, as use of knots with higher crossing number is associated with a wider range of knots being used. This suggests a wide range of knots needs to be used for these purposes with those knots tested and optimised to then necessitate the use of more complex knots. However the usage of more complex higher crossing number knots could also lead to the usage of a wider range of knots with mutation through transmission of these complex knots, whether intentional or accidental, leading to a range of other knots being tied. Mutation on knots of a higher crossing number results in a wider range of knots than mutation on knots of a lower crossing number, due to a greater amount of crossing changes being possible on knots of a higher crossing number.

The link between lower mean crossing number and a reduced range of knots used suggests that when a low crossing knot is suitable for the purpose there is no need to test and utilise a wide range of knots as the current more simple knot is best for the purpose.

### **Redundant features**

We define redundancy to be the difference between the crossing number in the ABOK picture for each knot and the mathematical reduced crossing number which is the minimal crossing number over all diagrams of the knot or link. This measure of redundancy gives the number of crossings that can be removed using Reidemeister moves and may be unnecessary to the knot. However the functionality of these features has not been explored so we cannot conclude all features removable by

Reidemeister moves are functionally redundant, but utilising this definition allows a measurement of potential redundancy.

We look at this redundancy measure across the knots that appear in ABOK and aim to identify factors affecting the scale of redundancy. Using a linear regression we find that there is a strong correlation between redundancy and amount of uses for each knot. That is knots appearing in ABOK with a higher amount of uses have lower redundancy levels and knots with fewer uses have more redundant features.

This could be due to knots being used more and then being optimised for the purpose, reducing the amount of redundant features. This seems to match with the link between high mean crossing number and a wider range of knots used as the wide range of knots used potentially optimises knots for the purpose and increases complexity. However it could also be that knots with fewer redundant crossings are less difficult to tie or demonstrate due to the necessity of most crossings in the knot, causing them to be more useful and used in more cases.

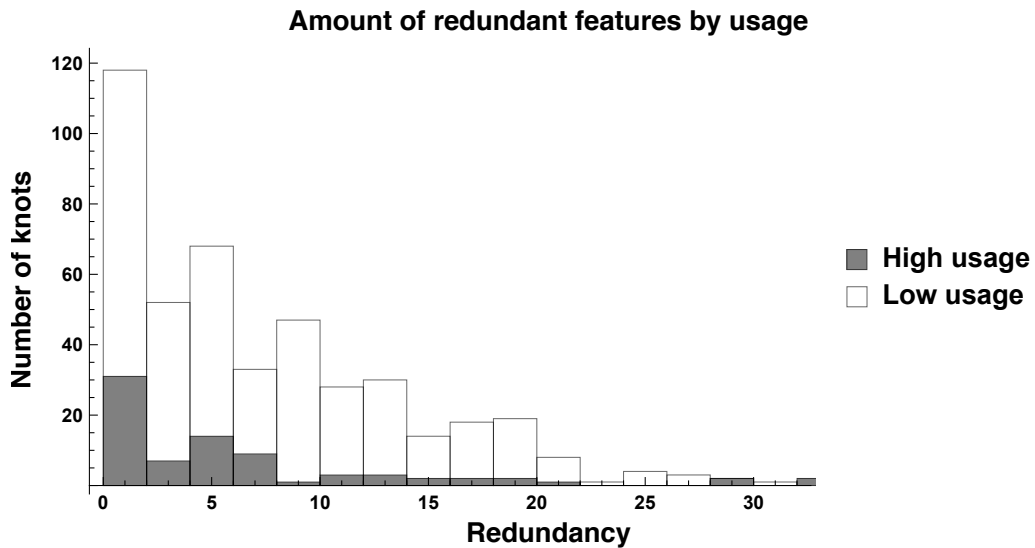


Figure 2.7: The plot shows the difference in the amount of redundant features for knots given in ABOK by their usage. Here high usage is given by knots with more than one use and low usage is given by knots with one or zero uses, with the median number of uses for a knot in ABOK being 1. We see from the plot that knots with higher usage seem to have fewer redundant features than those with only one use.

Figure 2.7 suggests that knots featured in ABOK that have more than one use

have fewer redundant features than those with one or zero uses. In order to check this Table 2.6 gives the mean, median and standard deviation for both groups with the Mann-Whitney U test [56] used to compare the medians for the two groups. The Mann-Whitney U test is the nonparametric equivalent of the Student's t-test [57] and can be used to compare unequal group sizes, as in our case. We see from Table 2.6 that the Mann-Whitney U test gives a result suggesting the medians are significantly different at the 0.0001 level, with the mean and medians from the groups suggesting that knots with higher usage have fewer redundant features but the standard deviation suggesting they have more variation in redundancy than lower usage knots.

	High usage knots	Low usage knots
Amount	81	451
Mean redundancy	6.98765	7.40575
Median redundancy	4	5
Standard deviation redundancy	10.3277	8.53317
Mann-Whitney U test result	0.0000246649	

Table 2.6: Comparison of the redundancy levels of knots that are given to have more than one use in ABOK and those with one or zero uses. We see from the table that knots with higher usage seem to have fewer redundant features than those with only one use.

We also see that prime knots are more likely to have more redundant features whilst composite knots have fewer. This might suggest that knots have attempted to be optimised for the purpose by the addition of crossings. For a prime knot, crossings have been added that may not aid the knot's function as they are more likely to be redundant whilst when compositions of knots are taken each crossing is more likely necessary as there are fewer redundant features.

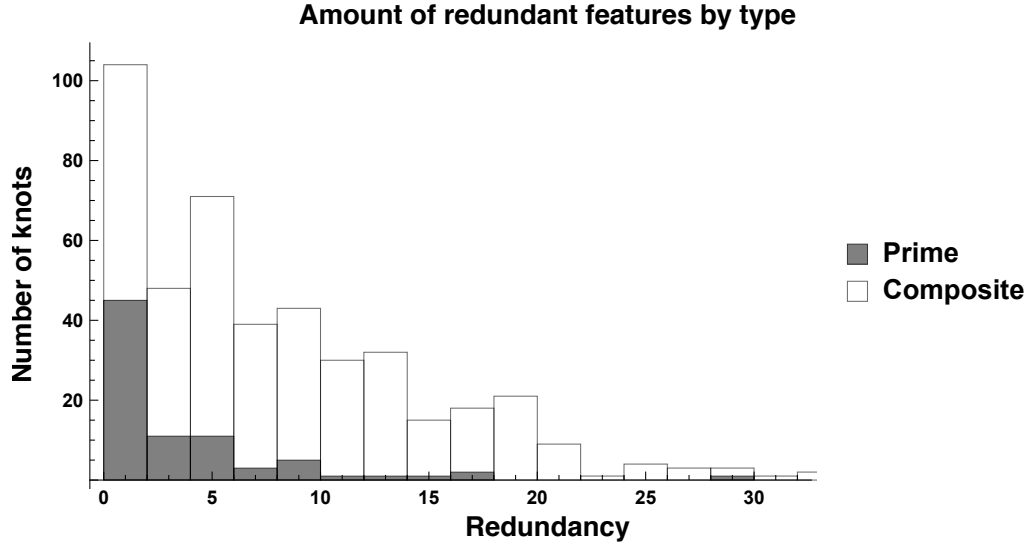


Figure 2.8: The plot shows the difference in the amount of redundant features for prime and composite knots in ABOK. We see from the plot that prime knots seem to have more redundant features than composite knots.

Figure 2.8 suggests that prime knots featured in ABOK have more redundant features than composite knots. Table 2.7 gives the mean, median and standard deviation for both groups with the Mann-Whitney U test [56] used to compare the medians for the two groups. We see from Table 2.6 that the Mann-Whitney U test gives a result suggesting the medians are significantly different at the 0.0001 level, with the mean and medians from the groups suggesting that prime knots have more redundant features and the standard deviation suggesting they have more variation in redundancy than composite knots.

	Prime	Composite
Amount	451	81
Mean redundancy	8.10421	3.09877
Median redundancy	6	1
Standard deviation redundancy	9.16638	4.71859
Mann-Whitney U test result	1.40611 x 10 <sup>-10</sup>	

Table 2.7: Comparison of the redundancy levels of prime and composite knots in ABOK. We see from the table that prime knots seem to have more redundant features than composite knots.

We also see a link between the amount of appearances of the knots in ABOK and the amount of redundancy, with the knots that appear more often having fewer redundant features and the ones that appear less often having more redundant features. Again this may suggest an optimisation for purpose as knots that appear more may be used more frequently and so may have some of the redundant features removed through use causing a lower redundancy overall. Again knots that have fewer redundant features may be easier to tie or teach due to the necessity of most of the crossings causing them to appear and be used more. The knots that appear more are likely to have more uses so this link between appearance and redundancy is similar to the link between use and redundancy.



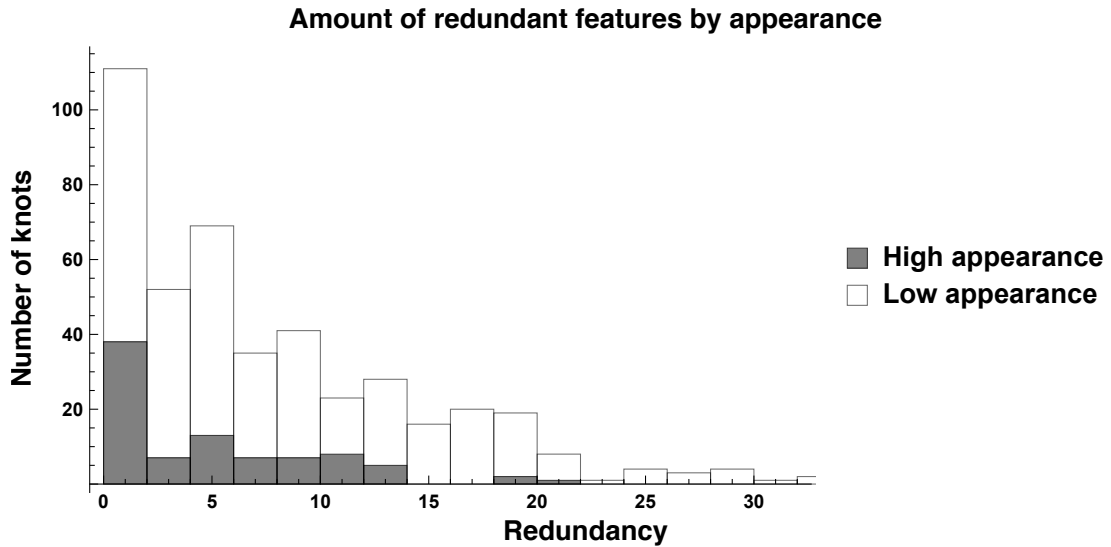


Figure 2.9: The plot shows the difference in the amount of redundant features for knots given in ABOK by the amount they appear. Here high appearance is knots with more than one appearance in ABOK and low appearance is knots with one appearance, with the median number of appearance for a knot in ABOK being 1. We see from the plot that knots that appear more in ABOK seem to have fewer redundant features than those that only appear once.

Figure 2.9 suggests that knots that appear more than once in ABOK have fewer redundant features than those that appear only once. Table 2.8 gives the mean, median and standard deviation for both groups with the Mann-Whitney U test [56] used to compare the medians for the two groups. We see from Table 2.8 that the Mann-Whitney U test gives a result suggesting the medians are significantly different at the 0.001 level, with the mean and medians from the groups suggesting that knots with fewer appearances have more redundant features and the standard deviation suggesting they have more variation in redundancy than those that appear more.

	High appearance	Low appearance
Amount	88	444
Mean redundancy	4.46591	7.91216
Median redundancy	2.5	5
Standard deviation redundancy	4.8017	9.31437
Mann-Whitney U test result	0.000316277	

Table 2.8: Comparison of the redundancy levels of knots that appear more than once in ABOK and those that appear only once. We see from the table that knots that appear more in ABOK seem to have fewer redundant features than those that only appear once.

However there is no difference between the amount of redundant features and whether the knot has a large amount of names or not, and there is no difference between the level of redundancy for knots with a lot of ABOK classifications (labels giving by Ashley, for example; best for purpose) or few. This suggests it is not just the popularity of the knot that correlates with redundancy.

## 2.4 Conclusion

In this chapter we have discussed knots in material culture and looked to the Ashley Book of Knots to study their range. We have discussed a method to categorise and create a database of these knots in order to answer our research questions. So far, the overall trends of prime and composite knots and links have been discussed with lower crossing knots and links appearing more often in ABOK and those of higher crossing number less often.

An analysis of the uses associated to the knots in ABOK suggests a likelihood that the knots that appear in ABOK have been optimised for their specific purpose.

The link between mean crossing number and standard deviation of crossing number suggests that a wide range of knots need to be used in order to use more complex knots, suggesting that more complex knots are only used when necessary for the pur-

pose and are found by trying a range of knots.

This optimisation is also suggested by knots with higher usage seeming to have fewer redundant features than those with fewer uses. This may suggest that as knots are utilised for more purposes their redundant features are reduced as they are optimised for those uses, or that knots with fewer redundant features are likely to be used for more purposes as they are simpler to tie and are best for the given purpose.

The link between prime knots and higher redundancy and composite knots and lower redundancy may suggest that composite knots are only formed when needed for the purpose leading to the optimal knot for that purpose and fewer redundant features.

Knots that appear more often in ABOK have fewer redundant features suggesting that as knots are used more often they are optimised and redundancy is reduced. This also suggests that knots that have fewer redundant features may be easier to tie and are not needlessly complicated, leading to them appearing in ABOK more often suggesting they are used widely.

The apparent optimisation seen here seems to fit with the findings of Muthukrishna et al. [33] in group size influencing complexity. The link between higher mean crossing number and higher standard deviation of crossing number suggests more knots need to be utilised to increase complexity, similar to the finding of Muthukrishna et al. that a wider range of demonstrators was necessary to preserve complexity.

However the measure of redundancy used in this analysis is determined by the number of crossings that can be removed from the projection of the knot or link through Reidemeister moves [42] and so does not take into account any potential functionality of these crossings, such as knots tied in looped ends as discussed in Figure 2.4. The presence of these features in prime knots, knots utilised more often and those that appear more often is nevertheless still interesting but does not necessarily indicate functional redundancy. The redundancy seen could still indicate optimisation with a preference for more compact features in a knot or link.

This analysis of the knots featured in the Ashley Book of Knots, whilst poten-

---

tially not indicative of the knots tied more broadly, gives us an idea of the potential features important in knot design, favouring knots with lower crossing number over those of higher crossing number. We also see possible optimisation in knot design reducing crossing number through increased usage, removing redundancy in the knot or link.

# Chapter 3

## An analysis of the transmission of granny and reef knots

### 3.1 Introduction

High fidelity social learning facilitates cumulative cultural evolution [58]. It enables individuals to acquire knowledge that exceeds that which any single individual could invent alone. Social learning has also been shown to increase the complexity of technology used [33] allowing humans to accumulate modifications over time [58].

However, social learning is not always perfect [18]. Errors in the imitation of actions may cause changes to material culture by affecting the fidelity of transmission. These errors can shape cultural evolution as copying error accumulates [59].

Kempe et al. present an experiment into the cultural mutation of the size of Acheulean handaxes [60]. The experiment involved transmission chains in which participants were asked to copy the size of the previous participants handaxe image on an iPad. This was compared with the mean and variance predicted by the Accumulated Copying Error model developed by Eerkens & Lipo [59], with the variance found to coincide but the mean deviating from that predicted. When participants were shown an initial image larger than the image they were copying, they tended to increase the image size resulting in a growing mean. This suggests that there was a biasing effect from the initial image size which caused the increasing mean, which was not factored into the errors in the initial model. This indicates

there are physiological factors causing non-random errors which may bias cultural evolution and may need to be factored into predictions.

As Kempe et al. showed a likelihood to increase image size caused a mutation in the appearance of this material culture over successive generations, we may expect other factors to bias cultural transmission. For example, Kalyanshetti & Vastrad present a study comparing reaction times using either hand of right and left handed individuals [61]. The study compared performance by monitoring auditory, visual and cutaneous reaction times of participants for either hand. Their study reported a significant improvement in the performance of right handed adult males when using their right hand over their left. However they found no significant improvement in left handed adult males when using their left hand over their right. This study shows that handedness affects performance of certain tasks, giving evidence of another physiological bias that may need to be factored in when considering copying error.

Actions are often mirrored when reproduced by the imitator, causing the imitator to perform the mirror image of actions shown [62] [63]. This propensity to perform the mirror image of actions shown automatically affects the fidelity of social transmission of actions and products that are laterally specified. Learners need to solve the correspondence problem when imitating actions [64] which can be difficult especially when actions are perpetually opaque. It has been suggested that performing the mirror image of actions is the spontaneous response [63] when reproducing actions, and so the prevalence of mirroring could greatly bias the transmission of culture as imitators mirror social information.

Biases are discussed in relation to cultural evolution and are referred to as factors of attraction [20] in cultural attraction theory. The effect of biases can be explored through experimental methods and modelling, using both transition matrices and parametric models [30].

We have seen biases limit and dictate the information transmitted culturally and expect similar biases to be present in the transmission of knot tying.

We are taught to tie knots from a young age, generally starting with learning to tie our shoelaces. The shoelace knot we are taught as youngsters is generally of the form shown in Figure 3.1 [8].

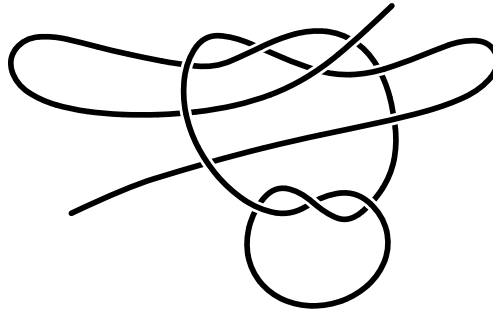


Figure 3.1: The standard shoelace knot tied, the ends of the lace can be pulled to release the knot

This knot is tied by forming an overhand knot and then forming a slipped overhand knot on top, allowing for the knot to be released by pulling the ends of the knot. We can look at the form of this knot without slipping the overhand knot on the top.

The shoelace knot takes the form of a reef knot, but is often incorrectly tied as the very similar granny knot, resulting in shoelaces that are liable to undo [65]. O'Reilly et al. explored factors influencing the untying of shoelace knots, including simulating the repeated impact of a shoe hitting the floor whilst walking, showing an increased liability for a shoelace tied in the form of a granny knot to undo [66]. These knots are some of the simplest, making them an ideal tool to explore biases in the learning process.

However, the appearance of the granny knot and the reef knot is extremely similar, making it difficult to know which knot has been tied. To make it easier to distinguish these two knots, we consider knots in a mathematical sense.

Intuitively we can think of a knot as a 3-dimensional closed curve, such as taking a piece of string, passing the string over and under itself in some way, and gluing the ends of the string together.

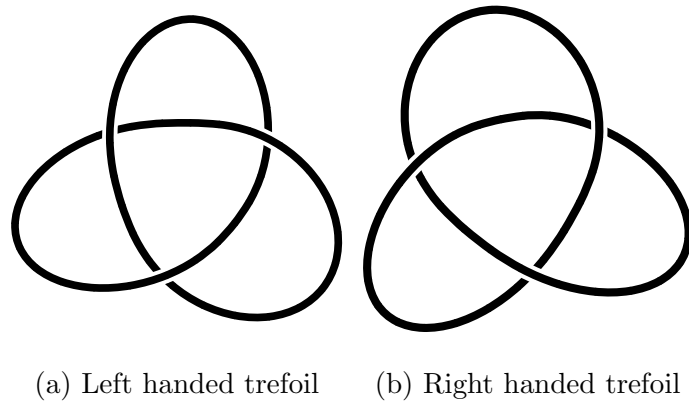


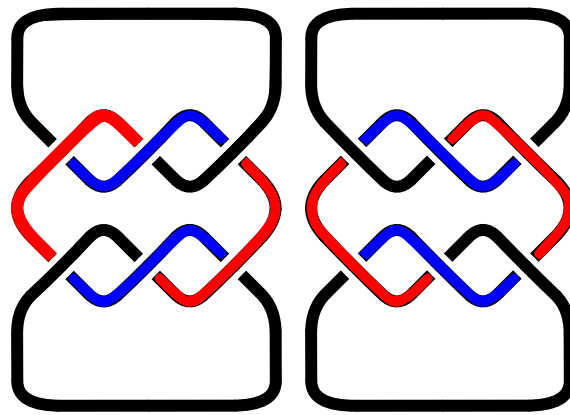
Figure 3.2: Both versions of the trefoil knot

Figure 3.2 shows the trefoil knot, which has the same form as the overhand knot with the ends glued together.

The trefoil knot has two forms, left handed (L) and right handed (R), which are mirror images of each other. These knots are mathematically distinct as they can not be transformed into each other by Reidemeister moves [42]. This means that no matter how much either knot is rotated or its strands moved, the only way to change the left handed trefoil to the right handed trefoil is to cut the knot open and retie it.

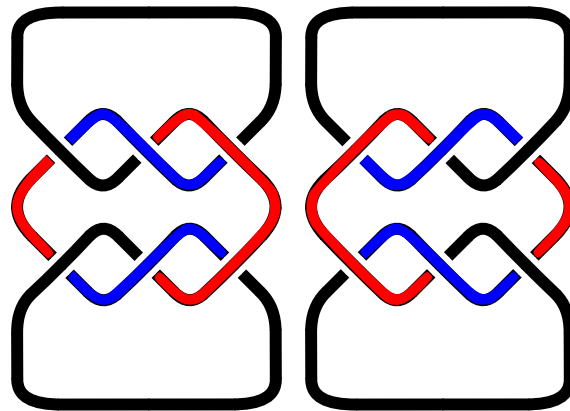
Both the granny knot and the reef knot are formed by first tying an overhand knot, then tying a second one on top. Mathematically they are composite knots formed by the trefoil knot. Although granny and reef knots are both formed of two trefoil knots joined together, they differ by the handedness of the trefoil knots.





(a) LL granny knot      (b) RR granny knot

Figure 3.3: Granny knots are formed by tying two trefoils of the same handedness one after the other, resulting in a left left (LL) granny knot and a right right (RR) granny knot. These knots are mirror images of each other, as shown by the coloured strands. These knots are distinct from each other, meaning there is no manipulation possible to make one look the same as the other. Both granny knots are also distinct from the reef knots



(a) LR reef knot      (b) RL reef knot

Figure 3.4: Reef knots are formed by tying two trefoils of different handedness one after the other, resulting in a left right (LR) reef knot and a right left (RL) reef knot. These knots are mirror images of each other, as shown by the coloured strands. These knots are not distinct from each other, as one can be rotated to match the other. However the reef knots are distinct from both granny knots

Granny knots are formed of trefoils of the same handedness, shown in Figure 3.3 and reef knots are compositions of trefoils of opposite handedness, shown in Figure 3.4.

The granny and the reef knot are distinct knots, and can be identified as such by knot invariants [67]. A knot invariant gives the same result when two knots are the same but may not always give a different result when the knots are distinct. The efficacy of each knot invariant in distinguishing knots depends on the invariant and the range of knots it is used upon. The Jones polynomial [43] is one such invariant, which assigns a polynomial with integer coefficients in one variable  $t^{1/2}$  to each knot and is discussed in Chapter 1. The Jones polynomial gives a unique result for all distinct prime knots of nine or fewer crossings. The Jones polynomial is given for the left handed granny knot in Equation 3.1.1, the right handed granny knot in Equation 3.1.2 and both reef knots by 3.1.3. These polynomials show that the granny knots are distinct from each other and both reef knots, but the two reef knots may not be distinct from each other. In fact, the two reef knots are not distinct, which can be seen by rotating one reef knot shown in Figure 3.4 to match the other. No such rotation is possible for the granny knots.

$$V_{LL}(t) = t^{-2} + 2t^{-4} - 2t^{-5} + t^{-6} - 2t^{-7} + t^{-8} \quad (3.1.1)$$

$$V_{RR}(t) = t^2 + 2t^4 - 2t^5 + t^6 - 2t^7 + t^8 \quad (3.1.2)$$

$$V_{reef}(t) = -t^3 + t^2 - t + 3 - t^{-1} + t^{-2} - t^{-3} \quad (3.1.3)$$

With the ends open, there are two ways a granny or reef knot can be tied. The knots shown in Figures 3.5 and 3.6 are a granny knot formed of two left handed trefoils (LL), a granny knot formed of two right handed trefoils (RR), a reef knot formed of one left handed trefoil then one right (LR) and a reef knot formed of a right handed trefoil then a left (RL).



(a) LL granny knot

(b) RR granny knot

Figure 3.5: Granny knots



(a) LR reef knot

(b) RL reef knot

Figure 3.6: Reef knots

The reef knot is generally considered more difficult to tie than the granny knot and is often incorrectly tied as such [65]. However we are not aware of any conclusive evidence to these claims.

The difference between the granny and reef knot is the handedness of the trefoils involved in the composition. We may expect that it is more difficult to tie two knots of a different handedness one after another, and that this is the reason for

the difficulty in tying reef knots. In order to explore this, we must look at the way knots are taught and tied.

By observing copying error for simple knots, such as granny and reef knots, we can see the effect of social learning biases and the barriers to high fidelity transmission. We present both experimental and modelling methods in order to explore these barriers and explore the effects on the accuracy in transmission of knot tying.

In Section 3.2 we discuss the set up and results of an experiment comparing the transmission of granny and reef knots through a one to many demonstration. The results are analysed using a Bayesian approach in Section 3.2.3. The outcome of the experiment is also explored using transition matrices in Section 3.2.3, using a linear approach to discuss the expected equilibria if these knots were transmitted through generations.

In Section 3.3 a parametric model is built to explore the biases affecting the transmission of granny and reef knots. The expected stability and equilibria of this model is also discussed. A parametric approach is used to take into account the biases affecting knot tying, in contrast to a linear approach.

In Section 3.4 the parametric model is matched with the experimental data in order to quantify the effect of the given biases on knot tying. The expected equilibria of these knots if transmitted through generations is discussed in Section 3.4.2 and contrasted with the linear approach shown in Section 3.2.3.

## 3.2 Experiment

In order to explore the transmission of granny and reef knots an experiment was conducted to test the biases that might affect the successful cultural transmission of these knots. Participants may have a bias towards tying particular knots, perhaps gained through prior teaching or knot tying experience, and so we aim to identify these biases.

The experiment was split into two stages. The first stage was intended to establish the handedness of the trefoil that participants would tie when given no guidance, in order to see if there was an ascocial bias towards a particular handedness of trefoil.

In the second stage, participants were shown a demonstration of tying a granny or a reef knot (LL, RR, LR and RL) and asked to tie the knot they saw, in order to compare the success rate in tying these knots. In total, 26 participants were in the LL treatment, 25 in the RR treatment, 25 in the LR treatment and 25 in the RL treatment.

### 3.2.1 Participants

Participants were recruited from the student population of Durham University, including undergraduate and postgraduate students across a range of subjects. They were rewarded with a £4 food voucher for their participation. In total 101 people took part in the experiment.

### 3.2.2 Procedure

A maximum of 10 participants took part in the experiment at any one time, and were sat sufficiently apart in a lecture theatre. Participants were given a large cardboard box and instructed to keep their hands inside it when tying any knots, to ensure no bias from observing other participants.

#### Stage 1

Participants were first asked to tie a “simple knot”. The word trefoil was not given as an instruction as it may have confused or caused participants to think too much about the knot they were tying. This was then checked to ensure that participants were tying a trefoil knot, and then untied.

Participants were then given 10 minutes to tie 10 trefoil knots in 10 pieces of string, each 25cm in length. They were asked at each minute interval to tie a “simple knot” and seal it in a small plastic bag. They were also asked to complete a distraction task in between tying each knot.

The distraction task involved participants drawing six concepts in order that another person could match the concepts to the drawings at a later time.

Both the plastic bag containing the 10 knots and the paper with the drawings from the distraction task were collected in at the end of the first stage.

### Stage 2

Participants were given an additional piece of string of length 35cm and then shown a video demonstrating the tying of either a LL granny knot, a RR granny knot, a LR reef knot or a RL reef knot, depending on the batch.

The video showed only hands tying a knot and contained no audio. The video was recorded from the point of view of an observer sitting across from the demonstrator. The video was chosen for each group by random attribution of batches to conditions, modified slightly to ensure roughly equal sample size in the end.

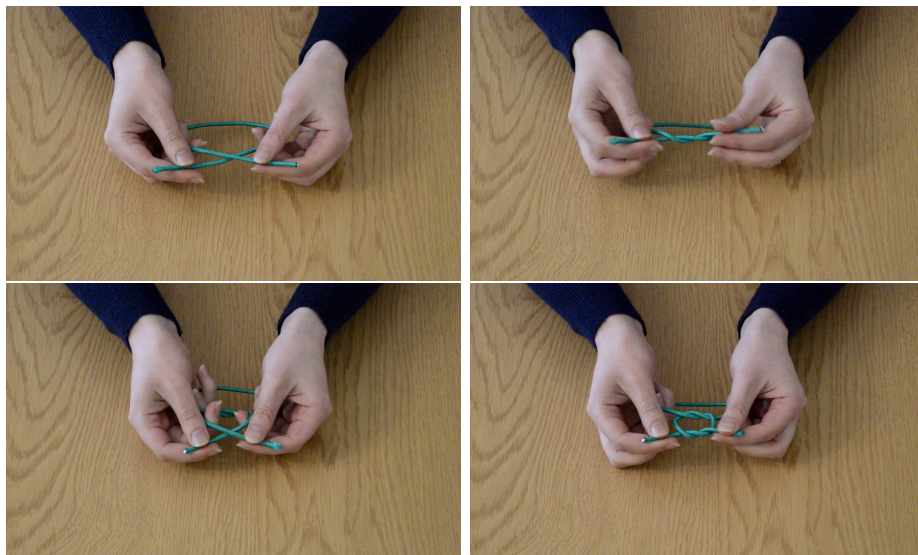


Figure 3.7: Screenshots from video showing the tying of RR granny knot

Participants were shown this video three times, with a pause of 30 seconds between each showing. They were told they could practice tying the knot whilst the video was being shown, and during the pauses between the showings. After the final showing of the video, they were told to untie any practice knots they had tied in the piece of string and asked to retie the knot shown in the video. This delay effect was to reflect the process of learning from a demonstration.

### Questionnaire

After both stages had been completed and all material collected, participants were asked to complete a short questionnaire detailing their name, gender, degree programme, handedness and hand usually written with, their knot tying experience and whether they knew how to tie a granny or reef knot. Details of the responses from the questionnaire can be found in Appendix A.1.1.

### 3.2.3 Results

For each participant in the experiment we recorded the handedness of each of the 10 trefoils. This gave us a measure of the handedness bias of each participant when left to tie a trefoil without guidance. The frequency of right handed trefoils tied by each person is shown in Figure 3.8, where participants who tied no right handed trefoils tied all left handed trefoils. Two participants who tied knots which were not trefoils have not been included in these data.

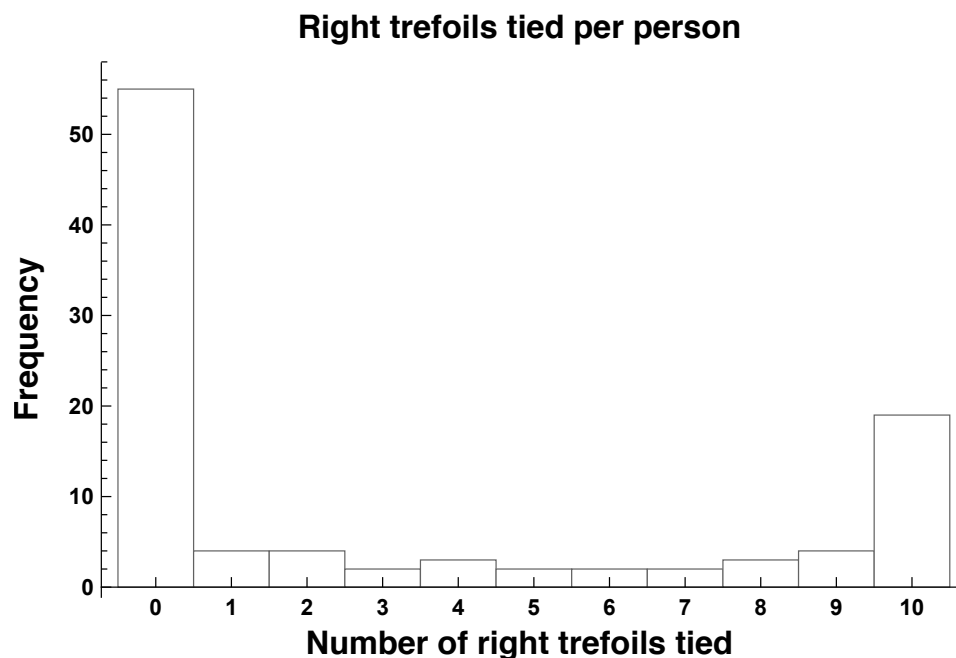


Figure 3.8: Frequency of right handed trefoils tied by participants, those who tied 10 right handed trefoils tied no left handed trefoils and those who tied 10 left handed trefoils tied no right handed trefoils

From Figure 3.8 we see that the majority of participants tied either solely all right handed or all left handed trefoils, with some tying a mixture of the two. Left handed trefoils were much more common than right handed trefoils. Taking the mean amount of right handed trefoils tied, divided by the amount of trefoils tied by each participant, we get a value of 0.32 at two decimal places. This is the likelihood that a participant tied a right handed trefoil, meaning that participants tied a left handed trefoil 68% of the time.

Participants were shown a video demonstrating how to tie one of four knots; a LL, RR, LR or RL.

Of the 101 knots tied after being shown the video, 100 of the knots were either LL, RR, LR or RL. One knot was a knot formed by a composition of the knot  $5_1$  and the knot  $3_1$ . This knot has been excluded from analysis and we give in Table 3.1 the rest of the knots tied given the video shown.

		Knot tied by participants				
		LL	RR	LR	RL	Total
Demonstration	LL	14	9	1	2	26
	RR	9	15	0	1	25
	LR	4	4	8	8	24
	RL	6	1	6	12	25
	Total	33	29	15	23	100

Table 3.1: Knots tied by participants given video shown in experiment

We notice that the highest numbers are on the diagonal of the table, indicating a high success rate in participants tying the knot shown in the video. We also notice that the number of mirror images tied given the video, are higher than the other knots. For example, more people tied the RR granny knot when shown LL, than tied either reef knot, LR or RL. As the videos were filmed from the point of view of a person sitting opposite the knot tyer, we might expect the knot to be misinterpreted



as its mirror image.

Overall we see the knot LL being tied most commonly, then RR, RL and least commonly LR.

Separating Table 3.1 into granny and reef knots, we see in Table 3.2 that granny knots are tied much more often than reef. However, we do notice that when a reef knot is shown in the video, a reef knot is tied quite frequently. This Table suggests that reef knots might be harder to tie than granny knots but that participants may recognise the form of the knot tied, often successfully tying it or its mirror image.

		Knot tied by participants		
		Granny	Reef	Total
Video shown to participants	Granny	47	4	51
	Reef	15	34	49
	Total	62	38	100

Table 3.2: Amount of granny and reef knots tied by participants given video shown

Both Table 3.1 and Table 3.2 suggest that the knots tied by participants are not independent of the knot in the video shown to participants.

### Bayesian analysis of results

Using a Bayesian analysis [68] of Table 3.1 we estimate and simulate posteriors for the data using the package Bayesian First Aid written by Rasmus Bååth for R [69].

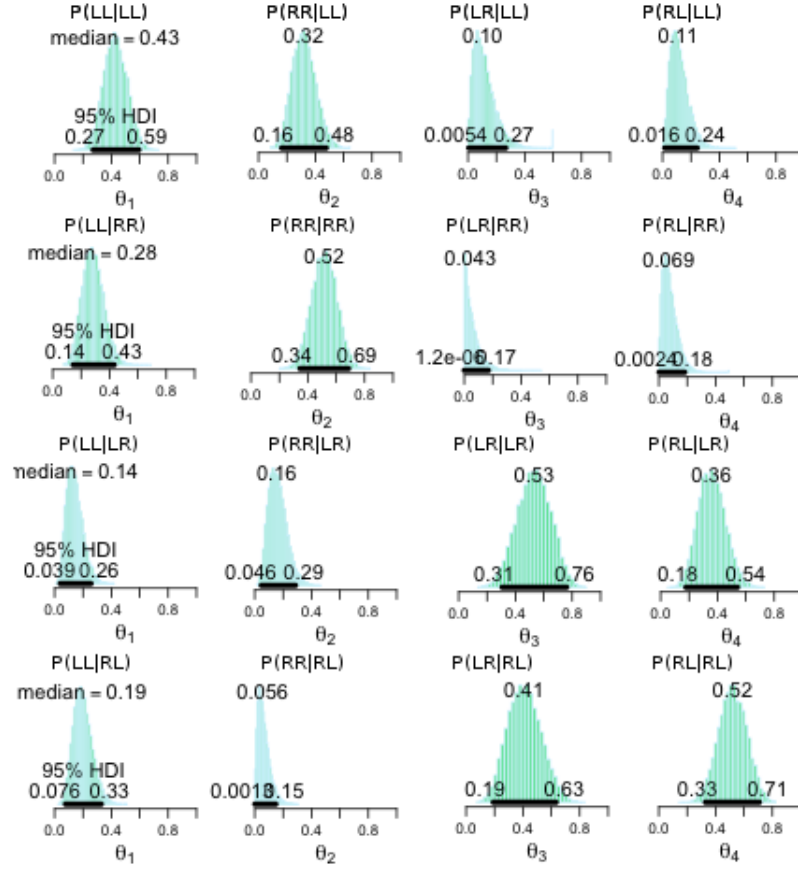


Figure 3.9: Posterior simulation of knots tied between each group. Each plot shows the likelihood  $\theta$  of tying a knot given the video shown. We see the highest likelihood for tying the knot shown in the video, with the second highest being the mirror image of that knot

Figure 3.9 shows the distribution of the posterior simulation of knots tied given the demonstration. Each line shows the posterior simulations for each knot in Table 3.1. Appendix A.1.2 contains the full posterior distributions for each knot, including between group simulations. We can see in each case the most likely knot to be tied is the knot shown in the video, with the next likely being the knots of mirrored form.

It may also be interesting to note that the 95% confidence intervals for both reef knots,  $P(LR|LR)$  and  $P(RL|RL)$  are slightly larger than those for both granny

knots,  $P(LL|LL)$  and  $P(RR|RR)$ . This could indicate that there is a greater uncertainty that reef knots will be correctly replicated after demonstration than granny knots. This is also seen in Table 3.1 with the lower numbers for both reef knots tied after demonstration than either granny.

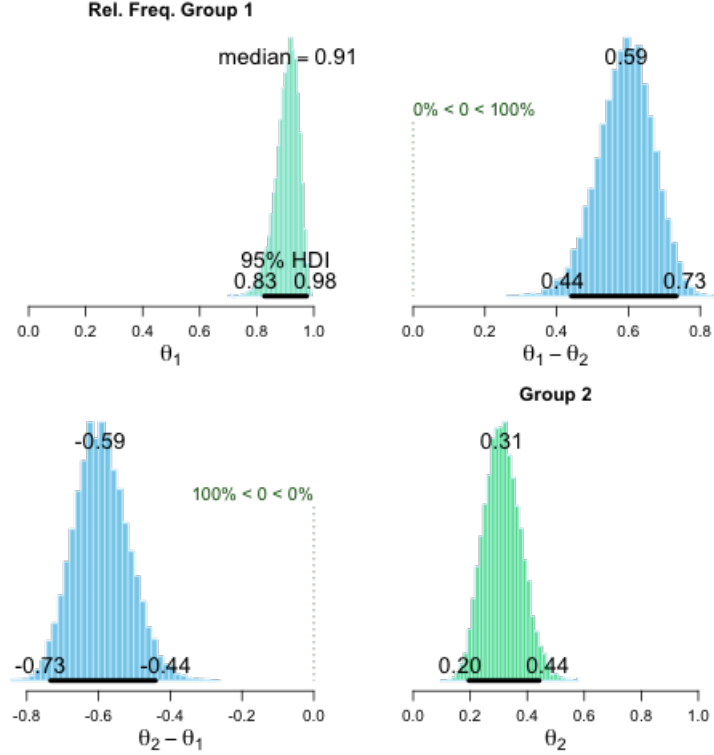


Figure 3.10: Posterior simulation of knots between groups. The green plots show the likelihood  $\theta$  of tying a granny knot when either knot. The plot with median 0.91 shows the likelihood of tying a granny knot when shown a granny knot and the plot with median 0.31, of tying a granny knot when shown a reef. The blue plots  $\theta_1 - \theta_2$ , the difference in likelihood between the groups

A similar analysis can be done using the overall values of granny and reef knots tied in Table 3.2. Figure 3.10 shows the posterior distributions for granny and reef knots, given the knot shown. The plot for group 1 shows the posterior probability that the demonstration of a granny knot results in a granny knot being tied, group 2 being the probability that a granny knot was tied after a reef knot was shown. We can see the median values were much higher for the granny knot demonstration than the reef and the plot  $\theta_1 - \theta_2$  shows a relatively large between group difference

of 0.59. This suggests that the probability of tying a granny knot was influenced by the video shown.

In Table 3.3 we display the number of trefoils tied per person by handedness and the knots participants tied. We split participants in to two groups, “Left” and “Right”, by which trefoil they tied the majority of the time. Participants who tied more than five left handed trefoils are in the “Left” category and those who tied more than five right handed trefoils are in the “Right” category. One participant tied an equal number of left and right trefoils and has not been included in the table. The two participants who did not tie all trefoils have not been included in this table.

		Knot tied by participants				
		LL	RR	LR	RL	Total
Trefoils tied by participants	Left	25	20	12	11	68
	Right	6	9	2	12	29
	Total	31	29	14	23	97

Table 3.3: Knot tied given handedness of trefoil tied by participants

Again using a Bayesian analysis from the package Bayesian First Aid [69] we compare the knots tied given the trefoils tied by participants. We see higher median values for knots starting with L when a participant tied a left trefoil and similarly higher median values for R knots when a right trefoil was tied. This suggests that the trefoils participants tied given no guidance had an effect on the knots tied following the demonstration, suggesting there is an underlying handedness bias relating to the tying of trefoil knots. It can be seen that participants that exhibited a handedness bias when tying the trefoils displayed the same bias in the first trefoil tied following the demonstration in the second stage of the experiment. For example, those who had a left handed bias in tying their trefoil were more likely to begin their post-demonstration knot with a left handed trefoil, L, than a right, R. This analysis can be seen in Figure A.6 Appendix A.1.2.

From the data in Tables 3.1, 3.2 and 3.3 we expect that when participants at-

tempted to tie the knot shown in the video, a few factors affected their performance.

The participant would first need to recognise that the video was filmed from the point of view of someone sat across from the demonstrator, and so replicate the demonstrator's actions, rather than perform the mirror image of those actions. The data shown in Table 3.1 suggests many participants performed the mirror image of the actions of the demonstrator, resulting in the mirror image of the knot shown being tied.

Participants would then need to correctly imitate the actions of the demonstrator. By the analysis of Tables 3.1 and 3.2 we see that many participants accurately imitated the perceived actions of the demonstrator, correctly tying the interpreted knot.

The knots participants tied were also affected by their “handedness bias”, as demonstrated in the analysis of Table 3.3. Participants needed to replicate the knot tied in the video rather than rely on their own bias.

From the data in Table 3.2 we also notice that granny knots seem to be tied more often than reef knots, suggesting granny knots are easier to tie than reef knots. We recall that granny knots are formed of two trefoils of the same handedness, whilst reef knots are formed of trefoils of different handedness. This suggests participants could be biased to simply repeat the first trefoil they tie, resulting in more granny knots tied than reef knots.

### Equilibria under a linear model

We can rewrite Table 3.1 as a transition matrix representing the probability of the change in knot types using an approach attributed to Markov [29]. For example  $x_{2,1} = P(LL|RR)$  the probability of tying knot LL when shown RR.

$$X = \begin{bmatrix} \frac{14}{26} & \frac{9}{26} & \frac{1}{26} & \frac{2}{26} \\ \frac{9}{25} & \frac{15}{25} & 0 & \frac{1}{25} \\ \frac{4}{24} & \frac{4}{24} & \frac{8}{24} & \frac{8}{24} \\ \frac{6}{25} & \frac{1}{25} & \frac{6}{25} & \frac{12}{25} \end{bmatrix}$$

$X$  is a right stochastic matrix containing the frequency of each knot tied given the knot demonstrated representing the experimental data. We simulate the teaching of these knots within future generations by taking powers of this matrix, basing future generations solely on the present state.

This has stationary distribution  $\pi$  such that  $\pi X = \pi$ ;

$$\pi = \begin{bmatrix} 0.401 \\ 0.391 \\ 0.072 \\ 0.136 \end{bmatrix}$$

We see that the knot  $LL$  has highest frequency in this distribution, followed by  $RR$  then the reef knots;  $RL$  and then  $LR$ .

This approach assumes each knot will be acquired in the same manner each generation, basing the probabilities off the experimental data independent from any other factors. Whilst the frequencies here are affected by biases in the transmission process, this approach does not explicitly take into account the biases discussed above and does not directly show their effect on the resulting knots tied. In order to observe the expected biases we present a parametric approach to the transmission of granny and reef knots in Section 3.3.

Various biases may cause mutation in the social learning process. In order to further analyse the affect of these biases on the transmission of knots we must take into account these factors; likelihood to mirror, accurate imitation of the perceived knot, handedness bias and repetition bias. In the next section we build a model of the transmission of granny and reef knots within a population, to quantify the effect of these proposed biases on the experimental results and explore their population-level consequences for the cultural evolution of our four knot types.

### 3.3 Parametric model

#### 3.3.1 Assumptions

We model the transmission of granny and reef knots within a population through oblique transmission [30] and assume that when a granny or reef knot is taught, the learned knot is always either a granny or a reef knot. There are four distinct granny and reef knots, the LL and RR granny knot and the LR and RL reef knot.

We assume that when a knot is demonstrated, the learned knot is affected by the probability the learner interprets the demonstrator's knot incorrectly as the knot's mirror image,  $g$ , the probability that the learner accurately imitates each trefoil in the perceived knot,  $s$ , the probability that the learner simply repeats the trefoil they tied for the first step of the knot,  $r$ , and the probability that the learner ties a right handed trefoil when given no guidance,  $p$ . These parameters represent probabilities and so take values in the interval  $[0, 1]$ .

These equations focus on the effect of learning biases on the transmission of these four knots and do not assume a preference for any particular knot.

#### 3.3.2 Equations

Using these parameters, we can build a system of recurrence equations to determine the change in frequency of each knot in the population between generations. The parameters represent the probability that the population as a whole is affected by the given learning biases.

The equations are recursive, so knot frequencies in the learner generation are a function of knot frequency in the demonstrator generation. We denote the proportion of knot  $ij$  tied in the demonstrating generation by  $f_{ij}$  where  $ij \in \{RR, LL, RL, LR\}$ , and the proportion of knots tied by the learner generation of the population after transmission as  $f'_{ij}$  where  $f'_{RR} + f'_{LL} + f'_{RL} + f'_{LR} = 1$  with each  $f'_{ij}$  taking values in the interval  $[0, 1]$ .

For example, take the frequency of the granny knot formed by tying two right handed trefoils and denote it by  $f_{RR}$ . This knot will be transmitted successfully if it is not mirrored and both trefoils that form it are accurately imitated by the next

generation, denoted by  $f_{RR}(s^2(1-g))$ . However, a right granny could also be formed by mirroring a LL with probability  $g$  and accurately imitating both trefoils of the perceived knot with probability  $s^2$ , giving  $f_{LL}(s^2g)$ . A right granny could also be formed with no accurate imitation at all, if the tyer has a bias towards tying right handed trefoils  $f_{RR}((1-s)^2p^2)$  or repeating the first knot tied,  $f_{RR}((1-s)^2(pr))$  and so we get the frequency of right grannies in the population as a function of grannies and reefs already in the population and the probability parameters;

$$\begin{aligned} f'_{RR} = & f_{RR}(s^2(1-g)) + \dots + f_{RR}((1-s)^2p^2) + \dots \\ & + f_{RR}((1-s)^2(pr)) + \dots + f_{LL}(s^2g) + \dots \end{aligned}$$

It is important to think about how the parameters interact with each other. If a learner imitates the knot correctly then the learner's likelihood to repeat or tie a right handed trefoil does not matter. They will do what is shown regardless of their biases, and so we can discount repetition and right hand bias when the knot is accurately imitated.

In the same way, when the learner simply repeats part of a knot their right hand bias does not matter, as they will repeat regardless of this bias. So we can discount right hand bias when repetition takes place.

The order in which each parameter acts does not matter as it is the way the parameters interact which is important. We assume the order of parameters is mirroring, accuracy, repetition then handedness bias. As the parameter  $s$  controls the learner's propensity to imitate the knot correctly regardless of handedness or repetition bias, it does not matter if  $s$  occurs before or after  $p$  or  $r$ , as  $s$  occurs regardless of  $p$  or  $r$ . It is therefore assumed  $p$  and  $r$  only come into effect when  $(1-s)$  occurs. As  $r$  controls propensity to repeat regardless of handedness bias it does not matter if  $p$  occurs before or after  $r$ , as  $r$  occurs regardless of  $p$  and  $p$  only comes into effect when  $(1-r)$  occurs. In this way it does not matter which order our parameters appear in in the tree, as rearranging will cause parameters to cancel with each other due to the way in which they interact.

A decision tree showing the effect of each parameter on the transmission of knot RR can be seen in Figure 3.11. A similar tree can be formed for LL, LR and RL, making the recursion equations easy to read off. The full equations are in Appendix



A.1.3.

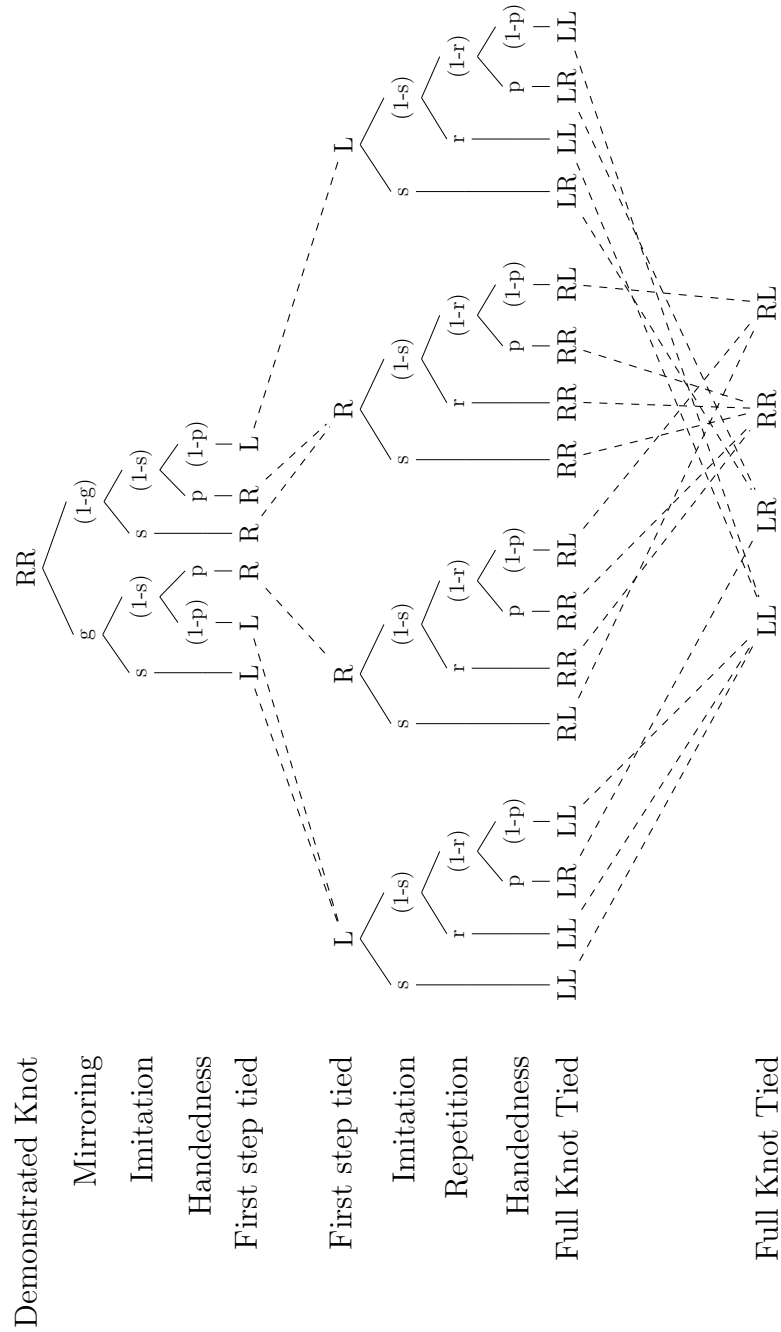


Figure 3.11: Decision tree showing the effect of parameters on the transmission of knot RR

### 3.3.3 Equilibria

We want to solve the system of equations for equilibria, to find the frequencies of each knot that do not change over successive generations. In order to do this we want to find the set of solutions when there is no change in the system. As we have a system of recurrence relations, change in this system is given by

$$\Delta f_{ij} = f'_{ij} - f_{ij} \quad (3.3.4)$$

Equilibria occurs when

$$\Delta f_{ij} = 0$$

and so we find the states  $\hat{f}_{ij}$  when

$$f'_{RR} = f_{RR}$$

$$f'_{LL} = f_{LL}$$

$$f'_{RL} = f_{RL}$$

$$f'_{LR} = f_{LR}$$

For each value of the parameters  $p$ ,  $g$ ,  $r$  and  $s$ , there exists a point of equilibrium, which is expressed in the equations in Appendix A.1.4.

It is important to discount the cases when these equilibria are undefined, that is when

$$(1 + s)(s(2g - 1)(rs - r - 1) - 1) = 0 \quad (3.3.5)$$

This occurs when either

$$(1 + s) = 0 \quad (3.3.6)$$

or

$$s(2g - 1)(rs - r - 1) - 1 = 0 \quad (3.3.7)$$

The case when  $s = -1$  in Equation 3.3.6 is automatically discounted as it is outside the range of the parameter  $s$ .

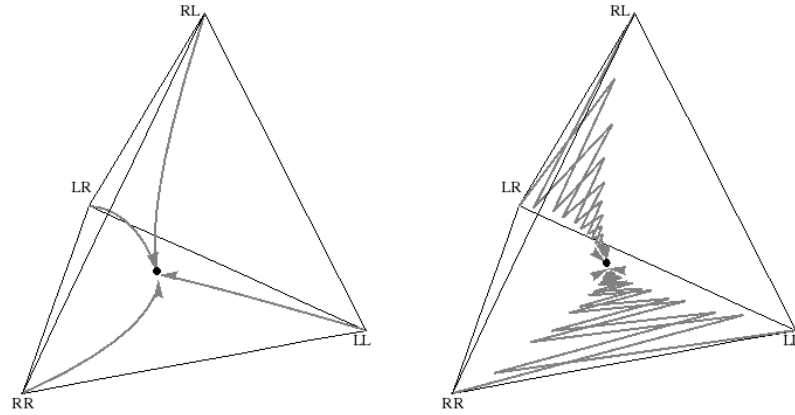
The case  $s(2g - 1)(rs - r - 1) = 1$  in Equation 3.3.7 holds when  $s = 1$ ,  $g = 0$ ,  $0 \leq r \leq 1$ . This is the situation when imitation is always accurate and mirroring

never occurs and so there is no change in the system. Although this situation is undefined by the parameters, it results in a trivial equilibrium.

We notice that the values of  $f_{LR}$  and  $f_{RL}$ , the frequencies of the two reef knots, at equilibria given by the equations above, are always equal. This is due to the fact that LR and RL represent the same knot mathematically, as shown by their Jones polynomial in Equation 3.1.3.

The equilibrium points for the system are determined by the parameters  $p, g, r$  and  $s$ . The way the system evolves to these points is also determined by these equations.

We plot evolutionary trajectories for this system in a tetrahedral plot. In order to plot the trajectories inside a tetrahedron, we need to plot values for our equations and convert these points to barycentric coordinates as shown in Appendix A.1.5.



(a)  $p=0.75, g=0.1, r=0.25, s=0.9$  (b)  $p=0.75, g=0.9, r=0.25, s=0.9$

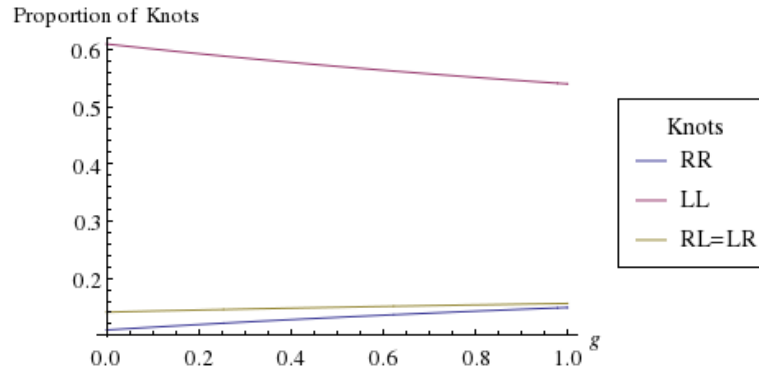
Figure 3.12: Evolutionary plots showing the change in frequency of knots. Each arrow represents the change in frequency of each type of knot in the population, starting from sole existence to a mixture of different knots. The solid disk is the equilibrium state which is evolved towards no matter the starting frequencies

In Figure 3.12a accuracy is high and mirroring almost never occurs. We see the system evolves in a smooth curve to a point determined by the values of  $p$  and  $r$ , the handedness bias and the repetition bias of the population. We note that the value of  $p$  in 3.12a causes the point to be closer to the corner  $f_{RR}$  than  $f_{LL}$  but the

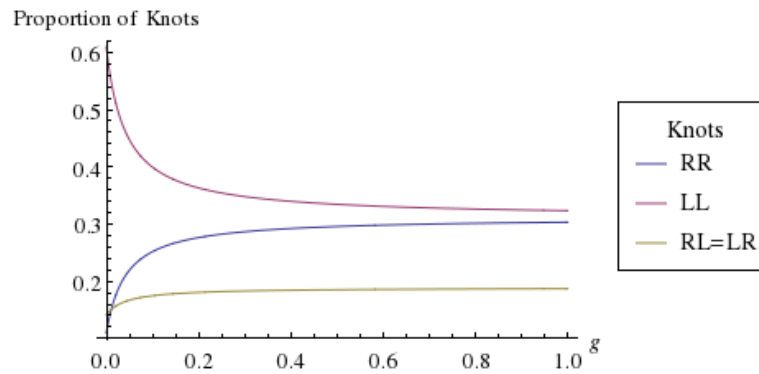
value of  $r$  does not cause the point to be as close to the  $f_{RL} + f_{LR} = 1$  boundary as we may expect.

In 3.12b, mirroring is likely to occur. Coupled with the high accuracy, the system evolves to a similar equilibrium point as shown in 3.12a, but the difference in mirroring causes the path to oscillate to the point rather than evolve in a smooth trajectory. The lower the value of  $g$ , the smoother the evolution towards equilibria.

We plot the equilibrium proportions  $\hat{f}_{ij}$  in Figure 3.13. These are plotted as a line graph, with three out of the four parameters fixed and the other varying between zero and one. The effect of the presence of accuracy on mirroring is shown in Figures 3.13a and 3.13b.



(a)  $p=0.25, r=0.25, s=0.1$



(b)  $p=0.25, r=0.25, s=0.9$

Figure 3.13: Line plots showing the proportion of knots at equilibria. The values of  $\hat{f}_{LR}$  and  $\hat{f}_{RL}$  are equal so these are represented by the same line on the graph, while  $\hat{f}_{RR}$  and  $\hat{f}_{LL}$  are represented by separate lines

In Figure 3.13a, the value of  $s$  is lower than in 3.13b, resulting in only a slight change in the values of  $\hat{f}_{RR}$ ,  $\hat{f}_{LL}$  and  $\hat{f}_{RL}$  and  $\hat{f}_{LR}$ . This is compared with the higher value of  $s$  in 3.13b and the curved lines representing the frequencies. This shows that imitation needs to be highly probable for mirroring to affect the proportion of knots tied in the population.

### 3.3.4 Stability

In this system, an equilibrium point is stable if no matter the starting values of  $f_{RR}$ ,  $f_{LL}$ ,  $f_{LR}$ ,  $f_{RL}$ , the system comes to rest at the same point. If the point changes depending on these starting values then it is not stable.

To find the stable equilibrium points we set  $f_{ij}$  equal to the equilibria points determined by the equations, plus some small perturbation  $\epsilon_{ij}$ . The equilibrium is stable if the value of  $f'_{ij}$ , moves towards the equilibria points given by Equations A.1.5 - A.1.9 in Appendix A.1.4.

Let

$$\begin{aligned} f_{RR} &= \frac{Q_1}{P} + \epsilon_{RR} \\ f_{LL} &= \frac{Q_2}{P} + \epsilon_{LL} \\ f_{LR} &= \frac{Q_3}{P} + \epsilon_{LR} \\ f_{RL} &= \frac{Q_4}{P} + \epsilon_{RL} \end{aligned}$$

where  $Q_i$  and  $P$  are as given in Equations A.1.5 - A.1.9 in Appendix A.1.4, and

$$\epsilon_{RL} = -\epsilon_{RR} - \epsilon_{LL} - \epsilon_{LR}$$

to ensure  $f_{ij}$  sum to one.

We then compute  $f'_{RR}$ ,  $f'_{LL}$ ,  $f'_{LR}$ ,  $f'_{RL}$  as in Equations A.1.5 - A.1.9 in Appendix A.1.4 and the distance:

$$\begin{aligned} d_{RR} &= f'_{RR} - \frac{Q_1}{P} \\ d_{LL} &= f'_{LL} - \frac{Q_2}{P} \\ d_{LR} &= f'_{LR} - \frac{Q_3}{P} \end{aligned}$$

$$d_{RL} = f'_{RL} - \frac{Q_4}{P}$$

We then have the following cases.

Case 1:

$$d_{ij} = 0$$

In this case the system jumps to an equilibrium point given by the parameters. The system then remains at this point for all generations. This occurs when there is no accurate imitation, when  $s = 0$ . The system is not affected by starting values of  $f_{ij}$ , the frequency of each type of knot is determined solely by the values of  $p$  and  $r$ .

Case 2:

$$d_{ij} = \epsilon_{ij}$$

In this case there is no change in the system, meaning the system is currently at equilibria, with the system remaining at this point for all generations. This occurs when imitation is always accurate and mirroring never occurs, when  $s = 1$  and  $g = 0$ . The equilibrium state is determined by the starting values of  $f_{ij}$  and is independent of the values of  $p$  and  $r$ . The frequency of each type of knot remains constant across generations.

Case 3:

$$d_{ij} < \epsilon_{ij}$$

In this case the system moves towards the equilibrium point given by the parameters. This occurs when  $s < 1$ , when imitation is not perfect and the system evolves towards equilibria over generations.

Case 4:

$$d_{ij} > \epsilon_{ij}$$

In this case the system moves away from the equilibrium point given by the parameters. This never occurs for any equilibrium point in the system, meaning all points are stable.

### Granny and reef knots at equilibria

Take

$$x = \hat{f}_{RR} + \hat{f}_{LL}$$

to denote the proportion of granny knots at equilibria and

$$y = \hat{f}_{RL} + \hat{f}_{LR}$$

to denote the proportion of reef knots at equilibria.

The proportion of granny knots is equal to the amount of reef knots in the population at equilibria when  $x = y$  which occurs in two cases.

The first case is when imitation is not perfect, the individuals never repeat the first knot tied and are no more likely to tie a right handed trefoil than a left. This is given by parameter values  $0 \leq s < 1$ ,  $r = 0$ ,  $p = 1/2$  and  $0 \leq g \leq 1$ . The absence of repetition bias allows reef knots to become more prevalent in the population, and the lack of handedness bias prevents the prevalence of either granny knot.

The second case is when accurate imitation always occurs, the population never repeats the first knot tied, and mirroring always occurs to some extent. This is given by parameter values  $s = 1$ ,  $r = 0$ ,  $0 \leq p \leq 1$  and  $0 < g \leq 1$ . Again, the absence of repetition bias allows reef knots to become more prevalent in the population. Perceived imitation is always perfect, however there is always an element of mirroring, causing knots to be replicated incorrectly.

In the plot in Figure 3.14, the values at equilibria of granny knots,  $x = \hat{f}_{RR} + \hat{f}_{LL}$  are shown in a density plot.

In Figure 3.14 the values of  $r$  and  $g$  are fixed with  $r = 0$  and  $g = 1/2$ , the population never repeat the first trefoil tied when given no guidance, making tying reef knots more likely, and are equally likely to mirror the demonstrated knot as not. Both the cases discussed for equality between granny and reef knots in the population are visible in these plots. We have equality when  $s = 1$  for all values of  $p$ , and when  $p = 1/2$  for all other values of  $s$ . Under these conditions we observe the lowest proportion of granny knots in Figure 3.14 causing higher proportions of reef knots.

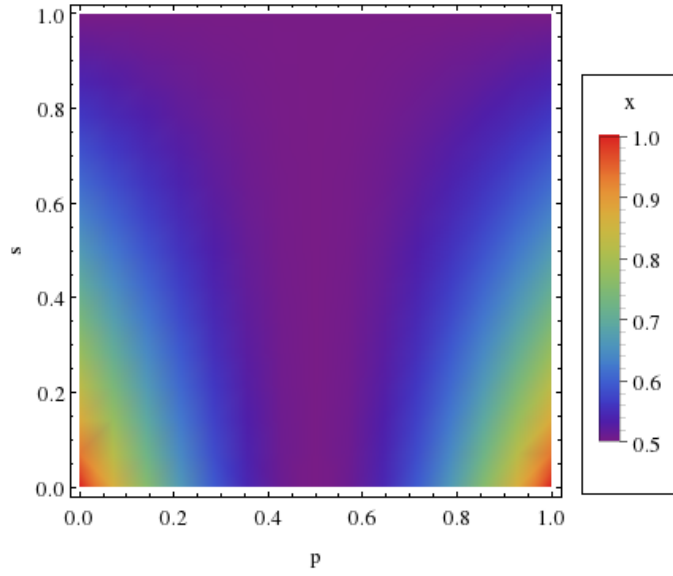


Figure 3.14: Density plots showing the change in proportion of granny knots as the values of  $p$  and  $s$  change with  $g=1/2$  and  $r=0$

The proportion of granny knots would be less than the amount of reef knots in the population at equilibria when  $x < y$ , however this inequality never holds. This means that the system can only ever come to rest at a point of equilibria, when there are either more granny than reef knots in the population, or they are equal as in the cases above. Even when repetition never occurs the population is still more likely to tie granny knots than reef knots, as their handedness bias makes tying a version of a granny knot more probable.

However, equilibria where more reef knots than granny knots exist in the population can still occur in the cases not governed by equations A.1.5 - A.1.9, namely when  $s = 1$  and  $g = 0$  as discussed in Section 3.3.3 and both  $f_{RR} = f_{LL}$  and  $f_{RL} = f_{LR}$ .

When  $s = 1$  and  $g = 0$  it is clear that there will be no change in the system, as everyone in the population will always accurately imitate the perceived knot and never mirror the knot they are shown, so the frequency of each knot in the population will always remain constant. In this case the equilibrium is always stable as the frequency of each knot will always remain constant.

When  $s = 1$  and  $g \neq 0$ , the only time the system will be at equilibria is when both



$f_{RR} = f_{LL}$  and  $f_{RL} = f_{LR}$ . In this case perceived knots are always accurately copied and some extent of mirroring always occurs. When knots are mirrored they are tied as their mirror image, so if frequencies of mirror images are equal to each other no change in frequency will occur in the system. Again, in this case the equilibrium is always stable as the frequency of each knot will always remain constant.

## 3.4 Applying the model to experimental results

Using Approximate Bayesian Computation (ABC) [70] we can evaluate our model using the experimental data.

### 3.4.1 ABC method

ABC works on the same premise as Bayes' theorem, relating conditional probability of parameters  $\theta$ , to data  $D$  by the rule;

$$p(\theta|D) = \frac{p(D|\theta)p(\theta)}{p(D)}$$

where  $p(\theta|D)$  is referred to as the posterior,  $p(\theta)$  represents the prior beliefs before any data is available,  $p(D|\theta)$  the likelihood of data  $D$  occurring given the prior and  $p(D)$  the evidence [68].

With this rule we can calculate the posterior by taking the product of prior beliefs with the likelihood of data occurring, divided by the evidence observed.

To obtain the probability of data  $D$  given parameter  $\theta$ , we use our model to simulate data for a given parameter. After simulating data, we need to decide whether it fits the observed data. We construct a metric to describe our observed data, in a manner so we can easily accept or reject the simulated data depending on whether it is in line with that observed. We then look at the parameters used to simulate the data that fits the observed, to get  $p(\theta|D)$  and compute the metric for  $p(D)$  and so can compute  $p(\theta)$  for a parameter  $\theta$ .

Taking our observed data from Table 3.1 as a  $4 \times 4$  matrix  $O$  and simulating data of the same form using our model to give a  $4 \times 4$  matrix  $S$ , we compare these

two sets of data using the metric;

$$d(O, S) = \sum_{i,j} a_{ij}^2 \quad (3.4.8)$$

where  $a_{ij}$  are the entries of the matrix  $O - S$ . This metric is proportional to finding the Euclidean distance between the points in the two matrices.

### 3.4.2 ABC results

We use a Monte Carlo simulation method [71] to simulate data for random values of each parameter  $p, g, r$  and  $s$  between 0 and 1, compute the outcome of walks through the decision tree in Figure 3.11 starting with each knot with the same frequency it was used as demonstration in the experiment, 26 for  $LL$ , 25 for  $RR$ , 24 for  $LR$  and 25 for  $RL$  and calculate the metric in equation 3.4.8. This procedure is repeated many times.

Below, we plot values of the parameters  $p, g, r$  and  $s$  for the simulations that result in a metric value,  $d(O, S) = \sum_{i,j} a_{ij}^2 \leq 0.0075$ , these values came from fewer than 0.5% of the simulations.

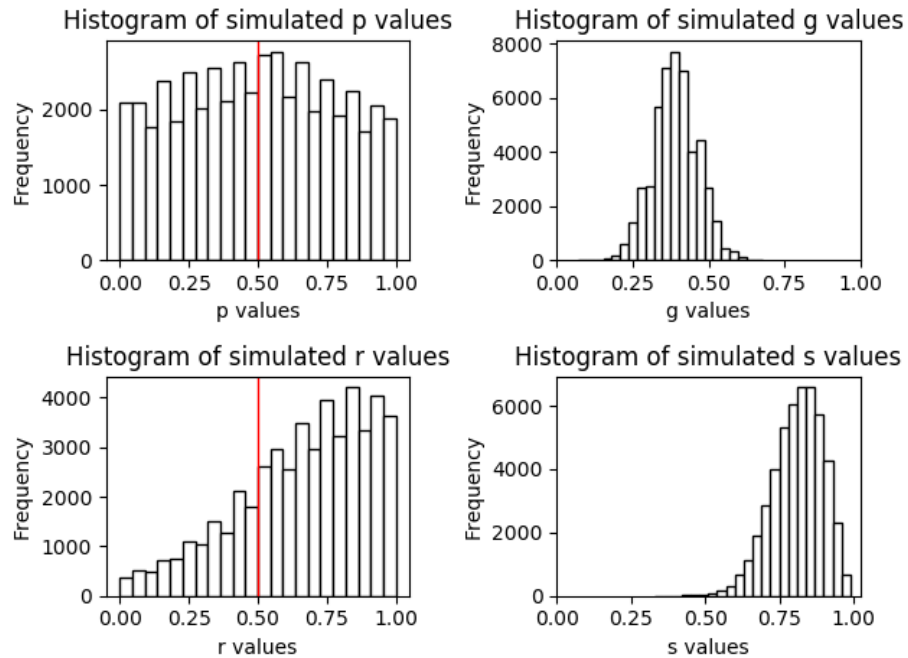


Figure 3.15: Histograms of parameter values simulated from experiment, with acceptance interval  $d(O, S) \leq 0.0075$

The red vertical lines in the histogram for  $p$  and  $r$  values represent random error, the value giving equal likelihood to tie right handed trefoils as tie left and equal likelihood to repeat the previous knot as not. We see from the difference between the bars in the histogram and these lines that the posterior value for  $r$  represents non-random error, with the value for  $r$  closer to 1 than 0.5 but the value for  $p$  well spread and close to representing 0.5 and random error.

These data were generated to simulate the tying of granny and reef knots in a population, using the experimental data to sample that population. Looking at each parameter in turn we can discuss the biases in the population by looking at the mean and standard deviation at 2 decimal places for each parameter.

Parameter	Mean	Standard Deviation
$p$	0.50	0.28
$g$	0.39	0.07
$r$	0.66	0.24
$s$	0.81	0.08

Table 3.4: Mean parameter values simulated from experiment, with acceptance interval  $d(O, S) \leq 0.0075$

We first look to the posterior right handed trefoil bias  $p$ . The  $p$  distribution for the parameter  $p$  is well spread and centered around random error. The distribution is centered at 0.5 contrasting the mean proportion, 0.32, of right handed trefoils tied observed in the asocial condition of our experiment described in Section 3.2. When analysing the trefoils tied in stage 1 of the experiment and the granny and reef knots in the second stage it looked like there would be a large emergence of left hand bias, however, using this model to analyse results it appears that there is only a very slight effect of handedness bias on the composite knots tied, although this may be fairly strong when tying a single trefoil. This apparent random error in tying composite trefoils helps preserve reef knots in the population despite a stronger repetition bias.

Next, we look to the mean value of  $g$  of 0.39 which indicates the knots are

mirrored less often than they are correctly interpreted, but are still mirrored fairly frequently. Looking back to the experimental data in Table 3.1 we see there was a high success rate of accurate knot tying but with a noticeable effect of mirroring, reflected by this value of  $g$ .

The values for  $r$  are distributed between 0.5 and 1, indicating participants are more likely than not to simply repeat the first part of the knot they tie. Again, this reflects the data shown in Tables 3.1 and 3.2, explaining the prevalence of granny knots tied over reef knots.

Finally, there is a relatively high value of  $s$  with mean value 0.81 and fairly small standard deviation, suggesting highly accurate perceived imitation. From the data in Table 3.1 we knew there was a high success rate in participants tying the knot interpreted from the video, and this is reflected by the high value of this parameter.

Assuming these values of  $p, g, r$  and  $s$  reflect the population as a whole, we can plug these values into the equilibrium equations to get the expected amount of each type of knot in the population.

The percentage of each type of granny and reef knot in the population at equilibrium, given by the mean values of  $p, g, r$  and  $s$  for simplicity, is shown in Table 3.5. This can be interpreted as the likelihood that an individual will tie each knot.

Knot	Percentage in population
LL	41.5%
RR	41.5%
LR	8.5%
RL	8.5%

Table 3.5: Percentage of each type of knot in the population at equilibria

The population evolves towards this distribution of knots as shown by the grey arrows in Figure 3.16 no matter the starting distribution. We notice that although perceived imitation  $s$  had a relatively high value, the population still evolves to a distribution of granny and reef knots determined by the biases. We see granny knots are more common than reef knots, caused by the high repetition bias and equal

proportion of both granny knots, caused by the lack of handedness bias,  $p = 0.5$ .

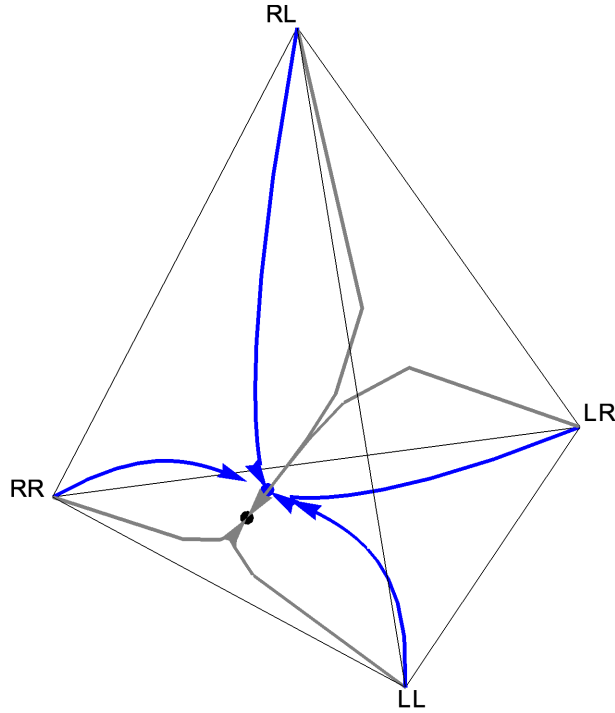


Figure 3.16: Evolutionary trajectory of frequency knots in the population using simulated parameter values

The grey arrows were plotted using the mean posterior values for the biases  $p, g, r$  and  $s$  and so represent the transmission in a population with non-random error. To contrast this the blue arrows represent the effect of random error on knot transmission, with random error being no mirroring occurs  $g = 0$ , equal likelihood to tie either handed trefoil  $p = 0.5$  and equal likelihood to repeat the previous knot tied as not  $r = 0.5$ . We see that there is not much difference between the position of the blue and black dot, with the parameter  $p$  having the same value in both cases, but the difference in values of  $r$  causes the difference in position of the two dots.

The usage of the mean posterior values in Figure 3.16 results in the grey arrow's smooth evolutionary trajectory. This gives the assumption that the parameter values are constant for each generation, however given the distribution of parameter values seen in Figure 3.15 it may be more accurate to the sample from that distribution to simulate evolutionary frequencies each generation. Taking parameter values in

this way, the result gives evolutionary frequencies distributed around the values resulting from taking the mean posterior values as constant parameter values for each generation, as can be seen in Figure 3.17.

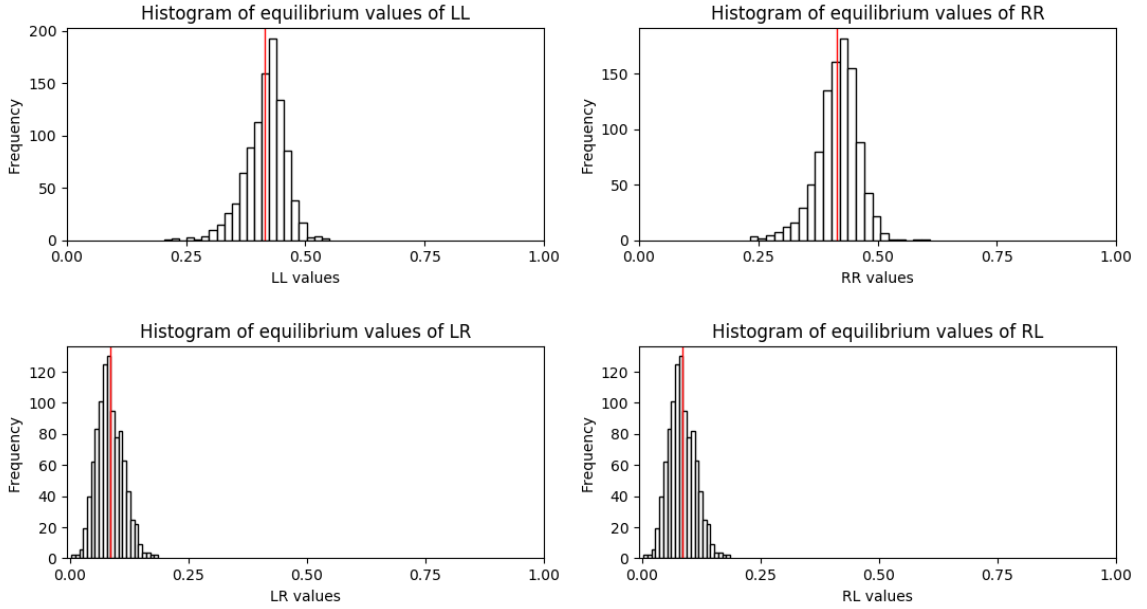


Figure 3.17: Equilibrium values of LL, RR, LR and RL determined by sampling from the distribution of parameter values. The red lines on each plot denote the equilibrium values determined by taking mean parameter values constant over generations

Knot	Percentage in population	
	Non-Random Error	Random Error
LL	41.5%	37.5%
RR	41.5%	37.5%
LR	8.5%	12.5%
RL	8.5%	12.5%

Table 3.6: Percentage of each type of knot in the population at equilibria under random and non-random error

Table 3.6 gives the expected percentage of knots in the population after transmis-

sion under both non-random and random error conditions, grey and blue trajectories respectively in Figure 3.16. Under non-random error we see a larger percentage of granny knots in the population than under random error. The non-random biases make granny knots more prevalent in the population and reduce the frequency of reef knots.

Under random error we may expect all knots to be equal in frequency but we see that granny knots have a much higher frequency than reef knots. Random error occurs when there is equal likelihood to tie either handed trefoil and equal likelihood to repeat the previous knot tied as not. Figure 3.18 gives a tree for tying each knot without demonstration.

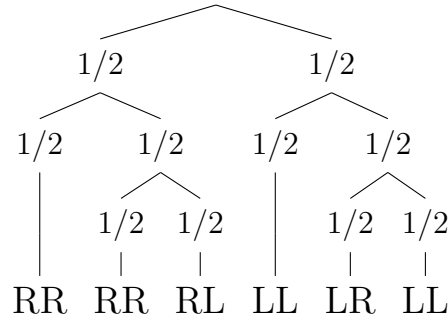


Figure 3.18: Tree showing knots tied given handedness and repetition biases

From this tree we can read off the probability of tying each knot with  $P(LL) = \frac{3}{8}$  and  $P(RR) = \frac{3}{8}$ , and  $P(RL) = \frac{1}{8}$  and  $P(LR) = \frac{1}{8}$ .

We can also calculate the probability of transmission of each knot within the population. This is the likelihood that when a particular knot is demonstrated the given knot is tied by the learner, calculated from the equations in Appendix A.1.3. Table 3.7 gives the probability of transmission of each knot.

		Knot demonstrated			
		LL	RR	LR	RL
Knot tied	LL	57.0%	37.0%	3.0%	3.0%
	RR	57.0%	37.0%	3.0%	3.0%
	LR	14.5%	14.6%	43.1%	27.8%
	RL	14.5%	14.6%	27.8%	43.1%

Table 3.7: Probability of tying each knot given knot shown using simulated parameter values under a parametric approach

We see from Table 3.7 that the probability of transmission of the granny knots is higher than the reef knots. Given that the value of  $s$  in this population is assumed to be high, we see that the probability of transmission of tying any given knot is reduced by the other parameters. The value  $r$  causes a bias towards repetition in the population, increasing the cultural fitness of the granny knots but the value of  $p$  helps preserve transmission of the reef knots.

### Comparing approaches

The values shown in Table 3.7 can be compared with the equilibria found using the transmission matrix in Section 3.2.

		Knot demonstrated			
		LL	RR	LR	RL
Knot tied	LL	53.8%	36%	16.7%	24%
	RR	34.6%	60%	16.7%	4%
	LR	3.8%	0%	33.3%	24%
	RL	7.7%	4%	33.3%	48%

Table 3.8: Probability of tying each knot given knot shown using transition matrix under a linear approach

Table 3.8 gives the probability of tying each knot given the knot shown from



the transition matrix approach. We see a difference in the probability of each knot type between the approaches. The linear approach shows that the probability of transmission of the LL granny is the highest but the parametric approach has both granny knots with equal fitness, from the random handedness bias when composite knots are tied. The transition matrix assigns different probabilities to the transmission of both reef knots whereas the parametric gives the same probability. The transition matrix approach assumes the transmission of these knots is linear and the first step is all the transmission is based on, not taking into account any other data. The parametric approach assumes more information is needed parametrisation of the transmission process based on the features of each knot. Although the model does not assume the reef knots are the same knot mathematically the parametrisation of the transmission process results in the same equations at equilibria for both reef knots shown in Equations A.1.7 and A.1.8 in Appendix A.1.4. As the knots are the same mathematically as shown in their Jones polynomial in Equation 3.1.3 the features present in each knot are the same, resulting in the equivalence in equations.

Table 3.9 shows the difference between both approaches in the frequency of each knot at equilibria. We see again the same high frequency of both granny knots in both approaches with the frequency of LL slightly higher than RR in the linear approach. However the frequency of both reef knots at equilibria is different in the linear approach, with their equivalence in the parametric approach again a consequence of the parametric approach taking into account the features present in each knot.

	Percentage in population	
Knot	Parametric Approach	Matrix Approach
LL	41.5%	40.1%
RR	41.5%	39.1%
LR	8.5%	13.6%
RL	8.5%	7.2%

Table 3.9: Percentage of each type of knot in the population at equilibria calculated using the parametric model and calculated using transition matrix

## 3.5 Conclusion

In this chapter we have discussed an experiment and model comparing the transmission success of granny and reef knots. Through experimental data we have seen that granny knots are more commonly correctly replicated than reef knots. The reasons for this were then explored using a model including four learning bias parameters; mirroring, accurate imitation, handedness and repetition.

By using Approximate Bayesian Computation to fit the model to experimental data, we saw that the participants in the experiment may have been unlikely to mirror the demonstrated knot and likely to accurately imitate the perceived knot, with a wide spread of bias towards tying handed trefoils and a bias towards repeating the first knot tied when given no guidance. By taking these participants to represent a sample of the population we could predict the evolution of these knots through future generations.

This modelling approach was also compared with a linear transmission matrix approach and the difference in equilibria states discussed. The transmission matrix gave an idea about the way in which these knots would be transmitted throughout the population but the parametric equations were needed to discuss the biases facilitating this transmission.

The biases discussed throughout the paper greatly effect the fidelity of cultural transmission of these knots, guiding the cultural evolution of knots tied. Although

accuracy of imitation of perceived information was found to be relatively high, a value of 0.79, the fidelity of knot transmission was affected by the other biases. The biases discussed were specific to the knots involved, but as the granny and the reef are two of the simplest knots and knots are a universal and ancient technology, this effect may be relevant to other cultural transmission.

Smith [72] discusses evidence to show that the biases of individual learners affects the stability of language. It was found through comparing models and experimental data that learners approach language learning tasks with individual biases, affecting the ease of learning of different language systems. These biases will be reapplied during the transmission of language, dictating the language systems seen in populations. In this way, language is dictated by non-random errors, as individual biases have a strong affect on the fidelity of transmission.

We present a further example of the effect of non-random errors on cultural evolution. Although individuals may be imitating the information they perceive extremely accurately, individual barriers limit and shape cultural transmission.

Non-random errors shape the evolution of knot tying. Under analysis of the knots formed from the composition of two trefoils in the Ashley Book of Knots [8], the granny knot appears in 75% of cases and the reef in 25% [46]. This is in line with the results found for the transmission of granny and reef knots in Table 3.6 exactly matching the equilibrium frequencies for random error and close to those for non-random error displayed in Figure 3.16.

One bias discussed here was mirroring, a well known issue relating to the correspondence problem [64]. The issue of interpreting mirrored actions has been discussed to be one of the largest barriers to accurate imitation, an effect seen in the transmission of these knots. Another bias discussed was handedness of the knots tied. This may related to the handedness of the individuals as shown in Appendix A.1.1 affecting the performance in the experiment. The final bias discussed was repetition, relating to the trefoils tied in each knot. The effects of repetition have been discussed in experiments showing improved performance in problem solving [73] and language learning [74]. However repetition has not always been shown to improve imitation but sometimes is shown to suppress neural activity [75], suggesting that

the effect of repetition is context specific. Nevertheless the factors discussed above of mirroring, handedness and repetition may need to be considered when approaching cultural evolution.

The model and experiment only considered the aspects affecting the reproduction of these knots, no functionality of the knots was considered. The model could be further extended to include preference for the reef knot, as it could be considered to be preferable to the granny. The model could also be applied to more complicated knots and other technology, by altering the parameters to best suit the technology. The factors influencing these biases were not explored through this analysis, just the presence and effect they have on the learning process. Future work could be done into the causes of these biases whether they were caused through prior learning of knot tying or from other factors.

The shoelace knot commonly tied is generally in the form of either a slipped granny knot or a slipped reef knot, with the reef knot being less likely to come undone. Using the data from the experiment and model, this suggests over 80% of the population are tying their shoelaces with a slipped granny knot, causing laces liable to come undone.

The experimental data and model suggested that there was a high level of accurate imitation in the population but that this was not the most important factor in successfully replicating the demonstrated knot. The bias towards repetition caused a prevalence in granny knots. On the individual level a bias was seen towards tying left handed trefoils, but when analysing the experimental results using ABC on a population level, it appeared the handedness bias was not as influential when tying double trefoil knots. The non-random errors caused by these biases greatly affect the frequency knots tied within a population, but the effects may be different when viewed at the individual and the population level.

This suggests that high levels of accurate imitation are not enough to maintain fidelity in the transmission of information, causing a mutation in information and technology through cultural evolution. The individual biases shape cultural evolution, causing a preference for a particular form of information or technology that cannot be controlled by accurate imitation. This suggests that the effect of non-

random errors on the imitation process is an important factor to consider in cultural evolution, but there may be a difference in the effect of these biases at the individual and population level. We have seen the effect of specific errors on the tying of some of the simplest knots and may expect similar errors to affect the evolution of other information and technology.

# Chapter 4

## A social and asocial learning model of knot transmission

### 4.1 Introduction

Knots appear in many disciplines and many forms, they are tied in material and used for many purposes [8], appear in protein structures [76] and DNA [77] and appear seemingly spontaneously in items such as telephone cords [78].

There are various models used in different disciplines to assess the formation and replication of knots [79]. These models use various methods to analysing random knots from those arising from random walks on a grid to exploring planar projections.

When considering the knots tied by humans the distribution in knots tied is varied [8] [46]. These knots have been tied by many people over many years and so we expect the knots used to have been guided by a process of social learning. In order to analyse this an analysis similar to the formation of knots in DNA through crossing changes may be appropriate.

The analysis of the change in the topology of DNA through topoisomerases, enzymes that change the crossing type in DNA, was analysed by Hua et al. [80]. They build a Markov Chain of Dowker-Thistlethwaite (DT) Codes [45], discussed in Chapter 1, of various knot types to simulate strand passage on DNA by topoisomerases. This is represented by a transition matrix representing the probability of a knot type becoming another through a strand passage process. This model

results in unknotting behaviour as knots can only simplify through the process of strand passages or crossing changes, causing knots to deform to the unknot over successive generations. The process of crossing changes in this way may be similar to the process of knot type deformation through teaching and learning and can be seen through the prevalence of the unknot in ABOK through the deformation of knot types over generations. However more complex knots do appear in ABOK so we ask is crossing changes the only method of transition to consider?

Cantarella et al. [81] discuss the fertility and lineage of knot types. A knot  $K$  is a parent of a knot  $H$  if  $H$  can be formed through a process of crossing changes on a minimal diagram of  $K$ ,  $H$  is then called a descendant of  $K$ . The descendant knots will have crossing number less than or equal to the parents, with a knot being both its own parent and descendant. Some knots are more fertile than others meaning they can be decomposed into more knots than others through crossing changes. This analysis is similar to that resulting from crossing changes on DT Codes discussed by Hua et al. [80].

In order to preserve the complexity of knot a method of transition other than crossing changes will be necessary.

Crossing changes can be thought of as an adaptation to a socially learned variant of the knot, with the knot demonstrated to a learner who may inherit the knot socially, replicating the crossings present in the knot. In order to increase the complexity of the knot crossing additions must be considered and as these additions can be considered independent of the demonstrated knot, can be assumed to be formed through an asocial learning process.

We now formulate a model of both social and asocial learning on knot types, with social learning given by crossing changes on knot types and some asocial learning to maintain complexity and prevent total deformation over generations to the unknot. A knot will be assumed to be demonstrated between a teacher and a learner, with the learner able to socially learn the knot correctly or incorrectly by making crossing changes on the knot. The learner can then add asocial learning by adding a crossing to the knot, increasing the complexity of that knot.

## 4.2 Model of social and asocial learning

In order to consider the evolution of knot types we consider a two parameter model on braid words whose closures represent knots and links. Crossings in the braid word are replicated correctly with probability  $s$  and incorrectly with probability  $1 - s$ , with the addition of a single crossing occurring with probability  $a$  and no crossings added with probability  $1 - a$ . Both parameters  $a$  and  $s$  are real numbers and take values in the interval  $[0, 1]$ . The parameters  $s$  and  $1 - s$  apply to individual crossings in the braid, with  $\sigma_i$  in the braid word replicated correctly with probability  $s$ , causing a left over right crossing  $\sigma_i$  to be adopted. However, if the crossing is replicated incorrectly with probability  $1 - s$ , it is adopted as  $\sigma_i^{-1}$ , a right over left crossing as opposed to left over right. The notation related to braid words is described in Figure 1.6 in Chapter 1.

The replication of crossings represents social learning, as the knot tied is influenced by a previous form, and the addition of new crossings represents asocial learning. Social learning takes place adopting the form of the knot tied with asocial learning occurring afterwards, adding a crossing to the adopted knot's form.

We consider the action of these parameters on each braid word in a given braid group up to a certain length  $n$  and explore the resulting braids. The closure of these braids result in knots or links and so we can see the affect of the probability of crossing additions and changes on the knots and links resulting from these braid words. From these we can build a network showing the probability of a knot or link transitioning to another through crossing changes and additions for some braid closure projection of the knots and links. In order to ensure a closed system, braid words of up to length  $n$  are considered and crossing additions on braid words of length  $n$  are assumed not to occur.

This system will give the frequency of a knot or link as a function of the probability of the knot or link in a previous iteration and the parameters  $a$  and  $s$ . This gives a “memoryless system” and so forms a Markov Chain [29], similar to that used by Hua et al. [80], representing the frequency a knot or link is tied in one generation on its frequency in the previous along with the parameters.



### 4.2.1 Braid words on two strands

The braid words on two strands are formed of compositions of  $\sigma_1$  and  $\sigma_1^{-1}$ . We consider all compositions of  $\sigma_1$  and  $\sigma_1^{-1}$  up to a length of eight and consider the effect of crossing additions and changes on those words. For words of length eight, only crossing changes are considered to ensure a closed system including only braids with a length of up to eight. Length eight is chosen as it includes the most common knots and links seen in the Ashley Book of Knots (ABOK).

**Example 4.2.1** The braid word  $\sigma_1\sigma_1$  represents a braid on two strands whose closure is the link  $L2a1$ .

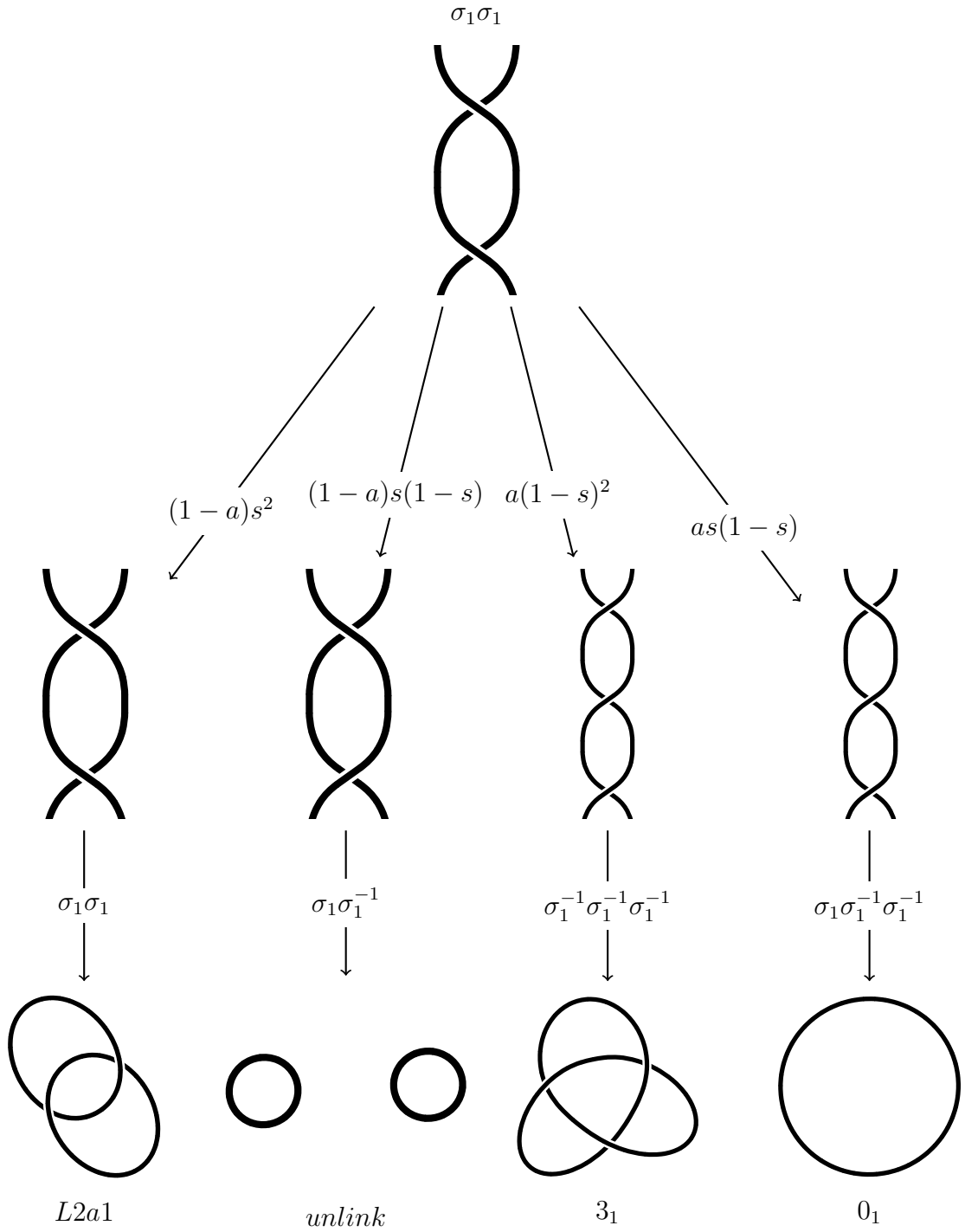


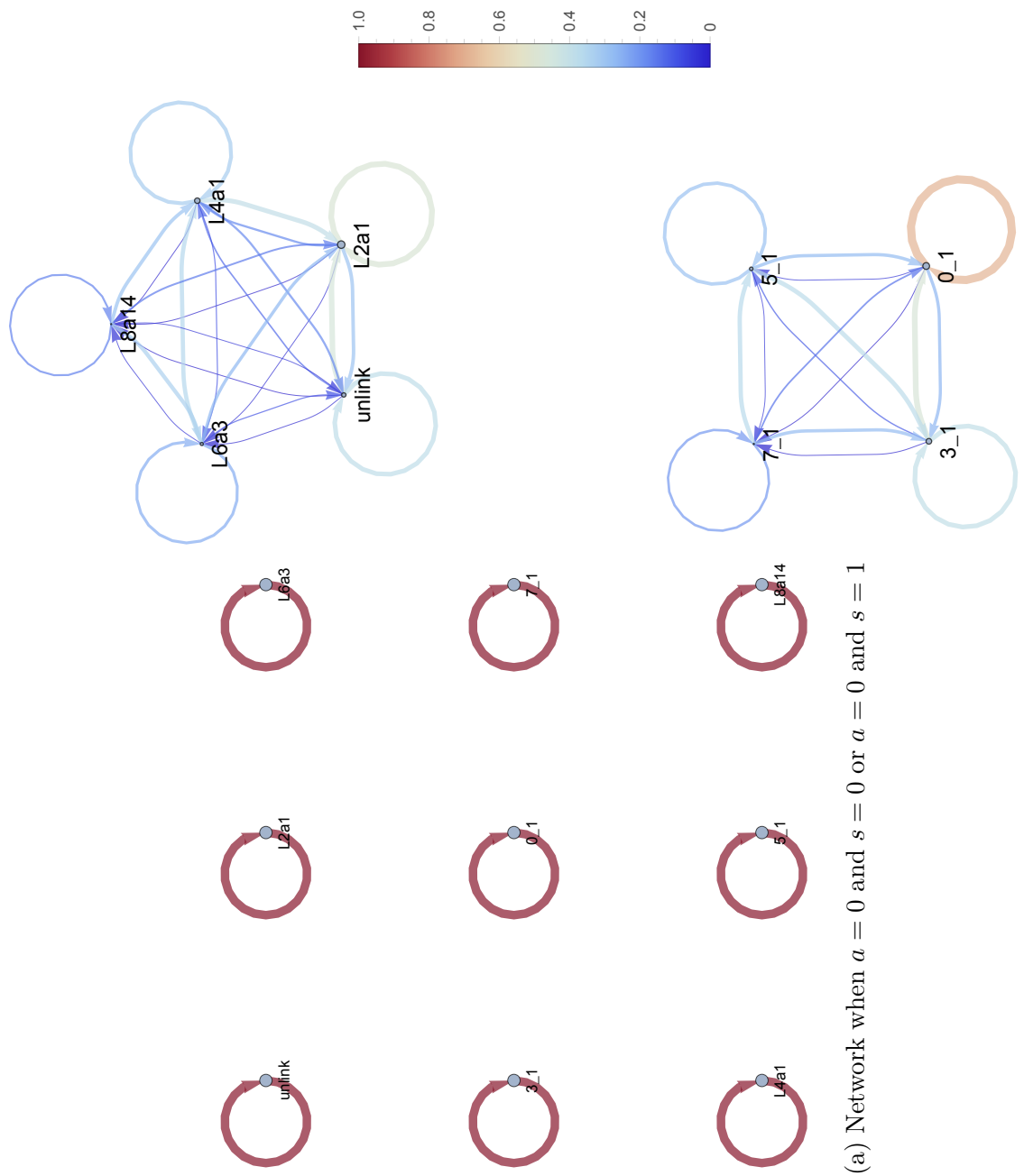
Figure 4.1: Example of some crossing changes on the braid word of  $L2a1$  given by the closure of the braid  $\sigma_1 \sigma_1$ . Both crossings in the braid word are socially learned correctly and no crossings added with probability  $(1-a)s^2$  to result in  $L2a1$ . One crossing in the braid word is socially learned correctly and one incorrectly and no crossings added with probability  $(1-a)s(1-s)$  to result in the *unlink*. Both crossings in the braid word are socially learned incorrectly and one crossing added with probability  $a(1-s)^2$  to result in the trefoil,  $3_1$ . One crossing in the braid word is socially learned correctly and one incorrectly and one crossing added with probability  $as(1-s)$  to result in the unknot,  $0_1$ .

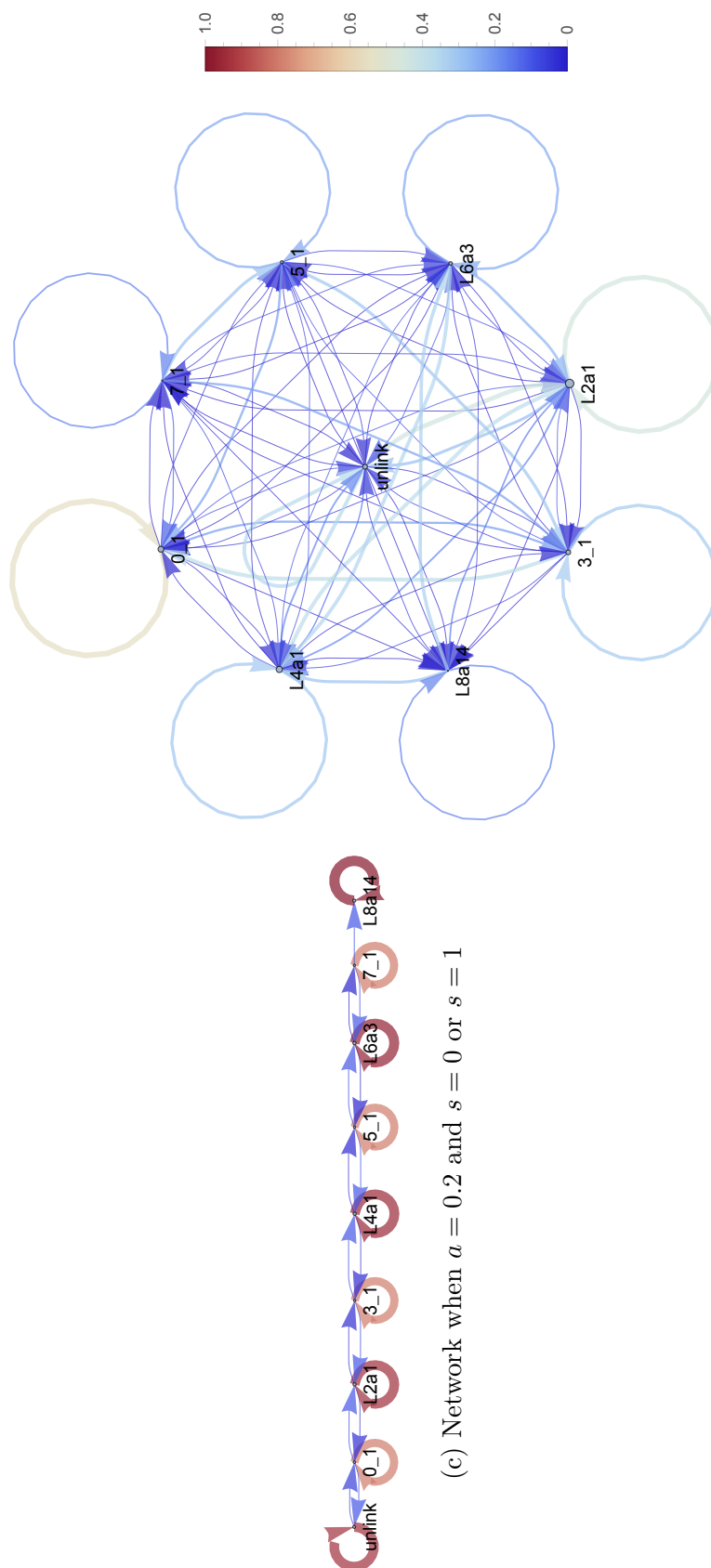
The probability of knots and links resulting from all possible crossing changes and additions are given in Table 4.1.

Braid word	Probability	Resulting knot or link
$\sigma_1\sigma_1$	$(1-a)s^2$	$L2a1$
$\sigma_1\sigma_1^{-1}$	$(1-a)s(1-s)$	$Unlink$
$\sigma_1^{-1}\sigma_1$	$(1-a)(1-s)s$	$Unlink$
$\sigma_1^{-1}\sigma_1^{-1}$	$(1-a)(1-s)^2$	$L2a1$
$\sigma_1\sigma_1\sigma_1$	$\frac{1}{4}as^2$	$3_1$
$\sigma_1\sigma_1\sigma_1^{-1}$	$\frac{1}{4}as(1-s)$	$0_1$
$\sigma_1\sigma_1^{-1}\sigma_1$	$\frac{1}{4}a(1-s)s$	$0_1$
$\sigma_1\sigma_1^{-1}\sigma_1^{-1}$	$\frac{1}{4}a(1-s)^2$	$0_1$
$\sigma_1^{-1}\sigma_1\sigma_1$	$\frac{1}{4}as^2$	$0_1$
$\sigma_1^{-1}\sigma_1\sigma_1^{-1}$	$\frac{1}{4}as(1-s)$	$0_1$
$\sigma_1^{-1}\sigma_1^{-1}\sigma_1$	$\frac{1}{4}a(1-s)s$	$0_1$
$\sigma_1^{-1}\sigma_1^{-1}\sigma_1^{-1}$	$\frac{1}{4}a(1-s)^2$	$3_1$
$\sigma_1\sigma_1\sigma_1$	$\frac{1}{4}as^2$	$3_1$
$\sigma_1\sigma_1\sigma_1^{-1}$	$\frac{1}{4}as(1-s)$	$0_1$
$\sigma_1^{-1}\sigma_1\sigma_1$	$\frac{1}{4}a(1-s)s$	$0_1$
$\sigma_1^{-1}\sigma_1\sigma_1^{-1}$	$\frac{1}{4}a(1-s)^2$	$0_1$
$\sigma_1\sigma_1^{-1}\sigma_1$	$\frac{1}{4}as^2$	$0_1$
$\sigma_1\sigma_1^{-1}\sigma_1^{-1}$	$\frac{1}{4}as(1-s)$	$0_1$
$\sigma_1^{-1}\sigma_1^{-1}\sigma_1$	$\frac{1}{4}a(1-s)s$	$0_1$
$\sigma_1^{-1}\sigma_1^{-1}\sigma_1^{-1}$	$\frac{1}{4}a(1-s)^2$	$3_1$

Table 4.1: The possible braids resulting from crossing changes and additions on the braid word  $\sigma_1\sigma_1$  with probabilities in terms of  $s$  and  $a$  and the knot or link corresponding to the closure of that braid. The probability of an addition is assumed to be the same regardless of addition or sign, so the probability of an addition is divided by the amount of possible additions, in this case 4, to ensure the probabilities sum to one. The knots and links resulting from these changes and additions are  $L2a1$  itself, the trefoil knot  $3_1$  which has higher crossing number than  $L2a1$ , the unknot  $0_1$  and unlink, which both have no crossings.

Example 4.2.1 contains the probability of knots and links resulting from a particular braid closure projection of  $L2a1$ . There are other braid closure projections on two strands that give  $L2a1$  and so we combine the probabilities resulting from all these braid words to get overall probabilities of knots and links resulting from any braid word projection on two strands. These probabilities are represented in the below networks for various values of  $a$  and  $s$ .





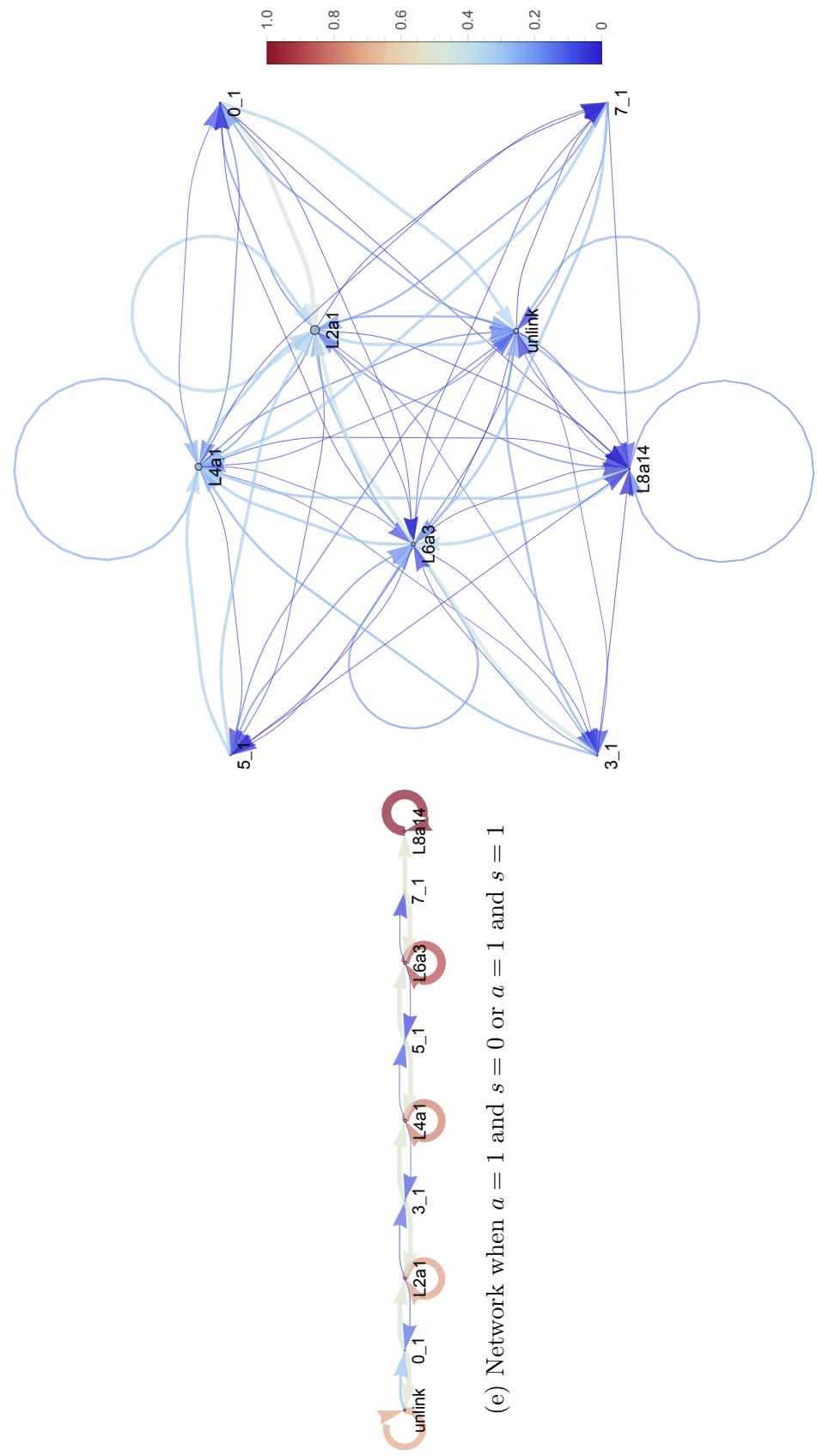


Figure 4.2: The six different forms of network graph are given in Figures 4.2a - 4.2f for various values of  $a$  and  $s$ . The size of each node represents the likelihood of each knot or link named on the node and the colour and thickness of the edges represents the likelihood of transition between two knot or link types.

Figure 4.2a applies for values  $a = 0$  and  $s = 0$  and  $a = 0$  and  $s = 1$  and represents the cases when no crossing additions occur and all crossings are either correctly replicated or all incorrectly, resulting in a mirror image of the given knot or link and so the same type tied. We see in this case that all knot and link types are correctly replicated with no transition between types.

Figure 4.2b applies for values  $a = 0$  and  $s = 0.2$  and has the same form for values  $a = 0$  and  $0 < s < 1$  with the edge and vertex weights differing. This is the case when no crossing additions occur but crossings are not always replicated solely correctly or incorrectly. This causes some transition between link types. As no crossing additions occur on the braid word, it is only possible for a knot to be replicated as a knot and a link as a link, giving the two disjoint graphs.

Figure 4.2c applies for values  $a = 0.2$  and  $s = 0$  or  $s = 1$  and has the same form for values  $0 < a < 1$  and  $s = 0$  or  $s = 1$  with the edge and vertex weights differing. This is the case where crossings are either all replicated correctly or all incorrectly and some addition of crossings occurs. This causes some transition of knots and links increasing or decreasing crossing number by one, with some replication of knots and links as themselves.

Figure 4.2d applies for values  $a = 0.2$  and  $s = 0.2$  and has the same form for values  $0 < a < 1$  and  $0 < s < 1$  with the edge and vertex weights differing. This is the case when some crossing additions occur but crossings are not always replicated solely correctly or incorrectly. This causes a lot of transition between knot and link types, including from knots to links and vice versa, with some replication of knots and links as themselves.

Figure 4.2e applies for values  $a = 1$  and  $s = 0$  and  $a = 1$  and  $s = 1$ , the case where crossings additions always occur and all crossings are either correctly replicated or all incorrectly. This causes some transition of knots and links increasing or decreasing crossing number by one, with some replication of knots and links as themselves. As crossing additions are assumed not to occur for braid words of length eight, the links which have braid words of length eight will be replicated as themselves, but no knots have braid word of length eight and so we see no correct replication of knots in this network.



Figure 4.2f applies for values  $a = 1$  and  $s = 0.2$  but has the same form for values  $a = 1$  and  $0 < s < 1$  but the edge and vertex weights differ, the case where crossing additions always occur but crossings are not always replicated solely correctly or incorrectly. This causes a lot of transition between knot and link types but, as in Figure 4.2e knots cannot be replicated as themselves as any braid word representing them will have a crossing added.

From these graphs we can see the fertility level of each knot for each range of parameters. This is the number of knots or links which result from any braid word projection on two strands up to eight crossings of a given knot or link, representing the number of descendants a link has. The fertility level here is analogous to that discussed by Cantarella et al. [81] in which the fertility level of a knot was determined by the number of knots that resulted from some crossing changes on any projection of the given knot. In this case the fertility level is given for knots and links and is determined by the number of knots or links resulting from crossing changes and additions on projections resulting from braid representations of the knot or link.

Parameter values	Descendants								
	$0_1$	$L2a1$	$Unlink$	$3_1$	$L4a1$	$5_1$	$L6a3$	$7_1$	$L8a14$
$a = 0$ and $s = 0$ or $s = 1$	1	1	1	1	1	1	1	1	1
$a = 0$ and $0 < s < 1$	4	5	5	4	5	4	5	4	5
$0 < a < 1$ and $s = 0$ or $s = 1$	3	3	2	3	3	3	3	3	1
$0 < a < 1$ and $0 < s < 1$	9	9	9	9	9	9	9	9	5
$a = 1$ and $s = 0$ or $s = 1$	2	3	2	2	3	2	3	2	1
$a = 1$ and $0 < s < 1$	5	9	9	5	9	5	9	5	5

Table 4.2: Fertility levels for each knot for a range of parameters. This is given by the amount of descendants each knot or link has, shown in Figure 4.2 by the arrows coming out of each node.

Table 4.2 gives the number of descendants for each knot or link given parameter values.

When  $a = 0$  and  $s = 0$  or  $s = 1$  all knots and links have only one descendant as they will be all replicated correctly as themselves.

When  $a = 0$  and  $0 < s < 1$ , all the knots have four descendants whereas the links have five. This is due to each knot being able to transition into every other knot and each link transitioning into the other links, with there being four knots and five links overall.

When  $0 < a < 1$  and  $s = 0$  or  $s = 1$ ,  $L8a14$  has one descendant and the *unlink* has two, whilst the rest of the knots and links have three. As all crossings in the knots and links are replicated correctly the only way knots and links can transition is through crossing additions. As no crossing additions are assumed to be possible for braid words of length eight,  $L8a14$  can only have itself as a descendant. The other knots and links have themselves and the knot or link one crossing number higher and lower resulting in three descendants, but the *unlink* can only become itself or  $0_1$ .

When  $0 < a < 1$  and  $0 < s < 1$ ,  $L8a14$  has five descendants whilst the others have nine. This is due to the assumption that crossings are not added on a braid word of eight crossings and so the only knots and links  $L8a14$  can become are those that result from crossing changes.

When  $a = 1$  and  $s = 0$  or  $s = 1$ ,  $L2a1$  and  $L4a1$  have three descendants,  $L8a14$  one and the others two. This is similar to case  $0 < a < 1$  and  $s = 0$  or  $s = 1$  but now crossings are always added.  $L2a1$  and  $L4a1$  and  $L6a3$  have projections that have braid length eight and as it is assumed that no crossings are added at length eight, they have to be replicated as themselves giving an extra descendant each.

When  $a = 1$  and  $0 < s < 1$  the knots and  $L8a14$  have five descendants whilst the other links have nine. This is again due to the assumption that crossings are not added to a braid word of length eight.

We can also look at the amount of parents each knot or link has, this is the amount of knots and links that have a braid projection that results in the given knot or link though crossing changes and additions.

Parameter values	Parents								
	$0_1$	$L2a1$	$Unlink$	$3_1$	$L4a1$	$5_1$	$L6a3$	$7_1$	$L8a14$
$a = 0$ and $s = 0$ or $s = 1$	1	1	1	1	1	1	1	1	1
$a = 0$ and $0 < s < 1$	4	5	5	4	5	4	5	4	5
$0 < a < 1$ and $s = 0$ or $s = 1$	3	3	2	3	3	3	3	2	2
$0 < a < 1$ and $0 < s < 1$	8	9	9	8	9	8	9	8	9
$a = 1$ and $s = 0$ or $s = 1$	2	3	2	2	3	2	3	1	2
$a = 1$ and $0 < s < 1$	4	9	9	4	9	4	9	4	9

Table 4.3: The amount of parents each knot or link has, shown in Figure 4.2 by the arrows going in to each node.

The amount of parents each knot or link has is the same as the amount of descendants for most values of  $a$  and  $s$  which is shown in Figure 4.2 by the edges going between most nodes occurring in both directions. This does not always happen, for example when  $0 < a < 1$  and  $s = 0$  or  $s = 1$  there is an edge from  $7_1$  to  $L8a14$  but not one in the reverse direction, shown in Figure 4.2c. This gives the difference in parents and descendants and is generally caused by the restriction on crossing number.

We see from Tables 4.2 and 4.3 that the number of descendants and parents for each knot and link is maximised when  $0 < a < 1$  and  $0 < s < 1$ . In this case some crossing changes and additions occur but do not always occur. This produces transition between knot and link types as  $s > 0$  and  $s < 1$  ensuring each knot and link is not always simply replicated as itself. It also ensures that complexity is maintained in the system as  $a > 0$  preventing deformation to the unknot over generations but also preventing overall evolution to the most complicated knot or link in the system as  $a < 1$ .

Equilibrium occurs in this system when the frequency of each knot type is stable over generations. The conditions for equilibria differ for parameter values.

### Case 1

Equilibrium occurs automatically when  $a = 0$  and  $s = 0$  or  $s = 1$  as each knot and link type is maintained through perfect crossing replication (or mirrored knots tied)

and no crossing additions as seen in Figure 4.2a. The frequency of each knot and link is therefore stable across generations.

### Case 2

When  $0 < a \leq 1$  and  $s = 0$  or  $s = 1$ , crossing replication is always perfect (or imperfect causing mirrored forms) and crossing additions occur, seen in both Figures 4.2c and 4.2e. In both these networks the link  $L8a14$  has no edges coming from its node to other knots of links but has one coming in. This causes the frequency of  $L8a14$  to increase over generations meaning equilibrium only occurs in this case when  $\hat{f}_{L8a14} = 1$ .

### Case 3

When  $a = 0$  and  $0 < s < 1$  the network of knots and links is represented by the disjoint graph in Figure 4.2b. In this case it is not possible for knots to change to links and vice versa meaning the evolution of these knots and links is determined by two disjoint cycles. Equilibrium still occurs in this case but is determined by the initial frequencies of each knot and link, giving the same equilibrium for all values of  $0 < s < 1$ . This equilibrium is determined by the start frequencies for each knot and link given by the following equations where  $\hat{f}_{knot}$  denotes the equilibrium frequency and  $f_{knot}$  denotes the start frequency of each knot and link. Equilibrium

occurs when

$$\begin{aligned}
\hat{f}_{0_1} &= \frac{49}{85} - \frac{49\hat{f}_{L2a1}}{38} \\
\hat{f}_{unlink} &= \frac{49\hat{f}_{L2a1}}{76} \\
\hat{f}_{3_1} &= \frac{27}{85} - \frac{27\hat{f}_{L2a1}}{38} \\
\hat{f}_{L4a1} &= \frac{35\hat{f}_{L2a1}}{76} \\
\hat{f}_{5_1} &= \frac{8}{85} - \frac{4\hat{f}_{L2a1}}{19} \\
\hat{f}_{L6a3} &= \frac{9\hat{f}_{L2a1}}{76} \\
\hat{f}_{7_1} &= \frac{1}{85} - \frac{\hat{f}_{L2a1}}{38} \\
\hat{f}_{L8a14} &= \frac{\hat{f}_{L2a1}}{76} \\
0 \leq \hat{f}_{L2a1} &\leq \frac{38}{85}
\end{aligned}$$

This is given by the start frequencies

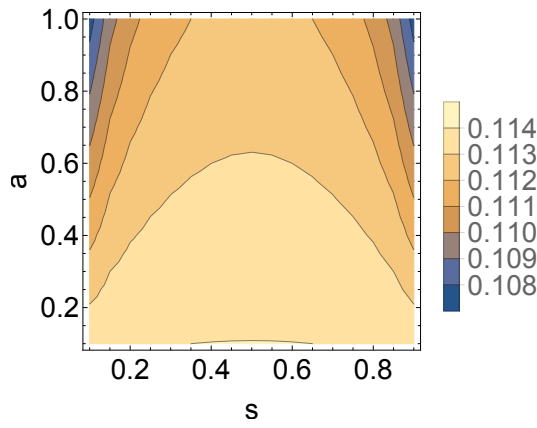
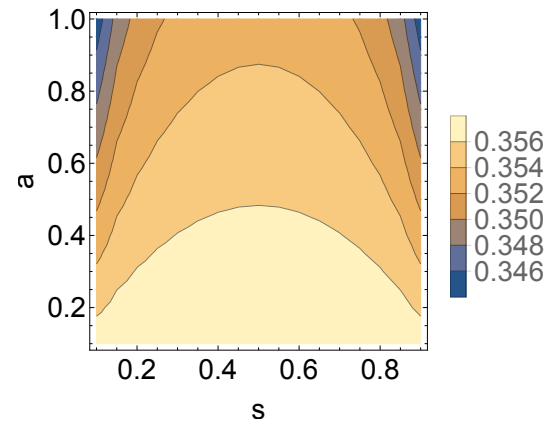
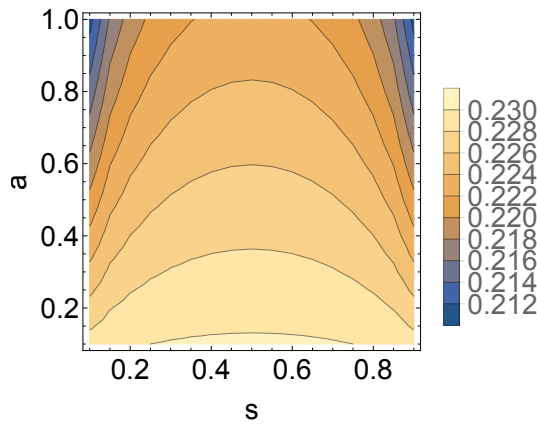
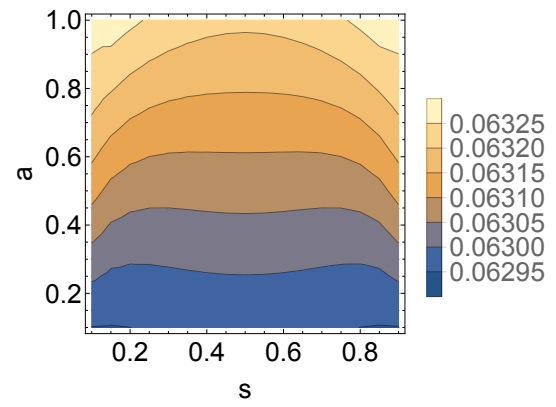
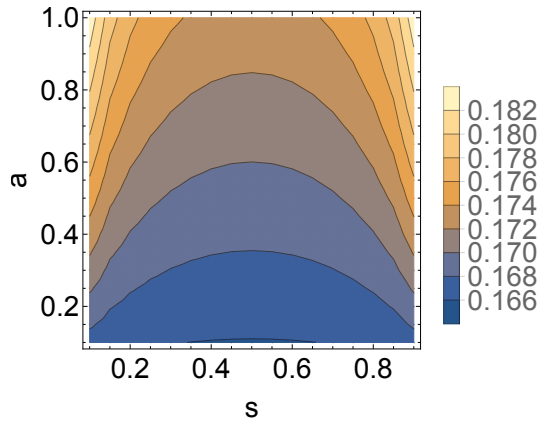
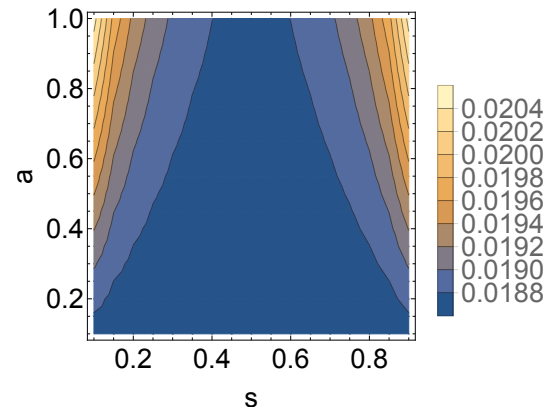
$$\begin{aligned}
\hat{f}_{0_1} &= \frac{49(f_{0_1} + f_{3_1} + f_{5_1} + f_{7_1})}{85} \\
\hat{f}_{L2a1} &= \frac{38(f_{L2a1} + f_{unlink} + f_{L4a1} + f_{L6a3} + f_{L8a14})}{85} \\
\hat{f}_{unlink} &= \frac{49(f_{L2a1} + f_{unlink} + f_{L4a1} + f_{L6a3} + f_{L8a14})}{170} \\
\hat{f}_{3_1} &= \frac{27(f_{0_1} + f_{3_1} + f_{5_1} + f_{7_1})}{85} \\
\hat{f}_{L4a1} &= \frac{7(f_{L2a1} + f_{unlink} + f_{L4a1} + f_{L6a3} + f_{L8a14})}{34} \\
\hat{f}_{5_1} &= \frac{8(f_{0_1} + f_{3_1} + f_{5_1} + f_{7_1})}{85} \\
\hat{f}_{L6a3} &= \frac{9(f_{L2a1} + f_{unlink} + f_{L4a1} + f_{L6a3} + f_{L8a14})}{170} \\
\hat{f}_{7_1} &= \frac{(f_{0_1} + f_{3_1} + f_{5_1} + f_{7_1})}{85} \\
\hat{f}_{L8a14} &= \frac{(f_{L2a1} + f_{unlink} + f_{L4a1} + f_{L6a3} + f_{L8a14})}{170}
\end{aligned}$$

We see the equilibrium frequencies of knots depend only on the start frequencies of the knots and the equilibrium frequencies of the links only on the links, which is

as expected from the network seen in Figure 4.2b.

#### Case 4

When  $0 < a \leq 1$  and  $0 < s < 1$ , represented in the networks in Figures 4.2d and 4.2f, there exists an equilibrium state determined by the parameters  $a$  and  $s$  giving the frequencies of each knot and link type. This equilibrium is not affected by the start frequencies of each knot and link as there do not exist any disjoint cycles, as in case 3, and each knot and link is present at equilibrium as there is no absorbing state, as in case 2 where frequencies evolved towards the link  $L8a14$ . The equilibrium frequencies are given by equations in two variables,  $a$  and  $s$ . Contour plots of the frequency of each knot and link at equilibrium are given in Figure 4.3 for values  $0 < a \leq 1$  and  $0 < s < 1$ .

(a) Frequency of  $0_1$  at equilibrium(b) Frequency of *unlink* at equilibrium(c) Frequency of  $L2a1$  at equilibrium(d) Frequency of  $3_1$  at equilibrium(e) Frequency of  $L4a1$  at equilibrium(f) Frequency of  $5_1$  at equilibrium

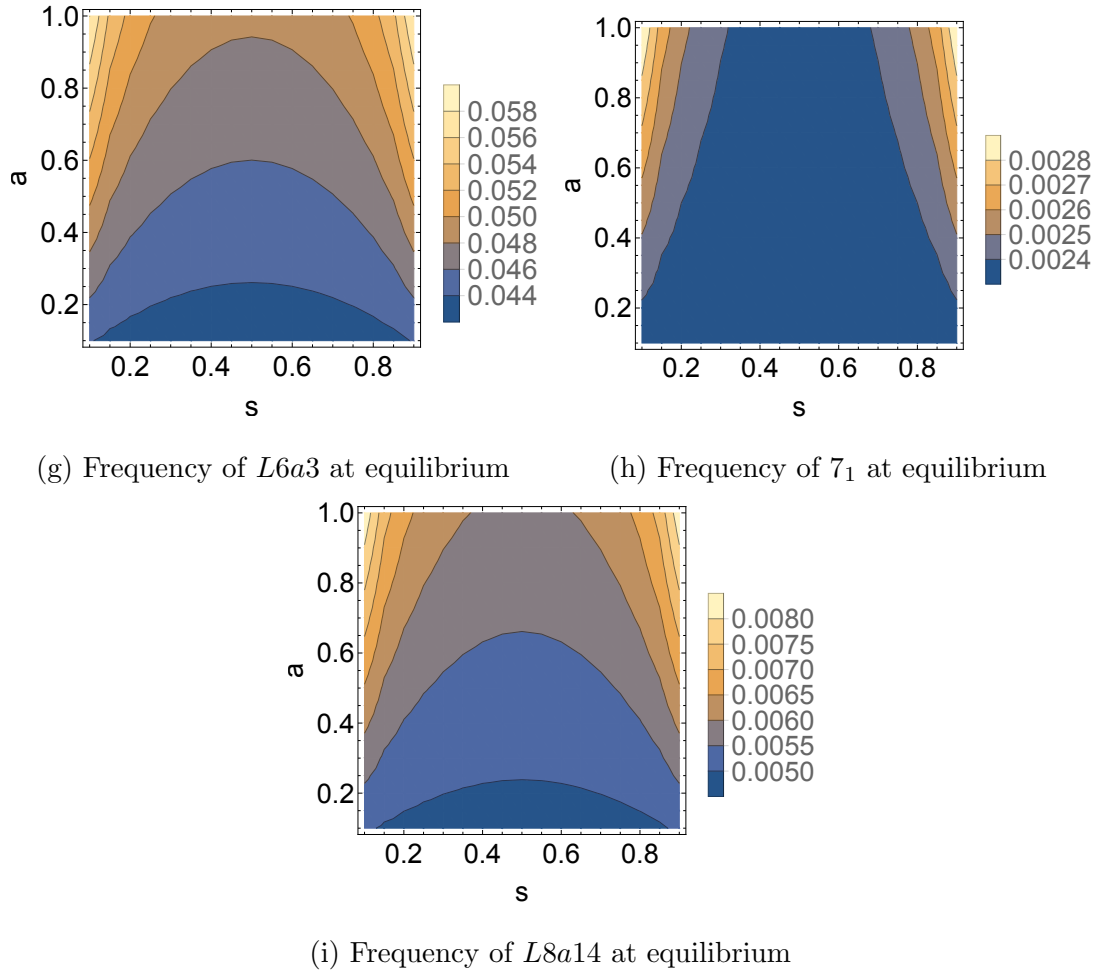


Figure 4.3: Contour plots of the frequency of each knot and link at equilibrium when  $0 < a \leq 1$  and  $0 < s < 1$ .

The frequency of  $0_1$ , *unlink* and  $L2a1$  are maximised when the value of  $s$  is around 0.5 and the value of  $a$  is relatively low, showing these links are most commonly tied through incorrect crossings and few crossing additions. The frequency of  $3_1$ ,  $L4a1$ ,  $5_1$ ,  $L6a3$ ,  $7_1$  and  $L8a14$  are maximised when  $s$  is closer to 0 or 1 and the value of  $a$  is relatively high, showing they result from the solely correct or solely incorrect replication of crossings and some crossing additions. From these plots we can see that  $L2a1$  is the most frequent knot at equilibrium, then the *unlink*, then  $L4a1$ ,  $0_1$ ,  $3_1$ ,  $L6a3$ ,  $5_1$ ,  $L8a14$  then finally  $7_1$ .

We see from these contour plots that the frequencies for each knot and link fall in a small range for different values of  $a$  and  $s$ , causing each frequency to be almost completely determined by the presence of  $a$  and  $s$ , independent of the precise value



of  $a$  and  $s$ .

The equilibrium states can be fit to the frequencies of the knots and links in the Ashley Book of Knots (ABOK), assuming the frequency of each knot in ABOK represents some stable state in the population. The frequencies in ABOK are

$$\begin{aligned}
 ABOK f_{0_1} &= \frac{111}{259} \\
 ABOK f_{L2a1} &= \frac{48}{259} \\
 ABOK f_{unlink} &= \frac{20}{259} \\
 ABOK f_{3_1} &= \frac{45}{259} \\
 ABOK f_{L4a1} &= \frac{14}{259} \\
 ABOK f_{5_1} &= \frac{12}{259} \\
 ABOK f_{L6a3} &= \frac{6}{259} \\
 ABOK f_{7_1} &= \frac{3}{259} \\
 ABOK f_{L8a14} &= 0
 \end{aligned}$$

Each case for equilibria can be discussed for the ABOK data.

**Case 1;**  $a = 0$  and  $s = 0$  or  $s = 1$

In case 1 all knots are replicated correctly with no crossings or additions and so starting with the frequencies in ABOK these frequencies are maintained at equilibrium. This assumes perfect social learning and replication over generations.

**Case 2;**  $0 < a \leq 1$  and  $s = 0$  or  $s = 1$

This case does not fit the data as it results in sole frequency of the link  $L8a14$ , whilst  $L8a14$  does not appear at all in the ABOK data.

**Case 3;**  $a = 0$  and  $0 < s < 1$

In this case the equilibrium frequencies are determined by a cycle, meaning they depend on the initial frequencies of the knots and links. In order to get the closest fit to the ABOK data, we take the ABOK data frequency for a link as the initial condition. We take  $\hat{f}_{L2a1} = ABOK f_{L2a1} = \frac{48}{259}$  and so the rest of the equilibrium

frequencies are determined;

$$\begin{aligned}
 \hat{f}_{0_1} &= 0.3375 \\
 \hat{f}_{L2a1} &= 0.1853 \\
 \hat{f}_{unlink} &= 0.1195 \\
 \hat{f}_{3_1} &= 0.1860 \\
 \hat{f}_{L4a1} &= 0.0853 \\
 \hat{f}_{5_1} &= 0.0551 \\
 \hat{f}_{L6a3} &= 0.0219 \\
 \hat{f}_{7_1} &= 0.007 \\
 \hat{f}_{L8a14} &= 0.002
 \end{aligned}$$

These frequencies give a metric value, using squared Euclidean distance;

$$\sum_{i=1}^9 (\hat{F}_i - ABOKF_i)^2 = 0.0113166$$

where  $\hat{F}$  is the vector containing the equilibrium frequencies and  $ABOKF$  the vector containing the ABOK data.

This looks to be a good fit for the data, however, this equilibrium state is determined by start frequencies for each knot and link. This gives an exact fit for the frequency of the link  $L2a1$  between the equilibrium frequency and the ABOK data lowering the metric value and improving the fit.

**Case 4;**  $0 < a \leq 1$  and  $0 < s < 1$

In this case equilibrium does not depend on the starting frequencies, it solely depends on the parameters  $a$  and  $s$ . Using Approximate Bayesian Computation and grid approximation [71] we simulate various equilibria for a range of the parameters  $a$  and  $s$ , keeping the parameter values giving the simulated data closest to the ABOK data. We use the squared Euclidean distance

$$\sum_{i=1}^9 (F\hat{sim}_i - ABOKF_i)^2$$

where  $F\hat{sim}$  is the vector containing the simulated data.

This results in a minimum metric value of 0.177309 and frequencies extremely different from the ABOK data, for example  $0_1$  has the fourth highest frequency in the simulated data whilst it has the highest frequency in the ABOK data.

A discussion of these cases suggests an absence of crossing additions and a likelihood to neither replicate all crossings correctly nor incorrectly ( $a = 0$  and  $0 < s < 1$ ) gives the best fit to the ABOK data. If the ABOK data was formed through knot tying over successive generations with these constraints this case would give the best fit but it does not seem an accurate assumption that crossings could never be added, given the appearance of knots and links with high crossing number in ABOK.

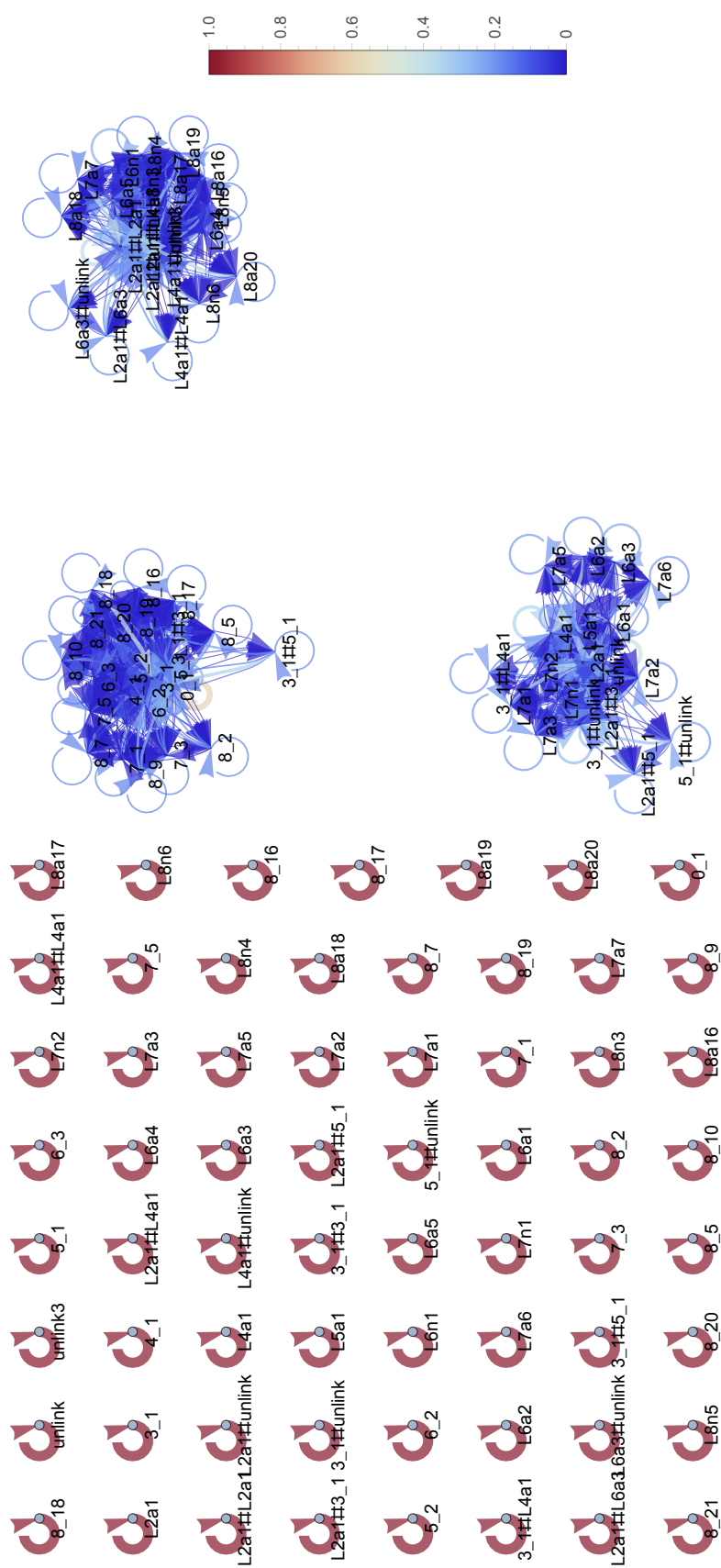
So far only knots and links resulting from braid words on two strands have been considered, we now extend analysis to braid words on three strands considering a wider range of knots and links.

### 4.2.2 Braid words on three strands

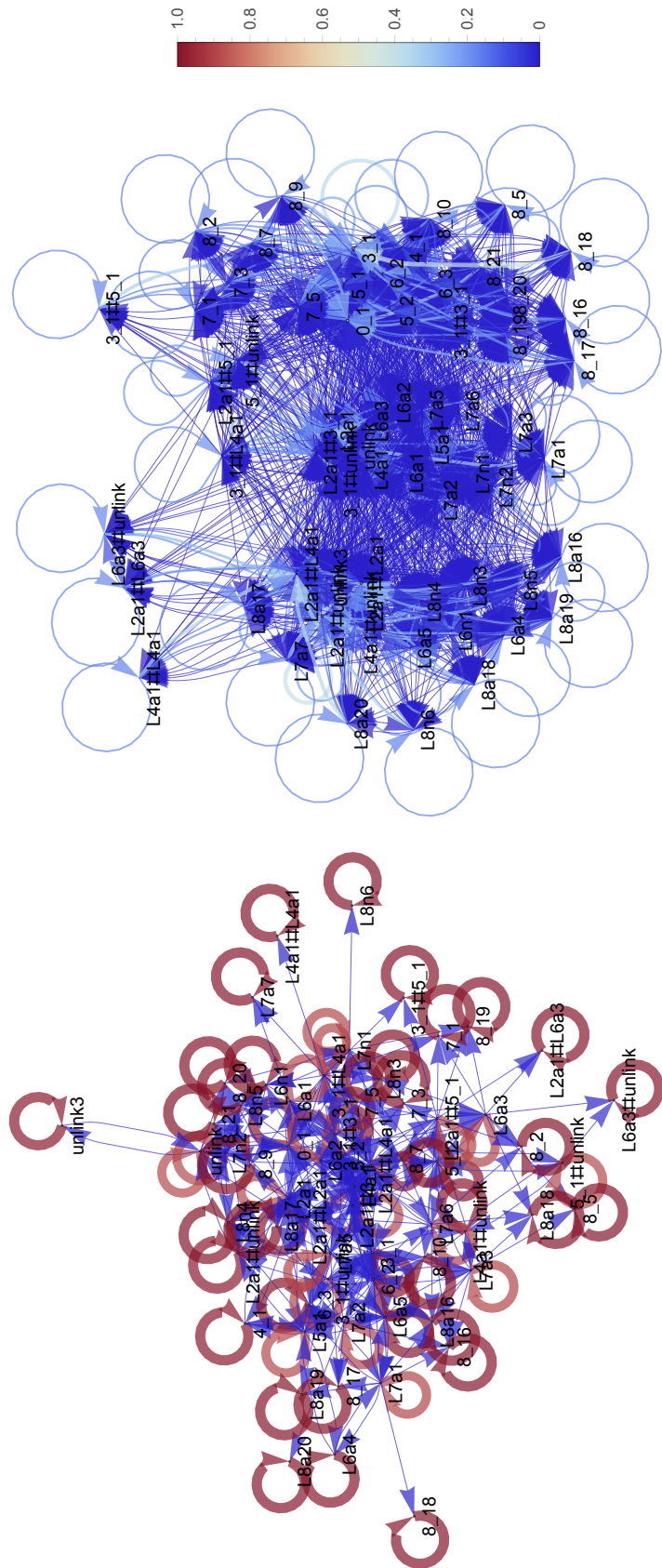
Braid words on three strands are formed of compositions of  $\sigma_1$ ,  $\sigma_1^{-1}$ ,  $\sigma_2$  and  $\sigma_2^{-1}$ . We consider all compositions of  $\sigma_1$ ,  $\sigma_1^{-1}$ ,  $\sigma_2$  and  $\sigma_2^{-1}$  up to a length of eight and consider the effect of crossing additions and changes on those words. As with the braids on two strands, for words of length eight, only crossing changes are considered to ensure a closed system including only knots and links with a length of up to eight.

As with the braid words on two strands, there are six different forms of networks representing transition between knot and link types for parameters  $a$  and  $s$ . These are given in Figure 4.4.

By considering braid words on three strands up to eight crossings we have a much wider range of knots and links than in the two strand case. There is only one prime link with crossing number up to six not included,  $6_1$ , whose minimal braid word has length seven on four strands. There are five prime links with crossing number up to seven not included, knots  $7_2$ ,  $7_4$ ,  $7_6$  and  $7_7$  and link  $L7a4$ . Of the prime knots with eight crossings only 11 appear out of 21 and of the prime links eight appear out of 29. A range of composite knots and links are included.



(b) Network when  $a = 0$  and  $s = 0.2$



(c) Network when  $a = 0.2$  and  $s = 0$  or  $s = 1$

(d) Network when  $a = 0.2$  and  $s = 0.2$

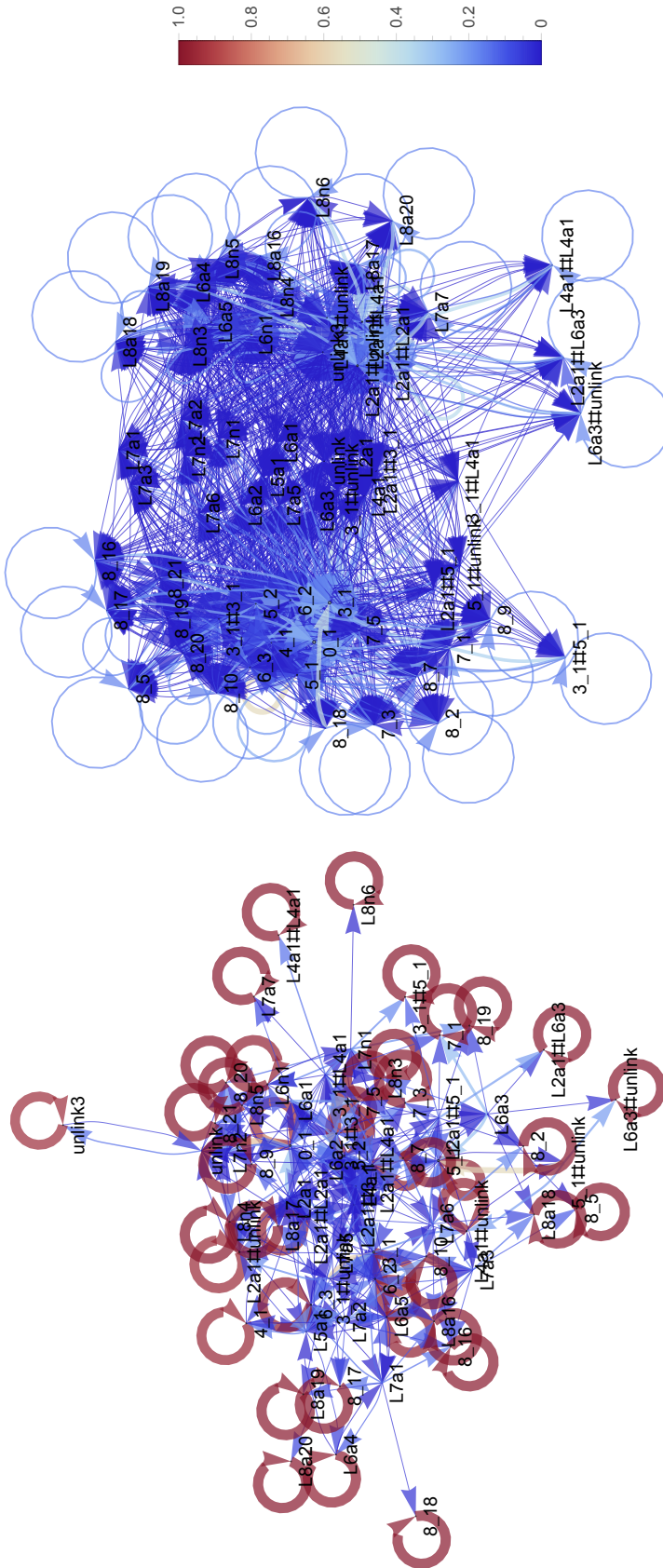


Figure 4.4: The six different forms of network graph are given in Figures 4.4a - 4.4f for various values of  $a$  and  $s$ . The size of each node represents the likelihood of each link named on the node and the colour and thickness of the edges represents the likelihood of change between two link types.

As with the case on two strands, Figure 4.4a applies for values  $a = 0$  and  $s = 0$  and  $a = 0$  and  $s = 1$ , the cases when no crossing additions occur and all crossings are either correctly replicated or all incorrectly resulting in no transition between types.

Figure 4.4b applies for values  $a = 0$  and  $s = 0.2$  but has the same form for values  $a = 0$  and  $0 < s < 1$  but the edge and vertex weights differ, the case when no crossing additions occur but crossings are not always replicated solely correctly or incorrectly. As in the case on two strands we have disjoint graphs, one including all the prime knots and the composite knots  $3_1 \# 3_1$  and  $3_1 \# 5_1$ , one including all the prime links with fewer than six crossings, some six crossing prime links and most seven crossing prime links and the composite links formed of one link and one knot component and the last the rest of the prime links and the composite links formed of two link components.

Figure 4.4c applies for values  $a = 0.2$  and  $s = 0$  or  $s = 1$  but has the same form for values  $0 < a < 1$  and  $s = 0$  with the edge and vertex weights differing, the case where all crossings are either replicated correctly or all incorrectly and some addition of crossings occurs. As correct replication or mirroring of all crossings occurs the only way to transition between link types is by crossing addition and so we get some knots and links that have an edge coming in but none in the reverse direction, for example  $8_{18}$ , giving some absorbing states.

Figure 4.4d applies for values  $a = 0.2$  and  $s = 0.2$  but has the same form for values  $0 < a < 1$  and  $0 < s < 1$  but the edge and vertex weights differ, the case when some crossing additions occur but crossings are not always replicated solely correctly or incorrectly causing a lot of transition between link types.

Figure 4.4e applies for values  $a = 1$  and  $s = 0$  and  $a = 1$  and  $s = 1$ , the case where crossings additions always occur and all crossings are either correctly replicated or all incorrectly. As with Figure 4.4c we see some absorbing states and as crossing additions always occur but some knots and links do not have a braid representation of length eight, some knots and links are never replicated as themselves.

Figure 4.4f applies for values  $a = 1$  and  $s = 0.2$  but has the same form for values  $a = 1$  and  $0 < s < 1$  but the edge and vertex weights differ, the case where crossing

additions always occur but crossings are not always replicated solely correctly or incorrectly. We again see some knots and links are never replicated as themselves, seen by the lack of a self loop on the node representing them.

The networks in the case of braids on three strands are similar to the networks for braids on two strands although the networks are much larger, containing 63 knots and link to the nine contained in the case on two strands. In both cases we see no transition of knot and link types when  $a = 0$  and  $s = 0$  and  $s = 1$ , disjoint graphs when  $a = 0$  and  $0 < s < 1$  and absorbing states in the network when  $0 < a \leq 1$  and  $s = 0$  or  $s = 1$  determining knot and link transition. Both cases include absorbing states in some networks, resulting from the assumption that no crossings are added on braids of length eight to ensure a closed system.

As with the braids on two strands, there are four cases to consider for equilibrium.

### Case 1

When  $a = 0$  and  $s = 0$  or  $s = 1$  all knots and links are replicated as themselves so equilibrium automatically occurs.

### Case 2

When  $0 < a \leq 1$  and  $s = 0$  or  $s = 1$  equilibrium is determined by the absorbing states, that is knots and links whose only descendant is themselves. These are the knots and links whose minimal braid representation on three strands has length eight and so when crossing additions are the only method to change type, it is assumed no crossings are added to them meaning they can only be replicated as themselves. These are the knots  $7_1, 7_3, 7_5, 8_2, 8_5, 8_7, 8_9, 8_{10}, 8_{16}, 8_{17}, 8_{18}, 8_{19}, 8_{20}, 8_{21}$  and  $3_1\#5_1$  and the links  $L7a7, L8a16, L8a17, L8a18, L8a19, L8a20, L8n3, L8n4, L8n5, L8n6, L2a1\#L6a3, L4a1\#L4a1$  and the *unlink* $\#L6a3$ . At equilibrium we require

$$\begin{aligned} &\hat{f}_{7_1} + \hat{f}_{7_3} + \hat{f}_{7_5} + \hat{f}_{8_2} + \hat{f}_{8_5} + \hat{f}_{8_7} + \hat{f}_{8_9} + \hat{f}_{8_{10}} + \hat{f}_{8_{16}} + \hat{f}_{8_{17}} + \hat{f}_{8_{18}} + \hat{f}_{8_{19}} + \hat{f}_{8_{20}} + \hat{f}_{8_{21}} \\ &+ \hat{f}_{3_1\#5_1} + \hat{f}_{L7a7} + \hat{f}_{L8a16} + \hat{f}_{L8a17} + \hat{f}_{L8a18} + \hat{f}_{L8a19} + \hat{f}_{L8a20} + \hat{f}_{L8n3} + \hat{f}_{L8n4} \\ &+ \hat{f}_{L8n5} + \hat{f}_{L8n6} + \hat{f}_{L2a1\#L6a3} + \hat{f}_{L4a1\#L4a1} + \hat{f}_{\text{unlink}\#L6a3} = 1 \end{aligned}$$

with the frequency of all other knots and links zero.

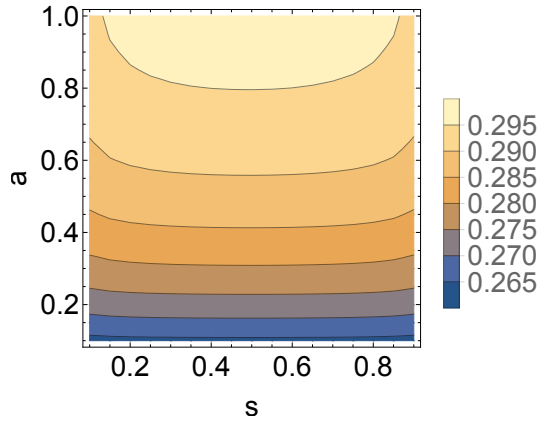
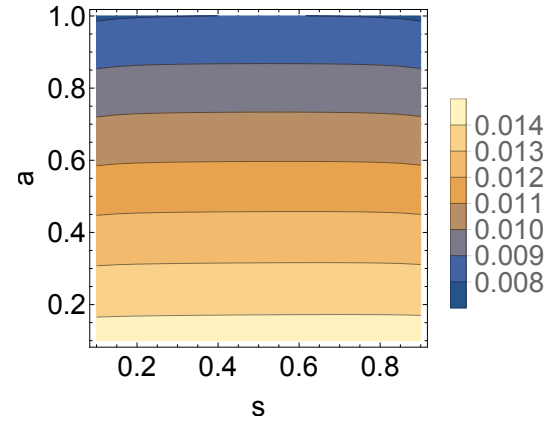
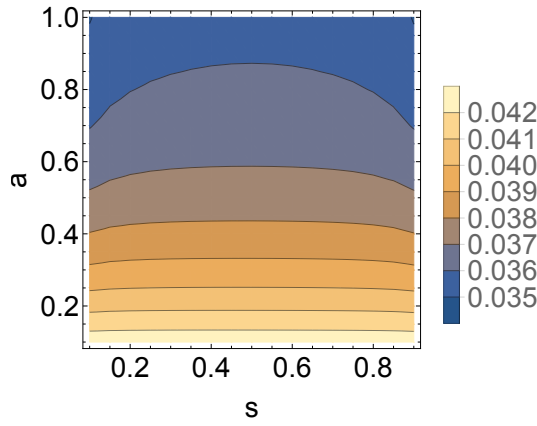
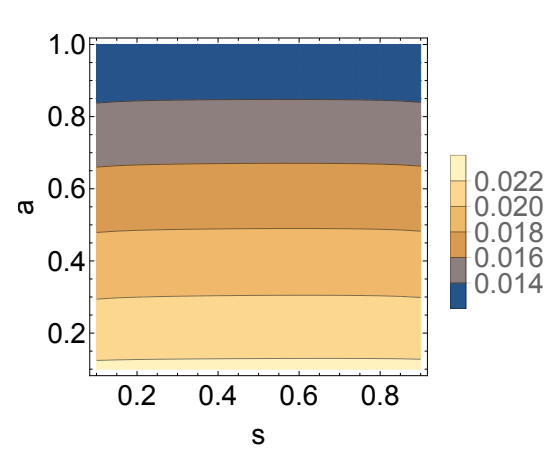
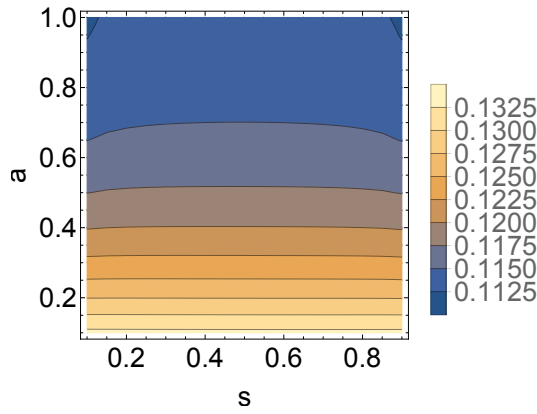
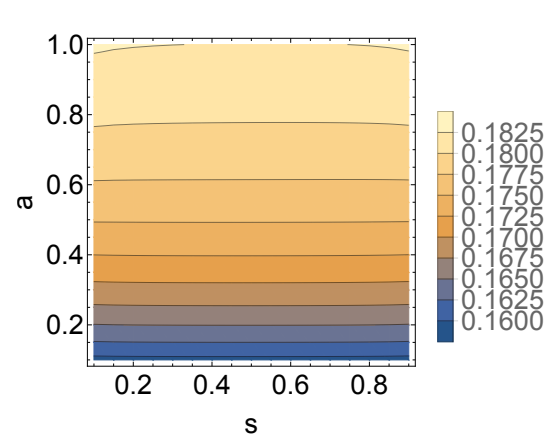
### Case 3

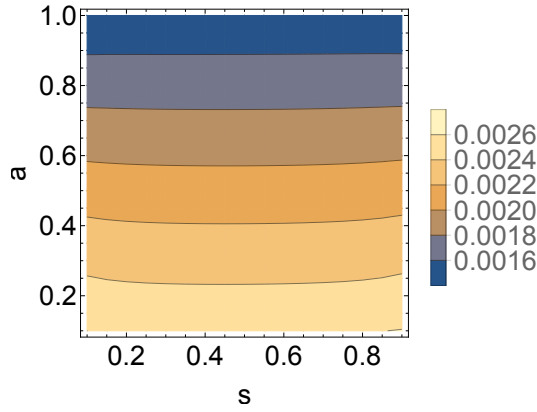
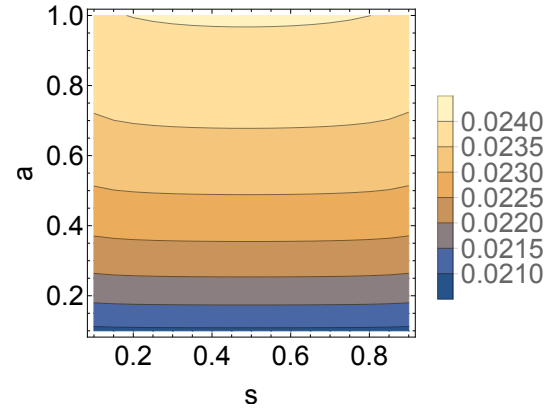
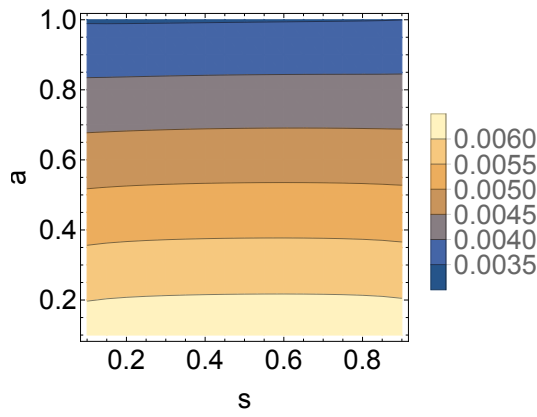
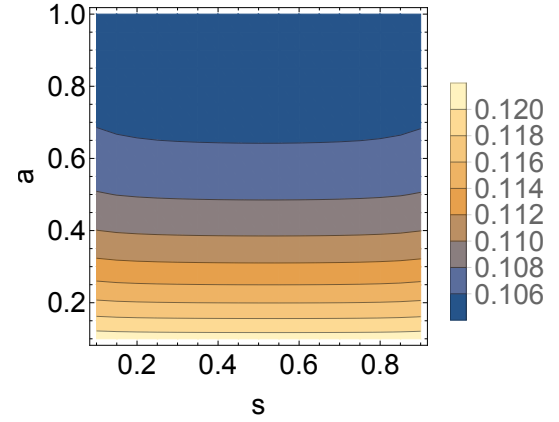
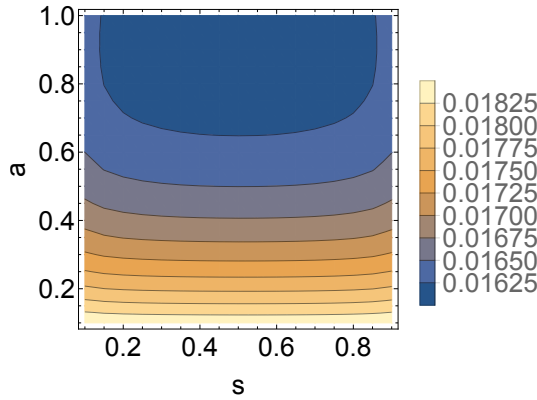
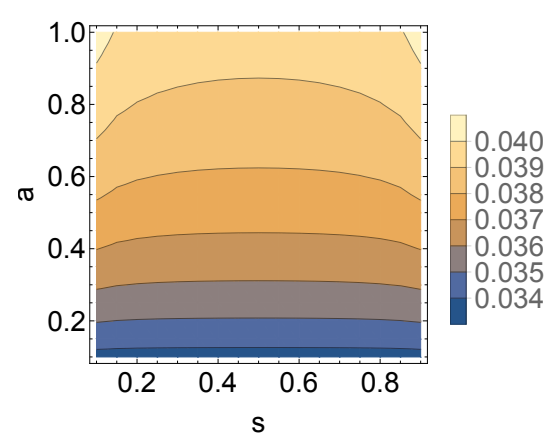
When  $a = 0$  and  $0 < s < 1$  equilibrium is determined by the initial frequency of

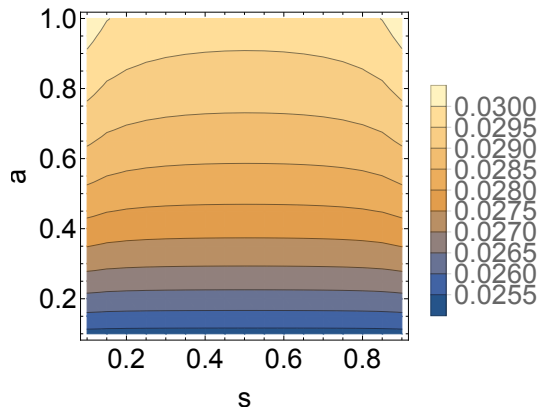
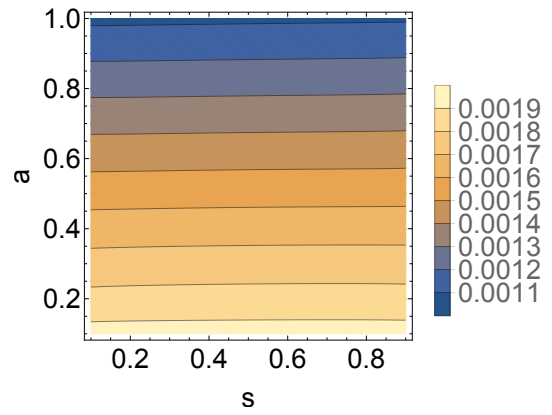
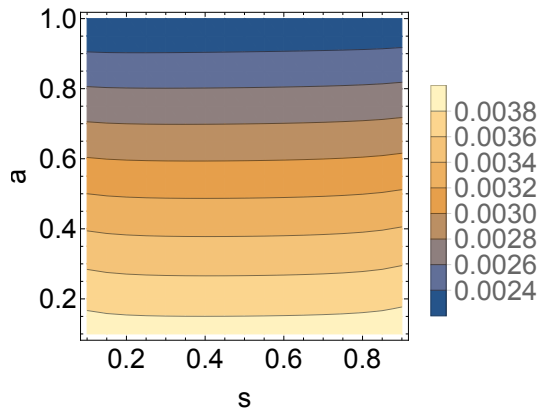
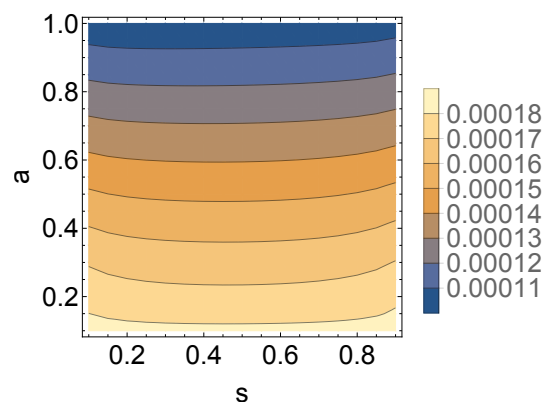
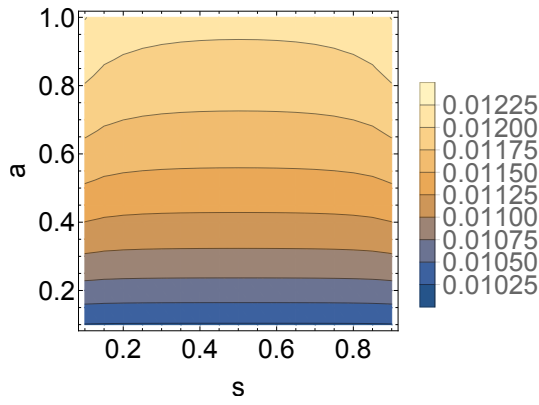
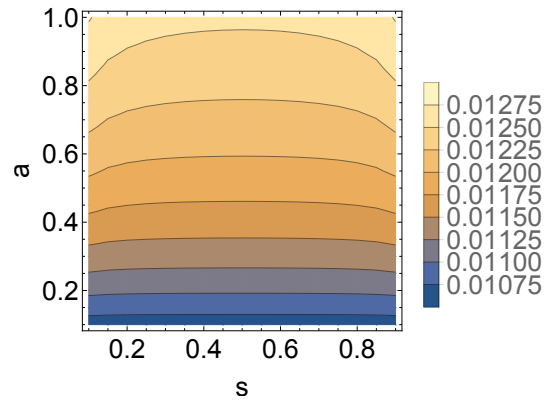


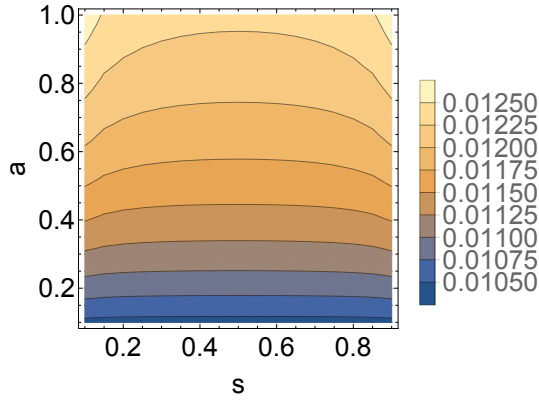
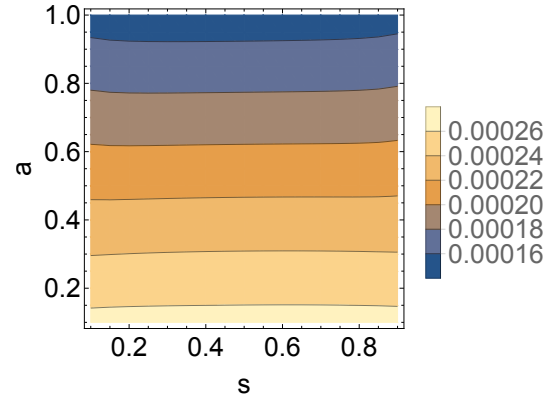
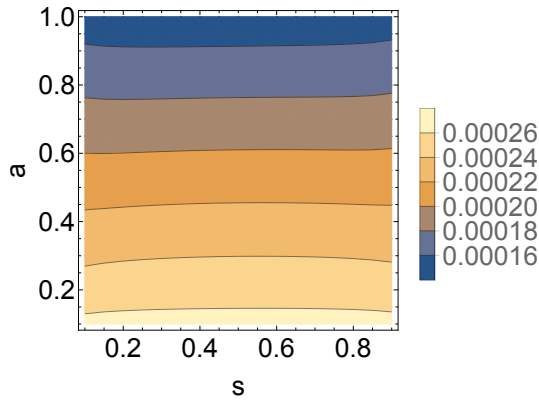
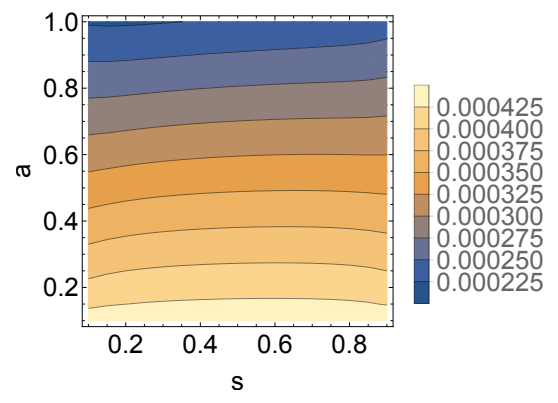
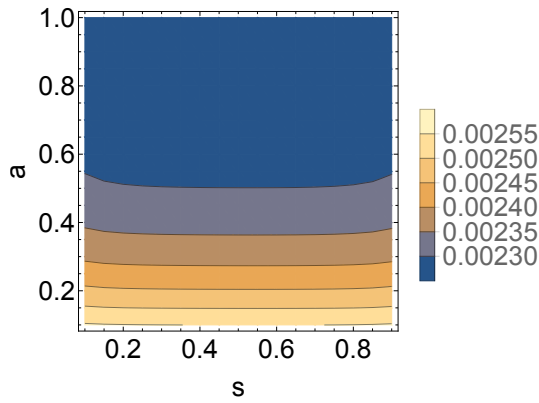
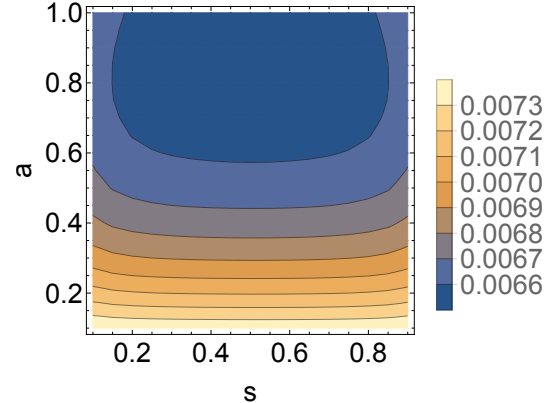
each knot and link due to the disjoint graphs present in the transition network. As in the case of braids on two strands, each frequency can be given in terms of the frequency of other knots and links. As there are three disjoint graphs, the frequency of knots in the cycle with  $0_1$  depend only on  $f_{0_1}$ , those in the cycle with  $L2a1$  on  $f_{L2a1}$ , with the remaining links a combination of the two. The full equations defining equilibrium for this case are given in Appendix A.2.

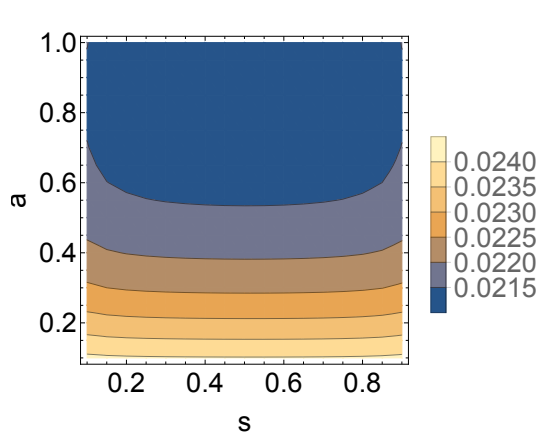
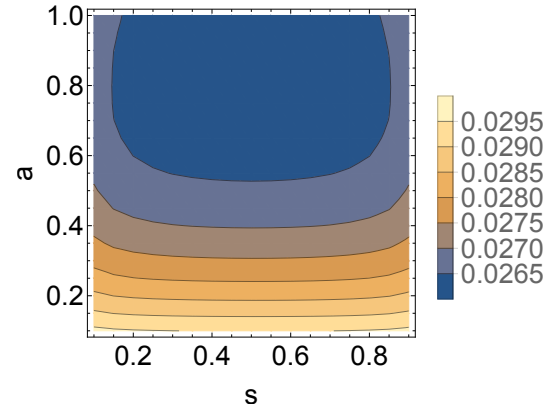
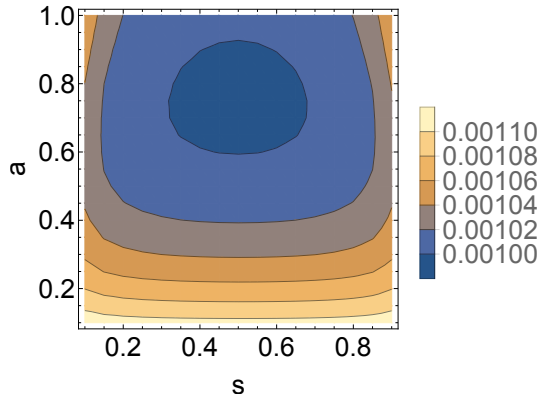
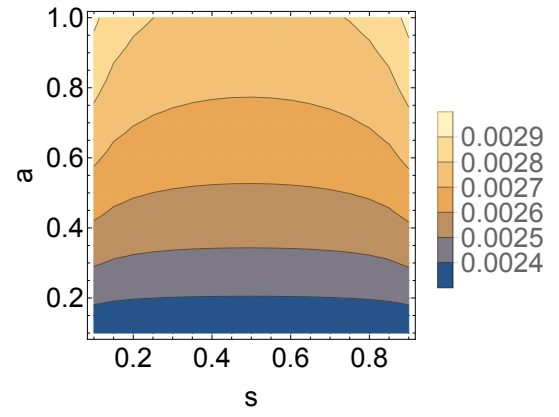
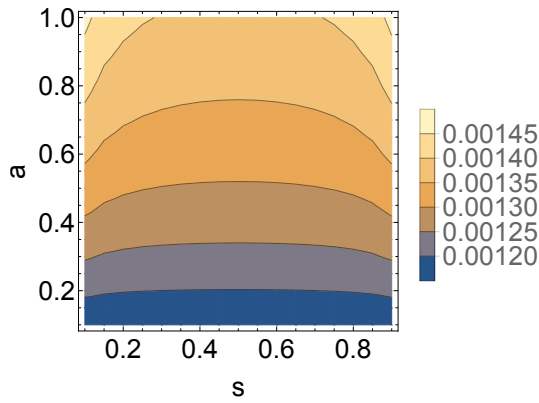
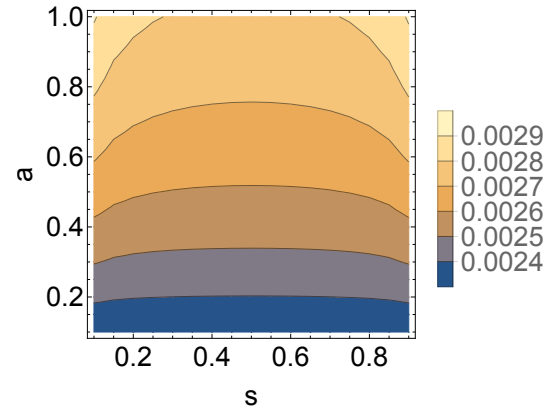
**Case 4** When  $0 < a \leq 1$  and  $0 < s < 1$  there are no cycles or absorbing states and so equilibrium do not depend on the initial frequencies of each knot and link but solely on the parameters  $a$  and  $s$ . Contour plots of the frequency of each knot and link at equilibrium are given in Figure 4.5 for values  $0 < a \leq 1$  and  $0 < s < 1$ . These plots show  $0_1$  and  $3_1$  are the two most common knots at equilibrium, but the range of values for each knot and link is quite small.

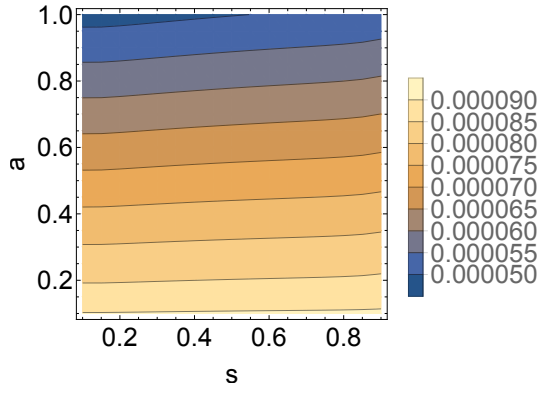
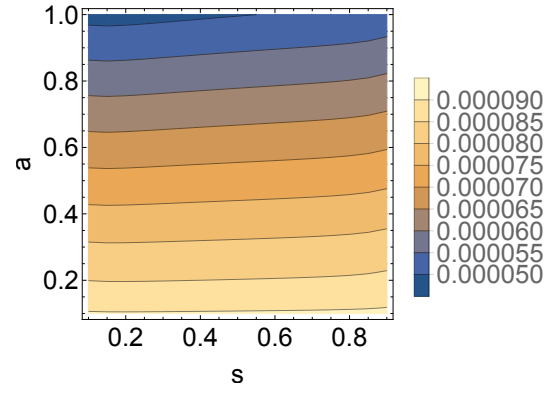
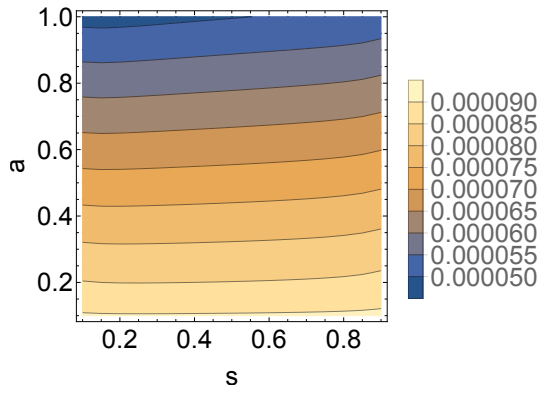
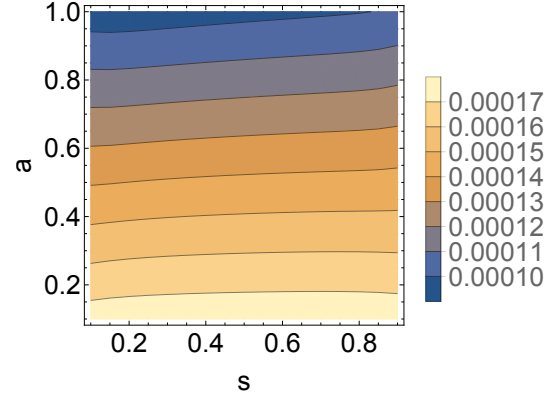
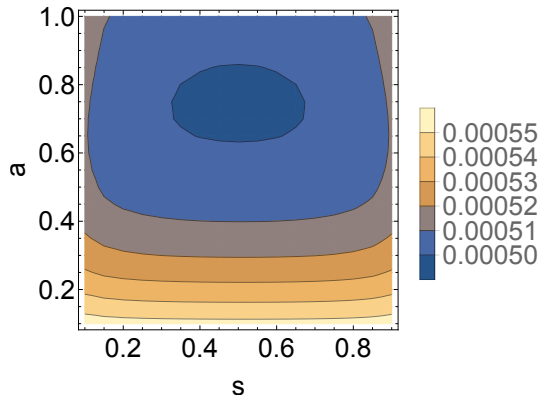
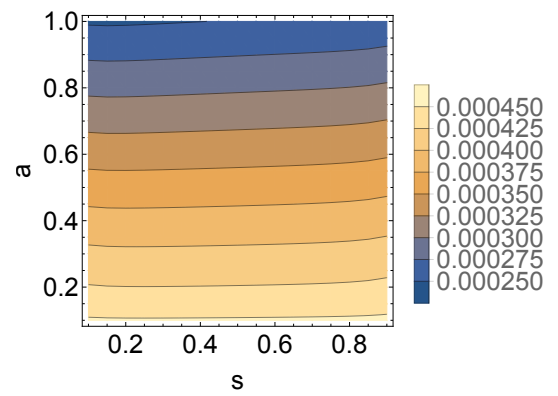
(a) Frequency of  $0_1$  at equilibrium(b) Frequency of *unlink* at equilibrium(c) Frequency of *unlink#unlink* at equilibrium(d) Frequency of *L2a1* at equilibrium(e) Frequency of *unlink#L2a1* at equilibrium(f) Frequency of  $3_1$  at equilibrium

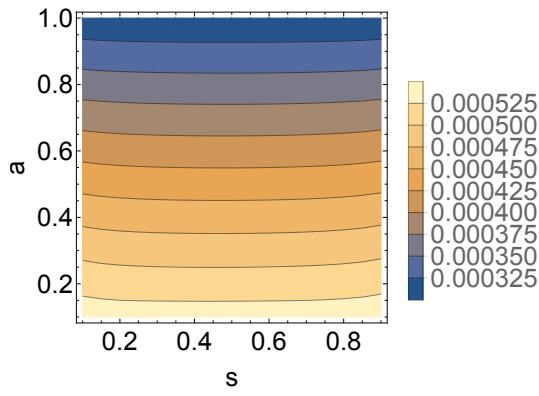
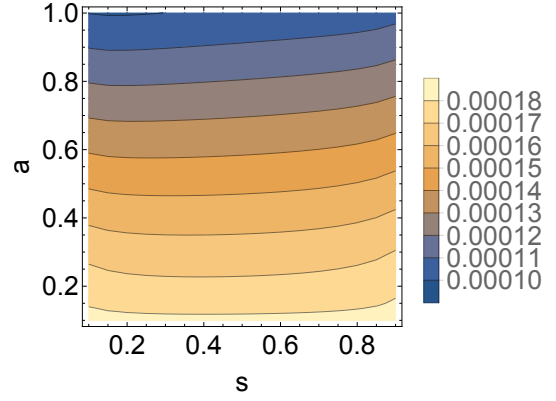
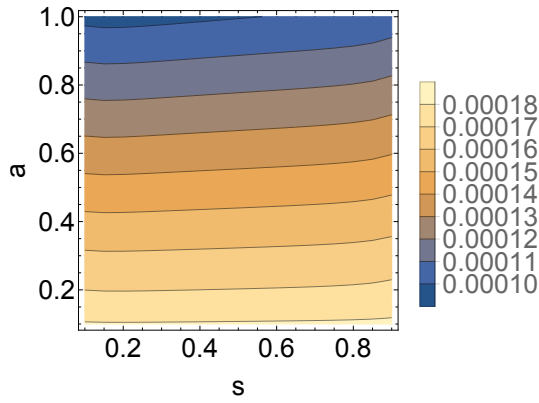
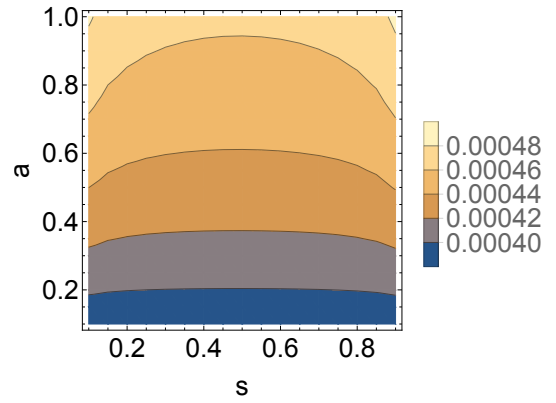
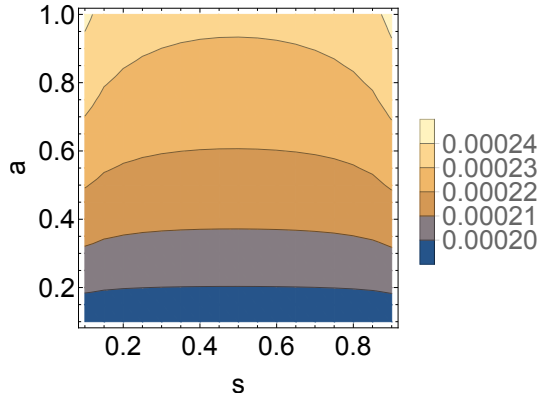
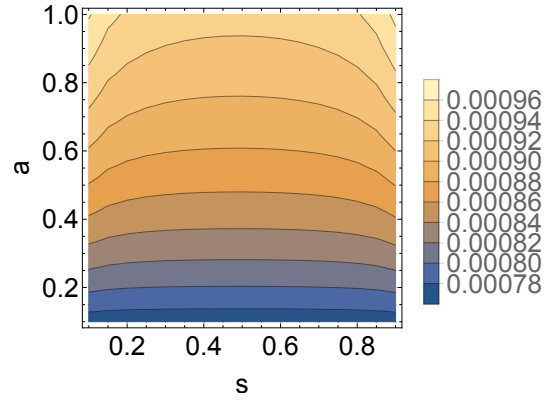
(g) Frequency of  $unlink\#3_1$  at equilibrium(h) Frequency of  $4_1$  at equilibrium(i) Frequency of  $L4a1$  at equilibrium(j) Frequency of  $L2a1\#L2a1$  at equilibrium(k) Frequency of  $unlink\#L4a1$  at equilibrium(l) Frequency of  $5_1$  at equilibrium

(m) Frequency of  $5_2$  at equilibrium(n) Frequency of  $L5a1$  at equilibrium(o) Frequency of  $L2a1\#3_1$  at equilibrium(p) Frequency of  $unlink\#5_1$  at equilibrium(q) Frequency of  $6_2$  at equilibrium(r) Frequency of  $6_3$  at equilibrium

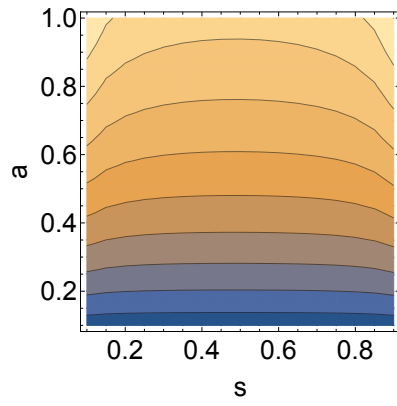
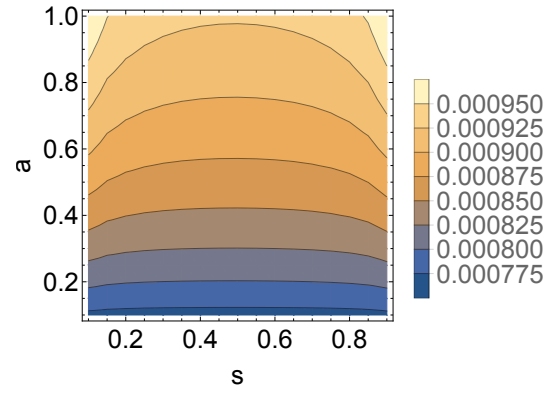
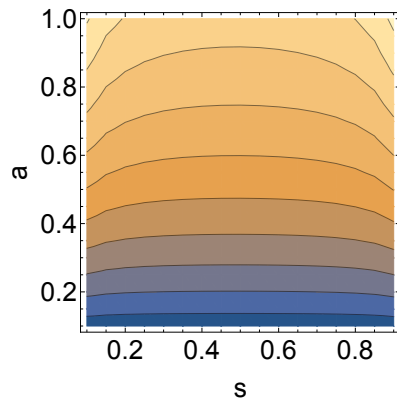
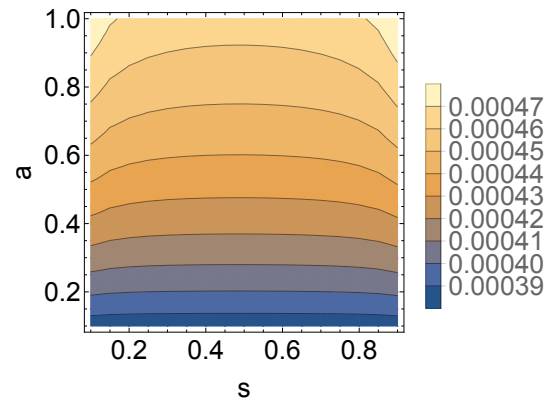
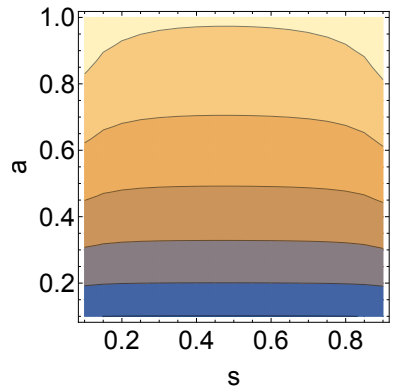
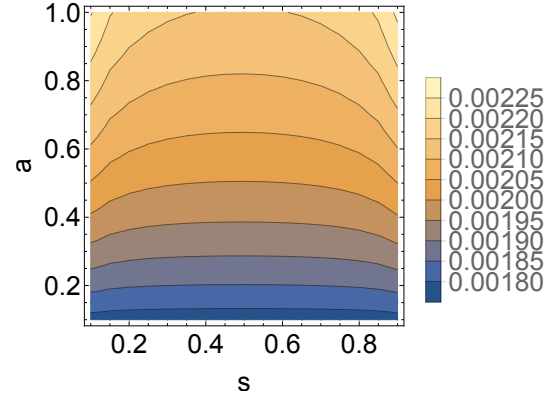
(s) Frequency of  $3_1\#3_1$  at equilibrium(t) Frequency of  $L6a1$  at equilibrium(u) Frequency of  $L6a2$  at equilibrium(v) Frequency of  $L6a3$  at equilibrium(w) Frequency of  $L6a4$  at equilibrium(x) Frequency of  $L6a5$  at equilibrium

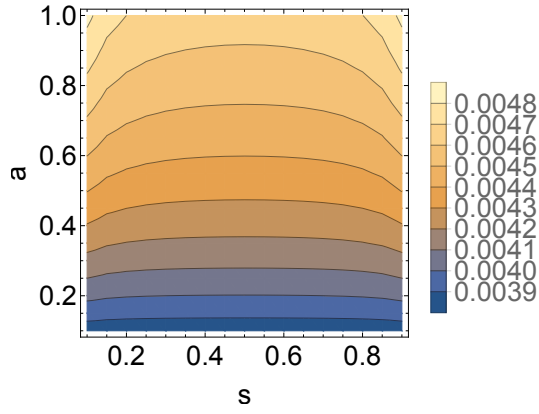
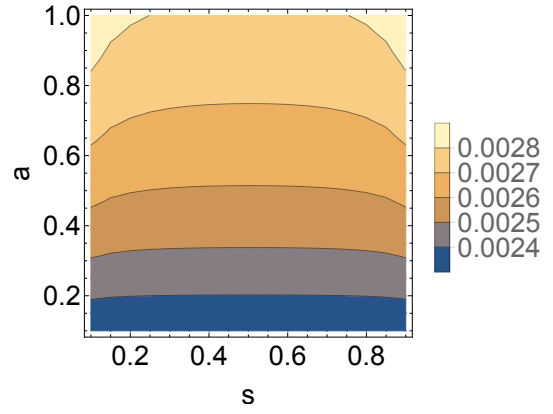
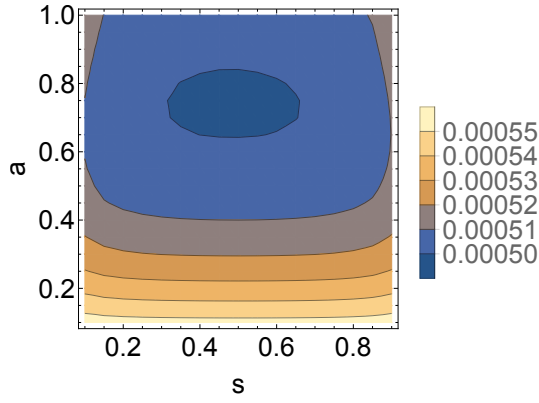
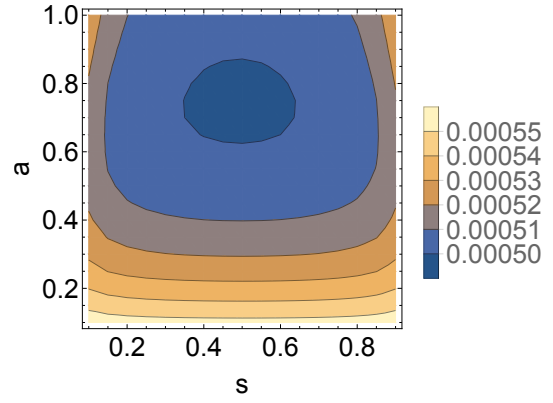
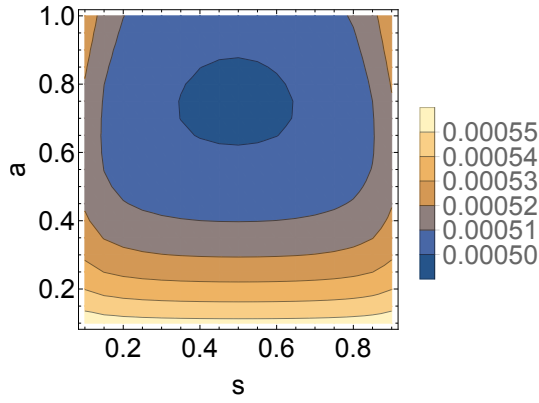
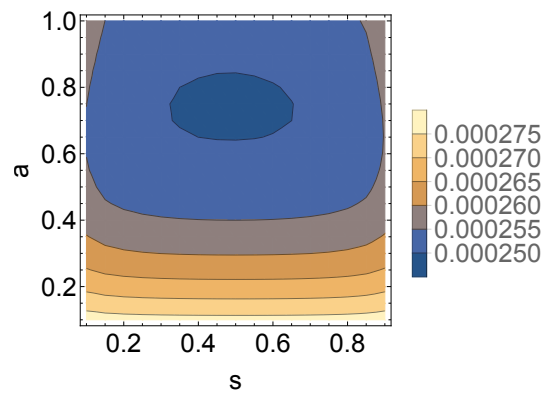
(y) Frequency of  $L6n1$  at equilibrium(z) Frequency of  $L2a1\#L4a1$  at equilibrium(aa) Frequency of  $unlink\#L6a3$  at equilibrium(ab) Frequency of  $7_1$  at equilibrium(ac) Frequency of  $7_3$  at equilibrium(ad) Frequency of  $7_5$  at equilibrium

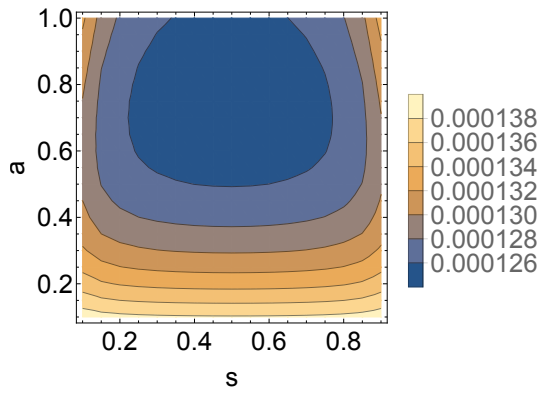
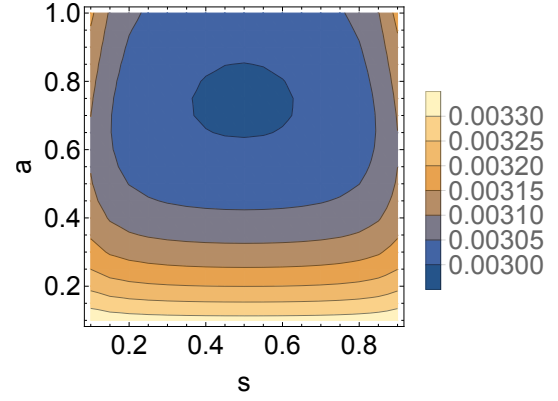
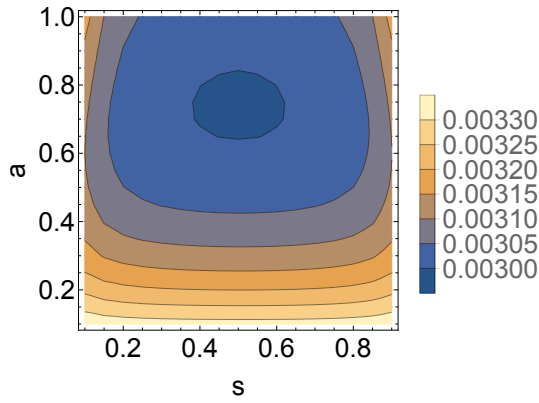
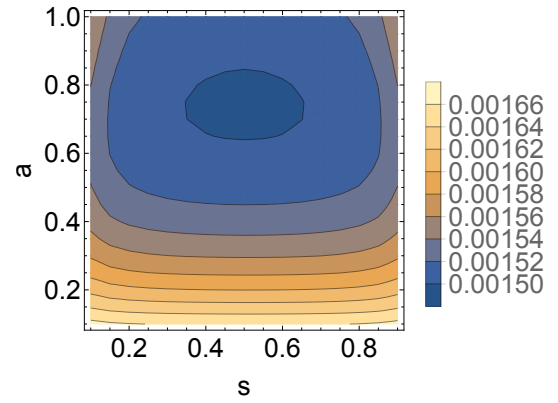
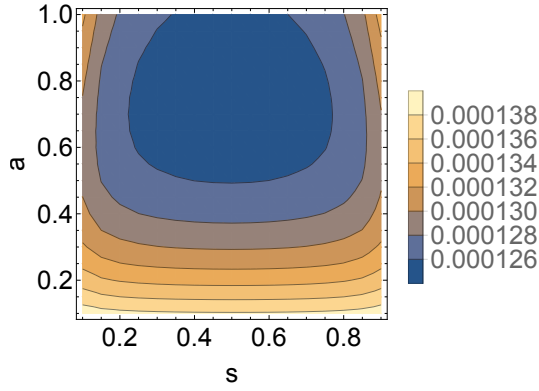
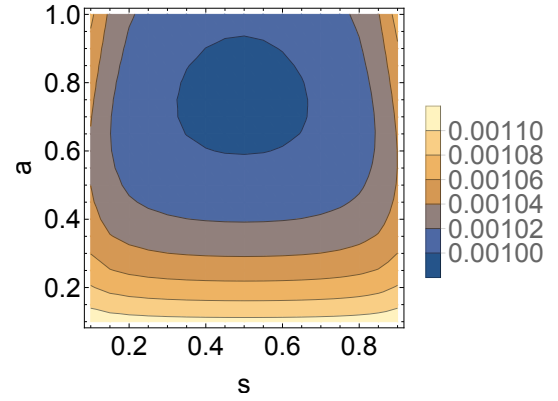
(ae) Frequency of  $L7a1$  at equilibrium(af) Frequency of  $L7a2$  at equilibrium(ag) Frequency of  $L7a3$  at equilibrium(ah) Frequency of  $L7a5$  at equilibrium(ai) Frequency of  $L7a7$  at equilibrium(aj) Frequency of  $L7n1$  at equilibrium

(ak) Frequency of  $L7n2$  at equilibrium(al) Frequency of  $L2a1\#5_1$  at equilibrium(am) Frequency of  $3_1\#L4a1$  at equilibrium(an) Frequency of  $8_2$  at equilibrium(ao) Frequency of  $8_5$  at equilibrium(ap) Frequency of  $8_7$  at equilibrium



(aq) Frequency of  $8_9$  at equilibrium(ar) Frequency of  $8_{10}$  at equilibrium(as) Frequency of  $8_{16}$  at equilibrium(at) Frequency of  $8_{17}$  at equilibrium(au) Frequency of  $8_{18}$  at equilibrium(av) Frequency of  $8_{19}$  at equilibrium

(aw) Frequency of  $8_{20}$  at equilibrium(ax) Frequency of  $8_{21}$  at equilibrium(ay) Frequency of  $L8a16$  at equilibrium(az) Frequency of  $L8a17$  at equilibrium(ba) Frequency of  $L8a18$  at equilibrium(bb) Frequency of  $L8a19$  at equilibrium

(bc) Frequency of  $L8a20$  at equilibrium(bd) Frequency of  $L8n3$  at equilibrium(be) Frequency of  $L8n4$  at equilibrium(bf) Frequency of  $L8n5$  at equilibrium(bg) Frequency of  $L8n6$  at equilibrium(bh) Frequency of  $L2a1\#L6a3$  at equilibrium

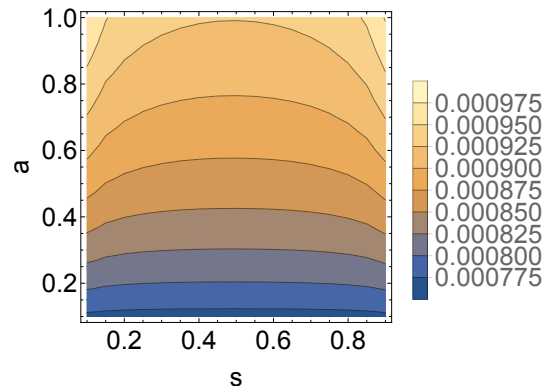
(bi) Frequency of  $3_1\#5_1$  at equilibrium

Figure 4.5: Contour plots of the frequency of each knot and link at equilibrium when  $0 < a \leq 1$  and  $0 < s < 1$

In the same way as case 1 for braids on two strands, case 1 for three strands is already at equilibrium as no transition of knot and link types or change in frequencies occurs. Case 2 is determined by the absorbing states for braids of length two and three, but more knots and links result in absorbing states on three strands than two, due to a higher amount of knots and links being included. For both braids on two and three strands, equilibrium in case 3 is determined by start frequencies of knots and links, resulting from disjoint network graphs, with all frequencies determined by the frequency of one link for braids on two strands and by two links in the case on three strands. In case 4, the range of frequencies for each knot and link given by the contour plots is quite narrow for both two and three strands, but the most frequent knots and links are different in both cases. For the braids on two strands the links  $L2a1$  and the *unlink* have the highest frequency in the contour plots whilst on three strands  $0_1$  and  $3_1$  are most frequent. This difference is due to the inclusion of more knots and links in the three strand case.

As with the case of braids on two strands, the frequencies do not differ much as the values of  $a$  and  $s$  change, with the frequencies almost completely determined by the presence of  $a$  and  $s$  in case 4, not the precise value.

As with the braids on two strands, these equilibrium states can be fit to the frequencies of the knots and links in the ABOK with each case equilibria discussed for the ABOK data. The ABOK frequencies for each knot and link included in the

case on three strands are given in Table 2.5 Chapter 2.3.4.

**Case 1;**  $a = 0$  **and**  $s = 0$  **or**  $s = 1$

The frequency of each knot and link type occurs in case 1 if all knots and links are replicated correctly with no crossings or additions as in the case on two strands.

**Case 2;**  $0 < a \leq 1$  **and**  $s = 0$  **or**  $s = 1$

In this case we require

$$\begin{aligned} & \hat{f}_{7_1} + \hat{f}_{7_3} + \hat{f}_{7_5} + \hat{f}_{8_2} + \hat{f}_{8_5} + \hat{f}_{8_7} + \hat{f}_{8_9} + \hat{f}_{8_{10}} + \hat{f}_{8_{16}} + \hat{f}_{8_{17}} + \hat{f}_{8_{18}} + \hat{f}_{8_{19}} + \hat{f}_{8_{20}} + \hat{f}_{8_{21}} \\ & + \hat{f}_{3_1\#5_1} + \hat{f}_{L7a7} + \hat{f}_{L8a16} + \hat{f}_{L8a17} + \hat{f}_{L8a18} + \hat{f}_{L8a19} + \hat{f}_{L8a20} + \hat{f}_{L8n3} + \hat{f}_{L8n4} \\ & + \hat{f}_{L8n5} + \hat{f}_{L8n6} + \hat{f}_{L2a1\#L6a3} + \hat{f}_{L4a1\#L4a1} + \hat{f}_{unlink\#L6a3} = 1 \end{aligned}$$

but these are among the least common knots in the ABOK data, so this case does not fit the data.

**Case 3;**  $a = 0$  **and**  $0 < s < 1$

In this case the equilibrium frequencies are determined by a cycle, meaning they depend on the initial frequencies of the knots and links. In order to get the closest fit to the ABOK data, we take the ABOK data frequencies for knots and links as the initial conditions. We require

$$0 \leq \hat{f}_{0_1} \leq \frac{2776}{5797}$$

and

$$0 \leq \hat{f}_{L2a1} \leq \frac{1747}{4284} - \frac{595727f_{0_1}}{699552}$$

in this case, which is satisfied using the ABOK values

$$\hat{f}_{0_1} = ABOK f_{0_1} = \frac{111}{415}$$

and

$$\hat{f}_{L2a1} = ABOK f_{L2a1} = \frac{48}{415}$$

These values then determine the rest of the equilibrium frequencies. These frequencies give a metric value using squared Euclidean distance of

$$\sum_{i=1}^{63} (\hat{F}_i - ABOK F_i)^2 = 0.0106668$$

where  $\hat{F}$  is the vector containing the equilibrium frequencies and  $ABOKF$  the vector containing the ABOK data.

This looks to be a good fit for the data, however, the low metric value is partly given by the exact fit between the frequencies for  $0_1$  and  $L2a1$  which were the values input. The equations predict much higher frequencies of some knots and links, for example  $L2a1\#L2a1$ ,  $L2a1\#unlink$  and  $unlink\#unlink$  which do not appear very often in ABOK but are weighted quite high in the equation frequencies.

**Case 4;**  $0 < a \leq 1$  and  $0 < s < 1$

In this case equilibrium does not depend on the starting frequencies, it solely depends on the parameters  $a$  and  $s$ . Using Approximate Bayesian Computation and grid approximation we simulate equilibrium for a range of the parameters  $a$  and  $s$ , keeping the parameter values giving the simulated data closest to the ABOK data using the squared Euclidean distance

$$\sum_{i=1}^{63} (F\hat{sim}_i - ABOKF_i)^2$$

where  $F\hat{sim}$  is the vector containing the simulated data. This results in a minimum metric value of 0.0369894 which seems to be a poorer fit than the fit in case 3. Again the equations predict large frequencies of some links which do not appear highly in ABOK and predict low frequency for  $L2a1$  which is the second most common link in the ABOK data, giving again a discrepancy with the ABOK data.

Both case 3 and case 4 look to give a good metric value but there is discrepancy over the difference in frequencies, so are not perfect fits to the ABOK data. However the fit for case 3 on three strands gives a metric value of 0.0106668 whereas case 3 on two strands gives 0.0113166, so increasing the number strands and the amount of knots included in the analysis gives a better fit to the ABOK data. This is also the case for case 4 with the metric value on three strands being 0.0369894, a much better fit than the value of 0.177309 on two strands. Longer braid words or braids on more strands could be considered to improve this fit, however, given the braids not included represent the least common knots and links in ABOK, this may not be useful for initial explanation of the ABOK data.

The values of  $a$  and  $s$  giving the best fit on both two and three strands are

$0 < s < 1$  and  $a = 0$  in case 3 and  $0 < a \leq 1$  in case 4. As the goodness of the fit in case 3 is partly determined by the exact fit of the two input frequencies, the fit in case 4 may be overall the best fit. This suggests the distribution of knots and links in ABOK is best explained by a model including both social and asocial learning where social learning is not always perfect or imperfect ( $s \neq 0$  and  $s \neq 1$ ) and some asocial learning always occurring to maintain complexity in the system ( $0 < a \leq 1$ ). However, as seen in Chapter 3 highly accurate social learning does not necessarily maintain fidelity of transmission through social learning and so biases towards certain knot forms may need to be considered. The discrepancy between this model and the ABOK data could be caused by biases towards certain knot and link types which were not included in this model.

As seen in the contour plots in both Figures 4.3 and 4.5, the frequency values do not differ much as the values of  $a$  and  $s$  change. It seems the frequencies of knots and links are almost determined by the parameters being in the range  $0 < a \leq 1$  and  $0 < s < 1$ , and not the exact value. This may suggest that it is difficult to determine the exact levels of social and asocial learning from population level data, such as the frequencies of knots and links in ABOK. Even though it may not be possible to establish the exact levels of social and asocial learning we can rule out the parameter cases (cases 1 and 2) and the parameters associated to them that do not fit the data.

## 4.3 Conclusion

The model examined in this chapter explored the affect of social and asocial learning on knots and links. This model compared crossing changes and additions on braids of two and three strands analysing the affect of these on knot and link types. Through this analysis we see that the transition between knot types is affected by the likelihood of crossing changes and additions, with low likelihood for crossing changes causing little transition between knot and link types and high likelihood for crossing changes causing high transition to the knot and link types with highest crossing number.

The analysis of the transitions of knots and links on braid words of two strands involved only nine knots and links with no composite knots and links included, whilst the analysis on three strands involved 63 distinct knots and links both prime and composite. In both sets of network graphs we see no transition of knot and link types when  $a = 0$  and  $s = 0$  and  $s = 1$ , disjoint graphs when  $a = 0$  and  $0 < s < 1$  and absorbing states in the network when  $0 < a \leq 1$  and  $s = 0$  or  $s = 1$  determining knot and link transition.

As expected, these transitions show that imperfection in social learning (crossings neither replicated all correctly nor all incorrectly,  $0 < s < 1$ ) increases the connectedness between knots and links. Without this imperfection in social learning all knots and links are either replicated as themselves (when  $a = 0$ ) or the transition between the different forms of knots and links collapses into a linear sequence when dictated solely by asocial learning (when  $0 < a \leq 1$ ). It is important to note that when crossings are either all replicated correctly or all incorrectly ( $s = 0$  or  $s = 1$ ) knots and links are replicated as themselves. This does not occur when imperfection in social learning occurs ( $0 < s < 1$ ) so perfect social learning results in the persistence of variants. However, when asocial learning always occurs ( $a = 1$ ) some knots and links are replicated as themselves due to the maximum crossing number of eight assumed in this model, instead of creating a new variant of higher crossing number. This is a direct result of this assumption to ensure a closed system and although it may be the case that asocial learning is reduced for higher crossing knots and links causing replication of the current knot or link type, the replication seen here is a result of the model set up and should not be taken as an indication of the effect of real world asocial learning.

When no asocial learning ( $a = 0$ ) occurs the transition between knots and links is given solely by social learning in the form of crossing changes on the braid words of knot and links. The crossing changes in this form are equivalent to the crossing changes on Dowker-Thistlethwaite (DT) Codes [45] given to analyse the affect of topoisomerases [80] and crossing changes on planar projections to analyse knot parentage [81]. However the model discussed in this chapter includes links in the analysis which are included in neither of these studies. The model discussed here



also allows control over the extent to which asocial and social learning occurs with adjustment of the parameters  $a$  and  $s$  respectively.

Using the data from the Ashley Book of Knots (ABOK) [8] we fit the equilibrium states to the ABOK data to obtain estimates for the parameters  $a$  and  $s$  which control crossing additions and changes respectively.

When  $a = 0$  and  $0 < s < 1$  no crossing additions occur but crossing changes always occur to some extent, the equilibrium states are determined completely by the frequencies of each knot and link. In both the two and three strand case this seemed to fit the ABOK data best suggesting low likelihood for asocial learning in the ABOK data. However as the fit was partly given by inputting the ABOK data into the equations this biases the result.

When  $0 < a \leq 1$  and  $0 < s < 1$  some crossing additions always occur and crossing changes always occur to some extent, giving equilibrium states that do not depend on the initial frequencies of each knot and link. Using this case to fit to the ABOK data gave a reasonable fit which was fairly uniform for all values of  $a$  and  $s$  in both the two and three strand case. The three strand case gave a better fit to the ABOK data, including more knots and links in the analysis so could be closer matched to the distribution in ABOK.

This suggests that in order to obtain the distribution of knots and links seen in the ABOK data some social and asocial learning must have occurred but the overall likelihood of either are unimportant as the presence of crossing changes and additions causes huge changes in knot and link types over generations, giving a prevalence for lower crossing knots and links as seen in ABOK but still preserving the presence of higher crossing, more complex knots and links.

We see in both Figures 4.3 and 4.5 that the exact values of  $a$  and  $s$  do not change the frequencies of knots and links much overall, suggesting the exact value is difficult to determine from the frequency data in ABOK. However through this process we can rule out the ranges of parameter values that do not fit the data and focus solely on those in the range  $0 < a \leq 1$  and  $0 < s < 1$ . This difficulty in determining the exact processes of transmission from population level is similar to that explored by Kandler et al. [28], with the analysis being useful in excluding the processes that

likely did not occur to explain that data.

The affect of this model on the transmission of knots and links is testable by experiment and could be used to investigate the parameters and assumptions used within this model, testing whether and for what range these two parameters give a reasonable assessment of the transmission of knots and links.

This model of social and asocial learning on knot and link types does not discuss or give any conditions as to when social and asocial learning occurs in the cultural transmission of knots and links but explores the effect on frequencies of knots and links given the frequency of social and asocial learning. A further model could explore the conditions on social and asocial learning informing the parameters  $a$  and  $s$  to give estimates on the extent of asocial and social learning.

Social and learning in this model operated on single crossings independent of neighbouring crossings whether they are of the same type or not. We may expect that this might not represent real knot tying as knots may be learned in sections or chunks of repeated crossings [82]. A similar model to that presented here was also considered, in which social learning operated on chunks of crossings in which all crossings in the chunk were replicated correctly or all incorrectly, with the chunks formed of neighbouring crossings of all the same type. This consideration of social learning in chunks produced almost the same results as considering social learning on individual crossings. The chunk model took longer to run than the model on individual crossings and provided no new information, and so the model on individual crossings discussed here became the sole model considered.

This model does not completely match the frequencies of knots and links seen in ABOK and so biases or other parameters may need to be factored into the model to give an exact fit to the data. However the inclusion of too many additional parameters may result in over-fitting.

Whilst we have only explored the transmission of knots and links the techniques explored in this model can be applicable to other socially transmitted technologies or traits through the assessment of social and asocial learning with tunable parameters.

# Chapter 5

## A fitness landscape analysis of knots and links

### 5.1 Introduction

Adaptive or evolutionary landscapes are a tool used to explore the processes of evolution. The first representation of these landscapes in this form are credited to Wright [83] who presented topographical peaks and valleys corresponding to the adaptive values of gene combinations [84]. This landscape can be used to explore evolution over time through selection for variants on the landscape, analysing the resulting adaptive value.

The  $NK$  model is a such a method used to explore adaptive evolution in systems. The fitness model is created using two parameters  $N$  and  $K$ , a form first presented by Kauffman and Levin [85]. The theory used in the  $NK$  model is based on Wright's formulation of a mathematical theory of evolution [86] [87] allowing the development of an adaptive model assigning fitness of variant through a combinatoric process.

The  $NK$  model assigns fitness, which is represented by scalar values, to strings of length  $N$ . If a distance metric is defined between strings then this model defines a landscape, allowing analysis of transition between variants. Fitness for individual strings is determined by the interaction between  $K$  neighbouring elements in the string.

Let  $S$  be a string of length  $N$ . Then the fitness of the string  $F(S)$  is given by

the sum

$$F(S) = \frac{1}{N} \sum_{i=1}^N f(s_i)$$

where  $f(s_i)$  denotes the fitness contributions of the  $N$  elements in the string. [88]

The fitness contributions of the elements in the string are determined by the interaction between  $K$  neighbouring elements in the string and is given by a scalar between 0 and 1.

$$f(s_i) = f(s_i, s_{i+1}, \dots, s_{i+K}) \in [0, 1]$$

The  $NK$  model is used to analyse interaction and evolution in many disciplines, with the fitness of strings in the model used to represent frequencies of features of the object in question, for example, applications of the  $NK$  model are seen in evolutionary biology, in the exploration of features optimising the use of antibodies [88] and economics, into the features associated in rapid technological shifts [89]. As the model involves only two parameters,  $N$  denoting the length of the observations and  $K$  the length of interaction within the observation, it is a widely applicable model allowing exploration of features in many domains with minimal assumptions, being applied to multiple problems within the social sciences [87]. When a distance metric is defined, the model forms a landscape with the distance between points defined allowing interactions and expected movements between points on the landscape to be observed.

The parameter  $K$  relates to the number of epistatic interactions affecting the fitness of a given element in the string of length  $N$ . The size of  $K$  relates to the ruggedness of the  $NK$  landscape, with the minimal value  $K = 0$  giving a smooth landscape and the maximal  $K = N - 1$  giving the most rugged landscape [85].

In their paper Curran et al. [90] explore the effects of cultural learning through the fitness and diversity of a population using  $NK$  landscapes. They contrast two  $NK$  models, one in which fitness is given through evolutionary learning, determined by a genetic algorithm, and the other in which fitness is affected by both evolutionary learning and cultural learning through imitation of selected teachers in the population. The use of the  $NK$  model allowed them to explore the evolution of

cultural learning parameters controlling the extent of cultural learning over generations. These two parameters detailed the probability of imitation by an agent from teachers in the population and the number of opportunities for teaching to occur. These parameters changed over generations of the model, stabilising at a probability of imitation of around 0.5 and opportunities of imitation of around 70 out of a maximum of 127. Their work found cultural learning to be beneficial to fitness and diversity over evolutionary learning alone, with the  $NK$  model allowing exploration of parameters contributing to this fitness.

Considering the global and local optima through these fitness models is good for exploring expected frequencies in the system in question. We may expect the “fittest” point on an  $NK$  landscape to correspond to the most frequent observation in a given system with the factors affecting the fitness of these traits also explored.

From the knots seen in ABOK, explored in Chapter 2, we see the same mathematical knot appearing in the form of many different material knots. As some knots appear more frequently than others in many forms this increase in frequency may be caused by some feature of the knot increasing its fitness leading to increased frequency of usage. As knots are formed of sequences of crossings it seems natural to consider the fitness of a given knot through the fitness of the crossings that form it. In this way we can consider an  $NK$  model exploring the fitness of various knot types.

## 5.2 Knot NK model

In Chapter 3 we saw that the accuracy of social learning may not be the only factor to consider when looking at transmission through social learning as we saw biases shape the frequencies of the knots tied. The social and asocial learning model discussed in Chapter 4 does not seem to fully fit the distribution in ABOK, suggesting an assessment of social and asocial learning is not enough to explain the distribution of knots in ABOK. An addition of relative fitness of knots can be explored using  $NK$  models, in order to assess the relative frequencies of knots and links in ABOK.

To assess the fitness of individual knots and links we apply the  $NK$  model to

braid words representing knots and links. The parameter  $N$  represents the number of crossings in the braid word and  $K$  the epistatic interactions affecting the fitness of a given crossing, that is the number of crossings affecting the fitness of a given crossing. When  $K = 0$  the fitness of each crossing depends on no neighbouring crossings, just the crossing itself, but when  $K = N - 1$  the fitness of each crossing depends on all crossings in the knot or link.

We first consider braids on two strands whose braid words are given by combinations of  $\sigma_1$  and  $\sigma_1^{-1}$  of length  $N$ . A natural distance metric to use is the Hamming distance [91], which counts the number of locations in which two strings differ and represents the difference in crossings for the two braids.

Fitness contributions are calculated by  $K$  neighbouring crossings and are represented by real numbers.

For given  $N$  and  $K$ , the fitness contributions are assigned randomly from a uniform distribution on the interval  $[0, 1]$ .

**Example 5.2.1** Consider an  $N = 3$ ,  $K = 1$  landscape for braids on two strands. Braid words on two strands are formed of compositions of  $\sigma_1$  and  $\sigma_1^{-1}$  and so when  $N = 3$  there are eight possible strings of length three of  $\sigma_1$  and  $\sigma_1^{-1}$  relating to only two knots.

Possible braids of length three on two strands	Knot they represent
$\sigma_1\sigma_1\sigma_1$	$3_1$
$\sigma_1\sigma_1\sigma_1^{-1}$	$0_1$
$\sigma_1\sigma_1^{-1}\sigma_1$	$0_1$
$\sigma_1^{-1}\sigma_1\sigma_1$	$0_1$
$\sigma_1\sigma_1^{-1}\sigma_1^{-1}$	$0_1$
$\sigma_1^{-1}\sigma_1\sigma_1^{-1}$	$0_1$
$\sigma_1^{-1}\sigma_1^{-1}\sigma_1$	$0_1$
$\sigma_1^{-1}\sigma_1^{-1}\sigma_1^{-1}$	$3_1$

Table 5.1: The possible braids on two strands and the knots they represent on an  $N = 3$  landscape of strings of length three, given by compositions of  $\sigma_1$  and  $\sigma_1^{-1}$ . The resulting knots in this landscape are the trefoil knot  $3_1$  and the unknot  $0_1$ .

The fitness of each of these eight strings is given by fitness contributions determined by the fitness of  $K + 1$  neighbouring crossings which make up the string. To determine the fitness of a string of length  $N$ , the string is split into sections of length  $K + 1$ . The fitness of each section is then summed and divided by the  $N$  to give the fitness of the string in total, division by  $N$  is to ensure fitness falls in the interval  $[0, 1]$ . For  $N = 3$  and  $K = 1$  the fitness is the sum of the fitness of the strings of length two, formed from positions 1 and 2, the positions 2 and 3, and then the positions 3 and 1. If  $K = 2$  strings of length three would be taken to calculate fitness, formed from positions 1, 2 and 3, the positions 2, 3 and 1, and then the positions 3, 1 and 2.

For example, take three strings in our  $N = 3$  and  $K = 1$  landscape for braids on two strands;

$$\begin{aligned}
F(\sigma_1\sigma_1\sigma_1) &= \frac{1}{3} \cdot (f(\sigma_1\sigma_1) + f(\sigma_1\sigma_1) + f(\sigma_1\sigma_1)) \\
F(\sigma_1\sigma_1\sigma_1^{-1}) &= \frac{1}{3} \cdot (f(\sigma_1\sigma_1) + f(\sigma_1\sigma_1^{-1}) + f(\sigma_1^{-1}\sigma_1)) \\
F(\sigma_1^{-1}\sigma_1^{-1}\sigma_1) &= \frac{1}{3} \cdot (f(\sigma_1^{-1}\sigma_1^{-1}) + f(\sigma_1^{-1}\sigma_1) + f(\sigma_1\sigma_1^{-1}))
\end{aligned}$$

Where  $F$  denotes the fitness of a string of length  $N$  and  $f$  denotes the corresponding fitness contributions.

In the  $K = 1$  landscape for braids on two strands the fitness contributions are given by strings of  $\sigma_1$  and  $\sigma_1^{-1}$  of length two. There are four possible strings of length two;  $\sigma_1\sigma_1$ ,  $\sigma_1\sigma_1^{-1}$ ,  $\sigma_1^{-1}\sigma_1$  and  $\sigma_1^{-1}\sigma_1^{-1}$ .

Assume fitness contributions are assigned to a scalar between 0 and 1 in the following way;

$$f(\sigma_1\sigma_1) = 0.5$$

$$f(\sigma_1\sigma_1^{-1}) = 0.2$$

$$f(\sigma_1^{-1}\sigma_1) = 0.7$$

$$f(\sigma_1^{-1}\sigma_1^{-1}) = 0.1$$

Then the fitness of each string is given by;

$$\begin{aligned} F(\sigma_1\sigma_1\sigma_1) &= \frac{1}{3} \cdot (0.5 + 0.5 + 0.5) = \frac{1}{2} = 0.5 \\ F(\sigma_1\sigma_1\sigma_1^{-1}) &= \frac{1}{3} \cdot (0.5 + 0.2 + 0.7) = \frac{7}{15} = 0.4\overline{66} \\ F(\sigma_1^{-1}\sigma_1^{-1}\sigma_1) &= \frac{1}{3} \cdot (0.1 + 0.7 + 0.2) = \frac{1}{3} = 0.\overline{33} \end{aligned}$$

Here we see that the string  $\sigma_1\sigma_1\sigma_1$  is the fittest of the three with these fitness contributions, but given different contributions another string may be fitter. We also notice that the string  $\sigma_1\sigma_1\sigma_1^{-1}$  has similar fitness, which may be unsurprising given it differs only in one position in the string, hence can be formed by one crossing change the braid  $\sigma_1\sigma_1\sigma_1$ . However, even though  $\sigma_1\sigma_1\sigma_1^{-1}$  differs from  $\sigma_1\sigma_1\sigma_1$  in only one position, the calculation of fitness has only one  $f(\sigma_1\sigma_1) = 0.5$  in common. We also see that although the highest fitness contribution is given by  $f(\sigma_1^{-1}\sigma_1) = 0.7$ , both strings that contain it have lower fitness than  $\sigma_1\sigma_1\sigma_1$ , showing containing the fittest feature is not the most important determination of fitness, as the fitness of all features in the string are considered.

Example 5.2.1 discusses the way in which fitness is calculated in an  $N = 3$ ,  $K = 1$  landscape for braids on two strands. For a larger  $N$  the strings of  $\sigma_1$  and



$\sigma_1^{-1}$  will be longer and so there will be more possible strings. As  $K$  changes the crossings that contribute to the fitness of the string change, with fitness calculated by strings of  $K + 1$  neighbouring crossings.

In the below table the knots and links represented by the fittest braid words are given with the percentage of the simulations that they are the fittest braid in the landscape for  $2 \leq N \leq 6$  with  $1 \leq K \leq N - 1$ .

N	K	Knot/Link	Proportion	N	K	Knot/Link	Proportion
2	0	$L2a1$	71.2%	5	3	$5_1$	55.8%
		$unlink$	28.8%			$0_1$	29.6%
	1	$L2a1$	70.9%			$3_1$	14.6%
		$unlink$	29.1%		4	$5_1$	55.7%
3	0	$3_1$	70.7%			$0_1$	29.4%
		$0_1$	29.3%			$3_1$	14.9%
	1	$3_1$	63.4%	6	0	$L6a3$	70.6%
		$0_1$	36.6%			$unlink$	29.4%
	2	$3_1$	62.6%		1	$L6a3$	57.2%
		$0_1$	37.4%			$L2a1$	28.1%
4	0	$L4a1$	70.8%			$unlink$	14.7%
		$unlink$	29.2%		2	$L6a3$	49.5%
	1	$L4a1$	57.9%			$L2a1$	25.6%
		$unlink$	32.5%			$unlink$	22.6%
		$L2a1$	9.6%			$L4a1$	2.3%
	2	$L4a1$	54.1%		3	$L6a3$	48.6%
		$unlink$	26.2%			$L2a1$	28.2%
		$L2a1$	19.7%			$unlink$	19.7%
	3	$L4a1$	54.2%		4	$L4a1$	3.5%
		$unlink$	26.1%			$L6a3$	46.8%
5	0	$5_1$	70.9%			$L2a1$	26.8%
		$0_1$	29.1%			$unlink$	20.3%
	1	$5_1$	60.9%		5	$L4a1$	6.1%
		$0_1$	34.6%			$L6a3$	46.5%
		$3_1$	4.5%			$L2a1$	26.9%
	2	$5_1$	58.1%			$unlink$	20.7%
		$0_1$	33.0%			$L4a1$	5.9%
		$3_1$	8.9%				

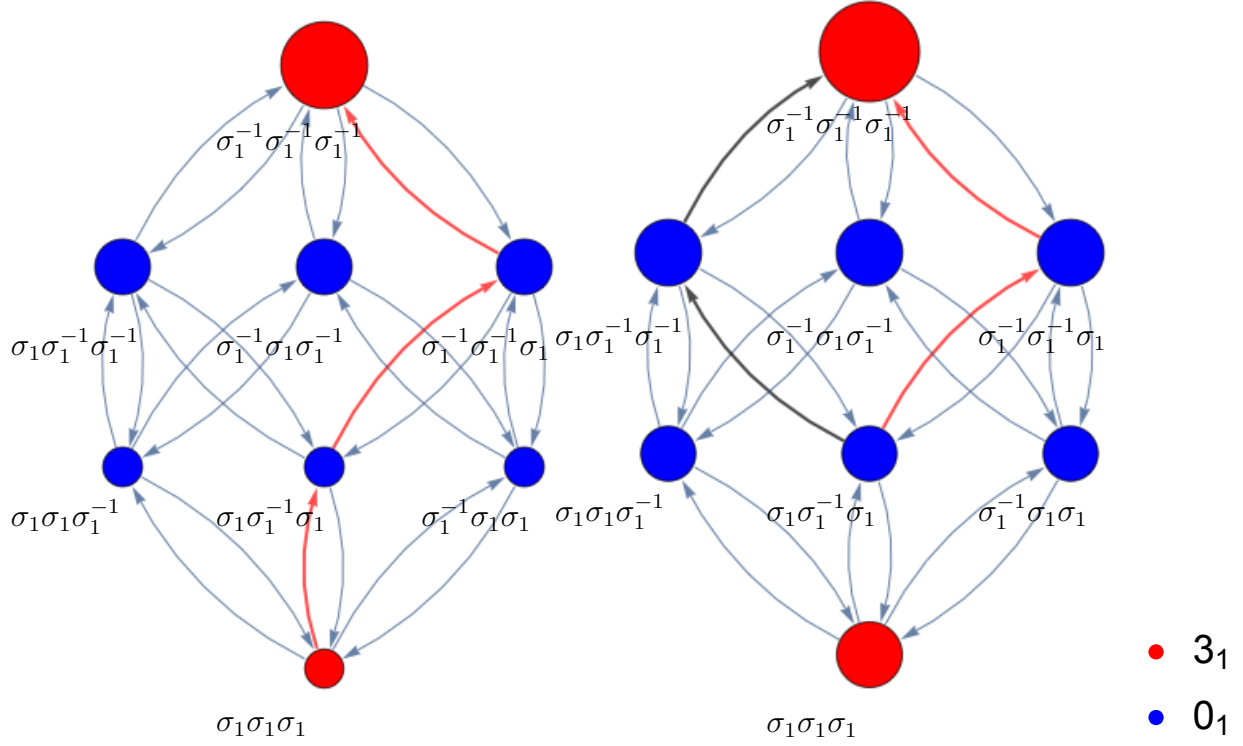
Table 5.2: Proportion of fittest knots and links for a range of landscapes for braids on two strands (strings of  $\sigma_1$  and  $\sigma_1^{-1}$ ). The knots and links in each landscape come from the closure of the fittest braids in the landscape.

We notice that the fittest knot or link in each landscape is the one with highest crossing number, for example when  $N = 6$  we see that the link  $L6a3$  is the fittest for all values of  $K$  over all 10,000 simulations of landscapes.

It is also interesting to note that when  $K = 0$  there are only two possible knots or links as the fittest in the landscape, a knot or link with  $N$  crossings or  $0_1$  or the *unlink*. This is due to fitness depending on a single crossing when  $K = 0$  and so if either  $\sigma_1$  and  $\sigma_1^{-1}$  has higher fitness contribution, the knot or link with  $N$  crossings of either  $\sigma_1$  and  $\sigma_1^{-1}$  has highest fitness. If  $\sigma_1$  and  $\sigma_1^{-1}$  have equal fitness the knot or link composed of both type of crossings has equal fitness to a knot or link of one type, resulting in  $0_1$  or the *unlink*, the knot or link with no crossings.

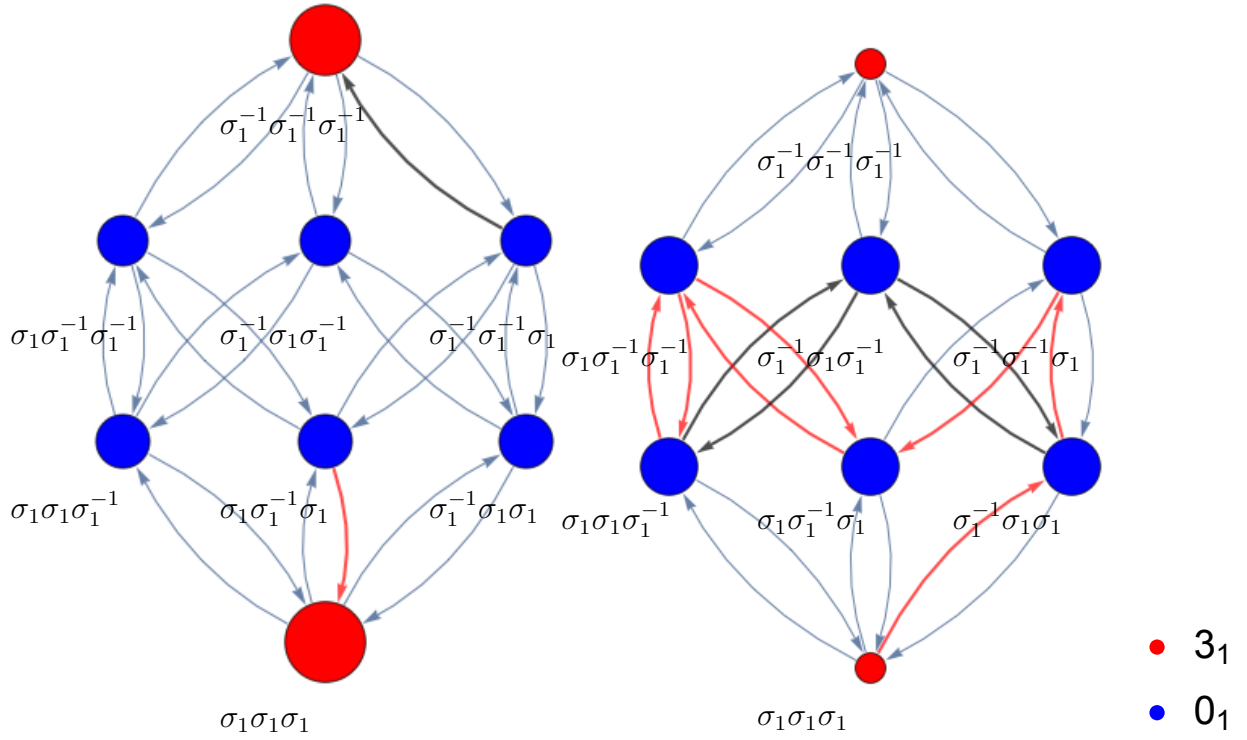
However a knot or link being the fittest in the landscape does not necessarily mean that knot or link is most often reached if we consider walks on the landscape where walks move between braids which have Hamming Distance one from another in favour of the braids with higher fitness.

**Example 5.2.2** We consider again the example of the  $N = 3$ ,  $K = 1$  landscape and consider walks on various forms of this landscape.



(a) An  $N = 3$ ,  $K = 1$  landscape in which the global maximum  $\sigma_1^{-1}\sigma_1^{-1}\sigma_1^{-1}$  is reached from walks starting anywhere on the landscape.

(b) An  $N = 3$ ,  $K = 1$  landscape in which the global maximum  $\sigma_1^{-1}\sigma_1^{-1}\sigma_1^{-1}$  is reached from walks starting anywhere on the landscape, except  $\sigma_1\sigma_1\sigma_1$ , a local maxima from which walks never move.



(c) An  $N = 3$ ,  $K = 1$  landscape in which the global maximum  $\sigma_1 \sigma_1 \sigma_1$  is reached from walks starting on the lower half of the landscape, whilst walks starting on the upper half terminate at  $\sigma_1^{-1} \sigma_1^{-1} \sigma_1^{-1}$ , a local maxima.

(d) An  $N = 3$ ,  $K = 1$  landscape in which there are multiple global maxima. The walks bounce around between equally fit nodes with Hamming Distance one.

Figure 5.1: A network representing the Hamming Distance between braids on two strands in an  $N = 3$ ,  $K = 1$  landscape. Each node represents one of the eight braids in the landscape with the node coloured by the knot it represents. Nodes are connected to other nodes that represent braids one crossing change away, and so have Hamming Distance one, by thin blue arrows. The size of the nodes represent the fitness of each braid under a random fitness landscape with the thick red and black arrows detailing walks from various start nodes, through nodes representing fitter braids, to terminate at the locally largest node representing the locally largest braid. There are many possible fitness landscapes for  $N = 3$  and  $K = 1$  on which some walks always reach the global maximum on the landscape and others terminating at or bouncing between multiple local maxima.

Figure 5.1 shows various landscapes for  $N = 3$ ,  $K = 1$  and some examples of walks on those landscapes. The walk starts at a random point on the landscape then moves to a braid one crossing change away with highest fitness, if there are multiple braids one change away with equal fitness then the next step is chosen randomly from those braids. We see that the fitness of each braid on the landscape and the starting point of the walk determines the termination point of that walk. We note that walks do not always terminate at the fittest braid on the landscape, sometimes becoming stuck at points of local maxima.

The analysis above discussed the knots which were given the highest fitness on various  $NK$  landscapes. Over the various landscapes with  $2 \leq N \leq 6$  and  $1 \leq K \leq N - 1$  the largest knot or link in the landscape generally has the highest fitness. However looking to the example of walks on an  $N = 3$  and  $K = 1$  landscape, walks sometimes never reach the fittest point in the landscape, terminating at a local maxima representing a knot or link with lower crossing number.

In general the knots in ABOK with higher crossing number appear with lower frequency. An analysis of these knots and links considering the fitness of each knot and link considered by the braid words representing them and the walks on these fitness landscapes may help understand knot frequency seen in ABOK.

### 5.2.1 Fitness from ABOK

The fitness landscapes discussed above have used fitness values for each string of length  $K + 1$  assigned randomly in order to explore the effect of different fitness levels of strings on the overall fitness of knots and links. In this case the “fitness” does not mean much at all, it is just a random scalar value assigned to braid words and does not give much information about the performance or preference of any knot type. If we use fitness values for certain strings influenced by the popularity of their corresponding knot type, what does this tell us about the fitness of other knot types?

For a given  $N$  and  $K$  we predict the fitness of the knots with braid words represented by strings of length  $N$  using the frequency in ABOK of the knots whose

braid words are represented by strings of length  $K + 1$ . In this way the fitness of knots and links with higher crossing number is predicted using the frequency from ABOK of knots and links with fewer crossings and similar features. As the value of  $K$  increases, longer strings are included in the calculation of the fitness of strings of length  $N$  and so the frequency of more knots and links from the ABOK data are used to calculate fitness. In this way, only the knots and links with lowest crossing number from the ABOK data are used when  $K$  is small, as fitness contributions for strings of length  $K + 1$ , and a range of knots and links is used when  $K$  is larger including those with low and those with high crossing number.

**Example 5.2.3** Let us consider again an  $N = 3$ ,  $K = 1$  landscape. We want to predict the fitness of knots and links with braid words of length  $N$  from the frequency in ABOK of the knots and links corresponding to the braids of length  $K + 1$ . There are eight possible braids on two strands in an  $N = 3$  landscape relating to two knots, as in Example 5.2.1.

When  $K = 1$  fitness contributions are given on strings of length  $K + 1 = 2$  and so fitness contributions are given for the braids  $\sigma_1\sigma_1$ ,  $\sigma_1\sigma_1^{-1}$ ,  $\sigma_1^{-1}\sigma_1$  and  $\sigma_1^{-1}\sigma_1^{-1}$  on two strands.

Braid word	Knot or link	Frequency in ABOK
$\sigma_1\sigma_1$	<i>L2a1</i>	$\frac{48}{415}$
$\sigma_1\sigma_1^{-1}$	<i>unlink</i>	$\frac{20}{415}$
$\sigma_1^{-1}\sigma_1$	<i>unlink</i>	$\frac{20}{415}$
$\sigma_1^{-1}\sigma_1^{-1}$	<i>L2a1</i>	$\frac{48}{415}$

Table 5.3: This table gives the braid words on two strands for  $K = 1$  with the knot or link they represent and their frequency in ABOK as detailed in Table 2.5 in Chapter 2.

The fitness of the  $N = 3$  braid words is calculated using these fitness contributions.

$$\begin{aligned}
F(\sigma_1\sigma_1\sigma_1) &= \frac{1}{3} \cdot (f(\sigma_1\sigma_1) + f(\sigma_1\sigma_1) + f(\sigma_1\sigma_1)) = \frac{48 + 48 + 48}{3 \cdot 415} = \frac{48}{415} \\
F(\sigma_1\sigma_1\sigma_1^{-1}) &= \frac{1}{3} \cdot (f(\sigma_1\sigma_1) + f(\sigma_1\sigma_1^{-1}) + f(\sigma_1^{-1}\sigma_1)) = \frac{48 + 20 + 20}{3 \cdot 415} = \frac{88}{1245} \\
F(\sigma_1\sigma_1^{-1}\sigma_1) &= \frac{1}{3} \cdot (f(\sigma_1\sigma_1^{-1}) + f(\sigma_1^{-1}\sigma_1) + f(\sigma_1\sigma_1)) = \frac{20 + 20 + 48}{3 \cdot 415} = \frac{88}{1245} \\
F(\sigma_1^{-1}\sigma_1\sigma_1) &= \frac{1}{3} \cdot (f(\sigma_1^{-1}\sigma_1) + f(\sigma_1\sigma_1) + f(\sigma_1\sigma_1^{-1})) = \frac{20 + 48 + 20}{3 \cdot 415} = \frac{88}{1245} \\
F(\sigma_1\sigma_1^{-1}\sigma_1^{-1}) &= \frac{1}{3} \cdot (f(\sigma_1\sigma_1^{-1}) + f(\sigma_1^{-1}\sigma_1^{-1}) + f(\sigma_1^{-1}\sigma_1)) = \frac{20 + 48 + 20}{3 \cdot 415} = \frac{88}{1245} \\
F(\sigma_1^{-1}\sigma_1\sigma_1^{-1}) &= \frac{1}{3} \cdot (f(\sigma_1^{-1}\sigma_1) + f(\sigma_1\sigma_1^{-1}) + f(\sigma_1^{-1}\sigma_1^{-1})) = \frac{20 + 20 + 48}{3 \cdot 415} = \frac{88}{1245} \\
F(\sigma_1^{-1}\sigma_1^{-1}\sigma_1) &= \frac{1}{3} \cdot (f(\sigma_1^{-1}\sigma_1^{-1}) + f(\sigma_1^{-1}\sigma_1) + f(\sigma_1\sigma_1^{-1})) = \frac{48 + 20 + 20}{3 \cdot 415} = \frac{88}{1245} \\
F(\sigma_1^{-1}\sigma_1^{-1}\sigma_1^{-1}) &= \frac{1}{3} \cdot (f(\sigma_1^{-1}\sigma_1^{-1}) + f(\sigma_1^{-1}\sigma_1^{-1}) + f(\sigma_1^{-1}\sigma_1^{-1})) = \frac{48 + 48 + 48}{3 \cdot 415} = \frac{48}{415}
\end{aligned}$$

Example 5.2.3 details the calculation of fitness in an  $N = 3$ ,  $K = 1$  for braids of length  $N = 3$  on two strands with the fitness contributions for  $K$  given by the ABOK frequency data.

The closure of both braids  $\sigma_1\sigma_1\sigma_1$  and  $\sigma_1^{-1}\sigma_1^{-1}\sigma_1^{-1}$  gives the trefoil knot,  $3_1$ , whilst the closure of all the other braids given relates to the unknot,  $0_1$ . The fitness of both braids representing  $3_1$  is  $\frac{48}{415}$  and the frequency of  $3_1$  in ABOK is  $\frac{45}{415}$ , a value not far away. The fitness of all braids representing  $0_1$  is  $\frac{88}{1245}$  with frequency in ABOK  $\frac{111}{415} = \frac{333}{1245}$ , a hugely different value.

Although the fitness of  $3_1$  is calculated to be quite close to the frequency in ABOK, the fitness of  $0_1$  is not close at all. This method predicts higher fitness of  $3_1$  over  $0_1$  but  $0_1$  is much more frequent in ABOK than  $3_1$ .

However, the frequency data from ABOK sums to one when all knots and links are considered and so when taking a subset of knots and links, the total of these elements will be less than one, whilst the total for the fitness values could be greater than one. In this way it does not make sense to compare the values of fitness and frequency directly. In order to compare the frequency and fitness we take both sets of values as vectors with both vectors first scaled so they both sum to one, by dividing each vector by the total of its elements.



$$NKFs_{scale} = \frac{NKF}{(\sum_{i=1}^n NKF_i)}$$

$$ABOKFs_{scale} = \frac{ABOKF}{(\sum_{i=1}^n ABOKF_i)}$$

Here  $n$  is the number of knots or links in the landscape,  $NKF$  is the vector containing their fitness values and  $ABOKF$  is the vector containing the corresponding frequency data from ABOK with  $NKF_{scale}$  and  $ABOKF_{scale}$  the vector of scaled values. If the knot or link does not appear in ABOK the frequency is zero.

This example only looked at an  $N = 3$ ,  $K = 1$  landscape on two strands, including eight braids relating to two distinct knots. Increasing the number of strands to three includes 64 braids and four distinct knots and links, potentially increasing accuracy. We now look to landscapes for increased  $N$  and  $K$  for braids on three strands.

When  $K = 0$  the fitness of each string is determined by the frequency of the unknot  $0_1$ , giving equal fitness to each string for any  $N$  and for each knot. When  $K = N - 1$  the fitness of each string is determined by the fitness of each string as a whole and therefore by the frequency of the knot or link represented by it in ABOK. For these reasons we consider only values  $1 \leq K \leq N - 2$ .

The fitness of knots and links is given for  $3 \leq N \leq 8$  and  $1 \leq K \leq N - 2$  in Appendix A.3. These are all the  $NK$  landscapes for values of  $N$  and  $K$  with the fitness values for the strings of length  $K$  informed by ABOK data.

To compare the fit of the landscape to the ABOK data we take the fitness value for each knot or link in the landscape and compare it to the frequency of that knot or link using the squared Euclidean metric;

$$d = \sum_{i=1}^n (NKFs_{scale_i} - ABOKFs_{scale_i})^2$$

We also use the Hamming Distance [91] between the ABOK data and knots and links in the  $NK$  landscape based on order of frequency and fitness. That is we give the ABOK data a natural number corresponding to its frequency, with value 1 if it is the least frequent knot or link in the data and value equal to the number of data items if it is the largest. We do the same for the fitness data, with value 1 if it is the

least fit knot or link and value equal to the number of data items if it is the largest. As the order of knots and links in both strings of data is the same, if two knots or links share the same fitness or frequency the one that appears first is given the next value in the order then the next the order plus one.

In each case we compare the knots and links that appear in the fitness landscape and do not take into account knots and links that appear in ABOK that do not appear in the landscape, that is those knots and links that have crossing number greater than  $N$  or those that cannot be formed from a braid on three strands.

**Example 5.2.4** Table 5.4 gives the frequency in ABOK and the fitness of each knot in an  $N = 3$  and  $K = 1$  landscape where the fitness values for strings of length  $K$  are given by the frequency data from ABOK. The order of the frequencies and fitness are given along with the squared Euclidean distance of the scaled vectors and Hamming distance.

Knot or link	ABOK frequency	Fitness	ABOK order	Fitness order
$3_1$	0.108	0.116	2	2
$L2a1$	0.116	0.217	3	4
<i>unlink</i>	0.048	0.194	1	3
$0_1$	0.267	0.071	4	1
Squared Euclidean distance	0.220			
Hamming distance	3			

Table 5.4: Fitness values for knots and links in an  $N = 3$  and  $K = 1$  landscape where the fitness values for strings of length  $K$  are given by the frequency data from ABOK. The order of frequencies and fitness values are given with two distance calculations. We see the fit is quite poor with Hamming distance of 3 for a total of four links in the landscape and with a squared Euclidean distance of scaled vectors of 0.220, far from zero. The poor fit is also easy to see in the difference in orders and values.

Table 5.5 gives both metric values for  $3 \leq N \leq 8$  and  $1 \leq K \leq N - 2$  landscapes with the fitness of strings of length  $K$  given by the frequencies in the ABOK data.

$N$	Knots and links in landscape	$K$	Squared Euclidean	Hamming distance
3	4	1	0.220	3
4	9	1	0.173	9
		2	0.164	7
5	9	1	0.208	9
		2	0.074	7
		3	0.148	7
6	20	1	0.150	19
		2	0.127	18
		3	0.110	19
		4	0.118	18
7	23	1	0.195	23
		2	0.128	21
		3	0.167	21
		4	0.080	21
		5	0.132	20
8	49	1	0.143	49
		2	0.128	47
		3	0.125	48
		4	0.113	47
		5	0.097	47
		6	0.107	48

Table 5.5: Distance values for  $3 \leq N \leq 8$  and  $1 \leq K \leq N - 2$  landscapes with the fitness values for strings  $K$  informed by the ABOK frequency data. We see the lowest Euclidean distance occurs when  $N = 7$  and  $K = 4$  with a value of 0.080 but the Hamming distance is 21 for 23 knots and links in the landscape, meaning the order between the fitness landscape data and the ABOK data agrees for only one knot or link. The Hamming distance between orders is poor for all landscapes and the squared Euclidean distances are fairly poor.

To put the metric values in Table 5.5 into context we compare these metric values

with those resulting from random assignment of fitness contributions.

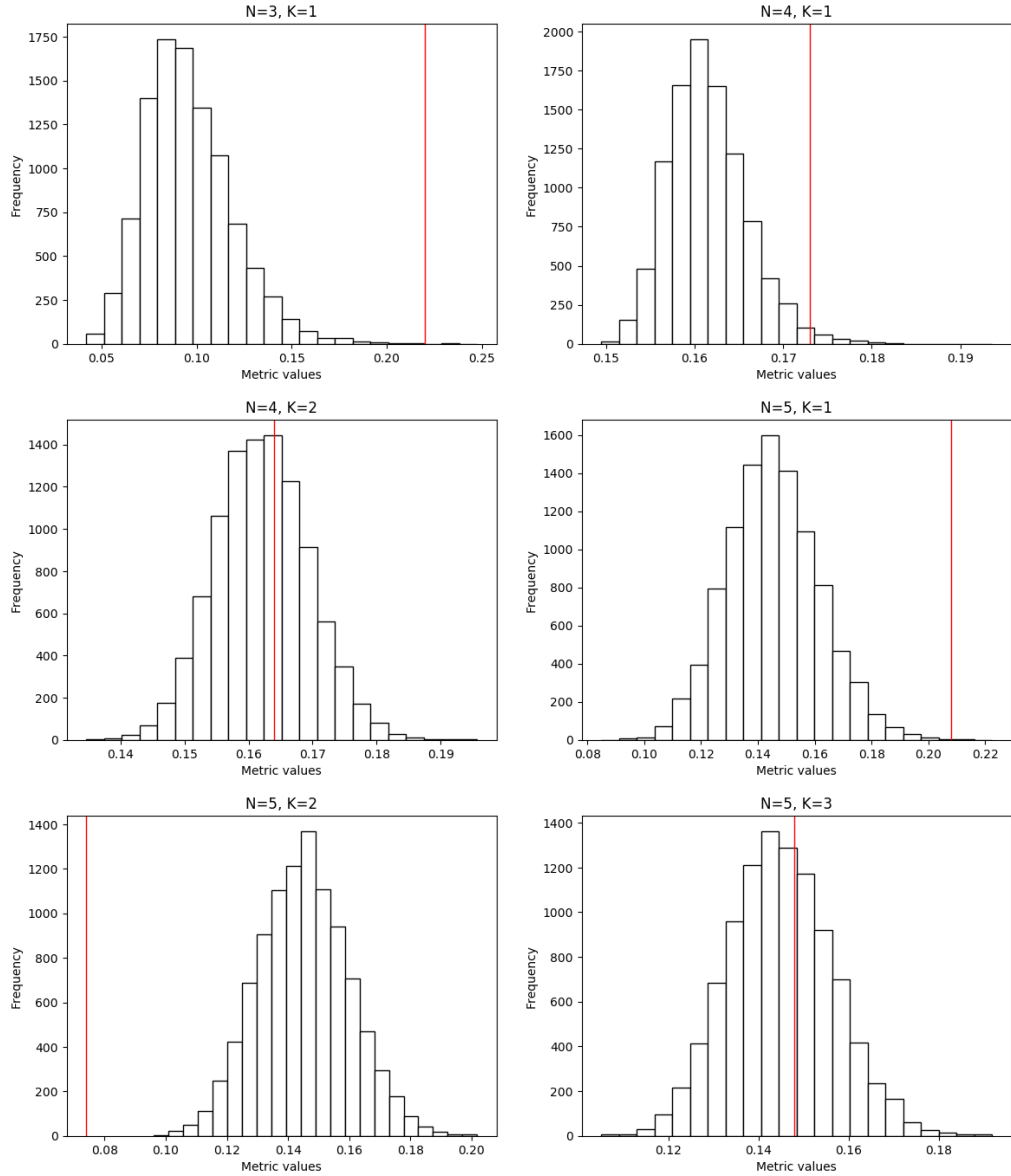


Figure 5.2: Distribution of squared Euclidean distance of scaled vectors on various landscapes with random fitness contributions between 0 and 1. The histogram plots the results of 10,000 simulations each with random fitness contributions selected from a uniform distribution between 0 and 1. The red line indicates the squared Euclidean value on the landscape with fitness contributions informed by ABOK frequency data. We can see that the metric value found using fitness contributions is varied, in some landscapes being much greater than the majority of metric values calculated with random fitness contributions and in others being lower.

N	K	$p = P(X < x)$	
		Squared Euclidean distance	Hamming distance
3	1	$p > 0.999$	$p = 0.152$
4	1	$p > 0.97$	$p = 1$
	2	$p > 0.6$	$p = 0.239$
5	1	$p > 0.999$	$p = 1$
	2	$p < 1 \times 10^{-8}$	$p = 0.202$
	3	$p > 0.6$	$p = 0.253$
6	1	$p = 0.998$	0.696
	2	$p < 0.014$	0.215
	3	$p < 3 \times 10^{-16}$	$p = 0.575$
	4	$p < 1 \times 10^{-12}$	$p = 0.181$

Table 5.6: Probability of the metric values given in Table 5.5 occurring as the result of randomly assigned fitness contributions from a uniform distribution between 0 and 1 for  $3 \leq N \leq 5$ ,  $1 \leq K \leq N - 2$  landscapes. The  $p$  values represent the probability that a randomly assigned fitness contribution results in a metric value less than that given in Table 5.5. We notice that the probability a randomly assigned value has lower squared Euclidean distance and the probability a randomly assigned value has lower Hamming distance varies case by case.

Table 5.6 gives the probabilities of the metric values resulting from the fitness values informed by ABOK data given in Table 5.5 resulting from randomly assigned fitness contributions from a uniform distribution on the interval  $[0, 1]$ . The probabilities given in Table 5.6 are calculated from 10,000 simulations with fitness contributions assigned from a uniform distribution on the interval  $[0, 1]$  for  $3 \leq N \leq 6$ ,  $1 \leq K \leq N - 2$  landscapes. Random fitness contributions from a uniform distribution on the interval  $[0, 1]$  were chosen as a comparison in order to see the difference between values given with no assumptions on the whole possible range of fitness values and those using the ABOK data.

We see that the probability of a squared Euclidean distance resulting from ran-

dom contributions being lower than that calculated using contributions from ABOK and the probability of a lower Hamming distance depends on the case. The lowest probabilities for Hamming distance occur when  $N = 5$ ,  $K = 2$ ,  $N = 6$ ,  $K = 3$  and  $N = 6$ ,  $K = 4$ . Simulations have not been included for landscapes with  $7 \leq N \leq 8$  as the larger the landscape the longer the simulation takes, but given that probabilities are generally lower given lower metric values and larger  $N$  we expect the same conclusions for landscapes with  $7 \leq N \leq 8$ .

The probabilities discussed in Table 5.6 demonstrate that the fitness of knots and links resulting from the assignment of fitness contributions informed by ABOK data sometimes gives a better fit to the frequencies seen in ABOK than assigning fitness randomly, but is sometimes far worse. As the fitness of larger knots and links under this assignment is predicted using the frequency of smaller knots and links, this suggests that there are patterns of crossings appearing in some smaller knots and links affecting their frequency that also affect the frequency of some larger knots and links, with these patterns varying as  $N$  and  $K$  vary. The calculation of fitness in an  $NK$  landscape is given through neighbouring features in a string and so by neighbouring crossings on the braid words of knots and links. The assignment of fitness contributions by frequency in ABOK give the knots that appear more often in ABOK, and therefore the features within them, and so the crossings that appear in more knots and links in ABOK higher fitness contribution, giving larger knots and links with similar features higher fitness. As this method results in lower metric values when compared with the ABOK data than random assignment it suggests that certain features in knots and links are common amongst those more frequent in ABOK.

The closest fit occurs here when  $N = 7$  and  $K = 4$ , resulting in a squared Euclidean distance of 0.080 and Hamming distance of 22. This fit is quite similar in value to the fit from case 4 of the social and asocial learning model discussed in Chapter 4.2.2, which resulted in a squared Euclidean distance of 0.045. However the case discussed in the social and asocial learning model included all braid words on three strands of length up to eight, resulting in 63 knots and links, and an  $N = 7$  landscape considers only braid words on three strands of length seven resulting in

23 knots and links.

We see that the squared Euclidean distance values for each  $3 \leq N \leq 8$  landscape fall as the value of  $K$  for each increases, with the second largest value of  $K$  producing the best fit for landscapes with a value of  $N$  of 5, 6, 7 and 8. These represent the most rugged landscapes, in which more fitness contributions are taken into account to determine the overall fitness of a knot or link. For a given  $N$  a larger value of  $K$  and so a very rugged fitness landscape gives the best fit to the ABOK data. The more rugged landscapes take more features of the knot or link into account when calculating their fitness allowing a closer fit to the ABOK data by the closer specification of the features that make up the knot or link. However this apparent good fit could purely be the result of overfitting to the sample data, with more parameters allowing a better fit. In the absence of correction for overfitting or a data set upon which to test the model we cannot conclude for certain that the most rugged landscape is the best model for the ABOK data.

We saw in Figure 5.1 that random walks on a fitness landscape may not always end up at the global optima of the fittest braid or knot in the landscape and, as the case in Figure 5.1 may end at local maxima knots rather than the global maxima. Given the fitness data does not seem to explain the distribution of knots in ABOK very well, considering random walks on these landscapes may explain the distribution better.

Table 5.7 gives results of the fittest knots or links in each fitness landscape for  $3 \leq N \leq 5$  and  $1 \leq K \leq N - 2$  discussed in Table 5.5 and the percentage that knot or link is reached in a random walk starting at various points on the landscape. The walk starts at a random point on the landscape then moves to a braid one crossing change away with highest fitness, if there are multiple braids one change away with equal fitness then the next step is chosen randomly from those braids. The data in Table 5.7 has been generated from 1000 walks starting at various points on the landscape and the knot or link represented by the braid they reach when the walk stops moving between types. Further random walks are given in Table A.11 and Tables A.12 and A.13 in Appendix A.3.

$N$	$K$	Fittest knots or links	Knots and links resulting from walks	Percentage
3	1	$L2a1$	$L2a1$	100%
4	1	$0_1, 3_1, 4_1$	$0_1$ $3_1$ $4_1$ $L2a1\#L2a1$	75.8% 12.1% 12% 0.1%
	2	$unlink$	$unlink$	100%
5	1	$unlink, L2a1, L4a1, L5a1$	$L2a1$ $L4a1$ $unlink$ $L5a1$	50.2% 23.7% 14% 12.1%
	2	$0_1, unlink$	$0_1$ $unlink$	75.6% 24.4%
	3	$unlink$	$unlink$	100%
6	1	$unlink\#unlink,$ $L2a1\#unlink,$ $L2a1\#L2a1, L6a4, L6n1$	$L2a1\#L2a1$ $L2a1\#unlink$ $L6n1$ $unlink\#unlink$ $L6a4$ $3_1$ $0_1$ $5_1$ $5_2$ $4_1$ $6_2$ $6_3$ $L6a5$	36.4% 32% 11.2% 7.9% 3.7% 3% 2% 1.5% 0.8% 0.5% 0.5% 0.3% 0.2%
	2	$unlink, L2a1$	$unlink$ $L2a1$	69.2% 30.8%
	3	$0_1, unlink\#unlink, L6n1$	$0_1$ $unlink\#unlink$ $L6n1$	91.8% 4.1% 4.1%
	4	$unlink$	$unlink$ $3_1$ $4_1$ $L2a1$ $0_1$	75.2% 11.1% 10.2% 3.1% 0.4%

Table 5.7: Random walk results  $3 \leq N \leq 5$  and  $1 \leq K \leq N - 2$  landscapes



The selection of knots and links in the random walks is through crossing changes. The walk will move to a point that represents a braid one crossing change away if that braid has higher fitness. This addition of selection through crossing changes is similar to the usage of crossing changes in the social and asocial learning model. We see that a more diverse range of knots and links emerge as the result of random walks than as the fittest point on the  $NK$  landscapes. Although the fittest knot distribution was similar to the ABOK distribution and the social and asocial learning model, taking random walks into account gives a more diverse range of knots. The range of knots and links reached through random walks is larger the lower the value of  $K$  for all  $3 \leq N \leq 8$ , that is the smoother the fitness landscape the more knots and links can be reached as the result of random walks on the landscape. As the value of  $K$  increases the landscape becomes more rugged, reducing the range of knots and links a walk can reach.

Taking the frequency each knot or link appears as the result of walks over all landscapes for  $3 \leq N \leq 8$  and  $1 \leq K \leq N - 2$  and comparing these frequencies with the ABOK data in the same manner as given in Table 5.5 gives a squared Euclidean distance of 0.0709418. This metric value is lower than those calculated for most landscapes in Table 5.5 and includes 38 distinct knots and links, more than those included in all landscapes with  $N < 8$ . Considering the frequency of knots and links in this way includes knots and links from all landscapes whilst resulting in a fairly low metric value, representing the ABOK data better than considering each landscape alone.

This analysis gives an idea of which knots and links may have highest fitness influencing selection, but this does not match up perfectly with the ABOK data. In the next section we discuss what particular features of a knot or link may increase the fitness of that knot or link for using a further  $NK$  landscape analysis.

### 5.2.2 Identifying fit crossings

In order to attempt to identify the features in a knot or link that increase its frequency in ABOK and potentially increase its usage or ease to learn, we use the frequency of each knot or link as seen in ABOK as target values for strings of length

$N$  in an  $NK$  landscape. We then use a machine learning procedure [92] to train the fitness contributions for  $K$  in order that the values for strings of length  $K + 1$  give an overall frequency for the strings of length  $N$  in the landscape that is close to the ABOK data. The strings of length  $K + 1$  are patterns of crossings in a braid word on three strands allowing us to identify features that would need to be the “fittest” to produce a distribution of knots as seen in ABOK.

Starting with random values from a uniform distribution on the interval  $(0, 1)$  fitness of strings of length  $K + 1$  is given. The fitness of strings of length  $N$  is then calculated and the fitness values of knots and link compared with their ABOK frequency data. The fitness contribution of the strings  $K$  to each string of length  $N$  is calculated and then adjusted by a small amount weighted by their contribution, to increase or decrease the fitness of strings of length  $N$  in line with the ABOK data. This process is repeated until the average difference between the fitness of each knot or link and the ABOK frequency is less than 0.01.

**Example 5.2.5** Consider the  $N = 3$ ,  $K = 1$  landscape. This landscape contains strings of length 3 made up of  $\sigma_1$ ,  $\sigma_1^{-1}$ ,  $\sigma_2$  and  $\sigma_2^{-1}$  whose fitness is given by the fitness of strings of length 2. The knots and links possible from braid words of length 3 on three strands are given below along with their frequency in ABOK;

Link	Frequency
$3_1$	0.108
$L2a1$	0.116
$unlink$	0.048
$0_1$	0.267

Table 5.8: ABOK frequencies for knots and links to be matched in an  $N = 3$ ,  $K = 1$  landscape.

The best fit to these data on the  $NK$  landscape occurs with the following fitness for strings of length 2;

Braid	Fitness	Braid	Fitness
$\sigma_1^{-1}\sigma_1$	0.4521	$\sigma_2\sigma_1$	0.0260
$\sigma_2\sigma_2^{-1}$	0.3179	$\sigma_1\sigma_2^{-1}$	0.0256
$\sigma_1^{-1}\sigma_1^{-1}$	0.2767	$\sigma_2^{-1}\sigma_2^{-1}$	0.0237
$\sigma_1\sigma_1^{-1}$	0.2427	$\sigma_1^{-1}\sigma_2$	0.0207
$\sigma_2\sigma_2$	0.1433	$\sigma_2^{-1}\sigma_1^{-1}$	0.0167
$\sigma_2^{-1}\sigma_2$	0.1401	$\sigma_2\sigma_1^{-1}$	0.0072
$\sigma_1\sigma_1$	0.1076	$\sigma_1\sigma_2$	0.0056
$\sigma_1^{-1}\sigma_2^{-1}$	0.0292	$\sigma_2^{-1}\sigma_1$	0.0002

Table 5.9: Crossing fitness required to match ABOK frequencies in an  $N = 3$   $K = 1$  landscape.

There are sixteen combinations of  $\sigma_1$ ,  $\sigma_1^{-1}$ ,  $\sigma_2$  and  $\sigma_2^{-1}$  in a  $K = 1$  landscape. All the combinations of  $\sigma_i\sigma_i^{-1}$  for  $i \in 1, 2$  are among the top six fittest combinations of crossings showing that in order to get the distribution of knots in this landscape, an over crossing then an under crossing, or vice versa, on the same strand is preferred. The combinations of  $\sigma_i\sigma_i$  for  $i \in 1, 2$  are between the third and eleventh fittest combinations showing that repeated crossings of the same type on the same strand are preferred over other combinations but are less favoured than a crossing of each type on the same strand.

In the below tables the fittest crossing types are given for various  $NK$  landscapes. There are four different possible crossing types forming a braid word in the  $K$  fitness contributions.

Here  $\sigma_i\sigma_i$  denotes braid words with all the same crossing type on the same strand, for example  $\sigma_1\sigma_1\sigma_1$  or  $\sigma_2^{-1}\sigma_2^{-1}\sigma_2^{-1}$ ,  $\sigma_i\sigma_i^{-1}$  denotes braid words with different crossing types on the same strand, for example  $\sigma_1\sigma_1\sigma_1^{-1}$  or  $\sigma_2^{-1}\sigma_2\sigma_2^{-1}$ ,  $\sigma_i\sigma_j$  denotes braid words with all the same crossing type on differing strands, for example  $\sigma_1\sigma_2\sigma_2$  or  $\sigma_2^{-1}\sigma_1^{-1}\sigma_2^{-1}$  and  $\sigma_i\sigma_j^{-1}$  denotes braid words with different crossing types on differing strands, for example  $\sigma_1\sigma_1^{-1}\sigma_2$  or  $\sigma_2^{-1}\sigma_1^{-1}\sigma_2$ .

		Average fitness of crossing type			
N	K	$\sigma_i\sigma_i$	$\sigma_i\sigma_i^{-1}$	$\sigma_i\sigma_j$	$\sigma_i\sigma_j^{-1}$
3	1	0.1378	<b>0.2882</b>	0.0194	0.0134
4		0.0368	0.0768	<b>0.1860</b>	0.0312
5		0.0223	<b>0.2780</b>	0.0047	0.0049
6		0.0026	<b>0.1546</b>	0.0579	0.0112
7		0.0001	<b>0.2823</b>	0.0037	0.0013

Table 5.10: Average fitness of crossing types in  $3 \leq N \leq 7$ ,  $K = 1$  landscapes, with the fitness of crossings calculated by matching knot and link fitness to the frequencies of knots and links in ABOK. Here  $\sigma_i\sigma_i$  denotes braid words with all the same crossing type on the same strand,  $\sigma_i\sigma_i^{-1}$  denotes braid words with different crossing types on the same strand,  $\sigma_i\sigma_j$  denotes braid words with all the same crossing type on differing strands and  $\sigma_i\sigma_j^{-1}$  denotes braid words with different crossing types on differing strands. The crossing type with highest fitness is given in bold for each case of  $N$ .

Here the fittest crossing types are those on the same strand of opposite kind  $\sigma_i\sigma_i^{-1}$ , either over then under or under then over. As these crossings occur on the same strand their actions undo one another, causing redundancy in the braid word. This redundancy is seen in the knots and links in ABOK. The next fittest feature seems to be those involving crossings of the same type on differing strands  $\sigma_i\sigma_j$ , these features will not undo one another and are so maintained in the braid and the corresponding knot or link, but this feature is not hugely fitter than the other two,  $\sigma_i\sigma_j^{-1}$  and  $\sigma_i\sigma_i$ . However the least fit crossing type seems to be those of the same type on the same strand  $\sigma_i\sigma_i$ , a string of repeated crossings in a braid word and repeated crossings in a knot or link.

N	K	Average fitness of crossing type			
		$\sigma_i\sigma_i$	$\sigma_i\sigma_i^{-1}$	$\sigma_i\sigma_j$	$\sigma_i\sigma_j^{-1}$
3	2	0.1084	<b>0.2675</b>	0.1467	0.0877
4		0.0447	0.0810	0.1424	<b>0.1895</b>
5		0.0175	<b>0.2123</b>	0.0349	0.0445
6		0.0087	<b>0.1102</b>	0.0243	0.0559
7		0.0001	<b>0.2541</b>	0.0250	0.0515

Table 5.11: Average fitness of crossing types in  $3 \leq N \leq 7$ ,  $K = 2$  landscapes, with the fitness of crossings calculated by matching knot and link fitness to the frequencies of knots and links in ABOK. Here  $\sigma_i\sigma_i$  denotes braid words with all the same crossing type on the same strand,  $\sigma_i\sigma_i^{-1}$  denotes braid words with different crossing types on the same strand,  $\sigma_i\sigma_j$  denotes braid words with all the same crossing type on differing strands and  $\sigma_i\sigma_j^{-1}$  denotes braid words with different crossing types on differing strands. The crossing type with highest fitness is given in bold for each case of  $N$ .

We see that sequences of differing crossing types on the same strand are most frequent, followed by sequences with differing crossing types on differing strands, followed by the same crossing type on differing strands, with sequences of the same crossing type on the same strands being the least common across these landscapes. This is almost the same pattern as seen on the  $K = 1$  landscapes. As with the  $K = 1$  landscape the fittest crossings for  $N = 3$  and  $N = 4$  is different to  $N = 5, 6, 7$  with the fittest crossings changing for smaller  $N$  and remaining the same for  $N = 6$  and  $N = 7$  in both cases. As with the  $K = 1$  landscape the fittest crossing has much higher average fitness than the others and least fittest  $\sigma_i\sigma_i$  much lower than the others, with the fitness of the other two crossing types not so dissimilar from one another.

		Average fitness of crossing type			
N	K	$\sigma_i\sigma_i$	$\sigma_i\sigma_i^{-1}$	$\sigma_i\sigma_j$	$\sigma_i\sigma_j^{-1}$
4	3	0.0337	0.0869	0.0914	<b>0.1838</b>
5		0.0274	<b>0.1946</b>	0.0347	0.0840
6		0.0050	0.0727	0.0247	<b>0.0979</b>
7		0.0005	0.1732	0.0452	<b>0.1801</b>

Table 5.12: Average fitness of crossing types in  $3 \leq N \leq 7$ ,  $K = 3$  landscapes, with the fitness of crossings calculated by matching knot and link fitness to the frequencies of knots and links in ABOK. Here  $\sigma_i\sigma_i$  denotes braid words with all the same crossing type on the same strand,  $\sigma_i\sigma_i^{-1}$  denotes braid words with different crossing types on the same strand,  $\sigma_i\sigma_j$  denotes braid words with all the same crossing type on differing strands and  $\sigma_i\sigma_j^{-1}$  denotes braid words with different crossing types on differing strands. The crossing type with highest fitness is given in bold for each case of  $N$ .

		Average fitness of crossing type			
N	K	$\sigma_i\sigma_i$	$\sigma_i\sigma_i^{-1}$	$\sigma_i\sigma_j$	$\sigma_i\sigma_j^{-1}$
5	4	0.0289	<b>0.1953</b>	0.0455	0.1481
6		0.0103	0.0819	0.0431	<b>0.1917</b>
7		0.0033	0.2273	0.1039	<b>0.3306</b>

Table 5.13: Average fitness of crossing types in  $3 \leq N \leq 7$ ,  $K = 4$  landscapes, with the fitness of crossings calculated by matching knot and link fitness to the frequencies of knots and links in ABOK. Here  $\sigma_i\sigma_i$  denotes braid words with all the same crossing type on the same strand,  $\sigma_i\sigma_i^{-1}$  denotes braid words with different crossing types on the same strand,  $\sigma_i\sigma_j$  denotes braid words with all the same crossing type on differing strands and  $\sigma_i\sigma_j^{-1}$  denotes braid words with different crossing types on differing strands. The crossing type with highest fitness is given in bold for each case of  $N$ .

We see the same pattern emerging in all cases for landscapes with  $1 \leq K \leq N-1$  and  $3 \leq N \leq 7$ , with the requirement of both over and under crossings on both strands as well as both under and over crossings on the same strand needed to be dominant to fit the ABOK data best, and successive over or under crossings on one set of strands being least common. The mixture of crossings on multiple strands may be needed to give the complexity of knots seen in ABOK incorporating complex features formed of both under and over crossings on multiple strands. The over then under crossing on the same strand may explain the redundancy seen in ABOK, with an over then under crossing on the same strand simply undoing one another, allowing a feature undone by Reidemeister moves which was the definition of redundancy given in Chapter 2. The fitness of these two features may explain the distribution in ABOK, one preserving complexity, the other increasing redundancy and the frequency of lower crossing knots and links.

### 5.3 Conclusion

The model discussed in this chapter involved an  $NK$  fitness model on the braid words of knots and links. The  $NK$  fitness model is a method used to search for combinations of a string that maximise the “fitness” of that string. Braid words of length  $N$  were used as the strings in this model with their “fitness” determined by the cumulative fitness of successive crossings of length  $K+1$ . The model can be used to define a landscape with the distance between braid words given by their Hamming Distance, that is the amount of crossings that differ between the two words. The fitness of knots and links given by the  $NK$  model could represent the selection of certain types of knots and links, increasing their frequency in the ABOK data.

The model was used with the fitness of strings of the  $K$  braids determined by the frequency of the knots and links representing them in ABOK giving the fitness of the  $N$  braids. This was calculated for landscapes with  $3 \leq N \leq 8$  and  $1 \leq K \leq N-2$  and the distance between the resulting fitness and the frequencies in ABOK calculated. This looked to give a better fit to the ABOK data for higher values of  $N$  and  $K$ , the cases with more knots and links in the landscape and more

data taken from ABOK to determine the  $K$  fitness. However the distributions did not fully match the ABOK data distributions.

However, it was seen that on these  $NK$  fitness landscapes the fittest knot and link was not necessarily the marker to use. By considering random walks on these landscapes, that is taking a random starting point on the landscape and moving towards a point representing a braid one crossing change away with higher fitness until the knot or link the points represent is unchanged, it was seen that the fittest knot or link in the landscape is not the one most commonly reached. This suggests that although certain knots and links may have higher fitness and therefore may seem like they should be tied commonly, the process of knot tying and changes coming from crossing changes, which were seen to always occur in the model discussed in Chapter 4, causes a reduction in their frequencies. Considering the knots and links produced by random walks on landscapes gave a much wider range of knots and links and so fit the ABOK distribution better, suggesting selection through crossing changes is necessary to explain the distribution seen in ABOK.

The difference between the ABOK distribution and the distribution of knots and links on  $NK$  landscapes is unsurprising. In their paper exploring the evolution technology using  $NK$  landscapes, Fleming and Sorenson use various patent data to explore the strategies of invention through evolution strategies on  $NK$  landscapes [93]. Although their findings support the application of the  $NK$  model to the evolution of technology, the  $NK$  model did not match up with the important factors in their data. They suggest that this may be due to selection in the replication of technology, whilst  $NK$  landscapes may well model biological evolution through simple search patterns the selection in technology may be more complex, needing a more complex strategy to explain the evolution in technology.

However a comparison of fit between the fitness determined by fitness contributions informed by ABOK data and those randomly assigned showed that those assigned by the frequency data matched the ABOK data much better than random assignment. As the fitness of larger knots and links in this procedure was calculated using contributions informed by the ABOK data of smaller knots and links, it suggests there are certain features increasing the fitness of similar knots and links.



Next the fitness of the  $N$  braids was given by the frequencies of their representative knots and links in the ABOK data in order to assess the fitness required for the  $K$  strings. This was assessed through a machine learning procedure [92], changing the fitness of a  $K$  string over generations to give the frequencies of  $N$  strings given in ABOK. This allowed us to identify the patterns of crossings in knots and links that would need to be optimised to give the distribution in ABOK.

The patterns of crossings that required the highest fitness value to fit the ABOK data were sequences involving crossings between multiple strands of the braid involving both over and under crossings. The next feature that required the highest fitness was sequences of both over and under crossings on the same strand. The first feature of both forms of crossings on multiple strands may aid in increasing the complexity of knots and links through the multiple strands and crossing types required. The second feature of both forms of crossing on one set of strands creates redundant features in the knot or link as the occurrence of both crossing types one after another has the result of undoing the crossing through Reidemeister moves, the definition used for redundancy in Chapter 2. The prevalence of these two may cause the complexity seen in ABOK but increase the frequency of redundant features, increasing the overall frequency of lower crossing knots and links. A bias towards these two features in knot tying during the social learning process could shape the distribution of knots to that seen in ABOK, high frequency of lower crossing knots and links with higher crossing, more complex, knots and links still present along with the presence of redundant features.

However this analysis only looked at the fitness of crossings on three strands and the landscapes were analysed for  $1 \leq K \leq N - 1$  and  $3 \leq N \leq 7$ , and so increasing  $K$  and  $N$  or the number of strands may cause different patterns to emerge. The crossings were analysed and grouped with similar crossings to identify overall patterns so a closer analysis could be possible to identify specific crossing patterns on each knot or for each crossing number, but this would be quite time intensive.

Overall this analysis shows us that although a given knot or link may seem to be optimal through its form it may not be the most commonly tied knot as the changes

caused by crossing changes and additions greatly affects a knots frequency. The form of the knot is also affected by the “fitness” of the crossings forming it, suggesting a preference for complex knot forms with crossings of multiple forms on multiple strands and preference for redundant crossings. This suggests that knots and links may not always appear in their minimal projection and gives an explanation for the high redundancy seen in ABOK.

The parameters used in the  $NK$  model allow it to be used as a diverse tool, allowing few assumptions in the exploration of the factors affecting the frequency in ABOK. The techniques utilised here are not specific to knots and links but can also be relevant to many other applications assessing the frequency of variants.

However, as few assumptions are needed to use the  $NK$  model, we may have missed certain important functional factors increasing the frequencies of knots and links by considering them simply as strings of crossings. Whilst this analysis of features gives a starting point to assess the important factors affecting knot frequency they may not be the only contributing factor to the preference of certain knot variants.

# Chapter 6

## Conclusions

In Chapter 2 an analysis of the various knots appearing in the Ashley Book of Knots (ABOK) [8] was presented. The knots appearing in ABOK were categorised by the mathematical knots and links they represented allowing us to see how many distinct mathematical knots and links are used. A large range of mathematical knots and links appear but many knots in ABOK that are reported to be distinct relate to the same mathematical knot or link.

The frequency of knots and links decreased as crossing number increased, meaning the knots tied most commonly tend to have lower crossing number. This could lead us to determine that the simpler a knot is, the more commonly it is tied, as it may be easier to tie or remember.

Section 2.3.4 explored some factors affecting the distribution of the knots and links in ABOK. An analysis of the knots for the usages given in ABOK found a link between the mean crossing number per usage and the standard deviation of crossing number, that is usages given in ABOK that had more complex knots associated with them utilised a wider range of knots. This suggests it is necessary to utilise a wide range of knots in order to increase complexity, a finding similar to that explored by Muthukrishna et al. [33] in which a wider range of demonstrations of knot tying were needed to maintain the complexity of knot types.

The factors affecting the amount of redundant features in ABOK were also explored in Section 2.3.4. Redundant features are measured by the difference between the crossing number of the picture of the knot in ABOK and the reduced mathe-

mathematical crossing number. It was found that knots with multiple uses associated with them have fewer redundant features than those with one or no uses, knots that have multiple appearances in ABOK have less redundancy than those appearing only once and composite knots have less redundancy than prime knots. These findings suggest the knots utilised are optimised for their purpose, with increased usage and a wider range of uses removing unnecessary features. The difference in redundancy between prime knots and composite knots suggests composite knots are only used when necessary with each crossing important to the knot, suggesting they are used as an optimisation for the given purpose.

In Chapter 3 the transmission of granny and reef knots was explored, motivated by the commonly reported issue of shoelaces that often come untied. The factors affecting the successful replication of granny and reef knots was explored using experimental and modelling methods. The experiment identified factors that may affect the faithful replication of granny and reef knots; a preference towards repeatedly tying the same handedness of trefoil and a slight likelihood to perform the mirror image of the action demonstrated. Although it appeared there was a preference to tie left handed trefoils the analysis identified that there was not an effect of a bias towards a particular handedness of trefoil when tying the composite knots. Although modelling methods identified the occurrence of highly accurate imitation, predictive methods forecast these factors would greatly influence the tendency to tie granny knots over reef knots. If these factors were to influence knot tying in the same manner over generations then this could have shaped the knots tied by humans and those seen in ABOK, giving an explanation to the issue of shoelaces frequently coming untied.

In Chapter 4 a model of social and asocial learning applying to all knots and links was presented in an attempt to explain the distribution of knots and links seen in ABOK. Social and asocial learning related to knots and links was analysed through a model reflecting crossing changes and additions on braid words of two and three strands. Crossing changes reflected social learning whilst additions represented asocial learning on multiple braid words of given knots and links. Through these changes and additions networks of expected mutation of knots and links were built

up, suggesting a preference to certain knots and links. The model predicted higher frequencies of lower crossing knots and links than higher crossing knots and links but still maintained the presence of the more complex variants, in a similar way to the ABOK data. However this model did not seem to fit the data on the frequency of knots and links in ABOK analysed in Chapter 2. As no biases were included in this model this would suggest there are factors influencing the usage of some knots over others which may result in selection for certain knots in the transmission process.

The fitness of given knots and links was analysed using various  $NK$  fitness landscapes [85] in Chapter 5. The fitness of braid words on fitness landscapes for various values of  $N$  and  $K$  were compared with the values for  $K$  informed by the frequency data in ABOK. Using values informed by the ABOK data for smaller knots and links to predict the fitness of larger knots and links gave a better fit to the ABOK data than randomly assigned fitness values. This suggested there were features present in knots and links, common across multiple types which affected their fitness and so frequency in ABOK. However, by analysing walks on these landscapes through crossing changes it was found that commonly the fittest knot or link or global maximum point in the landscape was not reached and could never be reached for some starting points of walks. The more rugged fitness landscapes gave a better fit to the ABOK data, allowing for greater specification of the fitness of features increasing the fitness of knots and links and incorporating the analysis of walks on these landscapes produced a good fit to the ABOK data, including more knots and links in the analysis than considering individual landscapes alone. However we cannot conclude for certain that this apparent goodness of fit of the most rugged landscapes to the ABOK data is not caused by overfitting of the model to the data through closer specification of parameters and more data with which to test this hypothesis may be necessary.

The similarity between the social and asocial learning model and the results on  $NK$  landscapes suggests that crossing changes need to be taken into account to explain the ABOK data. Both the social and asocial learning model and the  $NK$  model analyse the crossings in a knot or link, the social and asocial model through crossing changes and additions when knot tying information transitions and the  $NK$

landscape by associating fitness to strings of crossings to predict the resulting knot or link's frequency.

The fitness of crossings in braid words was then analysed by a machine learning procedure [92] in order to give landscapes that fitted the ABOK data. The crossings that needed the highest fitness to give this data were those including both over and under crossings, both across multiple strands and single strands. The crossings on multiple strands increase the complexity of knots through increasing the range and number of crossing types, whilst the crossings on single strands have the effect of undoing one another increasing the redundant features in knots and links.

Combining this finding with the networks of social and asocial learning could potentially explain the distribution of knots and links in ABOK, with the social and asocial learning showing crossing changes and additions are necessary for the distribution seen in ABOK. The  $NK$  analysis shows that although certain knots and links may be seen to be the fittest in the landscape they are not necessarily reached by walks through crossing changes on the landscape. The fitness of certain forms of crossings identifies suggests a reason for the appearance of higher crossing knots and links in ABOK but the prevalence of lower crossing knots and links with high redundancy.

Although here we have considered a social and asocial learning model separate to a fitness model the fitness here is informed by the frequency of the knots and links and so will be affected by a process of asocial learning. A combination of these models could be considered, perhaps informing fitness values in an  $NK$  landscape through the findings from the social and asocial learning model or considering an additional fitness parameter in the social and asocial model to represent the adaptive values found through the  $NK$  model increasing selection for those variants.

However the transmission of knots and links through social learning is not a simple process with various factors including handedness bias, mirroring and repetition affecting the fidelity of transmission of some of the simplest knots as seen in Chapter 3. These factors may also guide the variation on all knots and links but be a more complex process. We have only scratched the surface of the factors affecting the transmission of knots and links but have shown just how much information can be

gained from the learning process by considering knot tying in this way.

The modelling of the learning process utilised in this analysis did not include the various methods in which knots may be taught or learned in the real world and their possible effect on the learning process. The models analysed here included just one parameter to represent social learning and any specifics about the learning process could be incorporated into this parameter allowing a greater control over the extent and method of social learning in the model. The current models can be viewed as the simplest case and allow a starting point from which to specify more complex models with more parameters.

The analysis presented in this thesis may not be representative of knot tying by the wider population as most of the data presented was collected from ABOK and although ABOK presents over 3,800 knots tied by a wide range of people this may not be an accurate sample of knots tied by people as a whole. However the techniques presented here can be applied to wider data if such data is available and the findings presented could be testable through further experimental methods. In the models present in Chapters 3, 4 and 5 only a selection of knots were included in the analysis due to size limitations. This could have affected the findings resulting from these models, although the selections were justified by the frequency data in ABOK, the incorporation of wider range of knots could have produced different results.

In order to analyse the knots and links present in ABOK the material knots were considered as the mathematical knot they represent. As discussed in Chapter 2 these knots were considered by simply joining the ends on the picture of the knot given by Ashley to form a closed loop to be characterised mathematically, a technique which was not possible for some knots in ABOK. This procedure allowed the identification of redundant features through Reidemeister moves but this mathematical definition of redundancy did not include any consideration of the functionality of those features.

This exploration of the knots and links present in the Ashley Book of Knots, analysis of the transmission of granny and reef knots and modelling of the social and asocial learning and adaptive fitness of knots and links was possible by combining

both cultural evolutionary theory and mathematical knot theory. The identification of knot types in ABOK, analysis of the difference between granny and reef knots and exploration of the features relevant to transmission in both the social and asocial model and fitness analysis would not have been possible without the use of knot theory. The factors affecting the frequency and transmission of knots and links could not have been analysed without using cultural evolutionary theory and the modelling techniques associated to assess the social learning factors and selection for certain knot and link types and features.

This combination of specialist mathematical theories with experimental and modelling approaches from anthropology and cognitive psychology create powerful analysis tools and results that could not have using one method or discipline alone. The approach presented in this thesis integrates multiple disciplines and techniques highlighting the possibilities to the field of cultural evolution in incorporating mathematical theory.

The modelling and analysis techniques used throughout this thesis are not just applicable to knots. The identification of cognitive biases in the transmission process of knots and links explored in Chapter 3 can be applied to the cultural evolution of other tools and technologies, through experimental, modelling and parameter estimation methods. As too can the findings in Chapters 4 and 5 into the analysis of the transmission process and identification of features increasing the adaptive fitness of traits.

Throughout this thesis multiple techniques from various disciplines exploring knot tying have been utilised. Whilst these techniques may not fully explain knot tying as a whole the findings presented here give new approaches to the exploration of this technology also applicable to other technology and tools. More work is still to be done but the approaches detailed in this thesis show the results possible through an inter-disciplinary approach which can be applied more widely than just to knot tying.



# Appendix A

## Appendices

### A.1 Chapter 3 Appendix

#### A.1.1 Questionnaire information

As part of the experiment described in Section 3.2 the participants were asked to complete a questionnaire detailing their name, gender, degree programme, handedness and hand usually written with, their knot tying experience and whether they knew how to tie a reef or granny knot. The questionnaire was filled in by participants at the end of the experiment, when all materials had been collected.

Participants recorded the hand they usually write with.

		Trefoil Tied		Total
		Right	Left	
Hand usually written with	Right	25	62	87
	Left	4	6	10
	Total	29	68	97

Table A.1: Handedness of trefoils tied given hand usually written with

The majority of participants usually wrote with their write hand and tied a majority of left trefoils. Using a Bayesian analysis to test proportions [68] we see there is a larger probability of tying a left handed trefoil by participants who usually

wrote with their left hand than those who wrote with their right. Similarly there is a larger probability of tying a right handed trefoil by those who usually wrote with their left hand. However, the percentage of participants who usually wrote with their left hand is quite low so might not be wholly representative.

Participants were asked to record their gender in a free-form box.

		Tied correct knot		
		Y	N	Total
Gender	Male	19	17	36
	Female	28	33	61
	Other	2	1	3
Total		49	51	100

Table A.2: Performance in experiment given gender

Table A.2 shows the proportion of participants who tied the knot shown in the video given their gender. It is clear to see that their gender had no bearing on their performance in the experiment.

Participants were asked to rate their experience in knot tying on a scale of one to five, with one meaning they considered themselves a beginner and five an expert. They then had the opportunity to give details in a free-form box.

		Tied correct knot		
		Y	N	Total
Experience	1	18	19	37
	2	10	11	21
	3	14	14	28
	4	7	6	13
	5	0	1	1
Total		49	51	100

Table A.3: Performance in experiment given knot tying experience

Table A.3 shows the proportion of participants who tied the knot shown in the video given the experience rated on the questionnaire. It is clear to see that the self rated experience had no bearing on the performance in the experiment.

Participants were also asked whether they knew how to tie a granny and a reef knot.

		Knot tied		
		Granny	Reef	Total
Knew how to tie a granny knot	Yes	17	13	30
	No	45	25	70
	Total	62	38	100

Table A.4: Performance in experiment given knowledge of granny knots

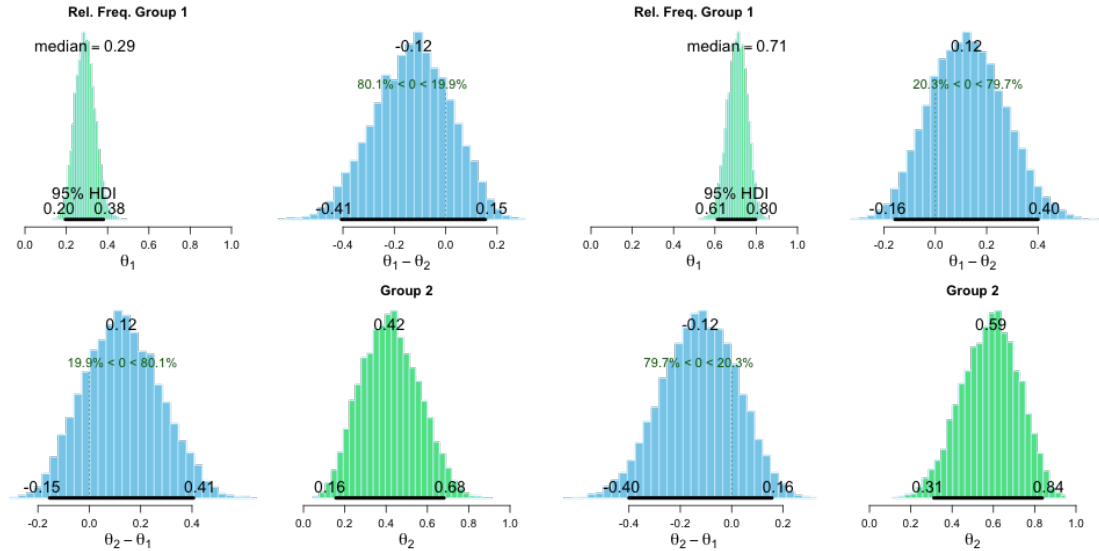
		Knot tied		
		Granny	Reef	Total
Knew how to tie a reef knot	Yes	17	17	34
	No	45	21	66
	Total	62	38	100

Table A.5: Performance in experiment given knowledge of reef knots

Tables A.4 and A.5 show the proportion of participants who tied granny and reef knots given the knowledge rated on the questionnaire. It is clear to see that the self rated knowledge also had no bearing on the knots tied in the experiment. It is interesting to note that more participants knew how to tie the reef knot than the granny. This could be due to the belief that the reef knot is superior to the granny and so more likely to be taught.

### A.1.2 Posterior simulations

Posterior simulations of the test of proportions generated using R package Bayesian First Aid [69]. The test of proportions assumes flat priors constructed as a Beta(1,1) distribution.



(a) Posterior simulation of right trefoils tied      (b) Posterior simulation of left trefoils tied

Figure A.1: Figure A.1a shows the simulations of tying right handed trefoils by those who wrote with either hand.  $\theta_1$  refers to those who wrote with their right hand and tied a right trefoil whilst  $\theta_2$  refers to those who wrote with their left hand and tied a right trefoil, the differences  $\theta_1 - \theta_2$  and  $\theta_2 - \theta_1$  refer to the difference between these groups. We see there is a larger probability of those who write with their left hand tying a right handed trefoil than those who wrote with their right hand. Figure A.1b shows the simulations of tying left handed trefoils by those who wrote with either hand.  $\theta_1$  refers to those who wrote with their right hand and tied a left trefoil whilst  $\theta_2$  refers to those who wrote with their left hand and tied a left trefoil, the differences  $\theta_1 - \theta_2$  and  $\theta_2 - \theta_1$  refer to the difference between these groups. We see there is a larger probability of those who write with their right hand tying a left handed trefoil than those who wrote with their left hand. However if we look at both Figures A.1a and A.1b we see those who wrote with their left hand were slightly more likely to tie a left handed trefoil than a right handed as the left handed trefoil was the most common amongst both groups and there were relatively few people reporting as writing with their left hand.

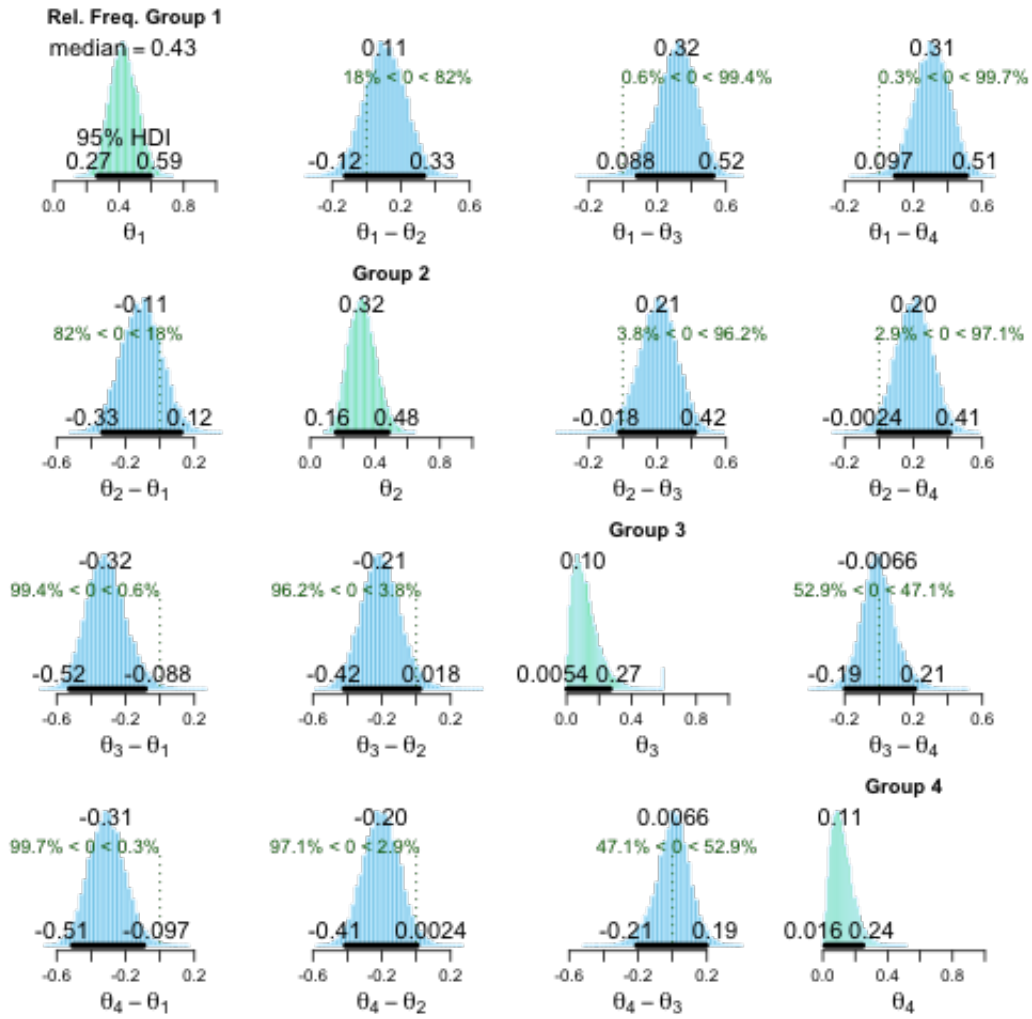


Figure A.2: Posterior simulation of LL knots tied given demonstration knot.  $\theta_1$  refers to those who were shown the knot LL and tied LL,  $\theta_2$  those who were shown RR and tied LL,  $\theta_3$  those who were shown LR and tied LL and  $\theta_4$  those who were shown RL and tied LL with  $\theta_i - \theta_j$ , ( $i, j \in \{1, 2, 3, 4\}, i \neq j$ ) referring to the difference between groups. We see a larger probability for those who were shown either LL or RR tying LL than LR or RL, with those shown LL having the largest probability.

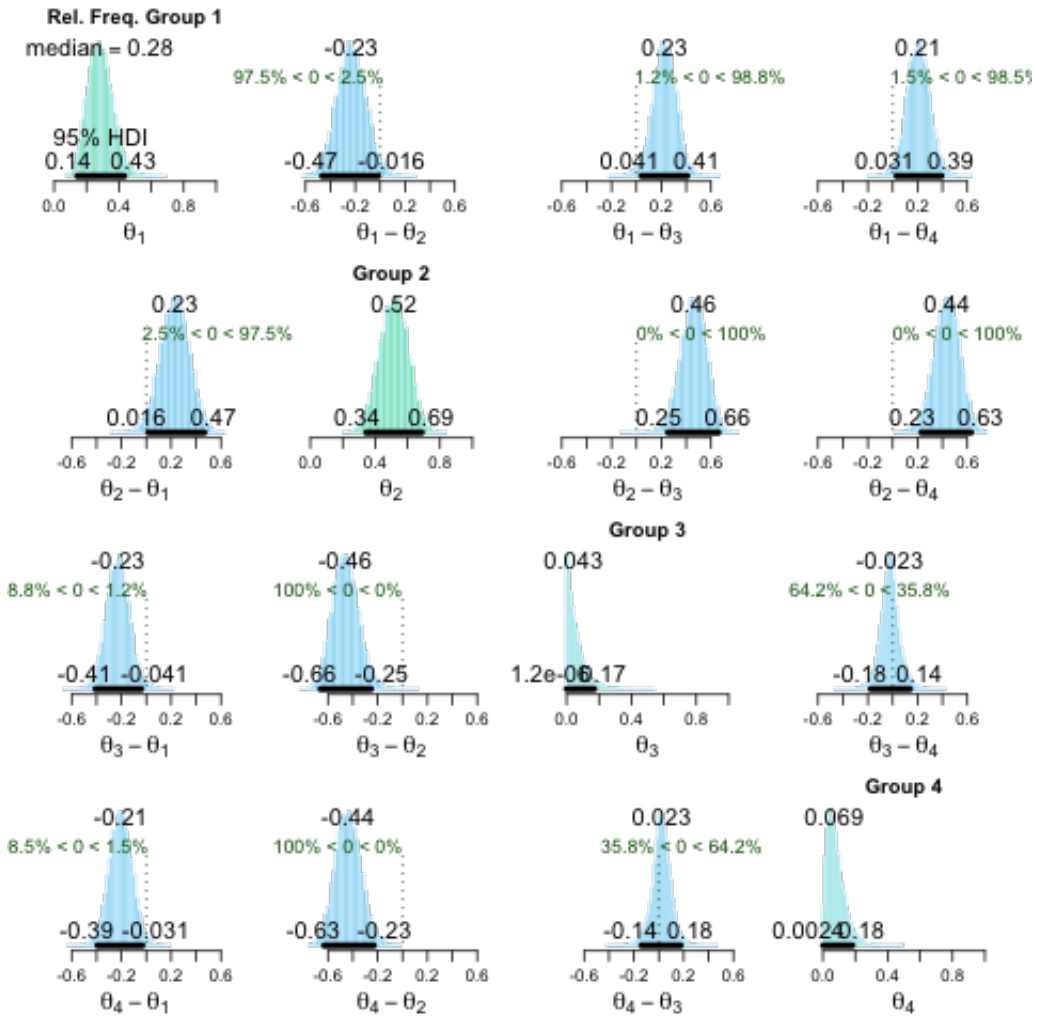


Figure A.3: Posterior simulation of RR knots tied given demonstration knot.  $\theta_1$  refers to those who were shown the knot LL and tied RR,  $\theta_2$  those who were shown RR and tied RR,  $\theta_3$  those who were shown LR and tied RR and  $\theta_4$  those who were shown RL and tied RR with  $\theta_i - \theta_j$ , ( $i, j \in \{1, 2, 3, 4\}, i \neq j$ ) referring to the difference between groups. We see a larger probability for those who were shown either LL or RR tying RR than LR or RL, with those shown RR having the largest probability.

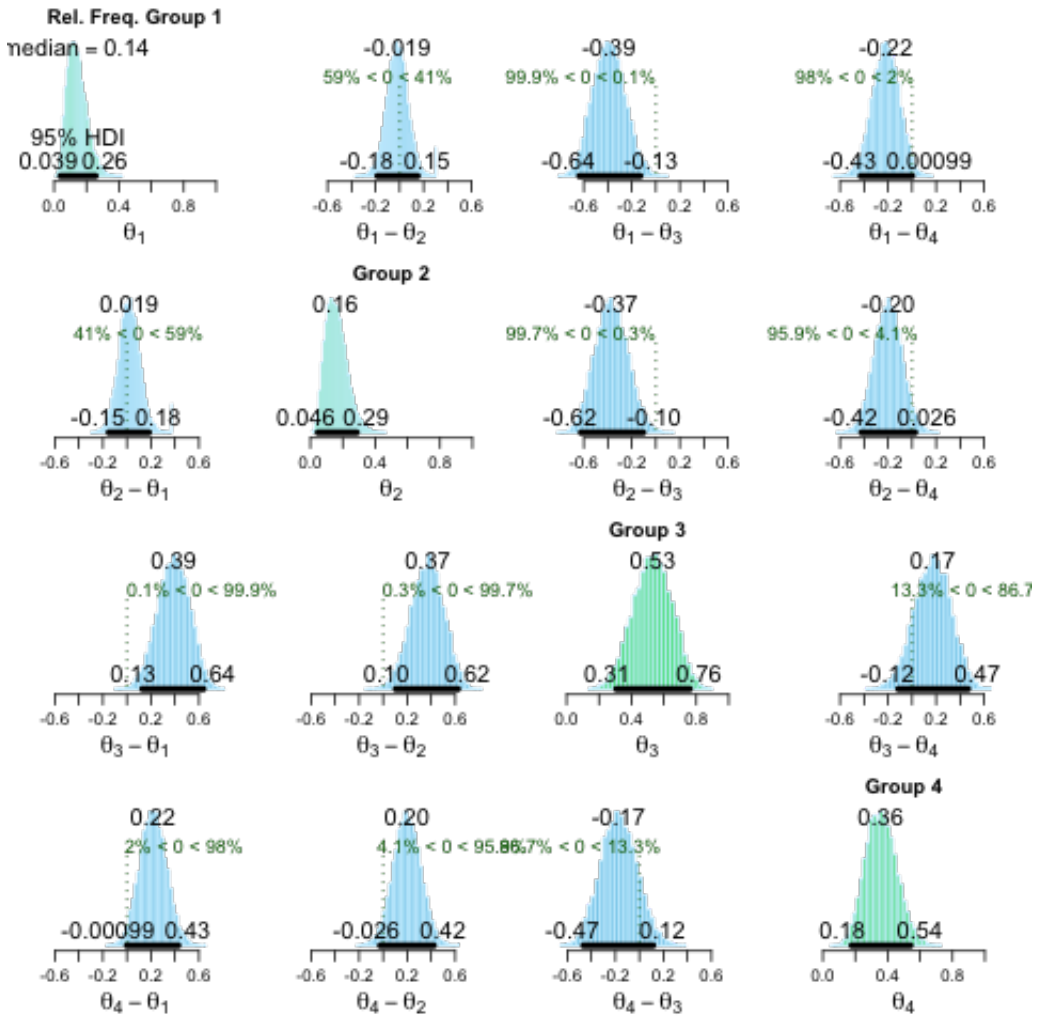


Figure A.4: Posterior simulation of LR knots tied given demonstration knot.  $\theta_1$  refers to those who were shown the knot LL and tied LR,  $\theta_2$  those who were shown RR and tied LR,  $\theta_3$  those who were shown LR and tied LR and  $\theta_4$  those who were shown RL and tied LR with  $\theta_i - \theta_j$ , ( $i, j \in \{1, 2, 3, 4\}, i \neq j$ ) referring to the difference between groups. We see a larger probability for those who were shown either LR or RL tying LR than LL or RR, with those shown LR having the largest probability.

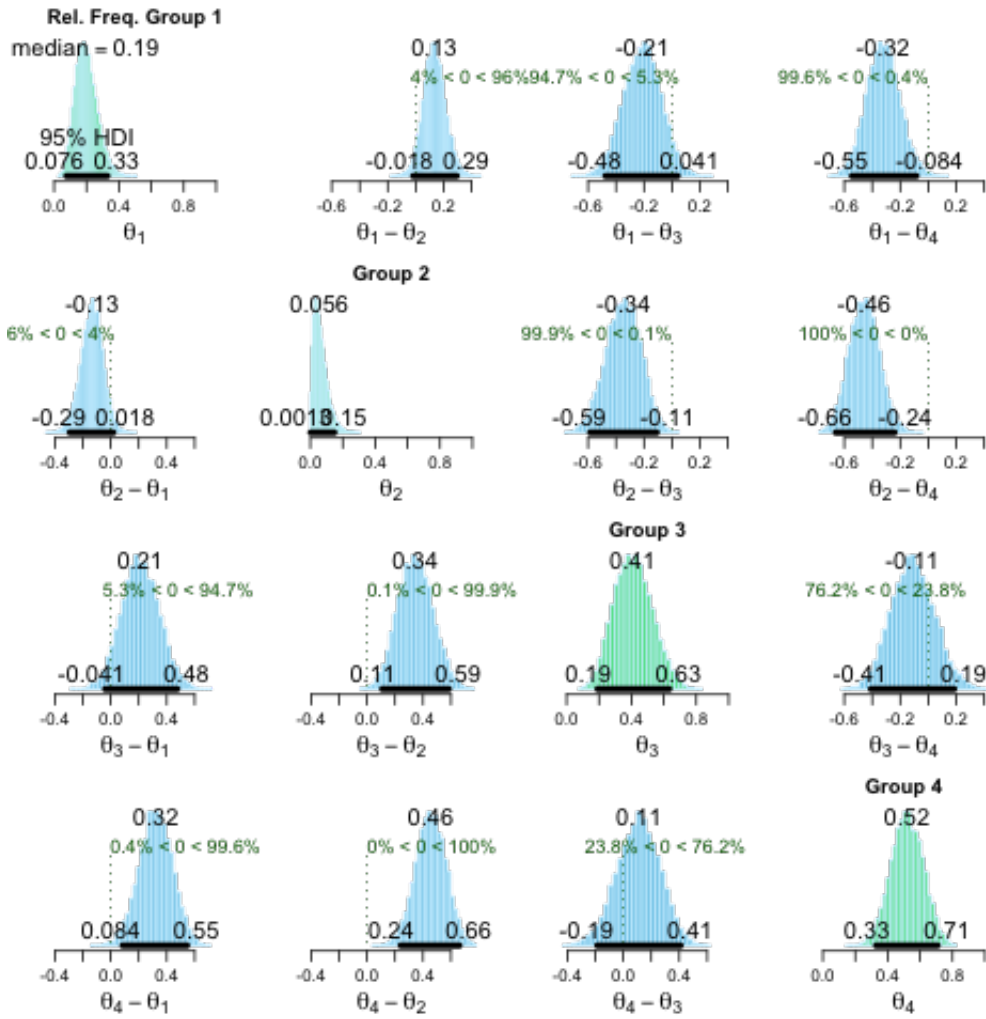
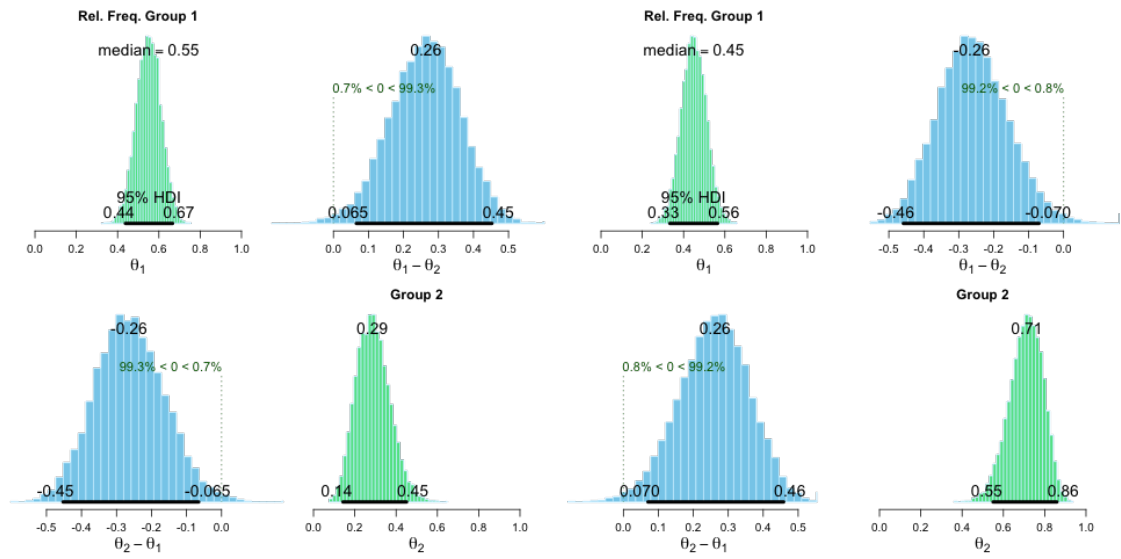


Figure A.5: Posterior simulation of RL knots tied given demonstration knot.  $\theta_1$  refers to those who were shown the knot LL and tied RL,  $\theta_2$  those who were shown RR and tied RL,  $\theta_3$  those who were shown LR and tied RL and  $\theta_4$  those who were shown RL and tied RL with  $\theta_i - \theta_j$ , ( $i, j \in \{1, 2, 3, 4\}, i \neq j$ ) referring to the difference between groups. We see a larger probability for those who were shown either LR or RL tying RL than LL or RR, with those shown RL having the largest probability.





(a) Posterior simulation of knots tied by those with a left hand bias in stage 1

(b) Posterior simulation of knots tied by those with a right hand bias in stage 1

Figure A.6: Figure A.6a shows the simulations of tying an L or R knot first post demonstration given a left hand bias in stage 1.  $\theta_1$  refers to those who had a left hand bias in stage 1 and tied an L knot first post demonstration,  $\theta_2$  those who had a left hand bias and tied an R knot first and  $\theta_1 - \theta_2$  and  $\theta_2 - \theta_1$  the difference between groups. We see there is a larger probability of those who had a left hand bias starting their post-demonstration knot with an L knot than an R. Figure A.6b shows the simulations of tying an L or R knot first post demonstration given a right hand bias in stage 1.  $\theta_1$  refers to those who had a right hand bias in stage 1 and tied an L knot first post demonstration,  $\theta_2$  those who had a right hand bias and tied an R knot first and  $\theta_1 - \theta_2$  and  $\theta_2 - \theta_1$  the difference between groups. We see there is a larger probability of those who had a right hand bias starting their post-demonstration knot with an R knot than an L.

## A.1.3 Equations

The equations are

$$\begin{aligned}
f'_{RR} = & f_{RR}((1-g)s^2 + (1-s)^2(1-r)p^2 + (1-s)^2rp + 2(1-g)s(1-s)r) \\
& + 2(1-g)s(1-s)(1-r)p \\
& + f_{LL}((1-s)^2(1-r)p^2 + (1-s)^2rp + gs^2 + 2gs(1-s)r) \\
& + 2gs(1-s)(1-r)p \\
& + (f_{RL} + f_{LR})((1-s)^2(1-r)p^2 + (1-s)^2rp + s(1-s)r) \\
& + s(1-s)(1-r)p)
\end{aligned} \tag{A.1.1}$$

$$\begin{aligned}
f'_{LL} = & f_{RR}(gs^2 + (1-s)^2(1-r)(1-p)^2 + (1-s)^2r(1-p) + 2gs(1-s)r) \\
& + 2gs(1-s)(1-r)(1-p)) \\
& + f_{LL}((1-g)s^2 + (1-s)^2(1-r)(1-p)^2 + (1-s)^2r(1-p) \\
& + 2(1-g)s(1-s)(1-r)(1-p) + 2(1-g)s(1-s)r) \\
& + (f_{RL} + f_{LR})((1-s)^2(1-r)(1-p)^2 + (1-s)^2r(1-p) \\
& + s(1-s)(1-r)(1-p) + s(1-s)r)
\end{aligned} \tag{A.1.2}$$

$$\begin{aligned}
f'_{RL} = & f_{RR}((1-s)^2(1-r)p(1-p) + (1-g)s(1-s)(1-r)(1-p) \\
& + g(1-s)s(1-r)p) \\
& + f_{LL}((1-s)^2(1-r)p(1-p) + (1-g)(1-s)s(1-r)p \\
& + gs(1-s)(1-r)(1-p)) \\
& + f_{RL}((1-g)s^2 + (1-s)^2(1-r)p(1-p) + (1-g)s(1-s)(1-r)) \\
& + f_{LR}(gs^2 + (1-s)^2(1-r)p(1-p) + gs(1-s)(1-r))
\end{aligned} \tag{A.1.3}$$

$$\begin{aligned}
f'_{LR} = & f_{RR}((1-s)^2(1-r)(1-p)p + (1-g)(1-s)s(1-r)(1-p) \\
& + gs(1-s)(1-r)p) \\
& + f_{LL}((1-s)^2(1-r)(1-p)p + (1-g)s(1-s)(1-r)p \\
& + g(1-s)s(1-r)(1-p)) \\
& + f_{RL}(gs^2 + (1-s)^2(1-r)(1-p)p + gs(1-s)(1-r)) \\
& + f_{LR}((1-g)s^2 + (1-s)^2(1-r)(1-p)p + (1-g)s(1-s)(1-r))
\end{aligned} \tag{A.1.4}$$

### A.1.4 Equilibria equations

Equilibria occur when

$$\hat{f}_{RR} = \frac{Q_1}{P}$$

where

$$\begin{aligned} Q_1 = & -p^2(r-1)(s-1)(1+s(2g-1)(r-1)+rs^2(2g-1))+gs(r(s^2-2)-s) \\ & +p(s-1)(2gs+r^2s(2g-1)(1+s)+r(1+s-2gs(2-s))) \end{aligned} \quad (\text{A.1.5})$$

$$\hat{f}_{LL} = \frac{Q_2}{P}$$

where

$$\begin{aligned} Q_2 = & s^2(1-g)-p^2(r-1)(s-1)(1+s(2g-1)(r-1)+rs^2(2g-1))-1 \\ & +r(s(1-2g)+s^3(g-1))+p(s-1)(r^2s(2g-1)(1+s) \\ & +2s(g-1)+rs(1+(3-4g)-2s^2(g-1))-2) \end{aligned} \quad (\text{A.1.6})$$

$$\hat{f}_{LR} = \frac{Q_3}{P}$$

where

$$Q_3 = (r-1)(gs-p(s-1)(1+p^2(s-1))(1+(2g-1)(s(r-1)+rs^2))) \quad (\text{A.1.7})$$

$$\hat{f}_{RL} = \frac{Q_4}{P}$$

where

$$Q_4 = (r-1)(gs-p(s-1)(1+p^2(s-1))(1+(2g-1)(s(r-1)+rs^2))) \quad (\text{A.1.8})$$

and

$$P = (1+s)(s(2g-1)(rs-r-1)-1). \quad (\text{A.1.9})$$

### A.1.5 Barycentric coordinates

We plot a tetrahedron with vertices at the points  $\begin{pmatrix} 1 \\ 0 \\ 0 \end{pmatrix}$ ,  $\begin{pmatrix} 0 \\ 1 \\ 0 \end{pmatrix}$ ,  $\begin{pmatrix} 0 \\ 0 \\ 1 \end{pmatrix}$  and  $\begin{pmatrix} 1 \\ 1 \\ 1 \end{pmatrix}$ .

Taking values of  $f'_{ij}$  from our equations, we can represent the values of  $f'_{ij}$  as points  $\mathbf{p}$  inside the tetrahedron using the conversion

$$\mathbf{p} = \begin{pmatrix} f'_{RR} + f'_{RL} \\ f'_{LL} + f'_{RL} \\ f'_{LR} + f'_{RL} \end{pmatrix} \quad (\text{A.1.10})$$

## A.2 Chapter 4 Appendix

### A.2.1 Social and asocial learning model

Equilibria for case 3 for braids on three strands

Equilibria occurs when

$$\begin{aligned}
 \hat{f}_{\text{unlink}} &= \frac{1142\hat{f}_{L2a1}}{1747} \\
 \hat{f}_{\text{unlink}\#\text{unlink}} &= \frac{89}{816} - \frac{30349\hat{f}_{0_1}}{133248} - \frac{1869\hat{f}_{L2a1}}{6988} \\
 \hat{f}_{\text{unlink}\#L2a1} &= \frac{485}{1428} - \frac{165385\hat{f}_{0_1}}{233184} - \frac{1455\hat{f}_{L2a1}}{1747} \\
 \hat{f}_{3_1} &= \frac{3345\hat{f}_{0_1}}{5552} \\
 \hat{f}_{\text{unlink}\#3_1} &= \frac{199\hat{f}_{L2a1}}{1747} \\
 \hat{f}_{4_1} &= \frac{439\hat{f}_{0_1}}{5552} \\
 \hat{f}_{L4a1} &= \frac{503\hat{f}_{L2a1}}{1747} \\
 \hat{f}_{L2a1\#L2a1} &= \frac{110}{357} - \frac{18755\hat{f}_{0_1}}{29148} - \frac{1320\hat{f}_{L2a1}}{1747} \\
 \hat{f}_{\text{unlink}\#L4a1} &= \frac{67}{1428} - \frac{22847\hat{f}_{0_1}}{233184} - \frac{201\hat{f}_{L2a1}}{1747} \\
 \hat{f}_{5_1} &= \frac{44\hat{f}_{0_1}}{347} \\
 \hat{f}_{5_2} &= \frac{265\hat{f}_{0_1}}{2776} \\
 \hat{f}_{L5a1} &= \frac{152\hat{f}_{L2a1}}{1747} \\
 \hat{f}_{L2a1\#3_1} &= \frac{304\hat{f}_{L2a1}}{1747} \\
 \hat{f}_{\text{unlink}\#5_1} &= \frac{14\hat{f}_{L2a1}}{1747} \\
 \hat{f}_{6_2} &= \frac{107\hat{f}_{0_1}}{2776} \\
 \hat{f}_{6_3} &= \frac{111\hat{f}_{0_1}}{2776} \\
 \hat{f}_{3_1\#3_1} &= \frac{109\hat{f}_{0_1}}{2776}
 \end{aligned}$$

$$\begin{aligned}
\hat{f}_{L6a1} &= \frac{21\hat{f}_{L2a1}}{1747} \\
\hat{f}_{L6a2} &= \frac{21\hat{f}_{L2a1}}{1747} \\
\hat{f}_{L6a3} &= \frac{35\hat{f}_{L2a1}}{1747} \\
\hat{f}_{L6a4} &= \frac{37}{5712} - \frac{12617\hat{f}_{0_1}}{932736} - \frac{111\hat{f}_{L2a1}}{6988} \\
\hat{f}_{L6a5} &= \frac{107}{5712} - \frac{36487\hat{f}_{0_1}}{932736} - \frac{321\hat{f}_{L2a1}}{6988} \\
\hat{f}_{L6n1} &= \frac{349}{5712} - \frac{119009\hat{f}_{0_1}}{932736} - \frac{1047\hat{f}_{L2a1}}{6988} \\
\hat{f}_{L2a1\#L4a1} &= \frac{107}{1428} - \frac{36487\hat{f}_{0_1}}{233184} - \frac{321\hat{f}_{L2a1}}{1747} \\
\hat{f}_{unlink\#L6a3} &= \frac{1}{357} - \frac{341\hat{f}_{0_1}}{58296} - \frac{12\hat{f}_{L2a1}}{1747} \\
\hat{f}_{7_1} &= \frac{3\hat{f}_{0_1}}{347} \\
\hat{f}_{7_3} &= \frac{3\hat{f}_{0_1}}{694} \\
\hat{f}_{7_5} &= \frac{3\hat{f}_{0_1}}{347} \\
\hat{f}_{L7a1} &= \frac{7\hat{f}_{L2a1}}{1747} \\
\hat{f}_{L7a2} &= \frac{7\hat{f}_{L2a1}}{1747} \\
\hat{f}_{L7a3} &= \frac{7\hat{f}_{L2a1}}{1747} \\
\hat{f}_{L7a5} &= \frac{14\hat{f}_{L2a1}}{1747} \\
\hat{f}_{L7a6} &= \frac{7\hat{f}_{L2a1}}{1747} \\
\hat{f}_{L7a7} &= \frac{1}{714} - \frac{341\hat{f}_{0_1}}{116592} - \frac{6\hat{f}_{L2a1}}{1747} \\
\hat{f}_{L7n1} &= \frac{35\hat{f}_{L2a1}}{1747} \\
\hat{f}_{L7n2} &= \frac{42\hat{f}_{L2a1}}{1747} \\
\hat{f}_{L2a1\#5_1} &= \frac{14\hat{f}_{L2a1}}{1747} \\
\hat{f}_{3_1\#L4a1} &= \frac{14\hat{f}_{L2a1}}{1747}
\end{aligned}$$

$$\begin{aligned}
\hat{f}_{8_2} &= \frac{\hat{f}_{0_1}}{694} \\
\hat{f}_{8_5} &= \frac{\hat{f}_{0_1}}{1388} \\
\hat{f}_{8_7} &= \frac{\hat{f}_{0_1}}{347} \\
\hat{f}_{8_9} &= \frac{\hat{f}_{0_1}}{694} \\
\hat{f}_{8_{10}} &= \frac{\hat{f}_{0_1}}{347} \\
\hat{f}_{8_{16}} &= \frac{\hat{f}_{0_1}}{694} \\
\hat{f}_{8_{17}} &= \frac{\hat{f}_{0_1}}{694} \\
\hat{f}_{8_{18}} &= \frac{\hat{f}_{0_1}}{5552} \\
\hat{f}_{8_{19}} &= \frac{37\hat{f}_{0_1}}{5552} \\
\hat{f}_{8_{20}} &= \frac{5\hat{f}_{0_1}}{347} \\
\hat{f}_{8_{21}} &= \frac{3\hat{f}_{0_1}}{347} \\
\hat{f}_{L8a16} &= \frac{1}{714} - \frac{341\hat{f}_{0_1}}{116592} - \frac{6\hat{f}_{L2a1}}{1747} \\
\hat{f}_{L8a17} &= \frac{1}{714} - \frac{341\hat{f}_{0_1}}{116592} - \frac{6\hat{f}_{L2a1}}{1747} \\
\hat{f}_{L8a18} &= \frac{1}{714} - \frac{341\hat{f}_{0_1}}{116592} - \frac{6\hat{f}_{L2a1}}{1747} \\
\hat{f}_{L8a19} &= \frac{1}{1428} - \frac{341\hat{f}_{0_1}}{233184} - \frac{3\hat{f}_{L2a1}}{1747} \\
\hat{f}_{L8a20} &= \frac{1}{2856} - \frac{341\hat{f}_{0_1}}{466368} - \frac{3\hat{f}_{L2a1}}{3494} \\
\hat{f}_{L8n3} &= \frac{1}{119} - \frac{341\hat{f}_{0_1}}{19432} - \frac{36\hat{f}_{L2a1}}{1747} \\
\hat{f}_{L8n4} &= \frac{1}{119} - \frac{341\hat{f}_{0_1}}{19432} - \frac{36\hat{f}_{L2a1}}{1747} \\
\hat{f}_{L8n5} &= \frac{1}{238} - \frac{341\hat{f}_{0_1}}{38864} - \frac{18\hat{f}_{L2a1}}{1747} \\
\hat{f}_{L8n6} &= \frac{1}{2856} - \frac{341\hat{f}_{0_1}}{466368} - \frac{3\hat{f}_{L2a1}}{3494} \\
\hat{f}_{L2a1\#L6a3} &= \frac{1}{357} - \frac{341\hat{f}_{0_1}}{58296} - \frac{12\hat{f}_{L2a1}}{1747}
\end{aligned}$$



$$\begin{aligned}
\hat{f}_{3_1\#5_1} &= \frac{\hat{f}_{0_1}}{347} \\
\hat{f}_{L4a1\#L4a1} &= \frac{1}{714} - \frac{341\hat{f}_{0_1}}{116592} - \frac{6\hat{f}_{L2a1}}{1747} \\
0 \leq \hat{f}_{0_1} &\leq \frac{2776}{5797} \\
0 \leq \hat{f}_{L2a1} &\leq \frac{1747}{4284} - \frac{595727\hat{f}_{0_1}}{699552}
\end{aligned}$$

where  $\hat{f}_{knot}$  denotes the frequency of the knot at equilibria and  $f_{knot}$  the initial frequency. Here the frequency of all knots and links is determined by the frequency of  $0_1$  and  $L2a1$ , which each appear in separate cycles, the frequency of the links in the third cycle is determined automatically as the frequency of all links must sum to one. We can see the equilibria frequencies for knots in the cycle with  $0_1$  depend only on  $\hat{f}_{0_1}$ , those in the cycle with  $L2a1$  on  $\hat{f}_{L2a1}$ , with the remaining links a combination of the two.

## A.3 Chapter 5 Appendix

Fitness values informed by frequency in ABOK

$N$	Link	Fitness for K		
		1	2	3
3	$3_1$	0.116		
	$L2a1$	0.217		
	$unlink$	0.194		
	$0_1$	0.071		
4	$4_1$	0.267	0.116	
	$L4a1$	0.116	0.108	
	$L2a1\#L2a1$	0.192	0.116	
	$3_1$	0.200	0.114	
	$L2a1$	0.082	0.228	
	$L2a1\#unlink$	0.175	0.082	
	$unlink$	0.071	0.267	
	$unlink\#unlink$	0.158	0.048	
	$0_1$	0.189	0.110	
5	$5_1$	0.116	0.108	0.034
	$L5a1$	0.237	0.116	0.057
	$L4a1$	0.207	0.107	0.122
	$3_1$	0.089	0.204	0.099
	$3_1\#unlink$	0.163	0.087	0.045
	$L2a1$	0.184	0.116	0.169
	$L2a1\#3_1$	0.176	0.114	0.045
	$unlink$	0.168	0.112	0.177
	$0_1$	0.075	0.252	0.075

Table A.6: Fitness values for knots with fitness contributions informed by ABOK data for  $3 \leq N \leq 5$  and  $1 \leq K \leq N - 2$  landscapes

$N$	Link	Fitness for K			
		1	2	3	4
6	$6_2$	0.217	0.114	0.084	0.022
	$6_3$	0.217	0.116	0.043	0.016
	$L6a3$	0.116	0.108	0.034	0.029
	$L6a4$	0.267	0.116	0.034	0.019
	$L6a5$	0.217	0.116	0.073	0.024
	$L6n1$	0.232	0.095	0.170	0.040
	$3_1\#3_1$	0.166	0.113	0.073	0.010
	$L2a1\#L4a1$	0.166	0.113	0.043	0.018
	$5_1$	0.192	0.114	0.083	0.030
	$5_2$	0.217	0.100	0.144	0.066
	$4_1$	0.206	0.112	0.182	0.104
	$L4a1$	0.093	0.188	0.088	0.095
	$L2a1\#L2a1$	0.187	0.115	0.130	0.094
	$L4a1\#unlink$	0.155	0.091	0.043	0.011
	$3_1$	0.179	0.117	0.147	0.087
	$L2a1$	0.080	0.236	0.083	0.178
	$L2a1\#unlink$	0.169	0.112	0.125	0.082
	$unlink$	0.075	0.252	0.075	0.213
	$unlink\#unlink$	0.155	0.109	0.127	0.048
	$0_1$	0.174	0.118	0.190	0.080

Table A.7: Fitness values for knots with fitness contributions informed by ABOK data for  $N = 6$  and  $1 \leq K \leq 4$  landscapes

$N$	Link	Fitness for K				
		1	2	3	4	5
7	$7_1$	0.116	0.108	0.034	0.029	0.014
	$L7a1$	0.246	0.116	0.051	0.019	0.009
	$L7a2$	0.202	0.116	0.033	0.016	0.009
	$L7a3$	0.202	0.115	0.093	0.026	0.012
	$L7a5$	0.202	0.115	0.067	0.017	0.014
	$L7a6$	0.202	0.114	0.076	0.028	0.015
	$L7n1$	0.220	0.104	0.127	0.041	0.072
	$L7n2$	0.224	0.096	0.153	0.062	0.087
	$3_1\#L4a1$	0.159	0.113	0.067	0.017	0.018
	$L2a1\#5_1$	0.159	0.113	0.042	0.019	0.010
	$L6a1$	0.202	0.108	0.093	0.074	0.026
	$L6a2$	0.202	0.101	0.145	0.042	0.058
	$L6a3$	0.185	0.113	0.081	0.029	0.026
	$5_1$	0.096	0.177	0.081	0.086	0.031
	$5_1\#unlink$	0.149	0.093	0.042	0.014	0.008
	$L5a1$	0.201	0.113	0.147	0.089	0.049
	$L2a1\#3_1$	0.183	0.114	0.118	0.075	0.056
	$L4a1$	0.184	0.115	0.150	0.077	0.102
	$3_1$	0.084	0.222	0.085	0.154	0.092
	$3_1\#unlink$	0.164	0.113	0.114	0.064	0.052
	$L2a1$	0.175	0.119	0.163	0.088	0.150
	$unlink$	0.166	0.119	0.167	0.075	0.178
	$0_1$	0.077	0.245	0.079	0.198	0.077

Table A.8: Fitness values for knots with fitness contributions informed by ABOK data for  $N = 7$  and  $1 \leq K \leq 5$  landscapes

$N$	Link	Fitness for K					
		1	2	3	4	5	6
8	$8_2$	0.192	0.113	0.071	0.028	0.020	0.005
	$8_5$	0.192	0.114	0.108	0.0277	0.020	0.005
	$8_7$	0.192	0.114	0.063	0.022	0.011	0.003
	$8_9$	0.192	0.114	0.086	0.018	0.019	0.004
	$8_{10}$	0.192	0.115	0.055	0.017	0.013	0.003
	$8_{16}$	0.230	0.116	0.063	0.021	0.007	0.007
	$8_{17}$	0.230	0.116	0.041	0.017	0.012	0.008
	$8_{18}$	0.267	0.116	0.034	0.019	0.002	0.012
	$8_{19}$	0.210	0.115	0.071	0.025	0.020	0.005
	$8_{20}$	0.222	0.095	0.159	0.063	0.102	0.033
	$8_{21}$	0.217	0.104	0.110	0.068	0.087	0.031
	$L8a14$	0.116	0.108	0.034	0.029	0.014	0.007
	$L8a16$	0.230	0.115	0.071	0.022	0.010	0.007
	$L8a17$	0.192	0.115	0.055	0.015	0.011	0.004
	$L8a18$	0.192	0.114	0.086	0.030	0.015	0.005
	$L8a19$	0.230	0.116	0.063	0.019	0.011	0.008
	$L8a20$	0.192	0.116	0.002	0.010	0.008	0.002
	$L8n3$	0.211	0.103	0.131	0.046	0.067	0.030
	$L8n4$	0.211	0.098	0.155	0.044	0.073	0.030
	$L8n5$	0.217	0.104	0.111	0.076	0.082	0.010
	$L8n6$	0.192	0.116	0.002	0.010	0.016	0.002
	$3_1\#5_1$	0.154	0.112	0.063	0.018	0.022	0.002
	$L2a1\#L6a3$	0.154	0.112	0.041	0.020	0.011	0.005
	$L4a1\#L4a1$	0.154	0.112	0.063	0.022	0.009	0.002
	$7_1$	0.179	0.113	0.079	0.029	0.024	0.012
	$7_3$	0.192	0.102	0.131	0.043	0.037	0.014
	$7_5$	0.192	0.109	0.101	0.051	0.044	0.006
	$L7a7$	0.192	0.115	0.055	0.066	0.017	0.007

Table A.9: Fitness values for knots with fitness contributions informed by ABOK data for  $N = 8$  and  $1 \leq K \leq 6$  landscapes

$N$	Link	Fitness for K					
		1	2	3	4	5	6
8	$6_2$	0.195	0.113	0.133	0.076	0.068	0.026
	$6_3$	0.200	0.112	0.127	0.078	0.058	0.022
	$L6a3$	0.099	0.168	0.075	0.079	0.029	0.026
	$L6a4$	0.218	0.113	0.134	0.086	0.030	0.019
	$L6a5$	0.195	0.113	0.132	0.076	0.053	0.021
	$L6n1$	0.199	0.109	0.183	0.075	0.128	0.035
	$L6a3\#unlink$	0.145	0.095	0.041	0.016	0.009	0.004
	$3_1\#3_1$	0.180	0.113	0.111	0.064	0.070	0.012
	$L2a1\#L4a1$	0.178	0.113	0.109	0.065	0.047	0.021
	$5_1$	0.180	0.116	0.124	0.069	0.064	0.025
	$5_2$	0.195	0.111	0.157	0.079	0.112	0.055
	$4_1$	0.187	0.116	0.172	0.091	0.146	0.096
	$L4a1$	0.087	0.211	0.084	0.137	0.077	0.089
	$L4a1\#unlink$	0.159	0.112	0.102	0.057	0.041	0.014
	$L2a1\#L2a1$	0.180	0.117	0.154	0.087	0.106	0.083
	$3_1$	0.173	0.119	0.150	0.082	0.128	0.076
	$L2a1$	0.080	0.236	0.081	0.181	0.083	0.208
	$L2a1\#unlink$	0.168	0.119	0.148	0.082	0.109	0.083
	$unlink$	0.077	0.245	0.079	0.198	0.077	0.267
	$unlink\#unlink$	0.157	0.121	0.146	0.072	0.122	0.048
	$0_1$	0.170	0.120	0.170	0.082	0.186	0.076

Table A.10: Fitness values for knots with fitness contributions informed by ABOK data for  $N = 8$  and  $1 \leq K \leq 6$  landscapes

## A.3.1 Random walks on NK landscapes

$N$	$K$	Fittest knots or links	Knots and links resulting from walks	Percentage
7	1	$unlink, L2a1, 3_1 \# unlink, L4a1, L2a1 \# 3_1, L5a1, L7n1, L7n2$	$L2a1$	25.2%
			$L2a1 \# 3_1$	22.2%
			$unlink$	10.1%
			$L7n2$	9.9%
			$3_1 \# unlink$	9.8%
			$L5a1$	6.9%
			$L7n1$	6.1%
			$L4a1$	5.7%
			$L7a1$	3.9%
			$L6a2$	0.1%
			$L7a5$	0.1%
	2	$0_1$	$0_1$	98.2%
			$L2a1$	1.4%
			$unlink$	0.3%
	3	$unlink, L2a1, L4a1$	$3_1$	0.1%
			$L2a1$	49.3%
			$unlink$	27.9%
	4	$0_1$	$L4a1$	22.8%
			$0_1$	88.4%
			$L2a1$	8.3%
	5	$unlink$	$3_1$	3.3%
			$unlink$	100%

Table A.11: Table giving the fittest knots or links on  $N = 7$  and  $1 \leq K \leq 5$  and the knots and links resulting from random walks on those landscapes

$N$	$K$	Fittest knots or links	Knots and links resulting from walks	Percentage
8	1	$0_1, 3_1, 4_1, 5_1, 5_2, 6_3, 3_1 \# 3_1, 8_{18}, 8_{19}, 8_{20}$	$0_1$ $3_1$ $5_2$ $5_1$ $6_3$ $8_{20}$ $3_1 \# 3_1$ $L2a1 \# L4a1$ $L2a1 \# L2a1$ $L2a1 \# unlink$ $L4a1 \# unlink$ $6_2$ $4_1$ $8_{21}$ $L8n3$ $8_{19}$ $L8n4$ $L6n1$ $L8n5$ $L6a5$ $8_{18}$ $L8a19$ $unlink \# unlink$ $L6a4$ $8_{17}$ $8_{16}$ $L8a16$	27.6% 24.6% 11.3% 6.9% 5% 5% 3.4% 2.6% 2.1% 1.7% 1.3% 1.2% 1% 1% 0.9% 0.8% 0.7% 0.6% 0.5% 0.4% 0.3% 0.3% 0.2% 0.2% 0.2% 0.1% 0.1%
	2	$unlink, L2a1$	$unlink$ $L2a1$ $0_1$ $3_1$ $L2a1 \# L2a1$ $L2a1 \# unlink$ $unlink \# unlink$	63.5% 32.3% 1.8% 1.1% 0.6% 0.5% 0.2%

Table A.12: Table giving the fittest knots or links on  $N = 8$  and  $1 \leq K \leq 2$  and the knots and links resulting from random walks on those landscapes



$N$	$K$	Fittest knots or links	Knots and links resulting from walks	Percentage
8	3	$0_1, unlink\#unlink, L2a1\#unlink, 4_1, L2a1\#L2a1, L6n1$	$0_1$ $L2a1\#L2a1$ $L6n1$ $L2a1\#unlink$ $unlink\#unlink$ $3_1$ $4_1$	31.7% 22.5% 14.8% 14.3% 9.9% 3.5% 3.3%
	4	$unlink$	$unlink$ $L2a1$ $L2a1\#L2a1$ $0_1$ $L2a1\#unlink$ $3_1$ $L6a4$ $L4a1$ $4_1$	62.1% 26.2% 3.9% 3.5% 2.2% 1% 0.5% 0.4% 0.2%
	5	$0_1$	$0_1$	100%
	6	$unlink$	$unlink$ $4_1$ $3_1$ $0_1$ $L2a1\#unlink$	41.1% 30.6% 27% 0.8% 0.5%

Table A.13: Table giving the fittest knots or links on  $N = 8$  and  $3 \leq K \leq 6$  and the knots and links resulting from random walks on those landscapes

# Bibliography

- [1] C. Warner and R. G. Bednarik, “Pleistocene Knotting,” in *Hist. Sci. Knots*, J. Turner and P. Van de Griend, Eds. World Scientific, 1998, pp. 3–18.
- [2] G. van der Kleij, “On Knots and Swamps: Knots in European Prehistory,” in *Hist. Sci. Knots*, J. Turner and P. Van de Griend, Eds. World Scientific, 1998, pp. 31–42.
- [3] W. Wendrich, “Ancient Egyptian Rope and Knots,” in *Hist. Sci. Knots*, J. C. Turner and P. van de Griend, Eds. World Scientific, pp. 43–68.
- [4] Encyclopedia Britannica, “Gordian knot.” [Online]. Available: <http://www.britannica.com/EBchecked/topic/239059/Gordian-knot>
- [5] L. H. S. Chen, “The Art of Chinese Knotwork: A Short History,” in *Hist. Sci. Knots*, J. C. Turner and P. van de Griend, Eds. World Scientific, 1998, pp. 89–106.
- [6] L. L. Leland, “The Ancient Quipo, a Peruvian Knot Record,” *Am. Anthropol.*, vol. 14, no. 2, pp. 325–332, apr 1912.
- [7] M. Medrano and G. Urton, “Toward the Decipherment of a Set of Mid-Colonial Khipus from the Santa Valley, Coastal Peru,” *Ethnohistory*, vol. 65, no. 1, pp. 1–23, 2018.
- [8] C. W. Ashley, *Ashley Book of Knots*. Faber and Faber Limited, 1993.
- [9] International Guild of Knot Tyers, “IGKT.” [Online]. Available: <https://www.igkt.net/> [Accessed: 2018-06-28]

- [10] H. N. G. Bushby, *Notes on Knots*, International Guild of Knot Tyers, Ed. International Guild of Knot Tyers.
- [11] The Mariner's Museum, "Henry Bushby's Manuscript Notes on Knots." [Online]. Available: <http://librarygallery.marinersmuseum.org/exhibits/show/bushby> [Accessed: 2018-06-25]
- [12] I. Fieggen, "Ian's Shoelace Site." [Online]. Available: <https://www.fieggen.com/shoelace/index.htm> [Accessed: 2018-06-25]
- [13] Grog, "Animated Knots by Grog." [Online]. Available: <http://www.animatedknots.com/index.php> [Accessed: 2018-06-25]
- [14] Yale University, "eHRAF World Cultures." [Online]. Available: <http://ehrafworldcultures.yale.edu/ehraf/>
- [15] P. T. Walsh, M. Hansell, W. D. Borello, and S. D. Healy, "Individuality in nest building: Do Southern Masked weaver (*Ploceus velatus*) males vary in their nest-building behaviour?" *Behav. Process.*, vol. 88, no. 1, pp. 1–6, 2011.
- [16] H. Adam, "Different types of body movement in the hagfish, *myxine glutinosa* L." *Nature*, vol. 188, no. 4750, pp. 595–596, nov 1960.
- [17] C. Herzfeld and D. Lestel, "Knot tying in great apes: etho-ethnology of an unusual tool behavior," *Soc. Sci. Inf.*, vol. 44, no. 4, pp. 621–653, 2005.
- [18] A. Mesoudi, *Cultural evolution: How Darwinian theory can explain human culture and synthesize the social sciences*. Chicago, IL: University of Chicago Press, 2011.
- [19] P. J. Richerson and R. Boyd, *Not by Genes Alone: How Culture Transformed Human Evolution*. Chicago, IL: University of Chicago Press, 2005.
- [20] N. Claidière, T. C. Scott-phillips, and D. Sperber, "How Darwinian is cultural evolution?" *Philos. Trans. R. Soc. B Biol. Sci.*, no. March, 2014.

- [21] J. Henrich and F. J. Gil-White, “The evolution of prestige: Freely conferred deference as a mechanism for enhancing the benefits of cultural transmission,” *Evol. Hum. Behav.*, vol. 22, no. 3, pp. 165–196, 2001.
- [22] N. Claidière, M. Bowler, S. Brookes, R. Brown, and A. Whiten, “Frequency of behavior witnessed and conformity in an everyday social context,” *PLoS One*, vol. 9, no. 6, 2014.
- [23] L.-A. Giraldeau, T. J. Valone, and J. J. Templeton, “Potential disadvantages of using socially acquired information.” *Philos. Trans. R. Soc. Lond. B. Biol. Sci.*, vol. 357, no. October, pp. 1559–1566, 2002.
- [24] O. Morin, “How portraits turned their eyes upon us: Visual preferences and demographic change in cultural evolution,” *Evol. Hum. Behav.*, vol. 34, no. 3, pp. 222–229, may 2013.
- [25] L. Cavalli-Sforza and M. W. Feldman, “Models for cultural inheritance I. Group mean and within group variation,” *Theor. Popul. Biol.*, vol. 4, no. 1, pp. 42–55, mar 1973.
- [26] R. Boyd and P. J. Richerson, “Culture and the evolutionary process,” p. 331, 1985.
- [27] A. Acerbi and R. Alexander Bentley, “Biases in cultural transmission shape the turnover of popular traits,” *Evol. Hum. Behav.*, vol. 35, no. 3, pp. 228–236, may 2014.
- [28] A. Kandler, B. Wilder, and L. Fortunato, “Inferring individual-level processes from population-level patterns in cultural evolution,” *R. Soc. Open Sci.*, vol. 4, no. 9, 2017.
- [29] B. Hayes, “First Links in the Markov Chain,” *Am. Sci.*, vol. 101, 2013.
- [30] L. L. Cavalli-Sforza and M. W. Feldman, *Cultural Transmission and Evolution: A Quantitative Approach*. Princeton University Press, 1981.

- [31] P. A. Gagniuc, “Building the Stochastic Matrix,” in *Markov Chain*. Hoboken, NJ, USA: John Wiley & Sons, Inc., jul 2017, pp. 25–35.
- [32] A. Mesoudi and A. Whiten, “The multiple roles of cultural transmission experiments in understanding human cultural evolution.” *Philos. Trans. R. Soc. Lond. B. Biol. Sci.*, vol. 363, no. 1509, pp. 3489–3501, 2008.
- [33] M. Muthukrishna, B. W. Shulman, V. Vasilescu, and J. Henrich, “Sociality influences cultural complexity.” *Proc. Biol. Sci.*, vol. 281, p. 20132511, 2014.
- [34] C. A. Caldwell, E. Renner, and M. Atkinson, “Human Teaching and Cumulative Cultural Evolution,” *Rev. Philos. Psychol.*, 2017.
- [35] W. Thomson, “On Vortex Atoms,” *Proc. R. Soc. Edinburgh*, vol. 6, pp. 94–105, sep 1869.
- [36] J. H. Przytycki, *Knots: From combinatorics of knot diagrams to combinatorial topology based on knots*, 2007.
- [37] P. G. Tait, “On Knots I, II, III,” *Sci. Pap.*, 1900.
- [38] “Knot Atlas.” [Online]. Available: <http://katlas.org>
- [39] J. C. Cha and C. Livingston, “KnotInfo: Table of Knot Invariants.” [Online]. Available: <http://www.indiana.edu/~7B{~}{%}7Dknotinfo/>
- [40] J. Hoste, M. Thistlethwaite, and J. Weeks, “The first 1,701,936 knots,” pp. 33–48, 1998.
- [41] M. Thistlethwaite, “Knotscape.” [Online]. Available: <http://www.math.utk.edu/~7B{~}{%}7D{~}{%}7Dmorwen/knotscape.html>
- [42] K. Reidemeister, “Elementare Begründung der Knotentheorie,” *Abhandlungen aus dem Math. Semin. der Univ. Hambg.*, vol. 5, no. 1, pp. 24–32, dec 1927.
- [43] V. F. R. Jones, “A polynomial invariant for knots via Von Neumann algebras,” *Bull. Am. Math. Soc.*, vol. 12, no. 1, pp. 103–111, 1985.

- [44] P. Freyd, D. Yetter, J. Hoste, W. B. R. Lickorish, K. Millett, and A. Ocneanu, “A new polynomial invariant of knots and links,” *Bull. Am. Math. Soc.*, vol. 12, no. 2, pp. 239–247, 1985.
- [45] C. H. Dowker and M. Thistlethwaite, “Classification of knot projections,” vol. 16, pp. 19–31, 1983.
- [46] L. A. Scanlon, “Study of knots in material culture,” *J. Knot Theory Ramifications*, vol. 25, no. 9, 2016.
- [47] P. Pieranski, S. Kasas, G. Dietler, J. Dubochet, and A. Stasiak, “Localization of breakage points in knotted strings,” *New J. Phys.*, vol. 3, pp. 0–13, 2001.
- [48] D. Rolfsen, *Knots and Links*. American Mathematical Soc., 1976.
- [49] T. M. A. Fink and Y. Mao, “Tie knots, random walks and topology,” *Phys. A Stat. Mech. its Appl.*, vol. 276, pp. 109–121, 2000.
- [50] D. Hirsch, I. Markström, M. L. Patterson, A. Sandberg, and M. Vejdemo-Johansson, “More ties than we thought,” *PeerJ Comput. Sci.*, vol. 1, no. e2, pp. 1–15, 2015.
- [51] M. G. Tytherleigh, T. S. Bhatti, R. M. Watkins, and D. C. Wilkins, “The assessment of surgical skills and a simple knot-tying exercise,” *Ann. R. Coll. Surg. Engl.*, vol. 83, pp. 69–73, 2001.
- [52] M. Derex, B. Godelle, and M. Raymond, “Social learners require process information to outperform individual learners,” *Evol. (N. Y.)*, vol. 67, pp. 688–697, 2013.
- [53] P. Traczyk and J. H. Przytycki, “Conway Algebras And Skein Equivalence,” vol. 100, no. 4, pp. 744–748, 1987.
- [54] J. C. Cha and C. Livingston, “LinkInfo: Table of Knot Invariants.” [Online]. Available: <http://www.indiana.edu/{%}7B{~}{%}7Dlinkinfo/>
- [55] R. G. Scharein, “The KnotPlot Site.” [Online]. Available: <http://www.knotplot.com/>

- [56] H. B. Mann and D. R. Whitney, "On a Test of Whether one of Two Random Variables is Stochastically Larger than the Other," *Ann. Math. Stat.*, vol. 18, no. 1, pp. 50–60, mar 1947.
- [57] M. P. Fay and M. A. Proschan, "Wilcoxon-Mann-Whitney or t-test? On assumptions for hypothesis tests and multiple interpretations of decision rules," *Stat. Surv.*, vol. 4, pp. 1–39, 2010.
- [58] H. M. Lewis and K. N. Laland, "Transmission fidelity is the key to the build-up of cumulative culture," *Philos. Trans. R. Soc. B Biol. Sci.*, vol. 367, no. 1599, pp. 2171–2180, aug 2012.
- [59] J. W. Eerkens and C. P. Lipo, "Cultural transmission, copying errors, and the generation of variation in material culture and the archaeological record," *J. Anthr. Archaeol.*, vol. 24, no. 4, pp. 316–334, 2005.
- [60] M. Kempe, S. Lycett, and A. Mesoudi, "An Experimental Test of the Accumulated Copying Error Model of Cultural Mutation for Acheulean Handaxe Size," *PLoS One*, vol. 7, no. 11, 2012.
- [61] S. B. Kalyanshetti and B. C. Vastrad, "Effect of handedness on visual , auditory and cutaneous reaction times in normal subjects," *Al Ameen J Med Sci*, vol. 6, pp. 278–280, 2013.
- [62] A. Wohlschläger, M. Gattis, and H. Bekkering, "Action generation and action perception in imitation: an instance of the ideomotor principle." *Philos. Trans. R. Soc. Lond. B. Biol. Sci.*, vol. 358, no. 1431, pp. 501–515, 2003.
- [63] C. Chiavarino, I. A. Apperly, and G. W. Humphreys, "Exploring the functional and anatomical bases of mirror-image and anatomical imitation: The role of the frontal lobes," *Neuropsychologia*, vol. 45, no. 4, pp. 784–795, 2007.
- [64] C. Heyes and G. Bird, "Mirroring, association, and the correspondence problem," *Sensorimotor Found. High. Cogn.*, pp. 461–480, 2007.
- [65] Grog, "Animated Knots: How to tie the Reef Knot." [Online]. Available: <http://www.animatedknots.com/reef/>

- [66] O. M. O'reilly, C. A. Daily-Diamond, and C. E. Gregg, "The roles of impact and inertia in the failure of a shoelace knot," *Proc. R. Soc. A Math. Phys. Eng. Sci.*, 2017.
- [67] C. C. Adams, *The Knot Book: An Elementary Introduction to the Mathematical Theory of Knots*. American Mathematical Soc., 2004.
- [68] A. Gelman, J. B. Carlin, H. S. Stern, and D. B. Rubin, *Bayesian Data Analysis*, 3rd ed. Chapman and Hall/CRC, 2003, vol. 2.
- [69] R. Bååth, "Bayesian First Aid: A Package that Implements Bayesian Alternatives to the Classical \* .test Functions in R," in *UseR! 2014 - Int. R User Conf.*, 2014.
- [70] M. Sunnåker, A. G. Busetto, E. Numminen, J. Corander, M. Foll, and C. Dessimoz, "Approximate Bayesian Computation," *PLoS Comput. Biol.*, vol. 9, no. 1, p. e1002803, jan 2013.
- [71] R. McElreath, *Statistical rethinking : a Bayesian course with examples in R and Stan*. CRC Press, 2016.
- [72] K. Smith, "Learning bias, cultural evolution of language, and the biological evolution of the language faculty." *Hum. Biol.*, vol. 83, no. 2, pp. 261–278, 2011.
- [73] V. N. Salimpoor, C. Chang, and V. Menon, "Neural Basis of Repetition Priming during Mathematical Cognition: Repetition Suppression or Repetition Enhancement?" *J. Cogn. Neurosci.*, vol. 22, no. 4, pp. 790–805, apr 2010.
- [74] K. Weber, M. H. Christiansen, K. M. Petersson, P. Indefrey, and P. Hagoort, "fMRI Syntactic and Lexical Repetition Effects Reveal the Initial Stages of Learning a New Language," *J. Neurosci.*, vol. 36, no. 26, 2016.
- [75] L. Mayrhauser, J. Bergmann, J. Crone, and M. Kronbichler, "Neural repetition suppression: evidence for perceptual expectation in object-selective regions," *Front. Hum. Neurosci.*, vol. 8, p. 225, apr 2014.



- [76] M. Jamroz, W. Niemyska, E. J. Rawdon, A. Stasiak, K. C. Millett, P. Sulkowski, and J. I. Sulkowska, “KnotProt: A database of proteins with knots and slip-knots,” *Nucleic Acids Res.*, vol. 43, no. D1, pp. D306–D314, jan 2015.
- [77] S. A. Wasserman, J. M. Dungan, and N. R. Cozzarelli, “Discovery of a predicted DNA knot substantiates a model for site-specific recombination.” *Science*, vol. 229, no. 4709, pp. 171–174, jul 1985.
- [78] D. M. Raymer and D. E. Smith, “Spontaneous knotting of an agitated string,” *Proc. Natl. Acad. Sci.*, vol. 104, no. 42, pp. 16 432–16 437, 2007.
- [79] C. Even-Zohar, “Models of random knots,” *J. Appl. Comput. Topol.*, vol. 1, no. 2, pp. 263–296, dec 2017.
- [80] X. Hua, D. Nguyen, B. Raghavan, J. Arsuaga, and M. Vazquez, “Random state transitions of knots: a first step towards modeling unknotting by type II topoisomerases,” *Topol. Appl.*, vol. 154, no. 7 SPEC. ISS., pp. 1381–1397, apr 2007.
- [81] J. Cantarella, A. Henrich, E. Magness, O. O’Keefe, K. Perez, E. Rawdon, and B. Zimmer, “Knot fertility and lineage,” *J. Knot Theory Its Ramifications*, vol. 26, no. 13, p. 1750093, nov 2017.
- [82] G. A. Miller, “The Magical Number Seven, Plus or Minus Two: Some Limits on Our Capacity for Processing Information,” *Psychol. Rev.*, vol. 63, no. 2, pp. 81–97, 1956.
- [83] S. Wright, “The roles of mutation, inbreeding, crossbreeding and selection in evolution,” pp. 356–366, 1932.
- [84] M. R. Dietrich and R. A. Skipper, “A Shifting Terrain : A Brief History of the Adaptive Landscape,” *Adapt. Landsc. Evol. Biol.*, vol. 7, pp. 3–15, 2012.
- [85] S. Kauffman and S. Levin, “Towards a general theory of adaptive walks on rugged landscapes,” *J. Theor. Biol.*, vol. 128, no. 1, pp. 11–45, sep 1987.

- [86] S. Wright, “Evolution in Mendelian Populations,” *Genetics*, vol. 16, no. 2, pp. 97–159, mar 1931.
- [87] L. Gerrits and P. Marks, “The evolution of Wright’s (1932) adaptive field to contemporary interpretations and uses of fitness landscapes in the social sciences,” *Biol. Philos.*, vol. 30, no. 4, pp. 459–479, 2015.
- [88] S. A. Kauffman and E. D. Weinberger, “The NK model of rugged fitness landscapes and its application to maturation of the immune response,” *J. Theor. Biol.*, vol. 141, no. 2, pp. 211–245, nov 1989.
- [89] R. Adner and D. A. Levinthal, “The Emergence of Emerging Technologies,” *Calif. Manage. Rev.*, vol. 45, no. 1, pp. 50–66, 2002.
- [90] D. Curran, C. O. Riordan, and H. Sorensen, “Evolving Cultural Learning Parameters in an NK Fitness Landscape,” *Lect. Notes Artif. Intell.*, vol. 4648, pp. 304–314, 2007.
- [91] R. W. Hamming, “Error Detecting and Error Correcting Codes,” *Bell Syst. Tech. J.*, vol. 29, no. 2, pp. 147–160, apr 1950.
- [92] C. M. Bishop, *Pattern recognition and machine learning*. Springer-Verlag New York, 2006.
- [93] L. Fleming and O. Sorenson, “Technology as a complex adaptive system: Evidence from patent data,” *Res. Policy*, vol. 30, no. 7, pp. 1019–1039, 2001.